GEOLOGICA ULTRAIECTINA

Mededelingen van de Faculteit Geowetenschappen Universiteit Utrecht

No. 321

Dissolved organic nitrogen dynamics in coastal ecosystems

Tom Van Engeland

Doctoral advisors:

Prof. dr. J. J. Middelburg	Utrecht University, The Netherlands Netherlands Institute of Ecology, The Netherlands
Prof. dr. K. Soetaert	Ghent University, Belgium Vrije Universiteit Brussel, Belgium Netherlands Institute of Ecology, The Netherlands

Members of the dissertation committee:

Prof. dr. ir. J. S. Sinninghe Damsté	Utrecht University, The Netherlands Netherlands Institute of Sea Research, The Netherlands
Prof. dr. H. J. Laanbroek	Utrecht University, The Netherlands Netherlands Institute of Ecology, The Netherlands
Prof. dr. R. W. P. M. Laane	University of Amsterdam, The Netherlands Deltares, The Netherlands
Prof. dr. N. Brion	Vrije Universiteit Brussel, Belgium
dr. T. J. Bouma	Netherlands Institute of Ecology, The Netherlands

ISBN 9789057441820

NIOO Thesis 77

Dissolved organic nitrogen dynamics in coastal ecosystems

Opgeloste organische stikstof dynamiek in kust-nabije ecosystemen

(met een samenvatting in het Nederlands)

Proefschrift

ter verkrijging van de graad van doctor aan de Universiteit Utrecht op gezag van de rector magnificus, prof.dr. J.C. Stoof, ingevolge het besluit van het college voor promoties in het openbaar te verdedigen op dinsdag 30 maart 2010 des middags te 2.30 uur

door

Tom Van Engeland
geboren op 14 januari 1979 te Lommel, België

Promotoren: Prof. dr. J.J. Middelburg
Prof. dr. K. Soetaert

This thesis was supported by NWO (Vlanezo2, 832.110.007) and Rijkswaterstaat (Canopy-DON).

Contents

Preface

Many aquatic ecosystems in the developed countries, including coastal systems, have gone through a phase of high inorganic nutrient levels, characterized by high primary production, strong heterotrophy and in many cases severe hypoxia. Many of these systems now experience a phase of decreasing inorganic nutrient concentrations because of nutrient reduction measures. However, primary productivity has not always decreased as expected. This is often attributed to internal loading of the systems combined with efficient nutrient recycling. Whereas some primary producers depend solely on dissolved inorganic nitrogen (DIN) forms, others are able to utilize dissolved organic nitrogenous (DON) compounds such as urea or amino acids. This ability to use various nitrogenous compounds is species and in some cases even stage dependent, giving these primary producers a competitive advantage under DIN depleted conditions over those restricted to DIN utilization. Changes in nitrogen substrate composition can thus cause changes in the composition of the primary producer community, changing seasonal succession or shifting dominance of the phytoplankton community over several years. Often opportunistic species, such as dinophytes and cyanobacteria, benefit most from inorganic nutrient reductions since they are often capable of utilizing organic substances without prior remineralization. However, because these species are less juicy for some heterotrophs, shifts in the higher trophic levels can occur as well. Moreover, some species produce toxins, cause shading, and hypoxia after the bloom collapses because of their large biomass, or cause large mortality among grazers that are not physically able to cope with for instance spines or the large volume of colonies. They can be harmful, not only to their direct environment, but often also from an economic point-of-view. En masse toxin production can either kill fish and shellfish populations, or accumulate in species that are harvested for consumption. Drinking water and recreational waters may be affected as well.

In many coastal ecosystems dissolved organic nitrogen (DON) is the largest pool of fixed nitrogen directly or indirectly available to bacteria and primary producers. Because of its large share in total dissolved nitrogen, even under inorganic nitrogen replete conditions, it used to be considered largely refractory, and was most often addressed concurrently with dissolved organic carbon (DOC). However, the scientific community has come to realize that these two components of the dissolved organic matter (DOM) pool function independently to a certain extent. DON is preferentially recycled relative to DOC in many systems, which is considered the way of natural systems bypass nitrogen limitation. Now, DON is often considered an intermediate in the recycling process of particulate organic nitrogen (PON) to dissolved inorganic nitrogen (DIN), available to primary producers and other osmotrophs.

Although quite some studies exist that illustrate the uptake potential of primary producers for small organics such as urea and free amino acids, our understanding of the fluxes in and out of the bulk DON pool is still very limited. It is for the majority of the better known ecosystems not even established if DON exhibits seasonality, and for those that have been investigated, why it does so in some systems and not in others. This thesis tries to fill in part of the gaps in our knowledge:

Chapter 1: In this chapter some basic definitions and notions are introduced concerning dissolved organic nitrogen and the approaches adopted.

Chapter 2 and 3: Time series analysis (TSA) presents a powerful tool to help us understand how ecosystems develop over time. It can help us to identify the characteristic scale at which ecosystem processes work, how particular parameters change over time, and how relationships between ecosystem parameters change over time. One of the more recent TSA techniques is wavelet-based analysis, which – as opposed to time-domain and frequency-domain analysis – retains both the temporal and scale aspect of a time series. Chapter 2 first gives a general introduction to discrete wavelet analysis with exemplary applications to monitoring data from one NO_3^- and DON time series. In chapter 3 these wavelet-based methods are applied to DON time series from the Dutch section of the North Sea (Rijkswaterstaat, 2009).

Chapter 4: Although organic nitrogen uptake is well established for terrestrial vascular plants, it has only very recently been illustrated for marine macrophytes in a natural environment. Uptake of DON compounds by bacteria, phytoplankton, and macroalgae has been reported throughout the last decades. In chapter 4 the potential uptake of several nitrogenous compounds by two temperate seagrasses and a macroalga are reported. Both root-mediated and leaf-mediated uptake of inorganic nitrogen, urea, and amino acids of varying molecular complexity are investigated. In addition, two artificial complex substrates, one derived from an axenic diatom culture and one from soil bacteria were tested for their utility as nitrogen source for marine macrophytes. The dual isotopic labeling (^{13}C and ^{15}N) allowed us to assess the fate of the carbon as well as the nitrogen.

Chapter 5: Seagrasses are usually assumed to take up only inorganic nitrogen, which is scarce in most seagrass meadows. A vast body of literature exists on strategies and adaptations of seagrasses to retain their valuable nitrogen. DON, however, often falls outside the scope of these studies or is considered a black-box from which regenerated nitrogen is drawn through heterotrophic breakdown. In chapter 5 the uptake of dissolved inorganic and organic nitrogen compounds by several macrophyte species, epiphytes, and phytoplankton are quantified in a temperate seagrass dominated ecosystem. Dual labeling (^{13}C and ^{15}N) again allows to follow the carbon and nitrogen from the dissolved organics separately. Biomarkers (PLFA: phospholid-derived fatty acids), and D-alanine (an amino acid specific for bacteria) allow for the assessment of bacterial contributions to the planktonic component of nitrogen uptake.

Chapter 6: Rooting marine macrophytes, such as seagrasses, take up most nitrogen via their root system. This gives them an advantage in nutrient acquisition relative to phytoplankton van free floating macroalgae. Dissolution of detritus, that enters the benthic environment, releases DON in the porewater, which is either used for biological activity or bound to the sediment. In some ecosystems nitrogen retention and remineralization are promoted by the seagrasses, most likely by stimulating bacterial hetetrotrophy via root ex-

udation of organic carbon. The complex composition of the benthic DON pool implies a spectrum of reactivities which could affect its retention in the sediment. In addition, a whole suite of benthic primary producers (seagrasses, macroalgae, microphytobenthos) and bacteria co-occur in sediments, with a wide variety of uptake capabilities. The question then arises how the sedimentary nitrogen is divided over different potential consumers. In chapter 6 the retention of inorganic and organic nitrogen compounds in different benthic biota (seagrasses, macroalgae, bacteria) is investigated over a period of 24 hours. Couplings between carbon and nitrogen uptake are studied by dual-labeling (^{13}C and ^{15}N). Biomarkers (D-alanine and phospholipid-derived fatty acids; PLFA) allow for a distinction between bacterial and microphytobenthic uptake and between different algal groups.

Chapter 7: An overview is given of the most important findings and their ecological and scientific implications. Potential future directions for DON research and long-term monitoring are discussed.

1. General introduction

1.1 Dissolved organic nitrogen?

Dissolved organic matter (DOM) is defined as a complex bulk pool of organic (biotically produced, carbon-containing) molecules that pass through a filter of nominal pore size 0.2 - 1 μm (Hedges, 2002). It is generally characterized in terms of carbon (DOC), nitrogen (DON) and/or phosphorus (DOP). Although DOM was for a long time considered largely unreactive, it has become increasingly apparent that the individual subpools (DOC/DON/DOP) function largely independently within many ecosystems. Here we will focus on the DON component, and relate it to the DOC component for which a larger body of literature exists.

DON is analytically determined as the difference of the total dissolved nitrogen (TDN) measured after conversion to some inorganic nitrogen form (destruction) and the dissolved inorganic nitrogen (DIN) concentration (Sharp, 2002). This approach has the disadvantage that measurement errors (ε) accumulate in the final calculation of DON (Bronk, 2002).

$$DON = (TDN \pm \varepsilon_{TDN}) - \left((NH_4^+ \pm \varepsilon_{NH_4^+}) + (NO_2^- \pm \varepsilon_{NO_2^-}) + (NO_3^- \pm \varepsilon_{NO_3^-})\right)$$

Different destruction methods exist of which none is really superior (Sharp et al., 2002). Coefficients of variation in an interlaboratory comparison ranged between 19 and 46% with lower concentrations (deep ocean) at the higher end of this range (Bronk, 2002), indicating that the uncertainty increases for lower concentrations.

1.1.1 Spatial variability

DON concentrations increase in different aquatic systems in the order deep ocean < surface ocean < coasts < estuaries < rivers (Tab. 1.1). DON concentrations increase drastically in the coastal systems, as reflected by the relatively large difference from the continental margin to the rivers (Tab. 1.1). This was for the North Sea demonstrated by Brockmann and Kattner (1997), although De Galan et al. (2004) could not find significant changes related to salinity for the Belgian continental shelf. However, they did report a steep increase in the DON/TDN ratio with increasing salinity, implying that DIN concentrations quickly decreased, whereas DON did not. Somewhere along this gradient of declining DIN levels, DIN will become scarce and the majority of the bioavailable nitrogen will have to be obtained from the DON pool (Suratman et al., 2008).

Rivers provide terrestrial organic matter to coastal systems, that is quickly transformed once it enters the estuary and coastal zone (Hedges et al., 1997; Seitzinger and Sanders, 1997). Important transformation processes occur at this land ocean interface, which is reflected in the large regional and local variability from the continental shelf to the rivers (Tab. 1.1). However, the nature of this local variability is poorly understood. In addition,

Table 1.1: Data from (Bronk, 2002)

	DON (μmol l^{-1})	DON/TDN (%)	C/N
deep ocean	4.3 ± 2.1	9.9 ± 2.6	14.7 ± 7.8
surface ocean	5.8 ± 2.0	61.6 ± 32.9	13.6 ± 2.8
continental shelf	9.9 ± 8.1	65.3 ± 30.4	17.7 ± 4.3
estuaries	22.5 ± 17.3	68.9 ± 22.4	21.1 ± 14.3
rivers	34.7 ± 20.7	60.1 ± 23.5	25.7 ± 12.5

the temporal variability is largely unknown. Some attempts to describe seasonality have been undertaken, but put together, they present no consistent picture of DON dynamics on the continental shelf as a whole or the coastal systems in particular (see e.g. Williams, 1995; De Galan et al., 2004; Suratman et al., 2008). The only long-term study with rigorous sampling at sufficiently high frequency over several years that we know of, demonstrated a consistent seasonal signal in the English Channel (Butler et al., 1979). This means that even simple descriptive studies can still provide valuable information on this poorly studied dissolved nitrogen pool.

1.1.2 Composition and reactivity

A part of the difficulty in research of DON (or DOM for that matter) is that it contains a wide variety of compounds. Only 4 - 14 % of total DON pool has been chemically characterized (Benner, 2002). The best studied constituents are urea, dissolved free amino acids, dissolved combined amino acids and humic substances. Bronk (2002) reported urea contributions to the total DON concentration of 5.2 ± 3.4 % (mean ± sd), based on data from different studies on different systems. Increasing contributions occurred with increasing terrestrial influence. Dissolved free amino acids (DFAA) contribute 5.9 ± 4.6 % to DON in marine systems. Particularly D enantiomers persist over longer times, and present potential markers for bacterial activity (Veuger et al., 2005, 2007). Dissolved combined amino acids (DCAA), dissolved amino acids after hydrolysis with a strong acid, comprised on average 7.2 ± 4.3 % of the DON. Of this pool 1 - 10 % is pure protein, that is rapidly assimilated, whereas 5 - 66 % is glucosylated protein and resists bacterial degradation to a certain extent (Keil and Kirchman, 1994). Up to 50 % of the DCAA is not proteinaceous in nature and resists break down over prolonged periods (Bronk, 2002). Humic (10-20 % of DOM) and fulvic substances (more than 50 % of DOM) form a class of relatively refractory organic compounds (mainly organic acids). A part of the nitrogen herein is bound as amino acids, nucleic acids, ammonium or amino sugars, and could be bioavailable (See et al., 2006). The remainder of the humic nitrogen is integral part of the compounds and is presumed biounavailable. Nucleic acids (DNA and RNA and parts thereof) are less studied in the context of DON dynamics but concentrations in the range of 4 - 960 μg l^{-1} have been reported for estuaries (Antia et al., 1991). It is clear that with this high variety of compounds comes a high variety of reactivities, which is not apparent when one value for turnover times, uptake, etc. for bulk DOM is used.

One tries to mitigate this problem by separating DON fractions based on physical and chemical characteristics. Filtration using a membrane with a 1000 Dalton cutoff results in a low-molecular-weight DON pool (LMW-DON) and a high-molecular-weight DON pool (HMW-DON) (Benner, 2002). The contributions of functional groups (esters, carboxyl-groups, amide-bounds, etc.) differs between the size-class (Benner, 2002), resulting in different reactivities. For instance, HMW-DON in open ocean has a turnover time of 0.5 to 1 year, whereas LMW-DON was found to be largely recalcitrant (Benner et al., 1997). Kerner and Spitzy (2001), however, observed an initial preferential degradation of LMW-DON relative to HMW-DON in the Elbe estuary, followed by a breakdown of HMW-DON until this latter had vanished, while some recalcitrant LMW-DON remained. This shows that bioavailability and reactivity are intrinsically connected with a time scale (duration). DON fractions are also separable by their optical properties. Optically distinct DON fractions exhibit a specific susceptibility for different types of degradation (Stedmon and Markager, 2005).

The composition and reactivity of the DON pool depend on the source (McCallister et al., 2006). DON of different rivers is chemically distinct (Retamal et al., 2007). This is reflected in the susceptibility for bacterial breakdown (Seitzinger et al., 2002). But even within a river system the DON reactivity varies during peak flow events and over the season (Stepanauskas et al., 2000; Wiegner et al., 2009). DON derived from specific biota has a specific reactivity. McCarthy et al. (1998, 2004) suggested that cyanobacteria rapidly remove new nitrogen from the bioavailable pool and store it in a refractory pool in the deep ocean. DON reactivity covaried in a study by McCallister et al. (2006) with the presence of microalgal material (estimated from poly-unsatured fatty acids).

Bulk DON concentration measurements present without doubt a first step towards understanding the dynamics of this pool, but do not allow to fully comprehend the mechanisms that govern this turnover. More in-depth analyses are possible using stable isotope analysis where the cycling of specific compounds or fractions can be traced through different stages of the ecosystem's nitrogen cycle.

1.1.3 Sources, sinks, and DON transformations in coastal systems

DON is most often the dominant reservoir of total dissolved nitrogen in ocean surface water (Bronk, 2002; Tab. 1.1). On a conceptual level it functions as an intermediate between dead particulate organic matter (detritus) and living particulate organic matter. Except for particle-associated bacteria and diazotrophs, nitrogen is only accessible in a dissolved, fixed form, and DON production thus presents a first and essential step in the re-cycling of nitrogen after immobilization in POM.

DON sources

There are several ways in which nitrogen enters the dissolved organic pool in marine systems. Firstly, DON production occurs through dissolution of phytodetritus (Carlson, 2002). Phytoplankton and seagrass detritus can contribute considerable amounts of bioavailable organic nitrogen for regenerated production in coastal systems (Mayer et al., 2009; Vonk

and Stapel, 2008). Dissolution is enhanced by solar irradiation. About 5 - 15 % of the phytoplankton-derived POM can undergo photodissolution before settling (Mayer et al., 2009). But also after settling significant amounts of DOM can become bioavailable again to the water column during resuspension events (Kieber et al., 2006).

Secondly, production of DOM from microbial biomass occurs through bacteria-induced and viral lysis of unicellular organisms (Carlson, 2002). Bacteria-induced lysis has received little attention so far, and estimates on the impact do not exist to the best of our knowledge. Virus-induced losses of DOM account for 3 % of the global primary production (Suttle, 2005). Bacterial and viral lysis can result in significant changes to the DON pool composition and reactivity (Gobler et al., 1997; Carlson, 2002; Frazier et al., 2007). The strength of the viral shunt (re-consumption of the DOM after lysis) determines the equilibrium between the bacterial growth efficiency and bacterial respiration, and hence DOM cycling pathways (Motegi et al., 2009). Obviously both bacteria and phytoplankton are prone to lysis.

Thirdly, living primary producers are a substantial source of DON to the marine environment (Bronk and Ward, 2000). Phytoplankton and cyanobacteria lose between 10 and 35 % of their gross DIN uptake as DON in the surface ocean (Bronk, 1999; Bronk and Ward, 2005). Differences in DON release rates are function of nutritional state (Bronk, 1999), day-night rhythm (Collos et al., 1992), location in the euphotic zone (Bode et al., 2004), substrate type (Bronk and Ward, 2005), and growth stage (Flynn and Berry, 1999), but relationships are often not consistent over different studies (Carlson, 2002). Whether the DON is actively excreted of passively lost, is usually not clear. Active DOC exudation is often invoked as explanation for carbon-rich DOM production in nitrogen-limited environments, because the photosystem keeps on functioning when nutrients for biomass production are not available (Carlson, 2002; Van den Meersche et al., 2004). But this does not explain DON exudation in nutrient-limited environments (Bronk, 2002). Collos et al. (1992) reported on DON release from diatom cells and subsequent uptake of the DON by dividing cells of the same species during the night, which could provide a competitive advantage over co-occurring primary producers that would not be able to take up these compounds. This does suggest an active excretion. Passive loss of DON from intact primary producers is probably due to osmotic gradients that are sustained by bacteria (Bjornsen, 1988). DOM exudation also occurs through root systems of seagrasses, thus fueling heterotrophic metabolism in the sediment (Benner et al., 1986; Findlay et al., 1986).

Finally, zooplankton presents another source of DON to the environment. They excrete 1 - 6 % of their body N per day under the form of ammonium, urea and amino acids (Carlson, 2002 and references herein). In addition, fecal pellets provide dissolved organic nitrogen over prolonged periods (Urban-Rich, 1999). Macrozooplankton misses out on 27% of its ingested organic matter as by sloppy feeding (Copping and Lorenzen, 1980). Microzooplankton loses less through sloppy feeding due to complete cell ingestion (Bronk, 2002). Obviously other fauna can excrete significant amounts of DON as well (30 % of total excreted nitrogen in *Mytilus edulis*; Tupas and Koike, 1990).

DON also enters marine systems through physical transport. Coastal systems are characterized by significant terrestrial DON inputs. Riverine DON is first used in the estuary or in the adjacent coastal zone, depending on the water residence time of the estuary (Seitzinger

and Sanders, 1997). Upon entering into marine waters the bioavailability of DON to bacteria sometimes increases (Stepanauskas et al., 1999). The reactivity of riverine DON is so high that the terrestrial signature almost vanishes before it has crossed the continental shelf (Hedges et al., 1997).

Another source of terrestrial DON is groundwater discharge. Santos et al. (2008) calculated that the amount of nitrogen that enters the Florida Gulf coast through submarine groundwater discharge could be similar to the discharge of its major rivers. They estimated the ammonium and DON loads from a small subterranean estuary at 58 and 28 % respectively, where the ammonium would be regenerated from DON. (Lorite-Herrera et al., 2009) found high variability in groundwater DON concentrations in a catchment of the Guadalquivir (Spain).

Atmospheric deposition under the form of rain (wet deposition), dust (dry deposition) and bacteria presents another source of nitrogen. Organic nitrogen would constitute 30% of the total atmospheric nitrogen deposition on average (Neff et al., 2002; Duce et al., 2008). This atmospheric organic nitrogen was for 45 - 75 % utilized by an estuarine microbial community in an experiment by Seitzinger and Sanders (1999).

In shallow systems DON can be released from the sediment to the overlying water after burial of POM. However, DON fluxes vary both in direction (in or out of the sediment) and magnitude, and are generally low compared to DIN fluxes (Burdige, 2002). The low C/N ratio of these fluxes suggests that part of it might be bioavailable (Burdige and Zheng, 1998). DON effluxes from the sediment are significantly altered at the sediment-water interface when macro- and microalgal mats are present (Eyre and Ferguson, 2002; Tyler et al., 2001).

DON sinks

Microbes are the dominant DON users in marine systems (Azam and Hodson, 1977; Carlson, 2002). Small organic (LMW-DON) and inorganic compounds are taken up through permeases, whereas larger compounds (HMW-DON) have to be broken down before uptake by extracellular hydrolytic enzymes (Antia et al., 1991; Bronk, 2002; Carlson, 2002, and references therein). Ammonium regeneration can be high, particularly during periods of inorganic nitrogen depletion, and at times it is vital for N demand in coastal systems (Bode and Dortch, 1996). Kerner and Spitzy (2001) measured DON remineralization rates of up to 79 μg N l^{-1} h^{-1} in the Elbe estuary. Badr et al. (2008) found similar rates for two English estuaries.

A large number of phytoplankton species use DON compounds (particularly amino acids and urea) to fulfill their nitrogen requirements (Bronk et al., 2007). Diatoms are often facultatively heterotrophic. Price and Harrison (1988) observed autonomous utilization (without bacterial intervention) of urea nitrogen by *Thalassiosira pseudonana*. They observed a quick ammonium uptake after it was released from the cells following intracellular urea breakdown. The urease enzyme to split urea into NH_4^+ and CO_2 is common in many primary producers and bacteria (see e.g. Glibert et al., 2006). An experiment by Collos et al. (1992) demonstrated the release of DON compounds by diatom cells in the light and an uptake thereof by dividing cells in the subsequent dark period. Still, diatoms are often associated with the

uptake of oxidized forms of nitrogen (Berg et al., 2003). Harmful algae are often associated with DON uptake (Anderson et al., 2002). Mulholland et al. (2004) observed nitrogen uptake from both urea and free amino acids by *Aureococcus anophagefferens*. Amino acid oxidation with production of ammonium appears frequent among phytoplankton species (Palenik and Morel, 1991). In addition, many phytoplankton species are able to hydrolyze peptides by themselves (Mulholland et al., 2002; Stoecker and Gustafson, 2003).

Beside phytoplankton, macroalgae and seagrasses can also take up DON (Tyler et al., 2001, 2005; Brun et al., 2003; Vonk et al., 2008). Although in some of those studies direct uptake by these end-users has not been demonstrated, they clearly illustrate a quick supply of organic matter derived nutrients to primary producers. Bacterial degradation of DON with subsequent uptake of inorganic nitrogen by phytoplankton is likely the largest flux of nitrogen out of the DON pool and into the plant compartment. Some marine fauna also use DON to supplement their nitrogen demand (Otake et al., 1993; Baines et al., 2005), but their contributions to DON uptake are more than likely small.

Different species have different preferences and capabilities to utilize DON. For example, *Ulva lactuca* takes up amino acid nitrogen after decarboxylation (Tyler et al., 2005). But the glycine residual after decarboxylation was taken up completely, whereas for alanine ammonium was taken up after deamination of the decarboxylated residual. *Gracilaria vermiculophylla*, however, appears to take up only the nitrogen from the amino acid molecules (Tyler et al., 2005). For a particular species uptake characteristics even differ with circumstances; Mulholland et al. (2004) reported differences in the choice of substrate (amino acids or urea) by *Aureococcus anophagefferens* between two similar coastal bays. Differences in the capacity to take up particular substrates imply differences in competitiveness, which can be responsible for species succession throughout a growth season (Berg et al., 2003), but also a permanent replacement of a particular species by a more competitive one under changing nutrient conditions (i.e. community shifts). In this sense, DON contributes to the complex interplay between nutrient ratios and community composition, which stresses the importance to understand DON dynamics.

Beside these metabolic fluxes, abiotic removal processes contribute to DON decreases. Adsorption onto sinking particles consumes DON either temporarily in stratified waters or permanently when particles are buried (Cauwet, 2002). Horizontal transport of water masses from the continental shelf to the open ocean presents a potentially large sink for the coastal and continental shelf DON (Bates and Hansell, 1999; Alvarez-Salgado et al., 2001).

1.1.4 DON versus DOC

Much of the research on dissolved organic matter has focussed on the DOC compartment due to methodological issues and because it was assumed that DON, like DOC, is largely unreactive and unimportant as nutrient for phytoplankton (Bronk et al., 2007). Indeed, since both carbon and nitrogen are part of a DOM pool, their cycling is partially intertwined. However, the N and C are unequally distributed within the bulk DOM pool. The C/N ratio of DOM differs with size-class; Biddanda and Benner (1997) observed a HMW-DOM

C/N ratio of 21, whereas the LMW-DOM showed a C/N ratio of 6. In addition, DON dynamics is different from DOC dynamics. Preferential recycling of DON relative to DOC has been observed in nutrient-poor systems such as seagrass systems (Ziegler et al., 2004) and the open ocean (Thomas et al., 1999; Osterroht and Thomas, 2000), but appears to be absent or diminished when DIN input is sufficient to support primary production (Aminot and Kerouel, 2004). By preferentially recycling DON, nitrogen limitation is avoided or alleviated (Thomas et al., 1999).

Bode et al. (2004) reported seasonal differences in nitrogen recycling mechanism. They also observed a spatial separation between DOC and DON release with a preferential DON release at the bottom of the euphotic zone. Artificial bloom experiments and in situ observations often reveal a production of carbon-rich DOM (Williams, 1995; Sondergaard et al., 2000; Engel et al., 2002). Engel et al. (2002) and Van den Meersche et al. (2004) reported a decoupling of DOC and DON production from the moment nitrogen was depleted. However, carbon partitioning into DOC occurred during and after a bloom in an experiment by Sondergaard et al. (2000), independent of the nutritional state or growth phase of the phytoplankton.

Focusing on individual organic compounds, the fate of the carbon and nitrogen can be coupled or uncoupled. *Aureococcus anophagefferens* used amino acid carbon but not urea carbon in two U.S. coastal bays. A similar decoupling between urea carbon and nitrogen uptake was observed by Veuger and Middelburg (2007) in an intertidal benthic community, where diatoms were the dominant N consumers. These authors also noted a partial decoupling between carbon and nitrogen uptake from amino acids, suggesting that deamination was involved but that it was not the only pathway of nitrogen utilization from amino acids. *Thalassiosira pseudonana* carbon and nitrogen acquisition from urea were uncoupled under nitrogen sufficient conditions, but they were coupled in nitrogen-starved axenic cultures (Price and Harrison, 1988). Utilization of carbon and nitrogen from small organic nitrogenous compounds can vary throughout the growth season (Andersson et al., 2006).

Tracing both DON and DOC (in the same and in different molecules) allows us to distinguish autotrophy, heterotrophy, and mixotrophy. Dual-labeled substances provide the means to investigate carbon-nitrogen couplings on the level of individual compounds.

1.2 Tools used in this research

Ecosystems are highly dynamic. Different processes operate at the same time, creating a net effect in an observable ecosystem variable. The notion of a process implies a certain time dependence that has to be described to understand its variation structure. Statistical analyses, however, often assume independence of observations, which is, depending on the scale of the experiment or measurements, either a valid or an incorrect assumption (Shumway and Stoffer, 2006). Time-series analysis encompasses a whole variety of statistical and filter techniques to deal with temporal dependence in data. In addition, influential factors often work with unequal and varying strength, and not all factors persist over the same time span. We are thus compelled to use statistical methods that take into account the limited duration

of these influencing processes. Wavelet transformations describe a data series in terms of sequence and sequence range. For a time series of data, for example, this is translated into time and time scale, for a depth profile this is translated into depth and depth range.

From a conceptual point of view, ecosystems comprise a number of reservoirs that interact with one another through fluxes of energy and matter, and influences on these fluxes. In this complex network of pathways (sequences of one or more fluxes) transfer of matter from one reservoir to another often occurs along different pathways. Isotope-based analysis present a way to quantify the transfer, and in some cases to distinguish among pathways. In addition, particular reservoirs are characterized by specific types of molecules, that can function as biomarkers (see below).

In the following subsections a basic overview will be given of time series analysis techniques with special emphasis on their application in ecological research. Special attention is given to the field of wavelet analysis, since it provides a natural way of dealing with scale aspects and the limited range of processes in ecology. Next, we will briefly elaborate on the application of stable isotopes and biomarkers in ecological research.

1.2.1 Time series analysis

In general, time series are regarded as either a series of points that reflect a certain progress over time, or a signal consisting of a number of subsignals with varying frequencies. The former view involves a description in a time-domain, the latter a description in a frequency-domain. In this section a short overview will be given of the fields of time-domain and frequency-domain approaches to analyze time series. It is intended as background information for readers that have never worked with time series analysis techniques, since some basic knowledge on this topic is required for chapter 2.

The time domain

Some estimators in the time domain A discrete time series is often looked upon as sequence of stochastic variables which are ordered according to time (Shumway and Stoffer, 2006). Each random variable has a distribution, and the values that make up the time series were drawn from these distributions. Such a series of random variables is also called a stochastic process. The actual series of values is then called a realization of this stochastic process (Shumway and Stoffer, 2006).

Two important measures are often used to describe or identify a process: the mean function (or the first moment in statistical terms) that describes its average behavior over time, and the autocovariance function (also termed the second moment) that describes the interdependence of observations. The mean function of a process X_t is

$$\mu_{xt} = E(X_t) = \int_{-\infty}^{\infty} x f_t(x) dx, \tag{1.1}$$

with E the expectation operator (Shumway and Stoffer, 2006), and $f_t(x)$ the density function

of the variable x. The autocovariance function of a process is given by

$$\gamma_x(s,t) = E\left[(x_s - \mu_s)(x_t - \mu_t)\right]), \tag{1.2}$$

Analogous to the covariance in classical inference, it measures linear relationships (Shumway and Stoffer, 2006). The subscripts s and t denote different time points. If s = t, one obtains the variance. Similar to classical inference, where the correlation is defined as the covariance normalized to the variances of the relevant stochastic variables, we define a correlation function as

$$\rho_x(s,t) = \gamma_x(s,t)/\sqrt{\gamma_x(t,t)\gamma_x(s,s)}. \tag{1.3}$$

In principle, these measures can be made at any time point. However, most often only one observation exists per time point. In this case, the mean and covariance (correlation) needs to be calculated based on the entire series. In order to make sense, these measures should thus not change over time, which is termed 'stationarity'. Put more accurately:

A discrete time series X_t (with discrete time steps) is strictly stationary if the joint distribution of X_{t1}, ..., X_{ti} is the same as the joint distribution of $X_{t1} + \tau$, ..., $X_{ti} + \tau$ for all time points t_i and time lags τ.

In strict stationarity all moments of the distribution are subject to the constancy. By restricting this constancy to the first two moments (mean and autocovariance), strict stationarity is reduced to a more practical form, called weak stationarity. Just as with stochastic variables in regression models, time series are often assumed to be normally distributed (time series are either considered series of stochastic variables or realizations of a stochastic process). If such normal processes are weakly stationary, they are also strictly stationary, since a multivariate normal distribution is completely defined by its first (mean) and second (covariance) moments.

Stationarity implies that equations 1.1, 1.2, and 1.3 are independent of time. The autocovariance and autocorrelation are then only dependent on the distance between the time points s and t (time lag; τ = t - s).

In analogy with the univariate measures autocorrelation and autocovariance, bivariate counterparts exist to detect the linear relationship between two time series as a function of time lags The cross-covariance function between two series is defined as:

$$\gamma_{x,y}(s,t) = E\left[(x_s - \mu_{xs})(y_t - \mu_{yt})\right], \tag{1.4}$$

with E the expectation operator. The cross-correlation function between a series X_t and Y_t is given by:

$$\rho_{x,y}(s,t) = \frac{\gamma_{x,y}(s,t)}{\sqrt{\gamma_x(s,s)\gamma_y(t,t)}}. \tag{1.5}$$

Time domain models Time domain models are mainly based on the principle of regression and averaging over time. Multiple regression of a time series onto lagged version of

this time series is called autoregression. A process that is modeled this way is called an autoregressive process (AR). Provided that the coefficients are smaller than 1 in absolute value, such a process is stationary (Chatfield, 2004). A second type of model is constructed by averaging a random series over a range of successive time points using a set of weights. This is called a moving average model (MA). Provided that these weights are in absolute value smaller than 1, we can find an autoregressive model that describes the same process (Chatfield, 2004).

These two classes of models are special cases of a more general autoregressive-moving average model (ARMA). An ARMA-model of orders p and q, denoted ARMA(p,q), is given by

$$X_t = \alpha_1 X_{t-1} + ... + \alpha_p X_{t-p} + \beta_1 Z_{t-1} + ... + \beta_q Z_{t-q}, \tag{1.6}$$

where α_1 to α_p are the autoregression coefficients, β_1 to β_q are the moving average coefficients, and Z_i are random normal variables with mean = 0 and variance is σ_Z^2. Provided that the aforementioned assumptions are satisfied, the same process can be modeled in terms of an AR-model a MA-model or an ARMA-model, where the ARMA-model usually has less coefficients and hence is the simpler model (Chatfield, 2004). The parameters in these models are independent of time and thus require stationarity of the modeled time series.

The frequency domain

Frequency domain techniques are based on a Fourier decomposition of a series in terms of sine and cosine functions. The contribution of different frequencies is given by the spectral density function (f(ω)) with ω the frequency. This is defined as

$$f(\omega) = \sum_{-\infty}^{\infty} \gamma(h) e^{-2\pi i \omega h}, \tag{1.7}$$

with -1/2 < ω < 1/2 and γ(h) the autocovariance function at lag h, provided that the latter is summable (Shumway and Stoffer, 2006). This spectral density function is estimated by the periodogram, which for a series, x_1, ..., x_n, is given by

$$I(\omega_j) = |n^{-1/2} \sum_{t=1}^{n} x_t e^{-2\pi i \omega_j t}|^2, \tag{1.8}$$

for j = 1, ..., n-1, where ω_j = j/n is called the fundamental frequency. This function allows to identify frequencies that explain large parts of the variation in a given series x_t. Intuitively, it is clear that here again stationarity is assumed since the dominance of these frequencies is assumed to occur over the entire time range of the function (sine and cosine functions are defined on the entire real axis).

The time-frequency domain, wavelets

As indicated before, both the time domain and frequency domain analysis assume a certain constancy in the characteristics of the series under investigation. Particularly, for biological

processes this is rarely the case. Wavelet analysis deals with non-stationarity in an elegant way, because it divides a time series in smaller intervals (scales) and describes the evolution of these intervals over time. In the context of time series analysis, a wavelet is a âĂŹsmall waveâĂŹ that is damped down to zero within a limited time range. In this sense it is localized in time, as opposed to the infinitely extending sine and cosine waves in Fourier-based analyses. In a wavelet transformation, wavelets of different âĂŸsizesâĂŹ or scales are fitted to the time series and the similarity of the series to this wavelet at a certain point in time is expressed by a so called wavelet coefficient (Percival and Walden, 2000). Wavelet analysis is therefore well-suited to deal with sharp spikes, jumps and 'changing behavior' in time series, because it describes the series based on local information, not global information as in ARMA-models and Fourier analysis. In chapter 2, some wavelet theory will be presented with examples to illustrate the working principles.

1.3 Isotope analysis of biomarkers

A biomarker is a compound that is produced specifically by one group of organisms and as such identifies this group. They can serve as a proxy for the presence and abundance of that particular group, because concentrations or variation therein are closely related to the abundance of members of that group. Pigments are one class of such biomarkers that allow to quantify biomass of particular groups of bacteria or phytoplankton within the microbial community (Mackey et al., 1996). Phospholipid-derived fatty acids (PLFA) comprise another class of biomarkers that can be used to identify algal and bacterial taxa (Viso and Marty, 1993; Mejanelle et al., 2005), and quantify their biomass (Dijkman and Kromkamp, 2006b). Although concentration variations due to environmental conditions and nutritional state occur (Viso and Marty, 1993; Renaud et al., 2002), there are compounds that have a stable abundance in particular groups or organisms, rendering them robust markers for these groups. Dijkman and Kromkamp (2006a) were able to develop signatures for a number of phytoplankton taxa occurring in the Schelde estuary. Moreover, using so-called mixing models (e.g. BCE; den Meersche et al., 2008), it becomes possible to derive the taxon composition, based on the biomarker composition ('signature') of an entire sample. However, these signatures cannot be used to derive rates and fluxes.

Stable isotope tracers have been used since years to quantify nutrient uptake and elucidate foodweb interactions (see for instance Dugdale and Wilkerson, 1986; Fry, 2006). By tagging a resource, and following the fate of the tag into the sink compartments, important information like the speed of the process (rate) is obtained. In recent years, approaches combining biomarkers and deliberate isotope tracers additions have emerged that allow to make a connection between taxonomic identity, biomass and (ecosystem-)metabolism (Boschker and Middelburg, 2002; Dijkman et al., 2009). Boschker et al. (2005) used isotope labeling with PLFA measurements successfully to detect differences in carbon subsidies to microalgae and bacteria in the Scheldt estuary. Whereas PLFA measurements alone only give information on abundance and biomass, the combination of PLFA measurements with

stable isotope chemistry does allow for a quantification of fluxes and rates (Boschker and Middelburg, 2002).

Another type of marker that helps to distinguish between bacterial and algal activity is D-alanine (Veuger et al., 2005, 2007). By combining ^{13}C and ^{15}N tracers with hydrolysable amino acids, it is not only possible to distinguish between bacterial and algal activity, but also to trace carbon and nitrogen cycling at the same time.

2. Wavelet approaches to analyze biogeochemical time series

Van Engeland T., T. J. S. Cox, K. Soetaert, R. W. P. M. Laane, F. J. R. Meysman & J. J. Middelburg. Submitted to Estuarine Coastal and Shelf Science

Abstract - *Long-term monitoring programs and remote sensing techniques have sparked an increasing need for statistical analysis techniques that model dependence in data. In this paper the potential of wavelet techniques for analyzing nutrient monitoring data in relation to time and scale (temporal range) are reviewed and investigated. Time series of three environmental variables of differential complexity are used to illustrate the application, advantages and disadvantages of wavelet methods. The wavelet based analysis methods provided extra information on top of that given by standard time series techniques, such as Fourier analysis. Due to the preservation of both the time and frequency or scale-related information, we were able to identify a methodological shift in the dissolved organic nitrogen measurements via its maximal overlap discrete wavelet transform. In addition, global correlation analyses were extended into the scale- and time-domain, allowing for a more precise explanation of the relationships between environmental parameters. Around 10 years of monthly samplings are considered a minimum to investigate within-year patterns of variation and their consistency over the longer term, a common issue with Fourier approaches. We conclude that, despite some limitations concerning series length and frequency resolution, wavelet techniques present a valuable addition to the toolbox of classical time series analyses.*

2.1 Introduction

Due to the inherent complexity of interactions, investigating the dynamics of ecosystem variables (e.g. concentrations, abundances) at relevant scales typically requires an enormous amount of temporal data. Continued monitoring efforts over the past decades have provided such long-term time series. This has brought along an increasing need for statistical methods that can handle time series data in a proper and flexible manner. Ecologists traditionally apply either time-domain (e.g. ARIMA) or frequency-domain methods (e.g. Fourier analysis) to time series. In ARIMA-type methods the observations at one point in time are described as a stochastic function of previous values. Fourier-type methods consider the time series to consist of periodic variations that can be captured by sines and cosines (Shumway and Stoffer, 2006). However, these statistical tools consider time series as a whole, and as a result they ignore that processes may only be acting in part of the time series. The assumption that the characteristics of the data series are invariant in time is called stationarity (see for instance Chatfield, 2004 for a mathematical treatment). Whereas time- or frequency-domain analyses can deal with non-stationary time series by splitting up the data, e.g. via moving data windows of a chosen width, these procedures for partitioning are rather arbitrary and often lack adaptivity (Vidakovic, 1999).

Wavelet analysis of time series deals with non-stationarity in an elegant way. A wavelet is a 'small wave' that is damped down to zero within a limited range of its time-domain, making it localized in time. The characteristic time period over which the wavelet persists or 'differs from zero 'is termed the scale of the wavelet (see examples in Fig. 2.1). During a wavelet transformation, wavelets of different scales are compared to the time series by shifting the wavelets through time. The similarity of the series to this wavelet at successive time points is expressed by wavelet coefficients. The ability to deal simultaneously with time and scale dependence suitably circumvents the stationarity assumption (Percival and Walden, 2000). Wavelet analysis is also well suited when signals exhibit sharp spikes or local discontinuities, features that are very poorly represented by Fourier analysis.

Wavelet-based methods have been used in areas where long time series have been available since decades, such as oceanography (Meyers et al., 1993; Mak, 1995; Percival and Mofjeld, 1997; Percival et al., 2008), geophysics and meteorology (Jevrejeva et al., 2003; Grinsted et al., 2004; Prokoph and Patterson, 2004; Alves Bolzan and Vieira, 2006; Schaefli et al., 2007), economics (Ramsey, 2002; Manimaran et al., 2008) and coastal engineering (Li et al., 2005). Biological wavelet applications include image processing in neuroscientific applications (Kolaczyk, 1996; Fadili and Bullmore, 2002), and also molecular biology (Lió, 2003). In recent years ecological applications of wavelet-based statistics have emerged because time series became long enough, and because holistic samplings were conducted, such as with remote sensors (Nezlin and Li, 2003). Applications in vegetation ecology encompass the assessment of canopy structure along transects in forests (Bradshaw and Spies, 1992; Mi et al., 2005) and changes in vegetation cover over time (Percival et al., 2004). Wavelets have been used to study fish stock fluctuations (Yndestad, 2004), and to find scale-specific community dynamics in relation to disturbance in wetland ecology (Keitt and Urban, 2005; Keitt and Fischer, 2006; Keitt, 2008). Braswell and coworkers (2005) also used a wavelet

decomposition to assess the scalewise performance of an ecological model. For an elaborate treatment of ecological applications we refer the reader to Cazelles and co-workers (2008), who mainly focus on the continuous wavelet transform.

There are some issues when using wavelet transformations. For instance, there exist many wavelet 'families', and there are no general and objective guidelines to determine which particular wavelet is the most appropriate for a certain application (Bruce and Gao, 1996). There are also other choices to be made, i.e. how to deal with boundaries (at the beginning and end of the time series), and whether to choose continuous or discrete wavelets or some intermediate form. This contrasts to Fourier analysis, because there is only one sine function underlying the Fourier transform. In addition, whereas the main output of spectral analysis can be easily understood, the results of wavelet analyses may not be so easily interpreted in terms of frequencies or cycles per unit time (Percival and Walden, 2000). Nevertheless, wavelet techniques present powerful approaches to explore large amounts of serially dependent data.

The Dutch national coastal monitoring program started in 1971. Between 1995 and 2004 17 stations were consistently sampled in the Dutch section of the North Sea. At monthly intervals, up to 18 different nutrient related variables were measured (Rijkswaterstaat, 2009). Because of the large amount of data, proper methods are needed to extract the interesting features of these time series. In this paper, we focus on the nitrogen data, and we test the usefulness of wavelets to analyze these data series.

This paper is first of all intended as a overview of the relatively simple discrete wavelet-based methods that are widely applicable in studies of biogeochemical/ecological time series. It is structured as follows: We start by presenting a general introduction to wavelet techniques, highlighting the relevant differences with the time- and frequency-domain methods, and describe the data sets that are used to exemplify the theory. We will illustrate the basic concepts of wavelet analysis with the discrete wavelet transform. For the continuous case we refer to the literature (Torrence and Compo, 1998; Liu et al., 2007; Maraun et al., 2007). Subsequently, the results obtained from time-domain, frequency-domain, and wavelet-based analyses are compared. We focus on the methods, only briefly dealing with ecological interpretations, as an elaborate ecological study of the nitrogen dynamics is given elsewhere (Van Engeland et al., submitted). We sacrifice some methodological accuracy for the benefit of comprehensibility and accessibility to the non-specialist. The interested reader may consult the works by Mallat (1999), Daubechies (1992), Bruce and Gao (1996), and Percival and Walden (2000) for a detailed treatment of the mathematics behind wavelet analysis. In addition, this paper is intended as a quick guide to more dedicated and advanced literature, which will be needed to accurately apply these methods with proper consideration of their strengths and limitations.

2.2 Materials & methods

2.2.1 The discrete wavelet transformation

In a discrete wavelet transformation, a given time series f(t) is written as a weighted sum of base functions $\Psi_i(t)$, the wavelets:

$$f(t) = \sum_i a_i \Psi_i(t) \tag{2.1}$$

This is similar to a Fourier analysis, where the base functions are sine and cosine functions. However, in contrast to the trigonometric functions, which persist infinitely, a wavelet is damped down to zero within a limited time range (the so-called scale of the wavelet). The base functions in equation 2.1 are constructed from a template wavelet by shifting (translating) it in time and stretching (dilating) it to a different scale. In a discrete wavelet transform, the wavelet is shifted within each scale over a distance proportional to its width, while it is doubled in temporal range in consecutive scales (equation 2.2). For finite time series there is a natural upper limit on the dilation given by the length of the time series. The maximum dilation or scaling depth J (= $\log_2$(N)) for a series is determined by the length of the series (N observations). To highlight these points, it is more common to write the sum (1) as

$$\begin{aligned} f(t) &= \sum_k s_{J,k}\Phi_{J,k}(t) + \sum_j \sum_k d_{j,k}\Psi_{j,k}(t) \\ &= \sum_k s_{J,k}\Phi_{J,k}(t) + \sum_j \sum_k d_{j,k}\Psi(\frac{t-2^j k}{2^j}) \end{aligned} \tag{2.2}$$

with the separate indices j and k denoting the dilation and translation of the original template wavelet $\Psi(t)$, also called mother wavelet. The father wavelet $\Phi(t)$ is an extra template wavelet that is needed in the transformation algorithm to split off the coarse scale information (Bruce and Gao, 1996) and is complementary to the mother wavelet (Daubechies, 1992). The coefficients $d_{j,k}$ of this sum are called the k^{th} wavelet coefficient at scale j. The $s_{J,k}$ are the scaling coefficients, and together they specify the discrete wavelet transform (DWT) of the time series. All the wavelet coefficients $d_{j,k}$ for a given j (scaling coefficients $s_{J,k}$) constitute the wavelet vectors $\mathbf{d}_j$ (scaling vector $\mathbf{s}_J$). Due to the doubling of the width of the template wavelet (equation 2.2), the vector $\mathbf{d}_j$ will be half the length of its predecessor $\mathbf{d}_{j-1}$, and $\mathbf{s}_J$ will contain at least one coefficient (this is called âĂŸdown-samplingâĂŹ).

Because of this down-sampling the DWT it is statistically less stable in certain respects (Nason and Silverman, 1995; Percival, 1995; Percival and Walden, 2000). The Maximal Overlap Discrete Wavelet Transformation (MODWT) is a variation on the DWT-theme with a âĂŸcontinuousâĂŹ time (as continuous as possible for a discretely sampled series), and a discrete scale dimension. Thus, within each discrete scale j the wavelet is shifted one time step instead of 2^j time steps (2^jk in equation 2.2, i.e. there is no down-sampling). In contrast to the DWT, where the time series is down-sampled by removing every other value,

the wavelet itself is doubled in length in consecutive scales in the MODWT. Hence, each coefficient vector $\mathbf{d}_j$ (and $\mathbf{s}_J$) is as long as the original signal. The MODWT is statistically more stable than the DWT but still has a discrete scale dimension (Percival and Walden, 2000).

Figure 2.1 shows a maximal overlap discrete wavelet transform (MODWT) of a Doppler signal, a function often used to illustrate a wavelet decomposition (see for instance Bruce and Gao, 1996). It is characterized by a continuously decreasing frequency. The decomposition depth was fixed at 7. The right side of figure 2.1 shows the translation and dilation of the mother wavelet. The wavelet vectors $\mathbf{d}_1$ to $\mathbf{d}_7$ at the various scale levels are different from zero only within limited time intervals, reflecting that the original signal only resembles the corresponding scale-specific wavelet during a limited time interval (wavelet coefficients are roughly interpretable as measures of correlation between the signal and the scale-specific wavelet; Percival and Walden, 2000). As such, the wavelet transform separates the variability in the original signal at progressively coarser scales. At the final step, the remainder of the variation in coarser scales is given by the scaling vector $\mathbf{s}_7$.

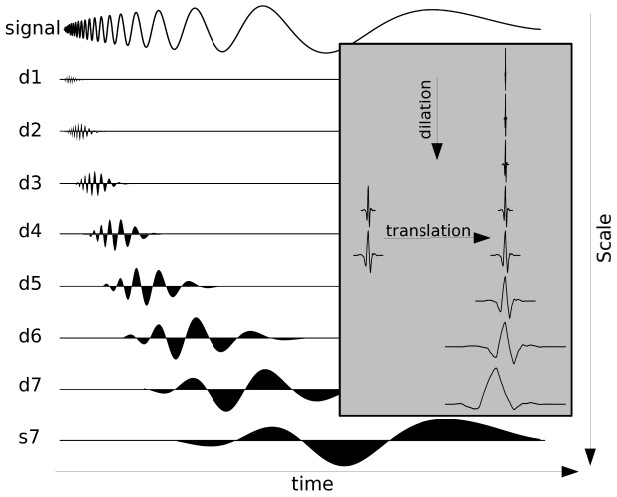

Figure 2.1: Maximal Overlap Discrete Wavelet Transformation (MODWT) of a Doppler signal. The decomposition depth was fixed at 7. The constructed scale-specific wavelet filters, based on the least asymmetric wavelet of width 8 (Daubechies, 1992) are shown on the right hand side. Note the difference between the wavelet at d_7, constructed from the mother template wavelet, and the wavelet at s_7, constructed from the father template wavelet.

The notion of 'scale' is perhaps the most important concept in wavelet analysis, as it distinguishes wavelet analysis from both Fourier and traditional time domain analysis. The scale is most closely related to the period of a periodic function, the time window that captures the variation in the signal. Because wavelets have a limited temporal range, they

have a range of neighboring frequencies in the frequency domain. This range is referred to as scale band, and is defined by the bandpass properties of the wavelet (Percival and Walden, 2000). Figure 2.2 expresses the power (squared gain, i.e. a measure for the amount of variance with a particular frequency) of the wavelet filters used in figure 2.1. At scale 1 the wavelet filter captures variation with frequencies in the band $[\frac{1}{4},\frac{1}{2}]$ (periodicities covering 2 to 4 observations), represented by the wavelet vector $\mathbf{d}_1$ (Fig. 2.1). At scale 2 the wavelet filter captures variation at frequencies between $\frac{1}{8}$ and $\frac{1}{4}$, which results in the $\mathbf{d}_2$ vector and so on. The filters have a particular optimum frequency (maximum values in figure 2.2). At the deepest level of the transform the scaling filter puts all variation at the remaining larger scales (frequency band $[0,\frac{1}{2^{J+1}}]$) into the scaling vector $\mathbf{s}_J$. The scale windows in figure 2.2 are determined by the construction of the wavelet transform, the curvature of the wavelet gain functions is a property of the chosen wavelet.

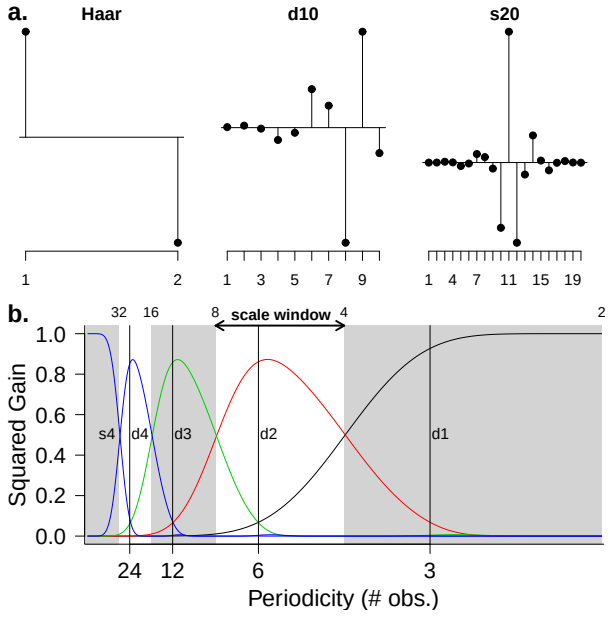

Figure 2.2: Three examples of discrete wavelets of different widths (a.). Squared gain functions of the normalized wavelet filters at scales 1 to 4 and the scaling filter at scale 4 (b.). Scales are expressed in number of observations. The nominal pass-bands (scale window) are indicated by the gray and white regions. The actual pass-bands are, indicated by the curves themselves. For an ideal band-pass filter the actual pass-band would be square and follow the edges of the nominal pass-band.

There exist many different families and shapes of wavelets. The choice for one or another wavelet will lead to slightly different properties of the wavelet analysis. Wavelets are often

selected to more or less match the shape of the signal under investigation. A stepwise signal is treated differently by wavelets with different smoothness (Bradshaw and Spies, 1992). Progressively wider wavelets (in time; Fig. 2.2a) have poorer temporal resolution. This is analogous to the influence of a moving average on an extreme value (spike) in a series. The spike is spread out depending on the width of the moving average. But wider wavelets, such as d10 and s20 (Fig. 2.2a) have better frequency resolution (steeper slopes in figure 2.2b), allowing for a clearer distinction between the scale bands. If a wavelet is not wide enough, variation at frequencies close to the edge of the band (e.g. a periodicity of 4 observations in figure 2.2) could show up in neighboring bands, a phenomenon called 'leakage'. Wavelet transformations using asymmetric wavelets (e.g. d10) introduce a temporal shift in the wavelet coefficients relative to the time series they were derived from. Symlets, such as s20 (symlet with 20 filter coefficients; Fig. 2.2a) minimize this shift (Daubechies, 1992).

The wavelet filter has a certain width and extends beyond the first/last observation, such that values outside these boundaries are needed to calculate the boundary wavelet coefficients. External values may be generated by repeating the signal (circular filtering, Percival and Walden, 2000), but this creates problems when the beginning and end of the signal do not 'match', for instance with decreasing values over time. Alternatively, the original signal may be extended with a mirrored version ('reflection boundary treatment'). Finally, the series can be padded with zeroes at the end (Cazelles et al., 2008). Clearly all these treatments produce artifacts at the boundaries, which persist a certain distance into the inner part of the series. Coefficients that are severely affected by boundary effects should be removed from analysis (cf. section 2.2.4).

2.2.2 Application of the wavelet transform

The wavelet transform coefficients are essentially measures of the changes in a signal at a number of scales, i.e. a scalewise and temporal distribution of the variation in a signal. They do not have a straightforward interpretation. In certain instances (depending on the wavelet) wavelet coefficients are interpretable as differences between values in the time series, while the scaling coefficients are weighted averages (Percival and Walden, 2000). The multiresolution analysis, discussed below, will provide a more intuitive interpretation (cf. section 2.2.2). However, a number of analysis techniques have been derived from the wavelet transforms, some of them are introduced here because of their usefulness and relatively straightforward applicability in ecology.

Analysis of variance (ANOVA)

A wavelet transformation decomposes the total variance of a signal according to scale, such that the sum of the variances in the individual transform vectors equals the total variance in the signal (Percival, 1995). By means of wavelet ANOVA, it is thus possible to examine the fractions of variance in the signal attributable to each scale (i.e. variance partitioning). This per-scale variance can be studied globally (one value per transform vector) or locally (changing over time within a wavelet vector) (Serroukh et al., 2000). The wavelet coefficients

are thus more easily interpreted as measures of variance than in terms of the actual signal. A similar ANOVA approach exists in the context of the discrete Fourier transform, where the variance is a function of individual frequencies rather than scales (Shumway and Stoffer, 2006). Note the difference with a standard analysis of variance in a linear models context. The latter determines the variation in a dependent variable attributable to a particular factor(set) and is essentially a bivariate technique. The wavelet ANOVA, however, determines the variation attributable to a scale and hence is a univariate technique.

Multiresolution analysis (MRA)

The multiresolution analysis is the reverse transformation of the individual coefficient vectors from the wavelet domain to the time domain. Wavelet vectors ($\mathbf{d}_j$) are transformed to detail vectors ($\mathbf{D}_j$), and scaling vectors ($\mathbf{s}_J$) to smooth vectors ($\mathbf{S}_J$). The smooth vector $\mathbf{S}_J$ represents the average signal at a certain scale level J and the detail vector $\mathbf{D}_J$ represents the deviation from this smoothed signal at scale J-1. The result of the elementwise summation of these two vectors is the smooth vector $\mathbf{S}_{J-1}$ at scale level J-1. If the detail vector $\mathbf{D}_{J-1}$ is added to the latter smooth vector the result is the smooth vector $\mathbf{S}_{J-2}$, and so on, until $\mathbf{S}_1 + \mathbf{D}_1$ results in the original signal. This summation process is given by the equation:

$$\mathbf{x(t)} = \mathbf{S_J} + \sum_{j=1}^{J} \mathbf{D_j} \tag{2.3}$$

where

$$\mathbf{D_j} = \textstyle\sum_k d_{j,k} \Psi_{j,k}(t)$$
$$\mathbf{S_J} = \textstyle\sum_k s_{J,k} \Phi_{J,k}(t)$$

(cf. Equation 2.2).

An MRA thus offers a more intuitive interpretation of a signal in terms of means and deviations when compared to the MODWT in terms of variance. However, the MODWT-based MRA does not preserve the variance like the MODWT does, and can not be used for a variance analysis. The MODWT and the MODWT-based MRA are therefore complementary.

Wavelet correlation and spin correlation

Similar to splitting the variance of one signal, the covariance/correlation between two signals can also be broken down into scale-dependent covariances or correlations (Serroukh and Walden, 2000a,b; Whitcher et al., 2000). This principle works for standard correlation without time lags, as well as for cross-correlations. The scale-dependent cross-correlation is also referred to as 'spin-correlation' (Whitcher, 2007). These techniques allow for the scalewise investigation of the relationship between two variables, and allow in some cases for the separation of irrelevant variation from the signal of interest.

Wavelet coherence and phase analysis

Whereas the wavelet and spin correlation are a measure for the time-averaged scale-specific covariation of two signals, the coherence between two series is a time dependent, instantaneous (local) measure for common scale-specific behavior. It is defined in analogy with a simple squared correlation on the interval [0,1]. Whitcher and coworkers (2005) have developed a MODWT-based coherence analysis, making use of the Maximal Overlap Discrete Hilbert Wavelet Transform (MODHWT) to calculate a coherence and the phase difference between signals. Essentially, a complex representation of both signals is generated using the MODWT with a specific sets of template wavelets (Hilbert wavelet pairs). From these representations the complex modulus and argument are used to derive a common strength, and mutual angular difference is calculated (similar to an amplitude and phase of sine/cosine waves). We refer to the specialized literature for more details (Selesnick, 2001, 2002; Selesnick et al., 2005; Whitcher et al., 2005). Note that coherence analysis is also well developed in the context of continuous wavelet transforms (Torrence and Compo, 1998; Jevrejeva et al., 2003; Grinsted et al., 2004; Maraun et al., 2007) and in the context of Fourier analysis (Shumway and Stoffer, 2006), but the time dependence is lost in the latter application.

2.2.3 The data

From the 17 stations in the North Sea regularly monitored by the Dutch national monitoring program, we selected one station, TSCH175 (54°43'6.2"N, 3°41'25.1"E), located at 175 km off the coast of the barrier island of Terschelling (Fig. 2.3). Two time series were investigated: dissolved organic nitrogen (DON) and nitrate (NO_3^-). While the seasonal variability of NO_3^- is well known and often clear, this is not the case for DON. Dissolved organic nitrogen is a variable whose signal is difficult to interpret, since it consists of a variety of compounds with differential complexity, bio-availability, and turnover times (Bronk, 2002). The DON and NO_3^- time series span the period from the beginning of 1992 to 2004. However, due to a methodological switch in the DON analysis, most of the analyses were performed on the data subset from 1995 to 2004. All the basic data used in this study are publicly available through a website (Rijkswaterstaat, 2009). The DON measurements from the other stations in the marine monitoring program were investigated elsewhere using the methods presented here (chapter 2).

The wavelet transforms used require observations to be equidistant. Most samples occurred on a monthly basis. When higher sampling frequencies were found, the values were averaged per month. Additionally, missing values were substituted by expected values from linear interpolation between adjacent measurements. If doubt existed about potential artifacts resulting from this interpolation strategy, an average value was used based on the surrounding values of the missing data point in a month-year two-dimensional plot, thus incorporating both information from successive measurements and measurement for the same period within-the-year of successive years.

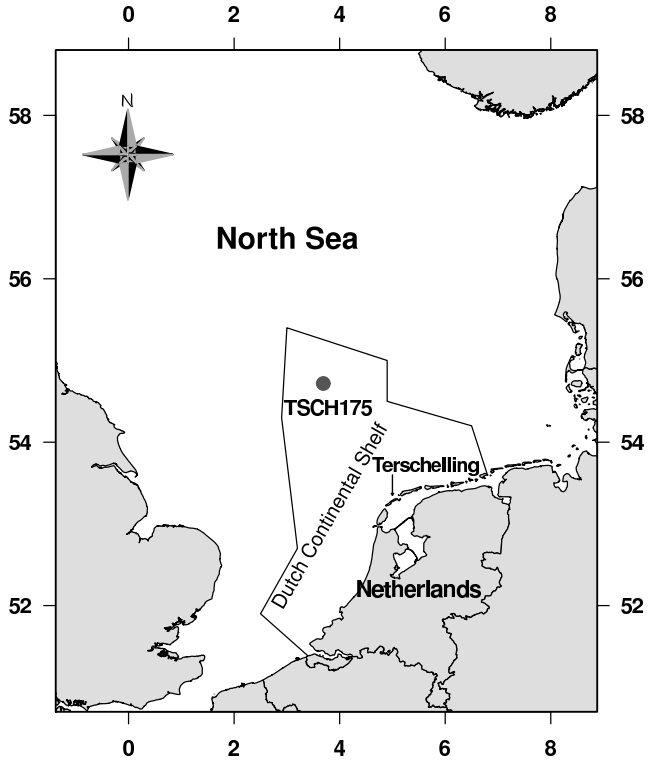

Figure 2.3: Location of the sampling station in the central North Sea, 175 kilometers from the coast of Terschelling.

2.2.4 The software

All statistical analyses were performed using the packages 'waveslim' (Whitcher, 2007) and 'wmtsa' (Constantine and Percival, 2007) in the Rstatistical software (R Development Core Team, 2009); see Table 2.1 for a summary of the most important functions, and section 2.6 for R-code examples). The Fourier analysis and auto-correlation were performed with functions from the standard R-package 'stats' (R Development Core Team, 2009).

All wavelet analyses were based on the MODWT. The least asymmetric wavelet of width 8 (la8; also called symlet or s8) was used because of its smoothness, its relatively small width, and because no significant leakage was present (see 2.3.2). The la8 wavelet is one of a large set of Daubechies wavelets (Daubechies, 1992), that are often used in discrete wavelet analyses, e.g. because the scales are easily interpreted in terms of the signalâĂŹs frequencies (see Fig. 2.2; Serroukh et al., 2000).

The decomposition depth (J) was fixed at four. In case of the monthly sampled data, this means that the seasonality (seasonal periodicity) resides in the $\mathbf{d}_3$ vector (8-16 months with an optimal band-pass periodicity around 12 months; Fig. 2.2), the year-to-year variability

in the $\mathbf{d}_4$ vector. A decomposition to more than the year-to-year scale ($\mathbf{d}_4$) was not feasible, because boundary effects would introduce artifacts over a considerable portion of the time interval (10 years x 12 months/year = 120 observations; cf. section 2.2.1). The temporal extent of the boundary coefficients amounts for a wavelet transformation using the la8 wavelet as template already to 106 observations in the $\mathbf{d}_4$ coefficient vector. Fortunately, only a fraction of these are severely affected, making a decomposition of 4 scales possible if some minor bias is allowed (Fig. 2.5).

Table 2.1: Summary of the most important R-functions used in this study. Two packages were used (first column), but more exist on the CRAN website (R Development Core Team, 2009). See section section 2.6 for R-code examples.

	Functions	Description
waveslim	modwt()	Construction of a (maximal overlap) discrete wavelet transformation of a series
	dwt()	
	phase.shift()	Shifts the coefficients in a modwt object back to the right position after the phase shift induced by the filtering
	wave.filter()	Converts a name of a wavelet to a set of coefficients for the father and mother wavelet
	wavelet.filter()	Converts a name of a wavelet to a filter at a specific scale
	mra()	Construction of a multiresolution analysis object, based on a DWT or MODWT
	wave.variance()	Calculates the wavelet variance and confidence intervals per scale
	wave.covariance()	Calculates the wavelet covariance/correlation and confidence intervals per scale
	wave.correlation()	
	modwt.hilbert()	Construction of a maximal overlap discrete Hilbert wavelet transformation of a series using Hilbert filter pairs
	dwt.hilbert()	
	hilbert.filter()	Same as wave.filter but for a Hilbert wavelet pair
	modhwt.coh()	Functions to calculate the coherence and phase difference between two signals. Both temporally and seasonally averaged values can be returned.
	modhwt.phase()	
	modhwt.coh.seasonal()	
	modhwt.phase.seasonal()	
wmtsa	wavDWT	Construction of a (maximal overlap) discrete wavelet transformation of a series (S4 object).
	waveMODWT	
	wavVar	Calculates the wavelet variance and confidence intervals per scale
	wavGain	Calculates the squared gain function of a given filter.

A reflection boundary treatment was used due to the asymmetry in the time series (cf. section 2.2.1). Because of the limited extent of the data set, we distinguished between coefficients that were only mildly affected and coefficients that could be severely biased by the circular filtering. The transition between these two classes was estimated by calculating

the e-folding time[1] of a wavelet (developed in the context of the CWT, where it is referred to as the 'cone-of-influence'; see for instance Torrence and Compo, 1998). Coefficients within the cone-of-influence defined by the e-folding time of the wavelet filter were withheld from analyses.

Phase shift corrections were performed using the functionality in the waveslim package (Whitcher, 2007) to realign the wavelet transform vectors with the original series (table 2.1). This is needed because the filtering of a series induces a temporal shift in the features in the transform relative to their origin in the series, due to the asymmetry of the filter relative to the position of the calculated coefficient.

2.3 Results

Our analyses will be performed on time series that differ in the strength of seasonality. NO_3^- exhibits a strong seasonality and has a well-known and easily interpreted behavior. Dissolved organic nitrogen (DON) exhibits more erratic behavior and its seasonality is more difficult to discern at the station. First, we discuss the Fourier spectra and auto-correlation functions. Next we compare them with the results from the wavelet transform analysis. And finally, more specific wavelet-based techniques are illustrated. We start with univariate techniques and then move on to bivariate techniques to investigate the relationship between two signals. The DON dynamics at other stations from the Dutch marine monitoring network and their ecological implications are dealt with elsewhere (chapter 3).

2.3.1 Traditional time series approaches

Nitrate (NO_3^-) data were log-transformed to obtain an approximate normal distribution. Transformation of the DON signal was not necessary. A KPSS stationarity test (Kwiatkowski et al., 1992) applied to the DON signal from 1992 to 2004 indicated significant deviations from level stationarity (KPSS level = 2.14, Truncation lag parameter = 2, p = 0.01) and trend stationarity (KPSS trend = 0.62, Truncation lag parameter = 2, p = 0.01). The DON signal was therefore non-linearly detrended by subtracting a spline smoother from the original data (Fig. 2.4). After the detrending step no significant deviations from trend or level stationarity remained. The $\log(NO_3^-)$ data showed no significant deviations from stationarity (Fig. 2.4a) and were used as such.

The time series, the periodograms, and the auto-correlation functions for nitrate and DON are plotted in figure 2.4. The strong seasonality in the $\log(NO_3^-)$ signal is indicated by the peak at frequency 1 yr^{-1} (red line) in the smoothed periodograms (Fig. 2.4b). Also the half-year periodicity was significant - the blue vertical bars in the periodograms represent the 95% confidence intervals. For the more irregular DON signal, a significant half-year periodicity was detected (Fig. 2.4e). The auto-correlation functions (ACF) gave

[1]The e-folding time/distance of a wavelet is roughly defined as the distance from the point of maximum power where the power is reduced to e^{-2} times this maximum power. This can be used to calculate at what distance from the endpoints of a signal a maximal bias at the endpoints would reduce to e^{-2} ($= \pm$ 13.5 %) times this maximal bias.

no additional information. The ACF of the NO_3^- signal exhibited a 12-month periodicity (Fig. 2.4c) due to the strong seasonality as already identified by the spectral analysis. The ACF of the detrended DON series showed no significance at any lag (Fig. 2.4f).

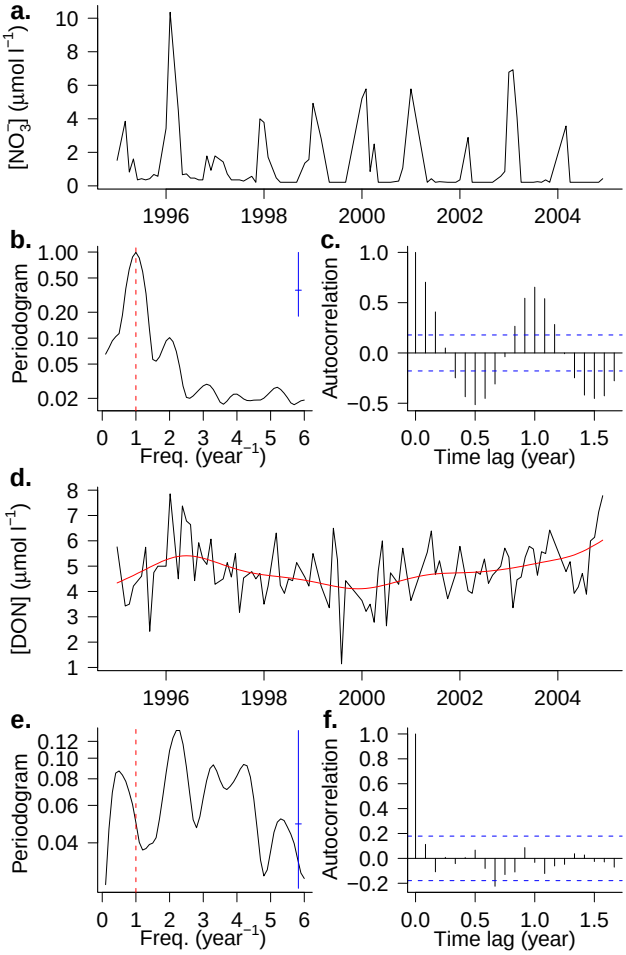

Figure 2.4: The time series of NO_3^- (a.) and DON (d.) with their respective periodograms (b., e.) and auto-correlation functions (c., f.). The blue vertical bar on the periodogram and the blue dashed lines on the auto-correlation plot (b., d.)delineate the approximate 95%-confidence intervals. The vertical dashed red line indicates the yearly periodicity (seasonality). The DON concentrations were detrended prior to the analyses using a spline smoother (red solid line in the DON time series plot).

2.3.2 Univariate wavelet methods

The Maximal Overlap Discrete Wavelet Transform (MODWT)

The MODWTs of the NO_3^- and DON concentrations are depicted in figure 2.5. The wavelet vectors - containing the wavelet coefficients in chronological order - are given, going from the finest scale ($\mathbf{d}_1$) to the coarsest ($\mathbf{d}_4$). The bottom graph depicts the scaling coefficients ($\mathbf{s}_4$) as a function of time, representing the remainder of the variability after the finer scales ($\mathbf{d}_1$-$\mathbf{d}_4$) have been isolated.

The inner red, solid, vertical lines represent the limits of the boundary coefficients. All coefficients outside these lines are affected to some degree by boundary effects. The regions outside the blue dashed lines on either side of the graphs are the coefficients within the e-folding distance (specific per wavelet filter) from the endpoints of the signal. The regions enclosed by either set of limits become progressively smaller as wavelet filters become wider. This illustrates the limitations imposed on the decomposition depth. However, by allowing some bias (i.e. as given by the region within the blue lines in each graph) even the coarser scales can be investigated over a relatively larger temporal range.

For $\log(NO_3^-)$ (Fig. 2.5, left) the seasonal component ($\mathbf{d}_3$) dominates, as indicated by the height of the coefficients (in absolute value). This is consistent with the results from the Fourier analysis and ACF (Fig. 2.4). However, some fluctuations in the strength of variability are visible (cf. $\mathbf{d}_3$ in Fig. 2.5) and co-vary with fluctuations in the scaling coefficients ($\mathbf{s}_4$).

The DON signal shows very little variability in the seasonal scale $\mathbf{d}_3$ (Fig. 2.5, right). The variation in the $\mathbf{d}_1$ wavelet vector appears to be dominant. A second important feature in the DON wavelet decomposition is the sudden drop in the scaling coefficients around 1994-1995 and the concurrent peaks in all wavelet vectors ($\mathbf{d}_1$-$\mathbf{d}_4$). This abrupt change coincided with a methodological transition from a manual destruction of the total dissolved nitrogen (TDN) following (Koroleff, 1983) to an online system with a similar procedure. It is possible that this methodological shift in the measurement procedure around 1995 has lowered the average measured value (scaling vector), possibly due to reduced contamination or a less thorough shorter online destruction. Note that the effects of the sudden decrease (high variation in some wavelet vectors and a decrease in the scaling vector) spread out progressively with increasing scale. This is due to the width of the wavelet and scaling filters.

Whereas the Fourier analysis already gave information on the dominance of the seasonality in the $\log(NO_3^-)$ signal and the smaller scale variability in the DON signal, the wavelet transform shows the time dependence of this variability for both variables. However, in comparison with the Fourier transform, direct interpretation of the wavelet transform coefficients is less straightforward.

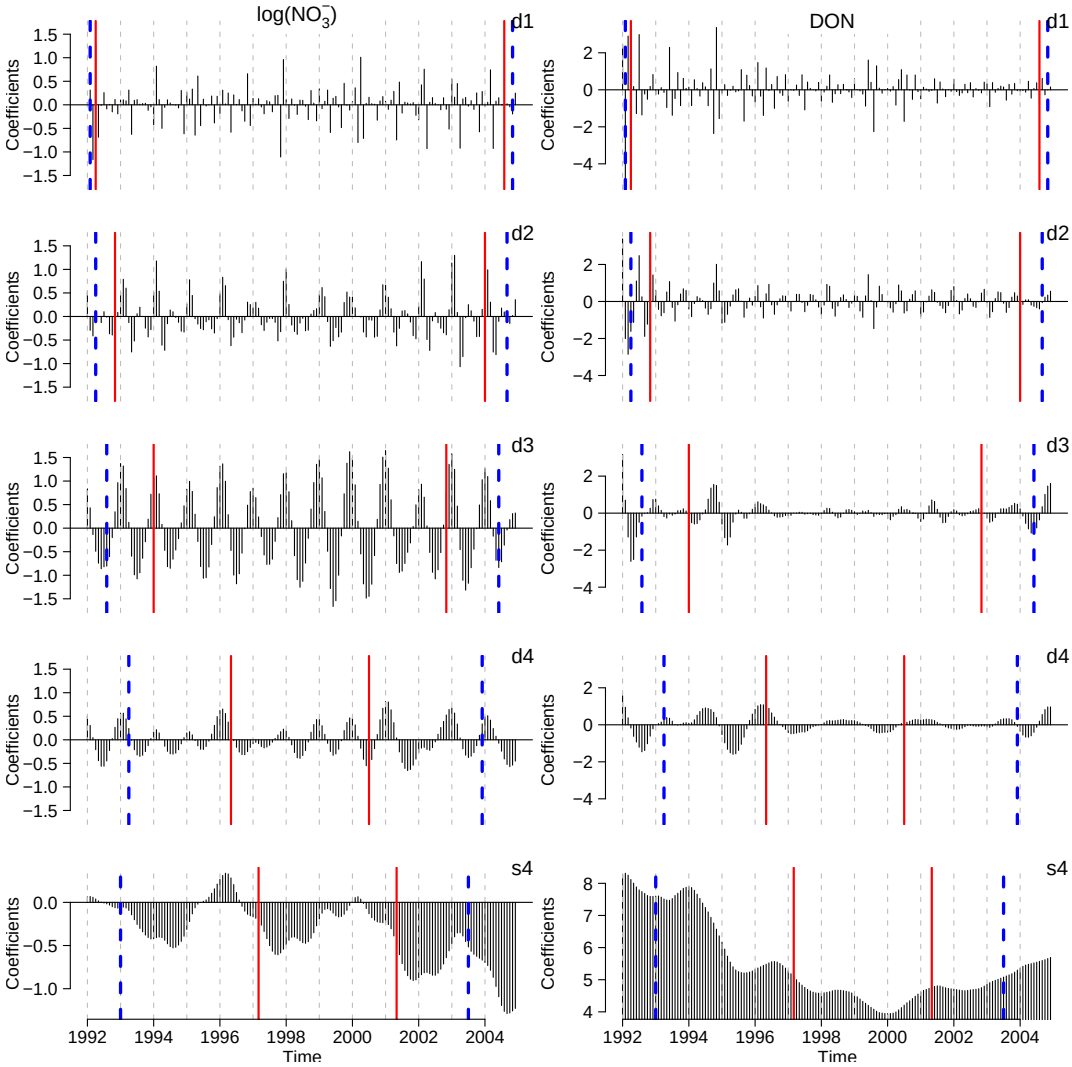

Figure 2.5: MODWTs of the $\log(NO_3^-)$ (left) and DON (right) concentrations at station TSCH175 at four scale levels. The series $\mathbf{d}_1$-$\mathbf{d}_4$ are wavelet coefficient vectors; the series $\mathbf{s}_4$ is the scaling coefficient vector at the coarsest scale. Coefficients not enclosed by the red solid lines are boundary coefficients (coefficients affected by circular filtering). The blue dashed lines are delineate the filter-specific e-folding distances from the beginning and end of the series (cone-of-influence in Torrence and Compo, 1998).

Wavelet analysis of variance

Wavelet analysis of variance (wavelet ANOVA) gives a comprehensive view of the distribution of the variance of a signal over different scales. Figure 2.6 shows the wavelet variance in the DON and $\log(NO_3^-)$ concentrations as a function of scale. For this analysis, we used

only the data from 1995 onwards to avoid influences from the measurement bias. Because the calculation of the confidence limits is based on the assumption of stationary normally distributed coefficients (Serroukh et al., 2000), log-transformed NO_3^- concentrations were used. The presence of leakage was checked by calculating the wavelet variances using progressively wider filters (least asymmetric wavelets of width 8 and 16), until the successive variance calculations converged. Once the difference per scale was negligible, the smaller of the two wavelets was taken. In our results no difference was found in the wavelet variance based on the la8 relative to that based on the la16 wavelet. Thus, the la8 was selected.

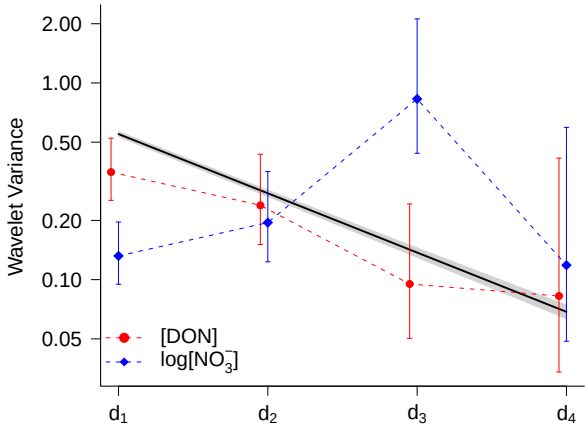

Figure 2.6: Wavelet variance for DON (red dots) and $\log(NO_3^-)$ (blue diamonds). The whiskers represent the 95%-confidence intervals. The thick black line embedded in a gray strip represent Gaussian white noise with the same overall variance as the DON signal and 95% confidence limits based on 10000 simulations.

The variance in $\log(NO_3^-)$ resides predominantly in the d_3 wavelet vector (blue diamonds in Fig. 2.6), whereas the variance in the DON concentrations appeared predominant in the finest scales (red bullets in Fig. 2.6). A linearly decreasing relationship between the wavelet variance and the scale, with slope -1 on a log-log plot is what is expected for a random Gaussian signal (Percival and Walden, 2000). In a random Gaussian signal all frequencies would be equally important, leading to a horizontal Fourier spectrum. However, since the scale bands in a wavelet transformation are not of equal width in terms of the frequencies that are captured (dyadic decomposition), the $\mathbf{d}_1$ component of the wavelet variance takes around half of the frequency range of a periodogram, the $\mathbf{d}_2$ components takes roughly a quarter, and so on (Fig. 2.2). This means that if all frequencies are equally represented in the signal, its wavelet variance in consecutive scales will decrease. This is represented by the thick black line (Fig. 2.6) with 95% confidence interval, based on 10000 simulated random white noise series with standard the same standard deviations as the DON signal.

Overall the DON wavelet variance closely resembled the expected variance from random noise, although being slightly lower in the first scale. Although the global trend in the Fourier spectrum was close to horizontal, some significant peaks were found at interannual frequencies and around the half-yearly frequency (Fig. 2.4), supporting the small deviation from randomness found by the wavelet variance analysis. Other stations showed even more deviation from this randomness, but these data are shown elsewhere (chapter 3).

Just as the periodogram (Fig. 2.4) the global wavelet variance (Fig. 2.6) is an average measure for the entire series. The temporal aspect is sacrificed. However, one advantage of the wavelet ANOVA over the Fourier spectrum is that no prior detrending or complicating transformations, such as differencing, are needed. A disadvantage is the decrease in frequency resolution of the wavelet ANOVA with respect to the periodogram, making wavelet ANOVA less easy to interpret.

Multiresolution analysis (MRA)

A multiresolution analysis results in a mathematical object of similar structure as the MODWT and allows to reconstruct the original signal. Because it is an additive decomposition, reconstruction of the original signal is accomplished just by taking the vector sum of the individual detail vectors and the smooth vector at the coarsest scale level. By including or omitting vectors it is possible to include or exclude variation at particular scales (filtering). The middle graph in figure 2.7 shows a reconstruction of the intra-annual part of the total DON signal (upper graph) that resulted from the vector sum of $\mathbf{D}_1$ to $\mathbf{D}_3$ (this is also called the level 3 'Rough' or $\mathbf{R}_3$ vector, Percival and Walden, 2000). The lower graph is the smooth vector $\mathbf{S}_3$ (lower graph), exhibiting the interannual variation. This method can thus also be used to eliminate long-term trends prior to spectral analysis, something that was accomplished in section 2.3.1 by subtracting a spline function from the original signal (see above). While this worked relatively well, the choice of the parameters is rather arbitrary and not related to scale. In contrast, by choosing the appropriate decomposition level J in an MRA we can just perform a spectral analysis on the level J Rough. Note that in the multiresolution analysis about twice as many boundary coefficients are generated compared to the wavelet transform, due to an extra filtering operation (Percival and Walden, 2000). Because of its additive nature and the resulting intuitive interpretation the multiresolution analysis is a more straightforward choice as exploratory tool than the wavelet transform.

2.3.3 Bivariate wavelet methods

Correlations and covariances between two variables can be investigated with increasing detail. They are decomposed across scales, resulting in scale-specific wavelet correlations (covariances). This allows for the identification of the dominant scale of co-variability. Just as with Pearson's correlation, time lags can be introduced in the wavelet correlations. In other words, cross-correlations between variables are decomposable over scales just as Pearson's correlation. This is sometimes addressed as spin correlation (Whitcher, 2007).

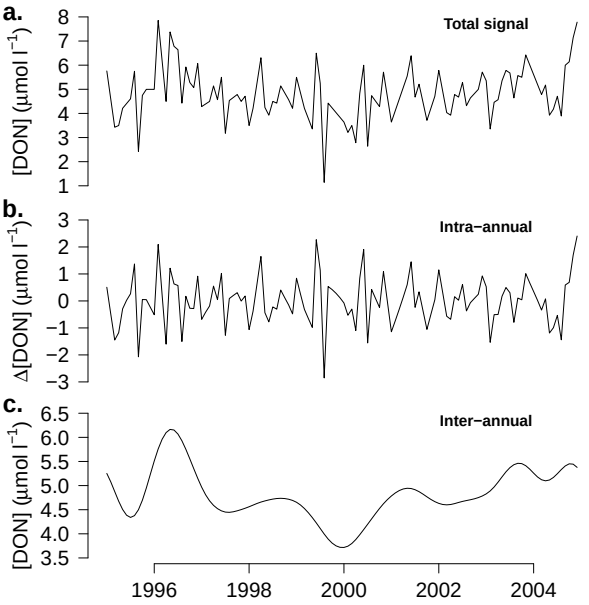

Figure 2.7: The original DON time series (a.), the intra-annual ($\mathbf{D}_1 + \mathbf{D}_2 + \mathbf{D}_3$; b.), and long-term ($\mathbf{S}_3$; c.) component signals. All units are μmol l^{-1}. The values in graph (b.) are deviations from the values of the underlying baseline signal (c.; $\mathbf{S}_3$).

We investigated the relation between DON and $\log(NO_3^-)$ using a sequence of steps (Fig. 2.8). First of all, no significant correlation was found between DON and $\log(NO_3^-)$ in a regular scatter plot (Fig. 2.8a). The wavelet correlations between DON and $\log(NO_3^-)$ did not show obvious deviations from linearity (data not shown). Secondly, scale-specific correlations were investigated. Although differences in the magnitude and even the sign of the scale-specific correlation are visible in figure 2.8b, no significance was attained at any scale. The half-yearly ($\mathbf{d}_2$) scale gives some indication of a potential negative relationship but the confidence interval is too wide to be significant. Thirdly, we looked at the presence of time lagged correlations (wavelet cross-correlations). At the second scale level the wavelet cross-correlation between DON and $\log(NO_3^-)$ was marginally significant for DON lagging 2 months relative to NO_3^- (Fig. 2.8c; indicated by an asterisk). It is worth mentioning that the global cross-correlation (without wavelet transformation) did not give any consistent patterns, let alone significant results (data not shown). Note that the lag 0 spin correlation at the second scale (thick line in Fig. 2.8c) equals the $\mathbf{d}_2$ wavelet correlation (thick whiskers in Fig. 2.8b).

The relationship between DON and NO_3^- can be understood as a transfer of nitrogen from the NO_3^- pool to the DON pool via the PON pool (microbial community). The transfer in the other direction (DON to NO_3^-) will occur through the pathway with NH_4^+

as intermediate. If only the first pathway (NO_3^- to DON) is considered and is assumed to be fast, one could expect a negative relationship at lag 0 (DON increases at the expense of NO_3^-). However, due to the extra steps and the presumed differential rates of transfer between the pools DON, PON, NO_3^- and NH_4^+ one can expect time lags, such as shown here (Fig. 2.8c).

The wavelet coherence measures how much two signals co-vary in a broad sense. If the coherence is close to 1, the signals show a strong 'common behavior '. If it is close to zero the signals do not behave in a coherent way. The coherence is also intrinsically connected with a phase difference, which is defined on the interval [-π, π[(2π = one period / one scale unit). This phase difference is the 'spectral' equivalent of a time lag (cf. complementarity of the periodogram and the auto-correlation function). A wavelet coherence/phase analysis gives essentially the same information as the wavelet cross-correlation, but introduces the extra dimension of time (the coherence and phase vary with time).

We analyzed the aforementioned relationship between DON and $\log(NO_3^-)$ for its stability over time. At the second scale (around half a year) the squared coherence between DON and $\log(NO_3^-)$ was initially low, but increased around 2000 (Fig. 2.8d). They are indicating a strengthening of the relationship between the respective concentrations around that time. From 2000 onwards the phase difference was more stable (dots in figure 2.8d). A constant phase means that the two processes vary 'at the same frequency'; in other words they behave in a coherent fashion. The average phase over the entire measurement period of 2.4 radians (after correction for the truncation in 1997-1998) is roughly equivalent to the time lag of 2.3 months, if a periodicity of 6 months (roughly the bandpass optimum) was assumed. This agrees quite well with the time lag from the wavelet cross-correlation analysis (Fig. 2.8c).

The scatter plot of the $\mathbf{d}_2$ component of the MODWT of DON versus that of $\log(NO_3^-)$ illustrates what the increased coherence means (Fig. 2.8e). All the dots together represent the temporal range 1995-2005. The red bullets are the subset of coefficients from 2000 to 2005. The squared correlation coefficient of the entire set ($R^2 = 0.13$) was smaller than that of the subset ($R^2 = 0.40$). This coherence analysis has thus illustrated that the global (over the entire time span) relationship between DON and $\log(NO_3^-)$ was very weak - only just significant if the time lag was taken into account - because a stronger relationship only occurred from roughly 2000 onwards. The added value of the coherence analysis to the wavelet cross-correlation is the elucidation of a time-dependent strength in a relationship, or its consistency over time.

2.4 Discussion

An ecological time series often results from a suite of processes working on different scales. However, not all scales are equally relevant. Wavelet transformations break down the variation in this time series on a per-scale basis, elucidating scale dependence of the underlying ecological processes. Consider an ecological variable that shows long-term variability, seasonality as well as short-term variation. The total variance in the signal gives no information on how much variation is attributable to the long-term trend and how much is due to sea-

sonality. In addition, it does not indicate whether the small-scale variation changes in time. Wavelet-based analysis of variation does provide this information. Similarly, for two ecological variables that vary seasonally and interannually, a standard (Pearson's) correlation analysis could indicate a significant relationship, but not whether this is due to a common long-term or seasonal trends or because of smaller-scale co-variation. This illustrates the fundamentally different nature of time series data from non-serially (or spatially) dependent data, which need to be analyzed by proper time series analysis techniques, rather than standard statistics.

Wavelets are just as Fourier analyses suited to detect **global (time-independent) patterns** in signals. Examples of this global approach are the wavelet variance analysis, the wavelet correlation, and the spin correlation, presenting measures of variance and linear relationships on a per-scale basis for the entire time domain. Similar Fourier-based approaches are the spectral variance analysis and spectral coherence analysis (Shumway and Stoffer, 2006).

Compared to wavelets, Fourier-based analyses will give higher frequency resolution, but if no particular frequencies dominate in the periodogram, such as for the DON signal (Fig 6), a wavelet variance plot will provide the same information in a more synoptic overview (Fig. 2.6). When a signal exhibits periodicities clearly resembling sine waves, a sine wave-shaped filter (i.e. Fourier analysis) is always the best way to describe it (Farge, 1992). However, if the signal exhibits periodic behavior other than sine waves, Fourier analysis will show strong variation at harmonic frequencies of the actual relevant frequency. By choosing a wavelet that resembles the signal better than a sine wave, these disturbing harmonics are reduced or eliminated.

Both the periodogram and the wavelet variance analysis (and wavelet and spin correlations) assume stationarity of the investigated signal or the wavelet coefficients (Serroukh et al., 2000). For the calculation of the periodogram demeaning and detrending have to be performed prior to analysis to obtain stationarity (Chatfield, 2004). Linear trends can be eliminated by subtracting a linear regression line from the actual data. Non-linear detrending involves more complicated functions such as spline, loess or lowess smoothers or moving averages. Here, a spline function was used to remove the long-term signal from the DON data, prior to the Fourier analyses (Fig. 2.4). In contrast, the wavelet transformation presents an automated way of detrending by filtering out the trend through the elimination of the scaling coefficients at a certain decomposition depth (note that this also eliminates the global mean) and subsequent inverse transformation (cf. imodwt in Tab. 2.1) or equivalently, summing the detail vectors of a multiresolution analysis with the same decomposition depth (Fig. 2.7). With a proper choice of the decomposition depth all the variation at larger scales is eliminated or at least reduced. Another way of transforming a signal to stationarity is by differencing (Chatfield, 2004; Shumway and Stoffer, 2006). Wavelet transformations using a Daubechies wavelet (Daubechies, 1992) have by construction a number of differencing operations and present an automated way of transforming certain classes of non-stationary signals to stationary wavelet coefficients. For a more elaborate treatment we refer to Percival and Walden (2000).

x

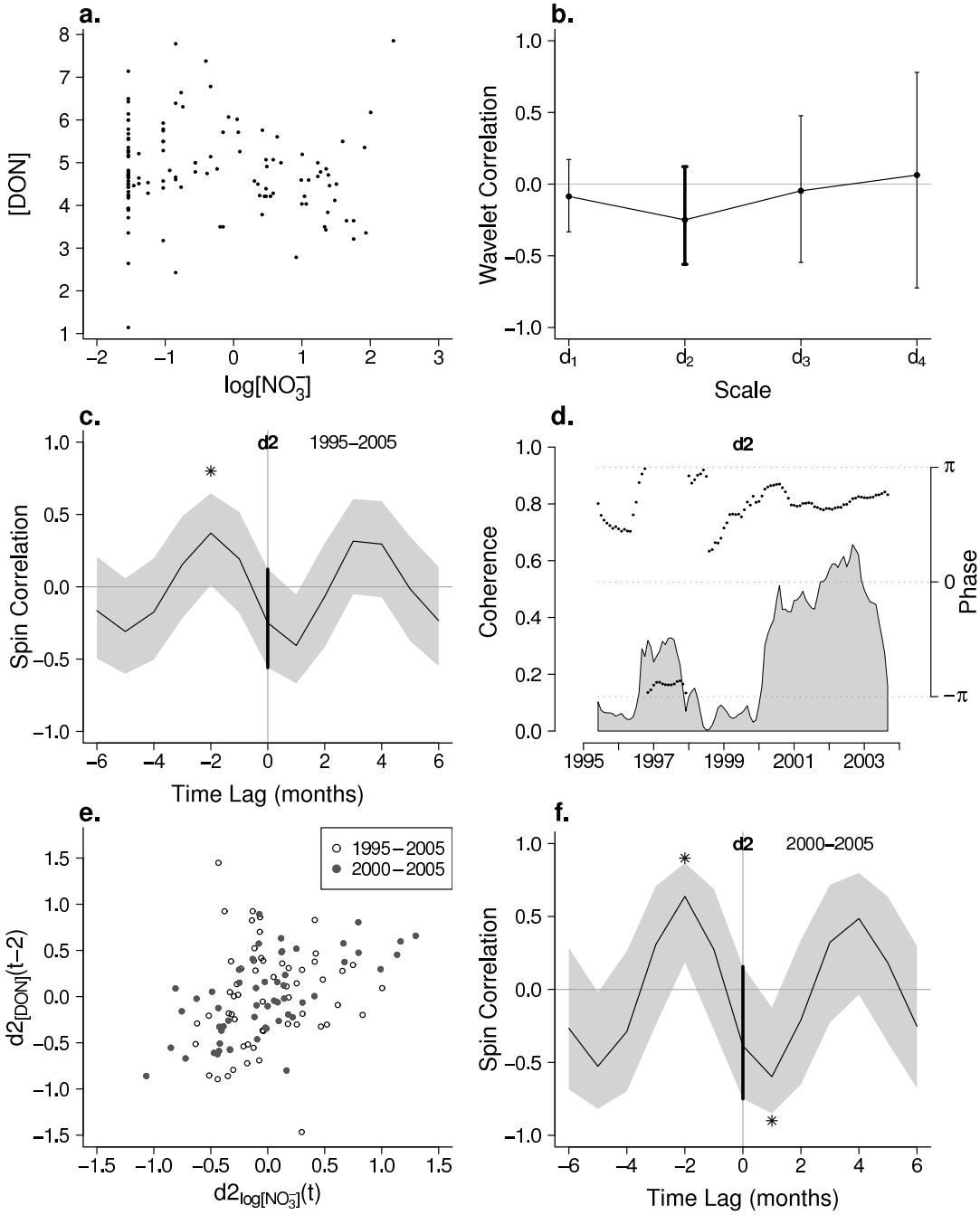

Figure 2.8: Scatter plot of DON vs. $\log(NO_3^-)$ (a.), scale-wise wavelet correlations (b.), d_2 wavelet spin-correlation (c.), d_2 wavelet coherence (grey polygon) and phase (black dots; d.), the scatter plot of the d_2 wavelet coefficients with a time lag of 2 months (e.) for the entire period (open circles) and for 2000-2005 (gray dots), and the $\mathbf{d}_2$ vector of the wavelet cross-correlation of the 2000-2005 subset (f.). Asterisks and thick lines indicate significance and 95%-confidence intervals respectively.

Both Fourier-based coherence analysis and wavelet correlation analysis can shed light on the global scale-specific relationships between processes (Whitcher et al., 2000; Shumway and Stoffer, 2006). Again, the Fourier-based approach provides higher frequency resolution. For wavelets, if the relevant scale is at the edge of a scale band of the wavelet transform, the correlation between the variables of interest (and also the variance of these variables) will be divided over two neighboring scales (Fig. 2.2). On the other hand, the wavelet correlation (and spin correlation) is more easily interpreted than the Fourier coherence and phase and the high frequency resolution of the Fourier techniques is not always needed.

Although wavelet analysis provides global information about time series similar to frequency-domain (Fourier) analyses, their real added value lies in the ability to investigate the temporal dependence of these phenomena, **local characteristics**. For instance, the MODWT (and MRA) of the DON signal showed that the baseline DON concentration dropped suddenly at the beginning of 1995 (Fig. 2.5), and this pointed to a potential artifact caused by the manual destruction in the DON analysis before 1995. The MODWT thus allows for a quick scan for sudden changes in the variability in a parameter throughout the measurement period, a valuable asset for analyzing data derived from long-term monitoring programs. In the MODWT coefficients of the $\log(NO_3^-)$ series a fluctuation in the scaling coefficient values and a concurrent fluctuation in the variability of the $\mathbf{d}_3$ wavelet coefficients was visible, which was attributable to an interannual periodicity in the yearly NO_3^- maxima. These results illustrate the exploratory strength of the MODWT and MRA because they pull apart the variability in scales and over time, making particular features more easily detectable than in the original signal. Beside non-stationarities in individual time series, temporal changes in relationship between variables are detectable using a wavelet coherence analysis (note that in contrast to the wavelet coherence the Fourier-based coherence is a global measure). Our analysis (Fig. 2.8) showed a change in the relationship between DON and NO_3^-. Whereas the wavelet and spin correlations gave some additional information on the dominance of scales in the correlation between DON and NO_3^-, the coherence analysis on these variables showed that a stronger relationship only occurred from 2000 onwards (Fig. 2.8). Coherence analysis is also useful to verify the consistency of periodic patterns, such as seasonality from one variable. An average annual profile (with averages per month) can be compared to the original signal from which it was derived. This gives indications on how well this seasonal model remains consistent over the entire time-series and it can highlight important deviations from the average seasonality occurring through time. This strategy was used by Kromkamp and Van Engeland (2009) to illustrate shifts in bloom phenology of the phytoplankton in the Westerschelde estuary, and by Van Engeland et al. (submitted) to detect a shift in DON seasonality at the Dogger Bank (central North Sea).

An additional application of wavelet analysis is based on the **decorrelating** nature of the standard **DWT** (Fan, 2003; Craigmile and Percival, 2005). By eliminating the serial dependence in the data, simple regression approaches or maximum likelihood methods based on DWT become possible. Fadili and Bullmore (2002) developed a way to use maximum-likelihood methods on dependent data by decorrelating their data with a DWT. Carl and Kühn (2008) investigated the distribution of species richness of plants in a two-dimensional spatial context using a DWT-based MRA. The Discrete Wavelet Packet Transform (DWPT)

could provide a valid alternative to obtain a higher degree of decorrelation (Percival et al., 2000), but this falls outside the scope of this work.

The above discussion clearly shows the advantages of wavelet-based approaches in addition to standard time and frequency domain analyses. There are, however, also drawbacks to using wavelet transformations; the most prominent being restrictions imposed by the length of the time series. In our analyses, the 120 sampling points restricted the width of the filter and the maximal depth of decomposition. Decomposition to more than the year-to-year scale ($\mathbf{d}_4$) was not feasible, as beyond this level boundary effects would dominate. Although boundary effects can be attenuated by a proper choice of boundary treatment (cf. section 2.2), some loss of data at the beginning and end of the signal is unavoidable.

In addition to the upper limit on the wavelet width, imposed by the length of the series, also a lower limit may be imposed. Narrow wavelets give a bad delineation of the frequency bands (impaired frequency resolution), inducing leakage of variance from one scale level to another (Percival and Walden, 2000). If the variance per scale is investigated this leakage should be kept to a minimum and the choice of the wavelet should be done carefully.

This freedom of choice of the wavelet provides flexibility but can also be considered a disadvantage since additional theoretical knowledge is needed to make the right choice, and because it introduces an element of arbitrariness.

Another drawback of the wavelet transformations is that the sampling frequencies have to be constant (values should be equidistant). This problem was here circumvented by introducing interpolated values and averaging per month, but it is clear that gaps in the series should be small and interpolation strategies could induce artifacts. Second-generation wavelets might provide a flexible way of dealing with non-equidistant observations (Cazelles et al., 2008; Jansen and Oonincx, 2005). Note that these limitations also exist for Fourier analysis.

Finally, other applications of discrete wavelet methods exist, e.g signal smoothing/denoising (Siddaiah et al., 2008), tests for homogeneity of variance in long-memory processes (Whitcher et al., 2002), expansion of the number of dimensions (spatial analysis), rotated cumulative variance plots and normalized partial energy sequences to characterize the signal's variability, the application of wavelet packet transforms for increased frequency resolution (Percival and Walden, 2000), and so on.

2.5 Conclusion

Specialized time series methods are a part of statistics that are relatively underused in ecology and biogeochemistry, yet they are a prerequisite for obtaining the maximal knowledge from monitoring campaigns. The increasing availability of data from large scale monitoring projects will make specialized statistical methods for time series analysis indispensable to ecological research. Wavelet-based analyses are situated on a continuum between the time and frequency domain, and present a valuable addition to a larger toolkit of methods for tackling ecological and biogeochemical questions by means of time series data.

2.6 Supplementary data: R-code to generate the graphs

The R-code used to construct the graphs in this paper were added as supplementary data in appendix A. It uses the functions that were presented in table 2.1.

3. Dissolved Organic Nitrogen Dynamics in the North Sea: a time series analysis (1995-2005)

Van Engeland T., K. Soetaert, A. Knuijt, R. W. P. M. Laane & J. J. Middelburg. Submitted to Estuarine Coastal and Shelf Science

Abstract - *Dissolved organic nitrogen (DON) dynamics in the Dutch North Sea were explored by means of long-term time series of nitrogen parameters from the Dutch national monitoring program. Generally, the data quality was good with little missing data points. Different imputation methods were used to verify the robustness of the patterns against these missing data. No long-term secular trends in DON concentrations were found over the sampling period (1995-2005). Interannual variability in the different time series showed both common and station-specific behavior. The stations could be divided into two regions, based on absolute concentrations and the dominant times scales of variability. Average DON concentrations were 11 $\mu mol\ l^{-1}$ in the coastal region and 5 $\mu mol\ l^{-1}$ in the open sea. Organic fractions of total dissolved nitrogen (TDN) averaged 38 and 71 % in the coastal zone and open sea, respectively, but increased over time due to decreasing dissolved inorganic nitrogen (DIN) concentrations. In both regions intra-annual variability dominated over interannual variability, but DON variation in the open sea was markedly shifted towards shorter time scales relative to coastal stations. In the coastal zone there was a consistent and strong seasonal DON cycle with high values in spring-summer and low values in autumn-winter. In the open sea the seasonal cycle was weak and more erratic behavior was apparent. A marked shift in the seasonality was found at the Dogger Bank, with a DON buildup towards summer and low values in winter prior to 1999, and a buildup in spring and decline throughout summer after 1999. Potential mechanisms for this change in seasonality are discussed. This study clearly shows that DON is a dynamic actor in the North Sea and should be monitored systematically to enable us to fully understand the functioning of this ecosystem.*

3.1 Introduction

Human activity has a major impact on nitrogen and phosphorus cycling in coastal systems all over the world (Nixon, 1995; Smith, 2003). Effects of coastal eutrophication have been described for, among others, the Baltic Sea (Larsson et al., 1985), the East Coast of the United States (Boyer et al., 2002), the German Bight (Hickel et al., 1993), and the southern North Sea (de Vries et al., 1998).

Increased nutrient levels in rivers led in most cases to increased primary production (e.g. Wadden Sea, Cadée and Hegeman, 2002), changes in community composition (Philippart et al., 2007), changes in nutrient ratios (Conley et al., 1993; Soetaert et al., 2006) and hypoxia (Welsh and Eller, 1991), and ultimately to an increased supply of nutrients and/or organic matter to the coastal systems because of a changing estuarine filter function (Soetaert et al., 2006). Although a mild form of nutrification could be beneficial to for instance fisheries yields (fertilization), the effects have generally been negative and severe (Cloern, 2001).

Recently, riverine nutrient loads to coastal ecosystems have decreased in many industrialized countries due to nutrient reduction measures taken from the mid 1980s onwards. Declining nutrient concentrations were reported for rivers throughout the United States (Alexander and Smith, 2006), and in Eastern Europe (Weilguni and Humpesch, 1999; Stålnacke et al., 2004) and Western Europe (e.g. van Beusekom and de Jonge, 2002 and de Jonge et al., 2002 for the Rhine, and Soetaert et al., 2006 for the Scheldt).

Reductions in nutrient concentrations have also been reported for coastal systems such as Chesapeake Bay (Kemp et al., 2005), the Danish coast (Conley et al., 2002; Carstensen et al., 2006), the Swedish Baltic coast (Elmgren and Larsson, 2001), and the Dutch coast (de Vries et al., 1998). However, primary producers (and whole ecosystems) did not always respond as expected. McQuatters-Gollop et al. (2007), for instance, reported increasing primary production in the presence of declining nutrient concentrations imposed by nutrient reduction strategies. Cloern (2001) already pointed out that ecosystem responses are generally non-linear.

To document and eventually understand these eutrophication/oligotrophication related changes rigorous long-term monitoring programs such as DNAMAP (Denmark; Carstensen et al., 2006) or MWTL (The Netherlands; see e.g. de Vries et al., 1998) are indispensable. Beside the more obvious goals such as monitoring reductions in nutrient concentrations and phytoplankton production, they should allow for the investigation of more subtle ecosystem changes such as changing seasonality (Cloern, 2001; Cloern and Jassby, 2008). It is clear that a more rigorous sampling at higher frequencies is needed for the latter set of goals than for the former.

Despite the growing awareness of the importance of organic substances as nutrient in the past decade, relatively few studies have addressed their dynamics in time and/or space. Often only inorganic parameters such as dissolved inorganic nitrogen (DIN) have been measured in monitoring efforts, and in the cases where total measurements (total dissolved nitrogen; TDN) were available, they were analyzed as such (Downing, 1997). The reason is twofold: (1) the measurement methodology for TDN and dissolved organic nitrogen (DON = TDN-DIN) is prone to error due to difficulties in making the destruction complete and the

accumulation of measurement errors in the calculating DON from TDN en DIN (Sharp et al., 2002), and (2) DON was initially considered nonreactive (Bronk et al., 2007). However, the seasonality present in DON and lack thereof in TDN in some systems (e.g. Butler et al., 1979) supports the idea of considering the organic fraction of the TDN separately instead of only studying TDN. Seitzinger and Sanders (1997) emphasized the weakness of both TDN and DIN as approximations of the real bio-available nitrogen, which is intermediate. Van Es and Laane (1982) also measured higher decomposition rates for dissolved amino acid carbon in comparison to bulk dissolved organic carbon.

The potential of DON as nitrogen source for primary producers has since long been recognized (see Bronk, 2002 and Bronk et al., 2007 for an overview). Four decades ago growth experiments with specific organic nitrogenous compounds already showed that axenic phytoplankton cultures could grow on organic substances (Antia et al., 1975). Admiraal and coworkers (1987) reported significant uptake of amino acids by estuarine benthic diatoms in a matter of hours. Both phytoplankton and bacterioplankton are known to use DON to fulfill at least a part of their nitrogen requirements (Bronk and Glibert, 1993; Bronk et al., 2007; Veuger et al., 2004). DON uptake rates and capabilities are taxon and compound/composition specific. The potential of DON as nutrient is further stressed by its dominance over inorganic forms in oligotrophic and mesotrophic systems (Bronk, 2002). But even in coastal systems affected by large amount of anthropogenic, atmospheric or riverine DIN input, DON can still make up 47 % of the total dissolved nitrogen (De Galan et al., 2004).

Microbes are not only consumers but also producers of DON (Bronk et al., 1994), through lysis or exudation. Lysis is induced by consumption by zooplankton (sloppy feeding), viral infection, or cell death after nutrient depletion (collapse of a bloom). The growth phase is known to play a role in the nitrogen content of the dissolved organic matter (DOM) that is exuded (e.g. Engel et al., 2002). In addition, DON originates from zooplankton excretion and defecation (leaching from fecal pellets). Beside these forms of in situ production, riverine discharge (Badr et al., 2008), atmospheric inputs (Jickells, 1995; Seitzinger and Sanders, 1999), release from sediments (Lomstein et al., 1998; Tyler et al., 2001) and groundwater discharge (Kroeger et al., 2006) are known to play a role.

The DON pool comprises a wide spectrum of compounds that cycle on a wide spectrum of temporal and spatial scales (Bronk, 2002). While ^{15}N tracer techniques and bio-assays have provided a wealth of information on short-term dynamics of DON cycling (e.g. Mulholland et al., 2002, 2004; Veuger et al., 2004; Andersson et al., 2006), far less is known about the evolution of the DON pool at larger scales (seasonal, interannual) in a particular system. Long-term monitoring efforts with sufficient spatial coverage are needed for this.

The Dutch national monitoring program is one of the few long-term monitoring projects that consistently measured TDN at a number of stations on a monthly basis. We analyzed DON concentrations derived from a subset of these TDN concentration series to investigate the patterns present at various temporal and spatial scales in the North Sea. Standard statistics are used in combination with wavelet-based approaches because the latter provide a rigorous framework to consider scale dependence without giving up the time dependence, as opposed to Fourier-based analyses (Shumway and Stoffer, 2006).

3.2 Materials & Methods

3.2.1 Area of study

The North Sea is a semi-enclosed continental shelf system that is hydrodynamically subdivided into a seasonally stratified northern part (north of 56°N) and a permanently mixed southern part (Ducrotoy et al., 2000). It receives water from the Atlantic Ocean through the English Channel in the south and from the North Atlantic Drift north of Scotland, implying a potentially large oceanic influence in these regions. Due to the complex interaction between tidal currents and bottom topography, oceanic water entering through the English Channel, is mainly deflected towards the Belgian and Dutch coast, thus creating a current parallel to the coastline which transports large quantities of terrestrial run-off and suspended matter from the rivers Scheldt, Meuse and Rhine (Dutch delta area) northward. As such, this southeastern part is more influenced by river run-off.

The total nitrogen and phosphorus loadings to the North Sea are 8870 ± 4860 kT N $year^{-1}$ and 494 ± 279 kT P $year^{-1}$ (Brion et al., 2004 based on data from the mid 1970s to the mid 1990s) of which 9 ± 3 % and 8 ± 2 % can be attributed to riverine input, the majority coming from the North Atlantic. The input of freshwater from the rivers is estimated at 91-97 km^3 $year^{-1}$. At the Dutch continental shelf (DCS) strong inorganic nutrient gradients are observed between 20 and 50 km offshore (de Vries et al., 1998) due to a combination of the coastal current and freshwater input.

Eutrophication effects have been observed for the coastal zone as well as for offshore regions, such as the Dogger Bank (Kröncke and Knust, 1995). The Dogger Bank region can exhibit higher primary production than the surrounding parts of the North Sea (Heip et al., 1992). Past research suggests that annual nitrogen budgets are balanced by nitrogen input from the Atlantic Ocean and internal recycling (Hydes et al., 1999; van Beusekom et al., 1999). Together with a favorable climatic regime this has led to an increase in chlorophyll and primary production at the end of the 1980s throughout large parts of the North Sea despite decreasing terrestrial nutrient inputs (McQuatters-Gollop et al., 2007).

3.2.2 Stations

Nutrient monitoring has been conducted at the Dutch Continental Shelf (DCS) since the mid 1970s. These data, stored in the DONAR database (Rijkswaterstaat, 2009), are publicly available via the Waterbase website. We extracted data from this database for 9 stations (Fig. 3.1), covering different zones with contrasting hydrodynamic regimes and nutrient supplies. All data points concern surface waters, and we deliberately excluded stations at intermediate distances to enhance the contrast between coast and open sea. The stations were taken from four transects perpendicular to the coasts of Walcheren (WAC, WAO), Goeree (GOC), Noordwijk (NWC, NWO), Terschelling (TC, TO, OG, DB) from south to north.

Two coastal stations (WAC and GOC) are in front of the Dutch delta system and receive large quantities of fresh water from the Rhine/Meuse and to a lesser extent from the Scheldt

(Lacroix et al., 2004). The stations NWC and TC are situated north of the mouth of the river Rhine. NWC experiences a large influence of this river due to the a predominant northward drift. TC receives water from the Wadden Sea and Lake Ijssel. All the coastal stations are subject to terrestrial runoff from different sources, potentially inducing station-specific differences.

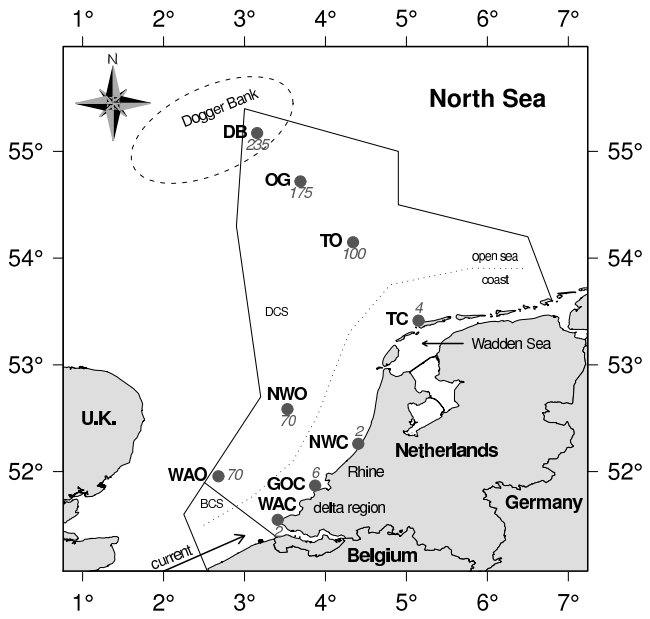

Figure 3.1: Sampling locations at the Dutch Continental Shelf (DCS). Terrestrial influences (Wadden Sea with inflow from Lake Ijssel and the Dutch delta area with water from the Scheldt, the Meuse and the Rhine) and the coastal northward current are indicated. The distances to the coast are indicated for each station in kilometers. The stations are divided into a coastal and open sea region (dotted line).

The stations in the open sea are subject to different hydrodynamic regimes as well. The most southern stations WAO and NWO, in this paper addressed as the southern North Sea, are in relatively shallow water with a vertically mixed water column throughout the entire year. While TO and OG are in deep water with a seasonal thermocline. Station DB is situated on the Dogger Bank in relatively shallow water.

Although the time series for dissolved inorganic nitrogen, dissolved organic carbon and other auxiliary data were longer, a systematic record for DON is only available from January 1995 onwards. All time series used here contained data points from januari 1995 until December 2004 at sampling frequencies of at least once per month.

3.2.3 Chemical analyses

DIN comprising ammonium, nitrate and nitrite has been measured by automated colorimetric techniques at the Rijkswaterstaat laboratory. DON was obtained by difference from TDN and DIN. TDN and DOC were analyzed using a UV-persulphate destruction (Koroleff, 1983) to NO_3^- and CO_2, respectively, and subsequently measured with an auto-analyzer. The same methods and laboratory procedures have been used during the entire period reported and analyzed here (1995-2004). DON values within DONAR were basically available from 1992 onwards but those from the first few years were not included because the measurement methodology was changed at the beginning of 1995 (switch from manual to online destruction of TDN).

3.2.4 Data quality

A long-term time series study requires assessment of the overall quality of the data (Loebl et al., 2009). The DONAR database contains more data than that covering the North Sea and there is overlap with data sets generated by other authorities. DIN and DOC data generated by the Netherlands Institute of Ecology (Soetaert et al., 2006) allow direct comparison with DONAR data. Where stations and sampling times of both databases were in close agreement, parameter values showed close agreement as well. The variability in both data sets was similar for all parameters. This at least supports the consistency between independently measured values. The laboratory of Rijkswaterstaat that has generated the DONAR data is an ISO-CERTIFIED 'Sterlab'. The laboratory participated on a regular basis in the QUASIMEME international calibration exercises for nutrients in seawater and in estuarine waters with satisfactory results (the average Z-score for TDN was 0.33).

3.2.5 Statistics

All statistical analyses were performed using the R statistical software (R Development Core Team, 2009). Linear modeling was performed using maximum-likelihood methods from the 'nlme' package (Pinheiro et al., 2008). Wavelet-based transformation and analyses were conducted by means of the 'waveslim' (Whitcher, 2007) and 'wmtsa' (Constantine and Percival, 2007) packages.

Regression analyses were performed using generalized linear models (GLM). Corrections for serial dependence were added if necessary by imposing an appropriate ARMA model on the residuals (Shumway and Stoffer, 2006). Logarithmic transformations were used to obtain normally distributed variables when necessary. Spatial variance partitioning was performed using a hierarchical mixed-effects model with a station-within-region design.

Standard time series analysis techniques, such as auto/cross-correlation analyses were supplemented with wavelet-based techniques. Wavelet-based transformations show quite some similarity to Fourier-based approaches but retain the time-domain aspect and allow for the modeling of local non-stationarities (Vidakovic, 1999). Here, we will only briefly explain the wavelet techniques so as to make our results understandable. We refer to chapter 3 for a more elaborate summary of the techniques that are used here, and are generally useful

for the analysis of ecological time series. The Maximal Overlap Discrete Wavelet Transformations (MODWTs) subdivides the total variation in a time series over scales without loss of information. In the context of DON, the concept 'temporal scale' can easily be understood by considering the differential turn-over times/rates of different organic compounds. Amino acids are quickly taken up again after they have been released into the environment by living organic matter (van Es and Laane, 1982). They have short turn-over time, hence cycle on short time scales. More complex substances need more effort to be broken down or only a small fraction of the microbial community is able to use them. They cycle on longer time scales. The same applies to DON versus DOC; Whereas DOC that contains large amounts of refractory humic carbon in some coastal systems is broken down slowly due to the low nutritional value, the DON pool contains larger amounts of more labile compounds that are immediately useful to autotrophs. Bio-availability is in this way associated with a wide spectrum of scales. Loh et al. (2006), for instance, found that ultra-filtered dissolved organic matter (UDOM) and particulate organic matter (POM) have different cycling times, which implies that they would show dynamic behavior on different time scales.

More general, a time scale corresponds to a time window of a particular width (a limited range of consecutive values in time). A representative value for process at a particular scale is then some kind of average representative value, and scale-dependent variability is associated with differences between those averages. For example, the difference between the yearly averaged DON values of 2001 and of 2002 determines the variability around this time at a year-to-year scale. For a more mathematically exact definition in a wavelet context we refer to the book by Percival and Walden (2000). We have adopted a MODWT of decomposition depth 4 that subdivides a time series into five scale levels (Tab. 3.1): four wavelet vectors ($\mathbf{d}_1$-$\mathbf{d}_4$) containing progressively coarser scale variation, and one scaling vector ($\mathbf{s}_4$) containing all the remaining coarse scale variation. Hence a MODWT transformation of a time series results in a set of new time series, each containing variability at a certain scale.

Table 3.1: Band-pass properties per wavelet/scaling coefficient vector ($\mathbf{d}_1$-$\mathbf{s}_4$) for a MODWT with a least asymmetric wavelet filter (Daubechies, 1992) and a decomposition depth of 4 (scales). The values are in months because the nutrient parameters were sampled monthly. The left column gives more trivial names that are used in this paper. They are based on the respective band-pass optima (last column). The upper and lower bounds are the nominal frequencies (cf. Percival and Walden, 2000).

Nomenclature	Transform vector	Lower bound	Upper bound	Band optimum
fine scale	$\mathbf{d}_1$	-	4	-
half-yearly	$\mathbf{d}_2$	4	8	6
seasonal	$\mathbf{d}_3$	8	16	12
year-to-year	$\mathbf{d}_4$	16	32	24
inter-annual	$\mathbf{s}_4$	32	-	-

In this paper, scales will be addressed using the scale number or their band-pass optimum. The third scale level will thus be addressed as d_3 (d for detail) or as the seasonal scale because the optimum frequency of the wavelet filter at this scale is roughly 12 observations

(12 months since samples were taken on a monthly basis; see also chapter 3).

A variance partitioning over temporal scales was performed by means of a wavelet-ANOVA (Serroukh et al., 2000). The scale-dependent variances are in this study presented as fractions of the total variance in the time series under investigation.

Wavelet coherence analysis was performed to investigate the association between parameters over time and scale (Whitcher et al., 2005). In addition, this analysis technique was used to check the consistency of the seasonal pattern over time. This was done by comparing the original signal (or time series) to an artificial signal that consisted of a repetition of the average seasonality (value as a function of month) to obtain a series of the same length as the original signal. Generally, this analysis results in a coherence and phase value per time point and scale. The former is defined between 0 and 1, in analogy with a coefficient of determination. The interpretation is also similar. The latter is the phase difference (an angle) between the signals and is defined between $-\pi$ and π. If the angle is $-\pi$ or π the signals are in counter-phase, a time lag of half a scale. If the angle is 0, both signals are in phase, a time lag of zero observations. If the angle is positive the first signal leads with respect to the second. If the angle is negative the first lags with respect to the second signal. This principle is similar to a Fourier-based coherence analysis (Shumway and Stoffer, 2006), except that coherence and phase values are allowed to vary over time.

The wavelet-based techniques used, do not allow missing data points the data have to be equidistant (i.e. constant sampling frequency). The few missing observations in our time series were filled in by values from linear interpolation between the adjacent data points (local information). Since the number of consecutive missing values was generally limited to two, no strong artifacts are expected from this strategy. When in doubt, a different interpolation strategy was used with a replacement of missing values by the average of the surrounding points on a year vs. month map of the parameter, allowing for the incorporation of information on the seasonality in the year before and after the missing value (cf. 3.3.2).

3.3 Results

The mean DON, DOC, DIN and DIP values show that the stations can be divided into two regions (Fig. 3.2; Tab. 3.2): the coastal zone and the open sea. DON concentrations varied in the coastal zone between 4 μmol l^{-1} and 25 μmol l^{-1} (average 11 $\pm$ 3 μmol l^{-1}) and in the open sea from 1 μmol l^{-1} to 13 μmol l^{-1} (average 5 $\pm$ 1 μmol l^{-1}). The highest average DON concentration for the coast was found for the station NWC, halfway the Dutch coast (12 $\pm$ 3 μmol l^{-1}), the lowest at TC downstream (11 $\pm$ 3 μmol l^{-1}). The differences between the stations in the coastal domain were significant (Generalized Linear Model with correction for short-term residual dependence by an ARMA(4,1), $F = 3.05$, $p = 0.03$). In the open sea domain long-term averages ranged from 6 $\pm$ 1 μmol l^{-1} at NWO to 5 $\pm$ 1 μmol l^{-1} at OG. Significant stationwise differences were not detected for the open sea.

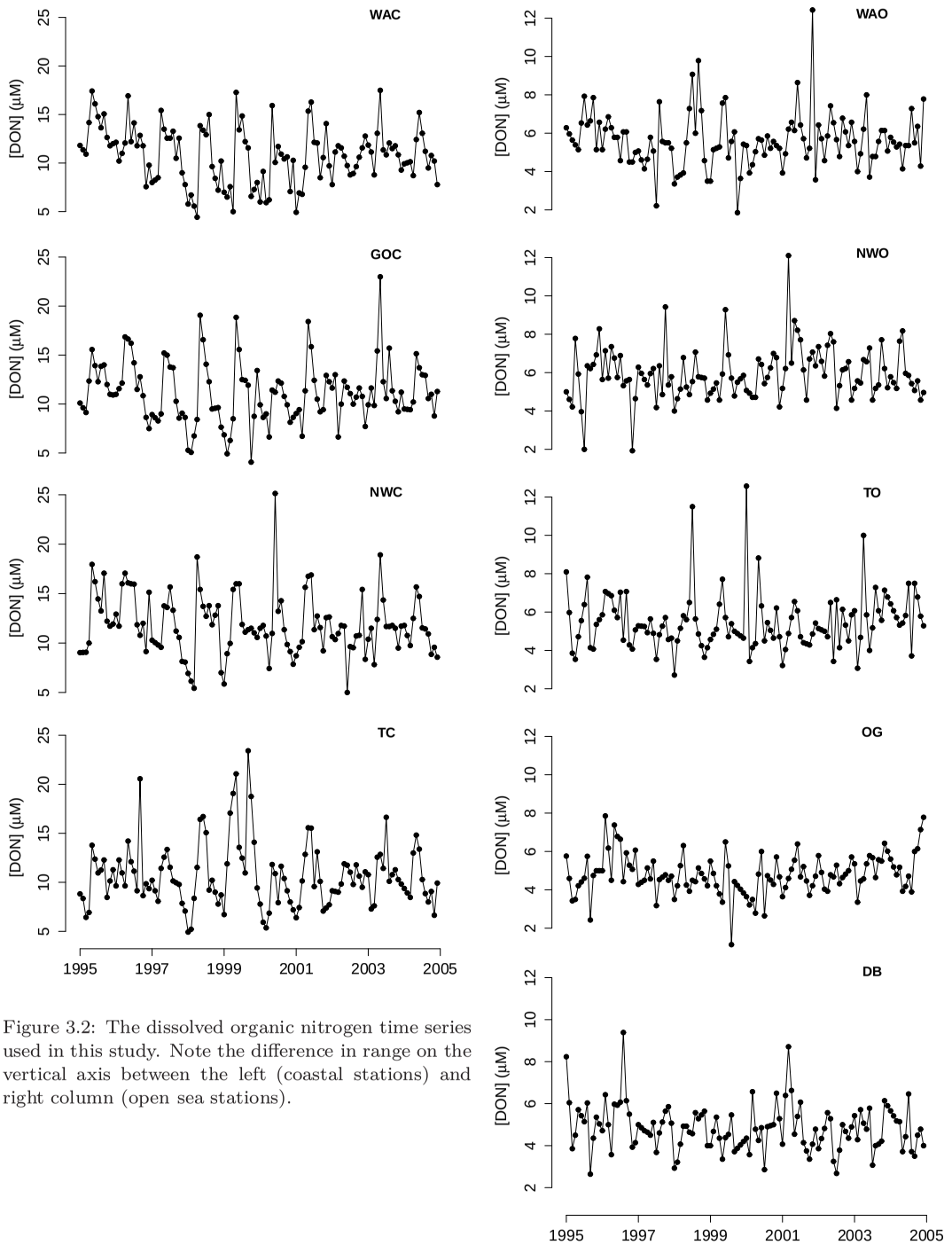

Figure 3.2: The dissolved organic nitrogen time series used in this study. Note the difference in range on the vertical axis between the left (coastal stations) and right column (open sea stations).

A visual inspection of the time series (Fig. 3.2) reveals that the DON signal in the coastal zone is more regular throughout the sampling period compared to the open sea. The irregularity in the open sea and the lack of similarity in the timing of features, such as extremes (e.g. the peak value in 2001 at NWO, compared to the peak value in 2002 at WAO), suggest that at short time scales the stations behave independently of one another with respect to the DON concentration. At a larger time scale, however, the common inter-annual trends in the DON (e.g. the increase in the Terschelling transect around 2000; Fig. 3.2 right) suggest common drivers that work on a larger regional scale.

Table 3.2: DOC, DON, DIN and DIP concentrations for the individual stations for the entire sampling period (1995-2005). All values are in μmol l^{-1} (mean $\pm$ sd).

	Station	DOC	DON	DIN	DIP
Coast	WAC	122 $\pm$ 28	11 $\pm$ 3	25 $\pm$ 20	0.8 $\pm$ 0.5
	GOC	129 $\pm$ 36	11 $\pm$ 3	30 $\pm$ 20	0.8 $\pm$ 0.5
	NWC	130 $\pm$ 25	12 $\pm$ 3	40 $\pm$ 24	0.9 $\pm$ 0.5
	TC	123 $\pm$ 27	11 $\pm$ 3	16 $\pm$ 15	0.5 $\pm$ 0.3
Open Sea	WAO	73 $\pm$ 13	6 $\pm$ 2	4 $\pm$ 4	0.3 $\pm$ 0.2
	NWO	78 $\pm$ 15	6 $\pm$ 1	3 $\pm$ 3	0.2 $\pm$ 0.2
	TO	77 $\pm$ 14	6 $\pm$ 2	3 $\pm$ 3	0.3 $\pm$ 0.2
	OG	75 $\pm$ 10	5 $\pm$ 1	2 $\pm$ 2	0.3 $\pm$ 0.2
	DB	74 $\pm$ 10	5 $\pm$ 1	2 $\pm$ 2	0.2 $\pm$ 0.1

None of the stations showed a significant net decrease or increase in DON between 1995 and 2005 (Generalized Linear Models; Fig. 3.2). Over the investigated period dissolved inorganic nitrogen concentrations decreased significantly in both the coastal zone (Mixed-effects Model with random intercept per station, $F = 42$, $p < 0.001$) and the open sea (Mixed-effects Model with random intercept per station, $F = 10.7$, $p < 0.01$). The yearly averaged organic fractions of total dissolved nitrogen (TDN) increased significantly in both the coastal zone (Mixed-effects Model with random intercept per station as random factor, $F = 5.4$, $p = 0.02$) and the open sea (same design, $F = 22.7$, $p < 0.001$), which was mainly attributable to the decreasing DIN values (for the coastal zone from 31.7 μmol l^{-1} in 1995-1996 to 22.5 μmol l^{-1} in 2003-2004 and for the open sea from 3.5 μmol l^{-1} in 1995-1996 to 2.4 μmol l^{-1} in 2003-2004). The increase in the organic nitrogen fraction was particularly clear for summer in the open sea and winter season in the coastal stations (Tab. 3.3).

The chlorophyll a (Chla) and DON values were averaged per month of the year to obtain an average seasonal profile for each individual station (Fig. 3.3). The Chla signal exhibited a clear bloom peak in spring (Fig. 3.3a and b), both in the coastal zone and the open sea. But in contrast to the open sea, the coastal Chla values remained relatively high in early summer and declined from July-August onwards (Fig. 3.3a). The open sea on the other hand exhibited a clear second bloom peak in autumn but the Chla concentrations were low in summer. The coastal DON concentrations peaked one month after the Chla peak, and seemed to decline more gradually than the Chla values (Fig. 3.3c). In contrast to the coastal zone, the DON profiles in the open sea (Fig. 3.3d) did not resemble the Chla seasonality.

Table 3.3: Percentages of DON in TDN per year (mean ± st.dev.) for the coastal zone and open sea in (summer = April-October; winter = November-March). The p values are based on simple regression models of the organic fraction as function of time. The data were log-transformed for these regressions.

Year	Summer		Winter	
	Coast	Open sea	Coast	Open sea
1995	46 ± 24	75 ± 18	18 ± 8	55 ± 13
1996	52 ± 18	81 ± 13	21 ± 6	47 ± 11
1997	55 ± 25	81 ± 11	18 ± 6	55 ± 14
1998	52 ± 25	81 ± 13	14 ± 5	48 ± 11
1999	54 ± 25	84 ± 12	15 ± 8	50 ± 10
2000	48 ± 25	83 ± 15	15 ± 4	45 ± 12
2001	47 ± 23	87 ± 10	19 ± 7	56 ± 20
2002	51 ± 22	87 ± 10	20 ± 5	53 ± 12
2003	65 ± 21	92 ± 3	26 ± 14	57 ± 22
2004	55 ± 26	87 ± 12	23 ± 6	58 ± 14
p value	0.07	< 0.001	< 0.001	0.02

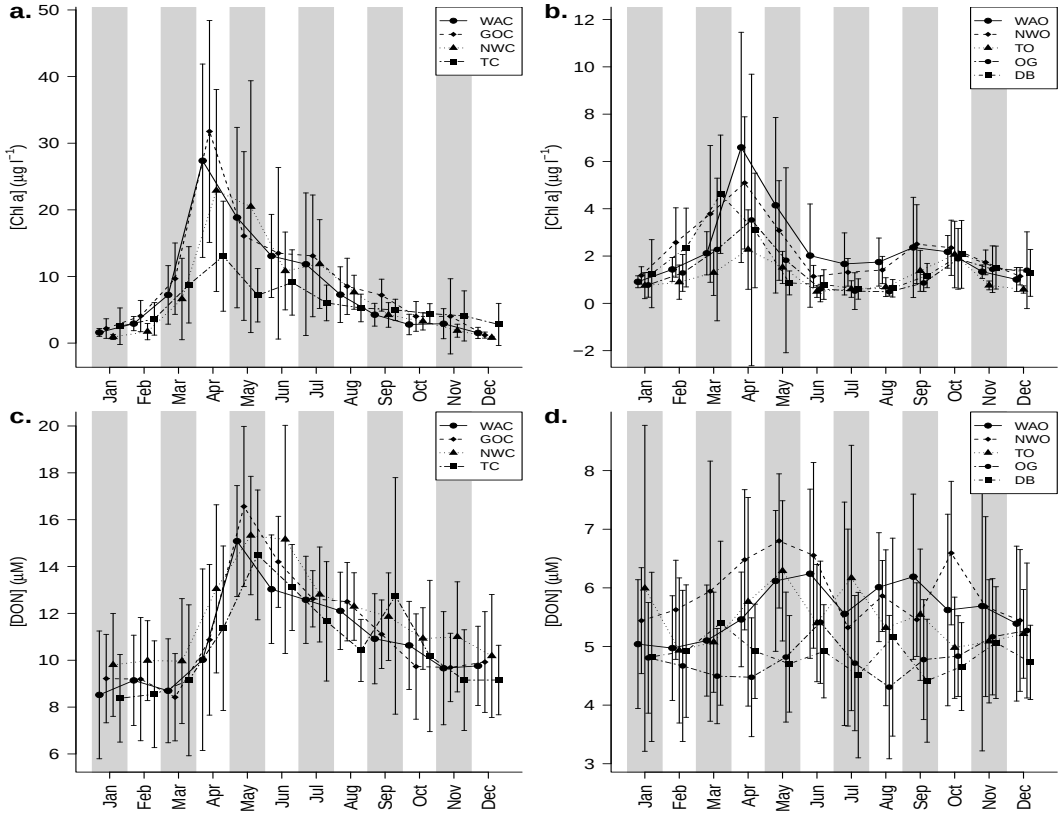

Figure 3.3: Seasonal profiles per station for the coastal (left) and offshore (right) DON (upper) and chlorophyll a (lower) based on the data from 1995-2005. The error bars represent standard deviations.

In addition, the per-station seasonal plots of DON exhibited a high degree of similarity in the coastal zone with relatively small standard deviation, but not in the open sea. These patterns illustrate that in the coastal zone the DON seasonality was consistent throughout the stations and over the years and appeared dependent on phytoplankton stocks and DOM production (DON lags with respect to Chla). In the open sea, however, little consistency in seasonality seemed present between the stations and throughout the measurement period.

3.3.1 Variance partitioning in Dissolved Organic Nitrogen

Spatial partitioning using a GLM approach revealed for DON a dominant variability (55 %) at the between-region level, while 38 % of the variability resided at the within-stations level. The remaining 7 % was attributable to a between-station effect within the regions. For DOC a similar pattern was found. Temporal variation partitioning was performed using a per-station wavelet-ANOVA approach. The coast exhibited the same scale-dependent variance distribution for DON and DOC signals with a major seasonal (d_3) component. The DON in the open sea showed a decreasing variance contribution with increasing scale (Fig. 3.4), i.e. DON variability occurred predominantly at short time scales. This almost linearly decreasing variance contribution with increasing scale level (on a log-log plot) is a reflection of the large measurement error that results from calculating DON (= TDN - (NH_4^+ + NO_2^- + NO_3^-)). However, considering individual stations (Tab. 3.4) quite some deviation from this average straight line (Fig. 3.4) are apparent. The variance fractions in DOC were very similar in both regions with the majority of the variability residing in the d_3 component (seasonality). The variance partitioning illustrated a clear dominance of intra-annual variation over interannual variation (Tab. 3.4), corroborating the absence of a long-term trend.

The discharge from the river Rhine was investigated for its impact on the seasonality in DON in the coastal stations. The DON concentration at Brienenoord (35 km upstream in the Rotterdam New Channel, which is the main discharge route for the Rhine) exhibited some seasonal variation with an absolute maximum in March-April and a second lower local maximum in September-October. Using the discharge values from near the mouth (Maassluis) and the DON concentrations at Brienenoord, the DON load to the coastal zone was calculated. A marine influence in the DON load is thus avoided by using DON data from the end of the freshwater part. The DON load exhibited a similar seasonality to the DON concentration at Brienenoord, except that the local peak in September-October was absent. A wavelet coherence analysis pointed out a relatively large coherence at the seasonal scale (0.68) between DON in NWC and the DON load from the New Channel until 1998. Thereafter the coherence decreased to virtually zero. A cross-correlation analysis of the data from 1995 until 1998 (the period of high coherence) revealed a time lag of 4-5 months. A positive significant linear relationship (simple regression, $F_{1,42} = 7.7$, $p < 0.01$) was found between the DON load and the DON concentration at NWC, lagging by 4 months, but the coefficient of determination was only 15.5 %. As expected from the coherence analysis, no significant relationship was found after 1998. This was attributable to a reduced seasonal variability and more irregularity in the DON load (data not shown).

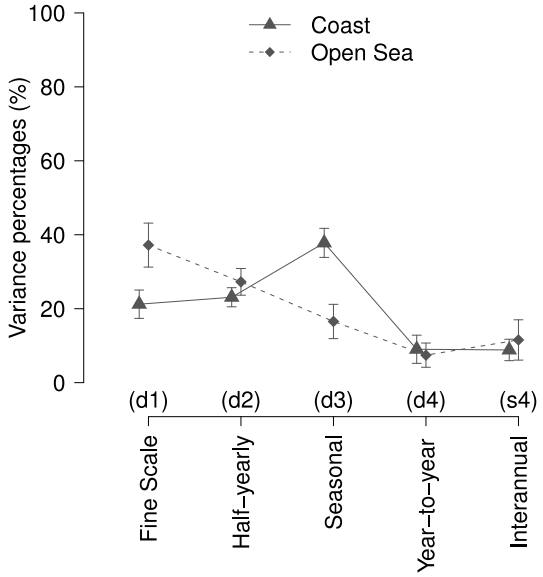

Figure 3.4: Percentages of the total variance per scale level for the DON series from the coastal (triangles, solid line) and offshore stations (diamonds, dashed line).

Table 3.4: For each scale the percentages of the total variance in the respective DON and DOC time series. The averages and standard deviations per region are for DON plotted in figure.

		Station	Fine scale (d_1)	Half-year (d_2)	Seasonal (d_3)	Year-to-year (d_4)	Inter-annual (s_4)
DON	coast	WAC	26	25	36	6	7
		GOC	23	20	40	7	10
		NWC	19	25	42	8	6
		TC	17	22	34	15	12
	open sea	WAO	34	31	15	7	13
		NWO	40	22	22	5	10
		TO	45	30	16	4	5
		OG	37	25	10	9	20
		DB	29	29	19	12	10
DOC	coast	WAC	19	28	39	8	6
		GOC	22	19	50	8	1
		NWC	17	25	49	8	2
		TC	14	23	50	9	5
	open sea	WAO	19	25	46	8	3
		NWO	19	24	41	9	6
		TO	21	30	34	4	10
		OG	18	26	34	7	16
		DB	15	21	45	6	13

3.3.2 Consistency of seasonality

Coherency analyses were performed between the DON concentrations (Fig. 3.2) and their average seasonality (Fig. 3.3) to further assess the consistency and/or year-to-year deviations from this average seasonality. Coherence of coastal DON signals with their average seasonal profile was high (median-values in the half-yearly and seasonal scale 0.39 and 0.84 resp.) corroborating the strength of the average seasonal profile as a descriptor.
In the open sea coherence between the average seasonal pattern and DON signals was relatively low at the seasonal scale (d_3) and generally even lower at the half-yearly (d_2) scale (median-values of 0.56 and 0.17 resp.), supporting our earlier findings from the station-specific seasonal profiles (see Fig. 3.3).

Coherency at the DB station (located on the Dogger Bank) was at the seasonal (d_3) scale very high between 1997 and 2005, except for the year 1999 when a phase shift of half a cycle occurred (Fig. 3.5b). This phase shift was only found in the seasonal scale (d_3) at this station. Unfortunately, the data set contains only one station at the Dogger Bank, which complicates independent verification. Neither TDN, nor any other nitrogen component exhibited a similar shift in our analyses (data not shown).

Figure 3.5 shows DON data at Dogger Bank with indication of the missing values, the result of the coherence analysis (only the seasonal scale is shown) and the seasonal distribution of DON prior and post 1999. The ecological interpretation of the phase shift in 1999

is obvious from the lower graph; Before 1999 (Fig. 3.5c) DON started to build up from April onwards (well within the spring bloom) and reached maxima in summer. After 1999 (Fig.3.5d) DON accumulated earlier, reached a maximum around March-April and then decreased to a minimum during summer.

The abrupt nature of the phase shift could in principle be attributable to the imputation of missing values in 1999 (Fig. 3.5a). However, the frequency and timing of the missing values were equal for all stations of the Terschelling transect, and none of the other stations showed a similar phase shift. Consequently, it is unlikely that the pattern at the Dogger Bank is due to missing values. Moreover, we used two different strategies to correct for missing observations. The first was a simple linear interpolation. The second strategy consisted of incorporating information on the seasonality in the year before and after the missing value. The missing value was then replaced by the average of the values surrounding the missing observation in a month-year map of the observations. Both strategies gave similar results, showing that the imputation method had no influence on the results of the coherence analysis. Because the signal is so strong in both periods (prior and post 1999) and does not depend on the presence or absence of missing data, and because the pattern is visible in the DON concentration data after the appropriate subdivision in time intervals, we believe that the pattern is genuine.

The DIN components were investigated to gain more insight in the nitrogen cycling at the Dogger Bank station (DB). No significant correlations existed between DON and NO_3^-, NH_4^+, or total DIN concentrations. Over the long term NH_4^+ decreased strongly at the Dogger Bank (and in the other offshore stations). Nitrate showed a tendency to decrease but this was less pronounced because winter values fluctuated throughout the years with a periodicity of around 4-5 years (data not shown). The concentration during the spring bloom (March-May), however, showed clear decreases at DB (Linear mixed-effects model with random month-effect, T = -3.34, $p < 0.01$). The number of months that concentrations fell below the detection limit (0.21 μmol l^{-1} for individual DIN components) increased throughout the period for all DIN components, but particularly for NH_4^+ from 1999 onwards (Fig. 3.6). Chlorophyll concentrations did not show any long-term trend, but high yearly averages occurred in 2000 and 2001 (1.9 $\pm$ 2.5 and 2.2 $\pm$ 2.6, respectively; mean $\pm$ sd; data not shown).

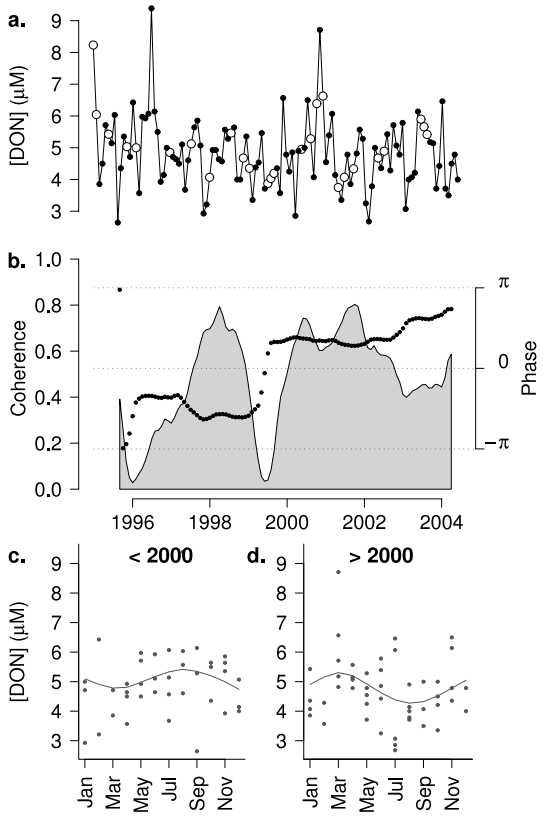

Figure 3.5: (a.) Time series of DON at DB (Dogger Bank). Interpolated values due to missingness are indicated by the open circles. (b.) Wavelet coherency (gray area; left axis) and phase difference (black dotted line; right axis) between the DON signal and its average seasonal profile as a function of time. (c. and d.) DON concentrations per month for the period before 2000 and from 2000 onwards with the global seasonal trend indicated by a spline smoother.

3.4 Discussion

Long-term records of inorganic nutrients have received considerable attention in the scientific literature as well as in policy and management. This is particularly true in the North Sea area because of its semi-enclosed nature and the high riverine nutrient inputs. The long-term inorganic nutrient record of the rivers and estuaries of the Scheldt (Soetaert et al., 2006; Billen et al., 2005), Rhine (de Jonge, 1997; van der Weijden and Middelburg, 1989; Nienhuis, 1992), Ems-Dollard (van der Veer et al., 1989; Essink, 2003) have been studied in

detail revealing increasing concentrations of N and P in the fifties to seventies and decreasing concentrations during the last two decades. The long-term evolution of inorganic nutrient concentrations in coastal waters of the North Sea area have been investigated in detail as well: Belgian Coastal Zone (Lacroix et al., 2004, 2007), Dutch coastal zone and Waddenzee (Cadée and Hegeman, 2002; van Beusekom and de Jonge, 2002; Philippart et al., 2007). De Vries and co-workers (1998) investigated the long-term record of the open North Sea based on the DONAR data set and compared model predictions with observations.

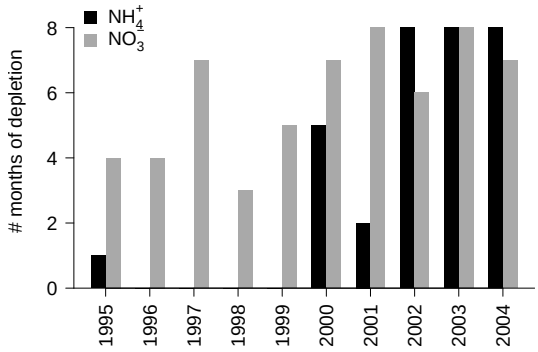

Figure 3.6: The number of months per year that the concentrations of ammonium and nitrate at the Dogger Bank (DB) remained below the detection limit.

Although DON contributed on average between 20 and 90 % (Tab. 3.3) to the TDN concentration, far less attention has been paid to this pool. This is problematic since DIN and DON pools are not separate entities because of intensive recycling via assimilation and regeneration processes involving prokaryotes and eukaryotes (Butler et al., 1979; Bronk, 2002). Moreover, atmospheric deposition results in significant anthropogenic organic nitrogen inputs (Jickells, 1995; Neff et al., 2002).

The North Sea was among the first systems to be investigated for DON distribution patterns (Tab. 3.5). Duursma (1961) was the first to analyze and report DON dynamics for a coastal station near the light vessel 'Texel' (53°1'N, 4°21'E), off the coast of the barrier island Texel, during the late 50-ies. Butler et al. (1979) reported DON dynamics and concentrations based on 9 years of data from the English Channel. De Galan et al. (2004) presented DON data for the Belgian Continental Shelf (BCS) from 1993-2000. More recently, van der Zee and Chou (2005), Badr et al. (2008), and Suratman et al. (2008) presented data for the 21st century but for a restricted number of years (Tab. 3.5). Our study adds significantly to this small, but increasing data set by presenting a medium to long-term study on dissolved organic nitrogen in the Dutch section of the North Sea.

Our data are largely consistent with those previous studies in the North Sea area and literature information for coastal systems in general. Bronk (2002) compiled existing literature and reported an average of 9.9 ± 8.1 μmol l^{-1} for coastal and continental shelf systems,

consistent with averages of 11.1 and 5.3 μmol l^{-1} for our coastal and open sea stations, respectively. Duursma (1961) reported DON concentrations between 5.8 and 12.4 μmol l^{-1} for a coastal station near Texel. Butler et al. (1979) reported DON values for the English Channel varying from 4.5 to 10.1 μmol l^{-1}. For waters of the Belgian continental shelf (BCS), De Galan et al. (2004) reported mean concentrations of 20.9 and 15.2 μmol l^{-1} for coastal waters with salinities higher and lower than 33, respectively. Their higher values are most likely attributable the strong influence of the nutrient-rich Scheldt estuary and its plume on the BCS. In addition, they used microwave-based destruction of TDN (Dafner et al., 1999), whereas combined persulphate-UV destruction was used in the Dutch monitoring (Koroleff, 1983). Our average DON percentages in TDN were in good agreement with those reported by De Galan et al. (2004) for the corresponding time interval. Suratman et al. (2008) reported DON concentrations for the British section of the North Sea adjacent to our study area and reported values between 4.2 and 8.9 μmol l^{-1}, again consistent with our data for the open sea (Tab. 3.2). This consistency in DON concentration levels between studies covering different parts of the North Sea and over a number of decades suggest that DON concentrations have experienced little if any changes, except for the coastal zone directly under influence of riverine inputs.

No net changes (secular trends) in DON concentrations throughout the measurement period (1995-2005) could be detected. On scales of a few years variation was apparent, but most of the temporal variability was situated at intra-annual scales (Tab. 3.4). The DIN concentrations, however, showed marked decreases, and consequently the organic fraction of TDN on average increased significantly in coastal and open waters of the North Sea. This was most pronounced during summer in the open sea, but was also observed during winter at most locations. At southern coastal stations WAC and GOC DON fractions initially decreased during winter (data not shown), corroborating the decreasing tendencies in the DON fraction in Belgian coastal waters between 1993-2000 (De Galan et al., 2004). DIN decreases have been repeatedly reported for estuaries (Soetaert et al., 2006; Billen et al., 2005), but less often for the coastal North Sea. De Vries et al. (1998) found significant decreases in DIN concentrations for the DCS, but De Galan et al. (2004) found no trend in total DIN for the Belgian coastal zone. McQuatters-Gollop et al. (2007) reported decreases in total nitrogen in the coastal North Sea between 1980 and 2000 as well; no distinction was made between DIN and DON. Loebl et al. (2009) found indications for nitrogen limitation (co-limitation with light) at stations from the NW transect (during small distinct periods at the coast, but more or less each year from 1998 until 2004). Peeters and Peperzak (1990) also demonstrated a predominant potential nitrogen limitation in the open southern North

Table 3.5: Study sites, sampling periods and sampling intervals of the DON related studies that were referred to in this work.

Study	Location	Period	Sampling interval
Badr et al. (2008)	Yealm and Plym estuaries, England	Feb 2002−Sep 2003	monthly
Banoub & Williams (1973)	English Channel	1968	monthly
Brockmann & Kattner (1997)	North Sea	May−Jun 1986/Jan−Mar 1987	2 campaigns
Butler et al. 1979	English Channel	1969−1977	monthly
De Galan et al. (2004)	Belgian Continental Shelf	Jul 1997−Oct 2000	3-monthly
Duursma (1961)	Light vessel 'Texel', Dutch Continental Shelf	Jun 1958−May 1959	2-weekly
Glibert et al. (2007)	Chincoteague Bay, Maryland, USA	1996−2004	monthly
Hansell & Carlson (2001)	Bermuda Atlantic Time-Series site, Sargasso Sea	1994−1998	monthly
Karl et al. (2001)	Station ALOHA, central Pacific Ocean	Oct 1988−Dec 1997	monthly
Knapp et al. (2005)	Bermuda Atlantic Time-Series site, Sargasso Sea	Mar 2000−May 2001	monthly
Suratman et al. (2008)	East Coast of UK -central North Sea	autumn 2004−summer 2005	3-monthly
van der Zee & Chou (2005)	Belgian Continental Shelf	September 2002−December 2003	monthly

Sea in their bio-assays from 1988, particularly in summer. The increasing DON to TDN ratio suggest that DON becomes more important as nutrient for algae and bacteria, and that more knowledge on DON dynamics is required to fully comprehend the N-cycle in this area.

Our wavelet-based variance partitioning showed distinct scalewise distribution patterns of DON and DOC. Whereas the coastal stations showed pronounced seasonality for both DON and DOC (i.e. a dominance of the d_3 wavelet variance), only DOC exhibited a clear seasonal cycle in the open sea (Tab. 3.4). DON in open sea showed temporal variability predominantly at finer scales (Fig. 3.4, Tab. 3.4).

A number of other studies have considered seasonality in DON, but there appears to be no simple systematic among them. Duursma (1961) investigated a coastal station near Texel in the 50-ies and found a seasonal pattern similar to ours for coastal stations. Banoub and Williams (1973) documented a seasonal cycle at a site in the English Channel for 1968, similar to findings by van der Zee and Chou (2005) for the BCS in 2002-2003: high values in early spring and decreasing values throughout summer. De Galan et al. (2004), however, reported for the same area an absence of a clear seasonal DON cycle for the period 1993-2000. But in the latter study samplings were performed only three to four times per year for four years, which would be insufficient clearly separate seasonality from other variability in their data. A consistent seasonal signal was found by Butler and co-workers (1979) for a coastal station in the English Channel, but maximal concentrations were reached only in August in their study, whereas the Dutch coastal stations exhibited maxima around April-May (Fig. 3.3). Williams (1995) made a meta-analysis of DOC and DON dynamics in coastal systems and reported high variability in the seasonality of DON. Nevertheless, Glibert and co-workers (2007) reported a consistent seasonality of DON in Chincoteague Bay (Maryland, USA) with increasing values towards July-September followed by a decrease towards January. It should be noted that the latter study and the Butler et al. study in the Channel area were the only investigations of seasonality based on long-term data sets. Comparing the seasonal profiles from Banoub and Williams (1973; data from 1968 only) with those from Butler et al. (1979) for the same region, it is clear that the seasonality in DON may be subject to change as we observed in this study in the Dogger Bank. This further emphasizes the need for rigorous monitoring to accurately describe the spatial and temporal consistency of ecological patterns. We have not been able to find studies on DON in the open North Sea. Suratman et al. (2008) reported seasonal DON data for coastal and open sea stations in the western part of the North Sea. The seasonal amplitude was comparable with our coastal stations, but with the highest values occurring in winter and lowest in summer. Open ocean studies at the BATS-station (North Atlantic Ocean; Hansell and Carlson (2001); Knapp et al. (2005)) and ALOHA-station (North Pacific Ocean; Karl et al. (2001)) revealed an absence or very low (undetectable) seasonal component in the DON variability, consistent with our findings for open North Sea stations (Fig. 3.3).

From a mechanistic point of view, the difference in strength of the seasonality between the coastal zone and the open sea at the DCS can most likely be attributed to difference in the contributions of transport fluxes and metabolic fluxes in and out of the DON pool; The Dutch coastal zone is heavily influenced by river discharge, particularly from the Rhine

(e.g. Cadée and Hegeman (1993)). While some seasonality was found in the riverine DON concentrations and loads, it only explained 16 % of the variability in the coastal station downstream along the northward coastal current (NWC). It is difficult to assess the exact contribution to the seasonal variation in the coastal zone, which would require extra modeling of the physical transport to the stations that were investigated here. But this would lead to far for this study. Beside the physical transport from the rivers, a buildup of DON throughout the growth season, followed by a period of remineralization at the end of the year could (partially) account for the consistent seasonal trend that was found in the coastal zone, as well. This was supported by the close agreement and 1-month time lag between the coastal chlorophyll a concentration and the DON concentration, which suggests a production during the bloom and a subsequent removal by remineralization and/or transport (Fig. 3.3). If however remineralization by bacteria or direct uptake of DON by algae becomes crucial for providing sufficient nutrients for plankton throughout the growing season (as expected for the open sea), a more erratic behavior lacking a large buildup could be expected. Both the on average lower concentration and the erratic seasonality indicate that DON was utilized by algae and/or bacteria in the nitrogen poor (Fig. 3.6) open North Sea stations. This is corroborated in figure 3.6, where we have plotted the number of months that NH_4^+ and NO_3^- were depleted (undetectable). From this graph it is clear that the period of NO_3^- depletion has increased over the time period. From 1999 on we observe significant NH_4^+ depletion as well.

DOC exhibited seasonal variability in both the coastal zone and open sea, possibly because of the more refractory nature of this pool. Primary producers generally require DIC for carbon supply, rather than DOC through heterotrophic uptake. Although uptake of certain organic molecules is possible (see Bronk et al. (2007) and references therein), it is likely that organic nitrogen is selectively removed from the less useful carbon skeleton (Palenik and Morel, 1991). This would render different proportions of the DOC and DON pool more or less refractory, ultimately leading to differential turnover times (i.e. rates). This could explain the differential distribution of variance over scales for DOC relative to DON (Tab. 3.4). Whereas the DOC builds up in the water column throughout the season to be remineralized once all the phytoplankton activity has decreased, the DON is constantly efficiently recycled by the microbial community thus preventing buildup on a larger seasonal scale.

Although the amount of variation was relatively low, the site on the Dogger Bank (DB) showed initially a DON seasonality with high concentrations in late-summer and low DON in winter (Fig. 3.5). This changed to high spring concentrations and low summer concentrations in a time span of two years (1998-2000). Considering the decline in dissolved inorganic nitrogen and the increase in number of months with inorganic nitrogen depletion, an increased recycling pathway of DON could be responsible for this pattern. Despite the decrease in dissolved inorganic phosphate (DIP), the DIN/DIP ratio decreased throughout the period from 6.9 to 3.8 (unpublished data), indicating a potentially severe nitrogen limitation. Loebl et al. (2009) found indications of nitrogen-light co-limitation at NWO from 1998 onwards. It is possible that this limitation pattern is stronger towards the central North Sea, due to the larger distance from riverine nitrogen sources. Baretta-Bekker and co-

workers (2009) also reported strong changes in the phytoplankton community composition of the North Sea station that were used in this study. At the Dogger Bank dinoflagellates increased quite abruptly from 1999 to 2000, while flagellates and *Phaeocystis sp.* decreased over a roughly two years time towards 1999 (Baretta-Bekker, pers. comm.). Dinoflagellates and flagellates have often been associated with DON dynamics (Berg et al. (2003); Palenik and Morel (1990b); Stoecker and Gustafson (2003); Mulholland et al. (2004); Glibert et al. (2006), 2007). Whether there exists a cause-effect relationship between the DON dynamics and the community structure is difficult to prove, but the similarity in timing is rather striking. And, if we can assume a direct link, the direction of the link is not clear, considering that dinoflagellates and Phaeocystis are known to produce DOM (e.g. HAB toxins and foam after the *Phaeocystis* bloom) and to consume DOM (Berg et al., 1997; Mulholland et al., 2004). Although the decline in inorganic N/P ratio was gradual, the sudden shift in community composition could indicate a threshold effect. Note that Weijerman et al. (2005) also found indications of a region wide regime shift around 1998. Stronger recycling of organic substances was also invoked by McQuatters-Gollop and co-workers (2007) to explain the higher productivity under lower nutrient conditions in the contemporary North Sea.

Considering the small fraction of DON variability in the seasonal scale (d_3), it is not surprising that this is not clearly visible in the DON time series plot. Although the quantitative importance of the seasonal scale in the overall variability in DON at Dogger Bank is limited, the shift can be qualitatively important.

Brockmann and Kattner (1997; Fig.3.3) reported slightly higher average DON values in the summer of 1986 than in following winter for the Dogger Bank region but the differences were small. However, Suratman et al. (2008) reported significantly lower summer concentrations than winter concentrations in 2004-2005 north of the Dogger Bank. These two papers are consistent with our findings on the Dogger Bank, but they did not report on the temporal stability of their seasonal patterns.

To our knowledge, this is the first study to investigate the temporal variability in DON in the North Sea. We have used 10 years of DON measurement data with a monthly sampling frequency, which allowed us to assess the seasonal consistency and multi-year variability in a part of the southern North Sea. Our study showed that the coastal DON dynamics fundamentally differ from those in the open sea, most likely due to the input of nutrients from the rivers, which are hypothesized to regulate nitrogen regeneration (effluxes from the DON pool). In addition, from combined time scale analyses it was clear that the mode of intra-annual variation can change over time. This emphasizes the need for rigorous monitoring on at least a monthly basis, and for the application of appropriate time series analysis techniques.

The wavelet variance analysis illustrated that the variability in the open sea is predominantly present in the finest temporal scales at our disposal. To fully grasp this variability and assess its statistical and ecological significance we would probably need higher sampling frequencies. This also follows from the numerous results in the literature on DON uptake in a matter of hours. The same applies to the spatial component of the variability. We were not able to correct for horizontal transport effects because these data were lacking. It is very likely that by using higher sampling frequencies, the uncertainty due to physical (pre-

dominantly wind-driven) transport would be reduced. In addition, although the variability at the between-station level was minimal, the patterns in the open sea were so distinctly different between the stations that a coherent picture in the spatial sense was not feasible. Considering the stability of typical hydrographic structures, such as East-Anglian plume (Weston et al., 2004), and the strong influence of rivers, extension of the spatial sampling pattern to include a good coverage of these structures is desirable. As the monthly sampling continues, it will become feasible to put the dissolved organic parameters against a climatological background.

3.5 Conclusion

This study has provided evidence for systematic variability in DON that can be understood in the light of nitrogen acquisition from this complex pool. This stresses the need to consider DON as a separate ecosystem component that should be monitored on a regular basis and included as such in eutrophication modeling. In addition, the use of appropriate time series analysis techniques is highlighted.

4. Potential uptake of dissolved organic matter by seagrasses and macroalgae

Van Engeland T., T. J. Bouma, E. P. Morris, F. G. Brun, G. Peralta, M. Lara, I. E. Hendriks, K. Soetaert & J. J. Middelburg. (In prep.)

Abstract - *Dissolved organic nitrogen (DON) acts as a large storage reservoir of nitrogen. Whereas DON utilization is common in the microbial community, little is known about DON utilization by macrophytes. We investigated the ability of two coexisting temperate seagrasses (Zostera noltii and Cymodocea nodosa) and a macroalga (Caulerpa prolifera) to take up nitrogen and carbon from small organic compounds of different complexities (urea, glycine, L-leucine, and L-phenylalanine) and from DON derived from algal and bacterial cultures (substrates with a complex composition). In addition to inorganic nitrogen, which was the preferred source, nitrogen from small organic compounds could be taken up in considerable amounts by all macrophytes. Preference for urea and individual amino acids was related to the substrate's structural complexity and/or C/N-ratio. The spectrum of compounds taken up by the aboveground tissue differed from that of the belowground tissue. No clear relationship between carbon and nitrogen uptake from small organic compounds was found. Uptake of algae-derived organic nitrogen was of the same order of magnitude as inorganic nitrogen, and was preferred over bacteria-derived nitrogen. This study demonstrates that aquatic macrophytes can take up significant quantities of nitrogen from a the DON reservoir within a matter of hours, suggesting that DON cycling must play an important role in these highly productive systems.*

4.1 Introduction

Seagrass ecosystems are highly productive and exhibit a strong nutrient retention capacity (Stapel et al., 2001). The affinities and uptake rates of seagrasses for dissolved inorganic nitrogen (DIN) are high (Stapel et al., 1996), keeping ambient DIN concentrations low and potentially limiting (Bulthuis et al., 1992). Efficient nutrient recycling then represents a vital ecosystem function (Boon et al., 1986; Ziegler and Benner, 1999b). Two major ecological pathways exist for the supply of regenerated nitrogen to primary producers: (1) DIN uptake after remineralization of dissolved organic matter, and (2) direct uptake of dissolved organic nitrogen (DON; Palenik and Morel, 1991; Berg et al., 1997; Stoecker and Gustafson, 2003). Regardless of which pathway is the more important, DON occupies a central position in the nitrogen recycling process, since it also represents the largest pool of fixed nitrogen which is directly or indirectly accessible (Bronk, 2002).

Dissolved organic matter (DOM) utilization is widespread in microbes and primary producers. Traditionally, DOM is regarded as a nutrient and energy source for heterotrophic bacteria, which represent a major sink for DON, not only via bacterial growth but also remineralization (Seitzinger and Sanders, 1997; Kerner and Spitzy, 2001). Many phytoplankton taxa, particularly dinoflagellates and pelagophytes are also able to use organic nitrogen (Admiraal et al., 1987; Palenik and Morel, 1990a; Berg et al., 2002). Urease activity appears widespread in microalgae (Solomon and Glibert, 2008), and some phytoplankton species exhibit proteolytic activity (Stoecker and Gustafson, 2003), amino acid uptake and/or amino acid oxidation (Mulholland et al., 2002). DON uptake has also been demonstrated in macroalgae. Urea uptake occurs in several seaweeds (Phillips and Hurd, 2003; Tyler et al., 2001). Tarutani et al. (2004) also observed autonomous uptake of amino acid nitrogen without bacterial intervention by *Ulva pertusa*. Tyler et al. (2005) investigated amino acid utilization in *Ulva lactuca* and *Gracilaria vermiculophylla*, and found different modes of uptake depending on the species and amino acid.

Whereas some information on DON uptake in macroalgae exists, virtually nothing is known about the uptake of DON by seagrasses. Bird et al. (1998) illustrated the axenic growth of *Halophila decipiens* on glutamic acid as sole nitrogen source. But until recently small organic compounds were not even considered as a direct nutrient source for seagrasses (Romero et al., 2006). Uptake of detritus-derived compounds by seagrasses has, however, been demonstrated by Brun et al. (2003), Evrard et al. (2005), and Barron et al. (2006). Although these studies did not indisputably show that the DOM was taken up as such without prior remineralization, they did illustrate the availability of organic nitrogen (or carbon) to primary producers in a matter of hours to days. Vonk et al. (2008) recently demonstrated significant nitrogen uptake of amino acid mixtures and urea in several tropical seagrasses. These few available studies clearly indicate that DON is a potentially important source of nitrogen in seagrass systems but at the same time remains a little understood aspect of seagrass nutrition.

To increase our understanding of nitrogen cycling and the role of DON uptake within seagrass meadows, we addressed the following questions: (1) Are macrophytes able to take up significant amounts of specific organic compounds? (2) What is the magnitude of up-

take of N from a composed DON pool (a semi-natural pool consisting of different types of compounds, such as urea, amino acids, purines, ...) when compared to DIN or uptake of individual compounds? (3) Is there an influence of compound complexity on organic nitrogen uptake? (4) How does the substrate spectrum of leaf-mediated uptake differ from that of root-mediated uptake. (5) Is there a concurrent uptake of the organic carbon? To address these questions, we conducted a laboratory experiment in which we measured the potential uptake of dissolved organic matter by three macrophyte species *Zostera noltii*, *Cymodocea nodosa*, and *Caulerpa prolifera*. Separate incubations of aboveground and belowground plant parts with ^{13}C and ^{15}N double-labeled organic substrates of differential complexity were used to investigate organic carbon and nitrogen uptake.

4.2 Materials & Methods

4.2.1 Experimental setup

Specimens of *Zostera noltii* Hornem, *Cymodocea nodosa* Ucria (Ascherson), and *Caulerpa prolifera* (Forsskål) J. V. Lamouroux were collected in the field near Santibañez (36°28'12.79"N, 6°15'7.07"W; Càdiz, Spain) and immediately brought to the laboratory. Epiphytes were removed from the macrophyte leaves by gently scraping with a razor blade. Filtered water (GF/F filter, Whatman) from the same location was used as incubation medium. Note that a GF/F filter retains a part of the bacterial community but not all bacteria. The incubations were performed in a climate-controlled room. Macrophytes were left intact with their aboveground and belowground parts in separate plastic cups (123 ml). Cups were filled almost to the top so as to minimize local desiccation of the plants where they protruded out of the water, while care was taken to prevent mixing of water between cups via capillary effects or spilling (Fig. 4.1). Inorganic and organic compounds of various complexities were added either to the 'aboveground' cup or to the 'belowground' cup at final concentrations indicated in table 4.1. Plants were incubated for approximately 3 hours in a three-way full-cross design with 3 species, 8 substrates, 2 plant parts (aboveground vs. belowground), and 3 replicates. The water in the cups was stirred constantly to prevent local depletion and the buildup of concentration gradients. To avoid experimental artifacts, concentrations were kept at realistically low levels as expected for the ambient concentrations (Tab. 4.1). Due to small volume of the cups this means that the substrate could have been depleted during the experiment. However, regarding the objective of determining if macrophytes could take up DON of different complexities under realistic conditions rather than quantifying the uptake kinetics, this was not a problem. After incubation the plants were rinsed with clean filtered seawater, dabbed with paper tissue, dissected, and stored at -20°C until they were freeze dried, weighed and ground to a fine powder in the laboratory. *C. nodosa* leaves, sheaths, rhizome, and roots were processed separately. No such separation was possible for the *Z. noltii* specimens because of the lower biomass per plant compared to the other macrophytes. The *Z. noltii* plants were dissected into an aboveground part further referred to as 'leaves', and a belowground part further referred to as 'roots' for simplicity. The *C. prolifera* individuals were dissected into three parts: the assimilators (from now on referred to as 'leaves'), the

stolons, and the rhizoids (from now on referred to as 'roots' for simplicity). The sheaths of the *C. nodosa* specimens and the stolons of the *C. prolifera* specimens were not analyzed, because no clear distinction was possible between the part in the 'aboveground' cup and the part in the 'belowground' cup.

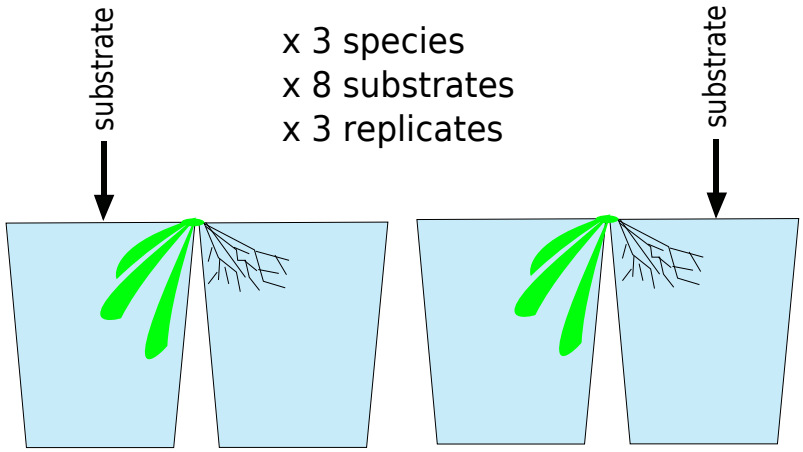

Figure 4.1: Incubation of macrophytes in cups. Root and leaf incubations were performed separately.

4.2.2 Inorganic and organic substrates

Ammonium and NO_3^- served as reference because a large body of literature exists describing their uptake kinetics by a variety of marine macrophytes. Urea and the amino acids glycine, L-leucine and L-phenylalanine were used as small organic nitrogen sources with increasing complexity; Glycine is a fairly simple achiral amino acid with hydrogen as R-group. Leucine is more complex and chiral with an iso-butyl group on the α-carbon. Phenylalanine has a benzene-like ring (phenyl) as R-group, which is considered chemically very stable (resistant to degradation). In addition, the C/N ratio of these amino acids also increases from glycine (2) to L-leucine (6) to L-phenylalanine (9). Finally, two composed DOM pools were used to mimic complex DON from the environment (see section 4.2.3). Both the nitrogen and carbon were present as the heavy isotope in the organic substrates (Tab. 4.1), thus enabling us to study the potential coupling of carbon and nitrogen uptake. Moreover, the use of isotope tracers allowed us to investigate uptake at nitrogen concentrations similar to these found in natural systems.

4.2.3 Preparation of algae and bacteria-derived DOM

Two complex pools of dissolved organic matter were created, one from a culture of soil bacteria grown on ^{13}C-glucose and $^{15}NH_4Cl$, and one from an axenic culture of *Skeletonema*

Table 4.1: The substrates (Cambridge Isotope Laboratories) used for this experiment, their final concentrations in the incubations, and the chemical structure of the small organics. The substrates marked by a * are only used in the DOM preparation.

Code	Name	Labeling	concentration (μM-N)	structure
CLM-441-5	$NaHCO_3$	(^{13}C, 99%)	*	
NLM-467-5	NH_4Cl	(^{15}N, 99%)	1	
NLM-157-1	$NaNO_3$	(^{15}N, 98%)	1	
CNLM-234-0.5	Urea	(^{13}C, 99%; $^{15}N_2$, 98%)	2	
CNLM-1973-0.25	Glycine	($U^{13}C_2$, 98%; ^{15}N, 98%)	0.1	
CNLM-281-0.1	L-Leucine (SILAC)	($U^{13}C_6$, 98%; ^{15}N, 98%)	0.1	
CNLM-575-0.25	L-Phenylalanine	($U^{13}C_9$, 98%; ^{15}N, 98%)	0.1	
CLM-1396-10	D-Glucose	($U^{13}C_6$, 99%)	*	

costatum grown on $NaH^{13}CO_3$ and $Na^{15}NO_3$ using a modified protocol from Miller (1972). After incubation, the cells were freeze dried. The biological material was added to 10 ml of milli-Q water and shaken for 48 hours at room temperature after addition of Devarda's alloy and MgO to remove inorganic nitrogen. The supernatants were collected after centrifugation, and diluted to 20 ml. These substances were frozen at -20°C until further use.

The DON concentrations in the algae-derived and bacteria-derived substrates were 14.6 mmol-N l^{-1} and 19.3 mmol-N l^{-1} with a ^{15}N atom percentage of 66% and 46 % respectively. The DOC concentrations were 124 mmol-C l^{-1} and 690 mmol-C l^{-1}, with a ^{13}C atom percentage of 8% and 46% respectively. Hence, after addition to the incubation medium, DON concentrations were 0.5 μmol-N l^{-1} and 6.7 μmol-N l^{-1} for algae-derived and bacteria-derived DOM respectively, and DOC concentrations were 4.3 μmol-C l^{-1} and 24 μmol-C l^{-1} respectively.

Note that the eventual DON pools in the incubations are a mixture of DON from various autotrophic and heterotrophic origins (which was already present in the incubation medium) with most likely a tasty donut fraction that is mainly in the added fresh DON (algal DON in one set of incubations, bacterial DON in another). Dissolved combined amino acids (DCAA) comprised 84 ± 24 % and 47 ± 11 % of the DON and 34 ± 11 % and 46 ± 12 % of the DOC in the algae and bacteria-derived substrates respectively. L-alanine and L-leucine were dominant in the DCAA fraction of DON substrates (Fig. 4.2a.). The free amino acid (FAA) fraction in total hydrolysable amino acids (THAA) was for algae-derived DON dominated by L-arginine and by L-glutamate (Fig. 4.2b).

4.2.4 Stable isotope and nutrient measurements

Dissolved inorganic nitrogen concentrations (DIN = NH_4^+ + NO_2^- + NO_3^-), urea and inorganic phosphate (DIP) were determined colorimetrically in filtered incubation medium (GF/F filter; Whatman; Middelburg and Nieuwenhuize (2000)). DON was calculated as the difference between total dissolved nitrogen (TDN), determined as NO_3^- after a alkaline persulphate destruction (Grasshoff et al., 1999), and DIN. Dissolved organic carbon (DOC) concentrations were measured with an auto-analyzer (Skalar SK12 organic carbon analyzer) after filtering the water over a GF/6 filter (Whatman). Dissolved free amino acids (DFAA) were determined prior to hydrolysis by HPLC on a Waters HPLC system with a 996 photodiode array detector (Fitznar et al., 1999), total hydrolysable amino acids (THAA) post hydrolysis, and dissolved combined amino acids by difference (DCAA = THAA - DFAA).

Bulk carbon and nitrogen content and relative abundances of ^{13}C and ^{15}N in the plant tissue and the concentrated DON substrates were measured using a Thermo EA 1112 elemental analyzer coupled to a Thermo Delta V Advantage isotope ratio mass spectrometer with a Conflo II interface (EA-IRMS; Vonk et al. (2008)). Concentrations and relative abundances of ^{13}C and ^{15}N for the amino acids in the DON concentrates were analyzed by gas chromatography-combustion-isotope ratio mass spectrometry (GC-c-IRMS) using a HP 6890 GC with a Thermo type III combustion interface and Thermo Delta Plus IRMS.

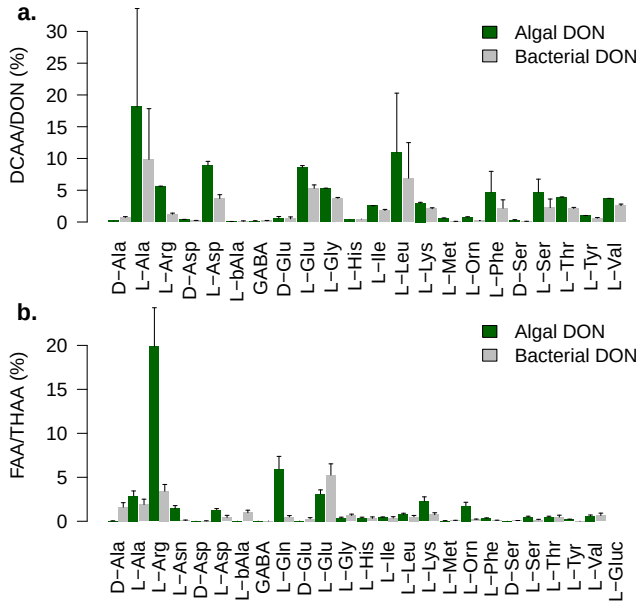

Figure 4.2: Percentages of the dissolved combined amino acids (DCAA) in the DON (a.) and percentages of free amino acids (FAA) in total hydrolysable amino acids (THAA) in terms of nitrogen for bacteria-derived and algae-derived DON.

4.2.5 Data treatment

Due to the wide range of labeling intensities our calculations were based on isotope fractions ($F^{15}N$ and $F^{13}C$) instead of δ-values (Fry, 2006). Isotope excesses were calculated as the difference between the isotope fraction in the sample and the natural abundance:

$$E_{sample} = F_{sample} - F_{nat.ab.}$$

Significance of the N and C uptake was tested as the difference between F_{sample} and $F_{nat.ab}$ using the t-statistics of a generalized weighted least-squares model in the statistical package R (R Development Core Team, 2009). Significance of an overall treatment effect was checked using the F-statistic of this model. All tests were done at the 5 %-significance level. Specific uptake rates of heavy isotope V were calculated as the quotient:

$$V = POM \times E_{sample}/(Time \times dryweight),$$

(where POM is organic matter content in terms of carbon or nitrogen) expressed in μmol (^{13}C or ^{15}N) mgDW^{-1} h^{-1}. Corrections for differential substrate concentrations were accomplished by dividing V by the substrate concentration in terms of nitrogen or carbon added (converted to percentages figs. 4.4 and 4.5):

$$\%V = 100 \times V/C(orN)_{added}.$$

This rate of uptake normalized to the amount of substrate available gives a rough indication of the preference for a particular nutrient source. Note that preferences in treatments with an equal of amount substrate added can be compared as if they were specific uptake rates. The total amount of heavy isotope taken up (I_i) during the incubation ($\approx$ 3 hours) was calculated as:

$$I = E_{sample} \times POM,$$

expressed in μmol, where POM is the amount of nitrogen or carbon in the macrophytes (in μmol).

4.2.6 Natural Abundances

Tissue ^{15}N natural abundances ranged between 1 and 4 ‰ and were different per plant part and per species (Fig. 4.3a.). No difference in ^{15}N abundance was apparent between aboveground and belowground tissue of *Zostera noltii*, while rhizomes of *Cymodocea nodosa* had a lower ^{15}N content than the roots and leaves. *Caulerpa prolifera* exhibited ^{15}N enrichment in the leaves relative to the roots. The seagrasses were enriched in ^{13}C relative to *C. prolifera* (Fig. 4.3b.). Belowground organs were enriched relative to leaves in all three species, likely due to storage of ^{13}C-rich carbohydrates.

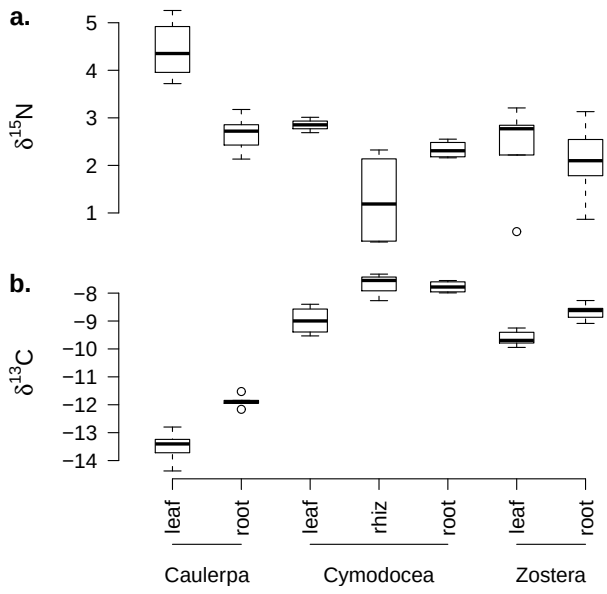

Figure 4.3: Natural isotope abundances ($\delta^{15}N$, a; $\delta^{13}C$, b) of the relevant plant parts.

4.3 Results

4.3.1 Potential uptake of nitrogen compounds

Leaf-mediated N uptake

For each species the type of labeled substrate had a significant effect on the atom percentage enrichment of ^{15}N over natural abundances when added to the aboveground parts (Generalized Linear Model with corrections for differential variance per treatment, $F_{8,18} = 39$, $p < 0.0001$ for *Zostera noltii*, $F_{8,18} = 23$, $p < 0.0001$ for *Cymodocea nodosa*, and $F_{8,18} = 76$, $p < 0.0001$ for *Caulerpa prolifera*). With the exception of the L-phenylalanine addition, all treatments exhibited significant uptake of ^{15}N in the *Z. noltii* plants (Pairwise t-tests; Fig. 4.4). For the *C. nodosa* plants significant nitrogen uptake was found for all treatments, except NO_3^- and urea for which uptakes were highly variable. *C. prolifera* individuals exhibited significant ^{15}N uptake for all substrates.

Tissue ^{15}N preferences (Fig. 4.4, left column) expressed as the percentage of the added substrate taken up per unit of time and per unit of dryweight were higher for inorganic nitrogen, than for urea and amino acids. *C. prolifera* leaves preferred NO_3^-, while NH_4^+ was preferred by the seagrass leaves. The seagrasses exhibited progressively declining preferences for the small organic compounds with increasing substrate complexity. The preference for algae-derived DO^{15}N was higher than for bacteria-derived DO^{15}N in all macrophytes.

Some statistically significant ^{15}N excesses over natural abundances were found in the belowground parts (e.g. for the glycine and leucine addition to *C. nodosa*; $t = 4.4$, $p = 0.036$ and $t = 4.3$, $p = 0.037$), but they were quantitatively negligible indicating a virtual absence of translocation from aboveground to belowground parts over the approximately 3 hours of incubation time.

Root mediated N uptake

For each species the type of labeled substrate had a significant effect on the specific ^{15}N uptake rates per amount of substrate when added to the belowground parts (Generalized Linear Model with corrections for differential variance per treatment, $F_{8,15} = 126$, $p < 0.0001$ for *Zostera noltii*, $F_{8,15} = 105$, $p < 0.0001$ for *Cymodocea nodosa*, and $F_{8,16} = 97$, $p < 0.0001$ for *Caulerpa prolifera*). *Z. noltii* exhibited significant ^{15}N uptake of all substrates (Paired T-tests, $p < 0.001$ for each treatment; Fig. 4.4, right column). Similar qualitative results were found for the *C. nodosa* roots. The rhizomes (data not shown) also exhibited similar patterns but the excesses were two orders of magnitude smaller and not significant. *C. prolifera* roots exhibited significant ^{15}N uptake in all substrate treatments, except the glycine addition.

The spectrum of compounds taken up by the belowground parts differed quantitatively from the uptake characteristics of the aboveground parts (Fig. 4.4). NH_4^+ was the preferred substrate in root-mediated uptake, whereas the NO_3^- and urea N fluxes per unit added nitrogen were relatively unimportant. Root-mediated glycine uptake was larger the seagrasses than the uptake of L-leucine and L-phenylalanine (preferences for the amino acids can be

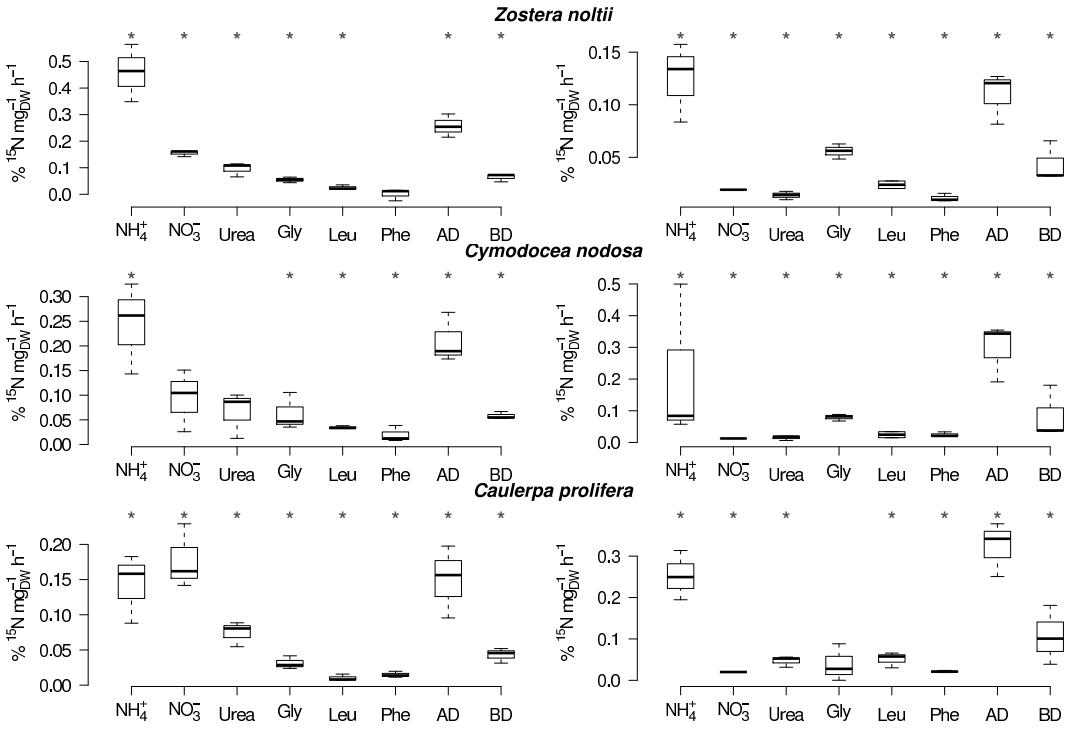

Figure 4.4: ^{15}N uptake rates in the leaves (left) and roots (right) of *Zostera noltii*, *Cymodocea nodosa*, and *Caulerpa prolifera* expressed as a percentage of the substrate added per milligram of dryweight and per hour of incubation time. Significant excesses are indicated with an asterisk.

compared as if it were specific uptake rates, since the added concentrations in terms of nitrogen were the same for all amino acid substrates). For *C. prolifera* no clear quantitative distinction existed between the amino acids (Fig. 4.4). Algae-derived and bacteria-derived DON uptake by the belowground tissue of *C. prolifera* and *C. nodosa* were quantitatively more important than by their aboveground parts (Fig. 4.4, added concentrations were the same in aboveground and belowground incubations). Algae-derived DON was again the preferred nitrogen source relative to bacteria-derived DON. Just as for the substrate additions to the aboveground tissue, those to the belowground parts showed no strong indications of translocation.

4.3.2 Concurrent organic carbon and nitrogen uptake

For the double-labeled (^{15}N and ^{13}C) organic substrates we also considered carbon uptake and its relation to nitrogen uptake. In general, the carbon signals were weaker than the corresponding nitrogen signals, more variable per treatment, and even negative excesses were observed (Fig. 4.5). Using a similar linear model as for the nitrogen uptake, significant

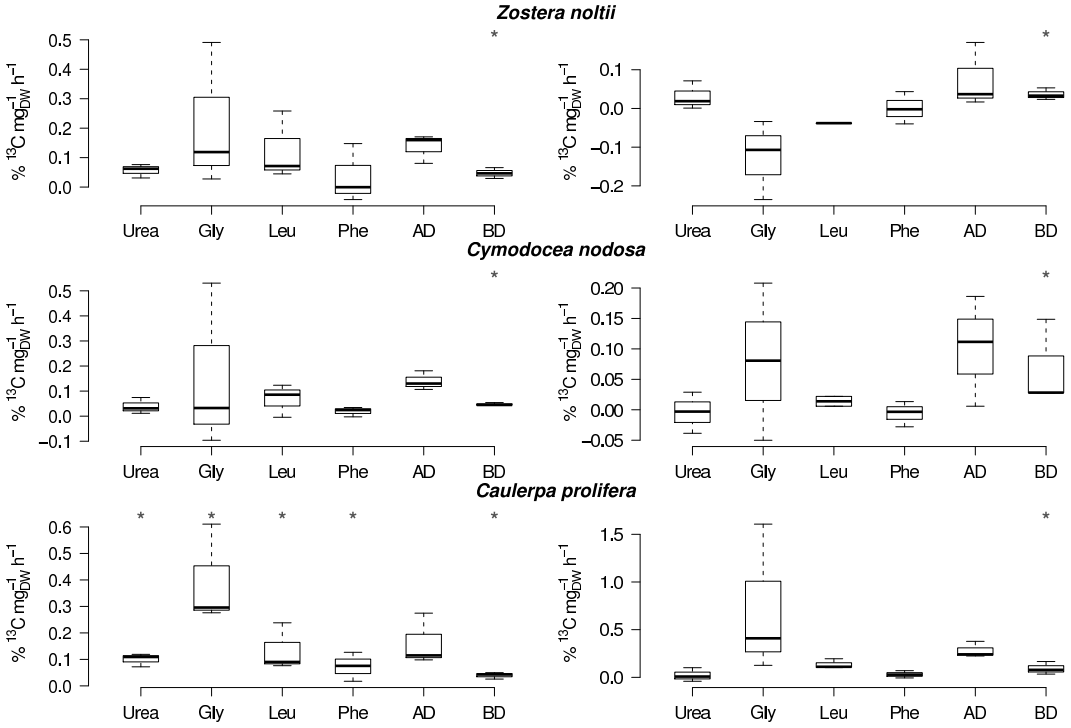

Figure 4.5: ^{13}C uptake rates in the leaves (left) and roots (right) of *Zostera noltii*, *Cymodocea nodosa*, and *Caulerpa prolifera* expressed as a percentage of the substrate added per milligram of dryweight and per hour of incubation time. Asterisks above the boxplots indicate statistical significance of excesses.

excesses in heavy carbon relative to natural ^{13}C fractions were found in the leaves for the bacteria-derived DOM additions in all species, and for urea, glycine, leucine, and phenylalanine in *Caulerpa prolifera* ($p < 0.05$). The carbon excesses for the amino acids in the latter species were no longer significant after correction for multiple testing. The decreases found in the preferences for amino acid carbon from simple to more complex amino acids (Fig. 4.5) were entirely due to the correction for differential amounts of substrate carbon (0.2 μmol l^{-1} for glycine, 0.6 μmol l^{-1} for leucine, and 0.9 μmol l^{-1} for phenylalanine), since the specific uptake rates of ^{13}C did not show this trend (data not shown).

4.3.3 Total ^{15}N uptake (I)

Because we aimed to identify uptake of different substrates at realistically low concentrations, rather than looking at uptake kinetics, the 3 hour incubations in relatively small volumes of water may have caused substrate depletion. On the other hand, total uptake of ^{15}N during the incubations was generally lower than the amount added (dashed line in Fig. 4.6).

In the NH_4^+ and NO_3^- incubations with *Caulerpa prolifera* leaves substrate depletion may have occurred, since the incorporation was close to the amount added. Urea and amino acid additions showed no indications of depletion. Algae-derived DON uptake was also high and close to depletion. Bacteria-derived DON was far from depleted (Fig. 4.6), but the label incorporation was stronger than in the algae-derived DON additions (data not shown). This seemingly contradictory result is due to the higher bacteria-derived $DO^{15}N$ addition compared to the algae-derived $DO^{15}N$ addition (see section 4.2.3). Similar analyses were performed for the belowground tissue, where no indications for depletion were found for any treatment (Fig. 4.6). The total incorporation via the roots was always lower than through the leaves most likely due to the lower biomass.

It is also obvious that *C. prolifera* took up more nitrogen for most of the substrates compared to seagrasses, but this can be due to its larger biomass in our incubations (data not shown), which is supported by the specific uptake rates that were similar or lower than those for the seagrasses (Fig. 4.4).

4.4 Discussion

4.4.1 Water column DON as nutrient source

Our results show that DON derived from algae presents an important source of nitrogen for seagrasses and macroalgae. The specific uptake rates per amount of substrate (preference) for DON derived from an axenic diatom culture were comparable to those for NH_4^+, the preferred inorganic nitrogen of seagrasses (Romero et al., 2006). This highlights the potential importance of DON as an immediate source of bioavailable nitrogen. The potential of detritus-derived nitrogen utilization by seagrasses was already illustrated by Evrard et al. (2005) and by Barron et al. (2006) for oligotrophic systems. However, their incubations lasted one to several days and focussed on sediment associated processes, thus illustrating the potential of organic nitrogen recycling and remineralization. By restricting the incubations to 3 hours, significant remineralization is minimized in our experiment. Recently, nitrogen uptake through leaves and roots was demonstrated for seagrass species in a tropical oligotrophic system (Vonk et al., 2008). To our knowledge, this study is the first to systematically address organic nitrogen utilization in temperate seagrasses.

Algae-derived DON was clearly preferred over bacteria-derived DON, which consisted of 84% and 47% amino acid nitrogen respectively, mainly in the form of DCAA (Fig. 4.2). This higher amino acid content may explain why algae-derived DON was the preferred DON pool. Many microalgae are also able to utilize amino acid nitrogen (Antia et al., 1975; Linares and Sundback, 2006). Utilization of free amino acids by seagrasses was demonstrated by Vonk et al. (2008), but was not compared to more complex mixtures with non-amino nitrogen. The lower fraction of amino acid nitrogen in bacterial DOM implies that other compounds are more abundantly present. It is possible that a large fraction is therefore more resistant to breakdown. This agrees well with the observation that bacterial DON contributes substantially to the refractory part of oceanic DOM in McCarthy et al. (1998, 2004), although these results concerned mainly autotrophs. Our findings are in good agreement with the

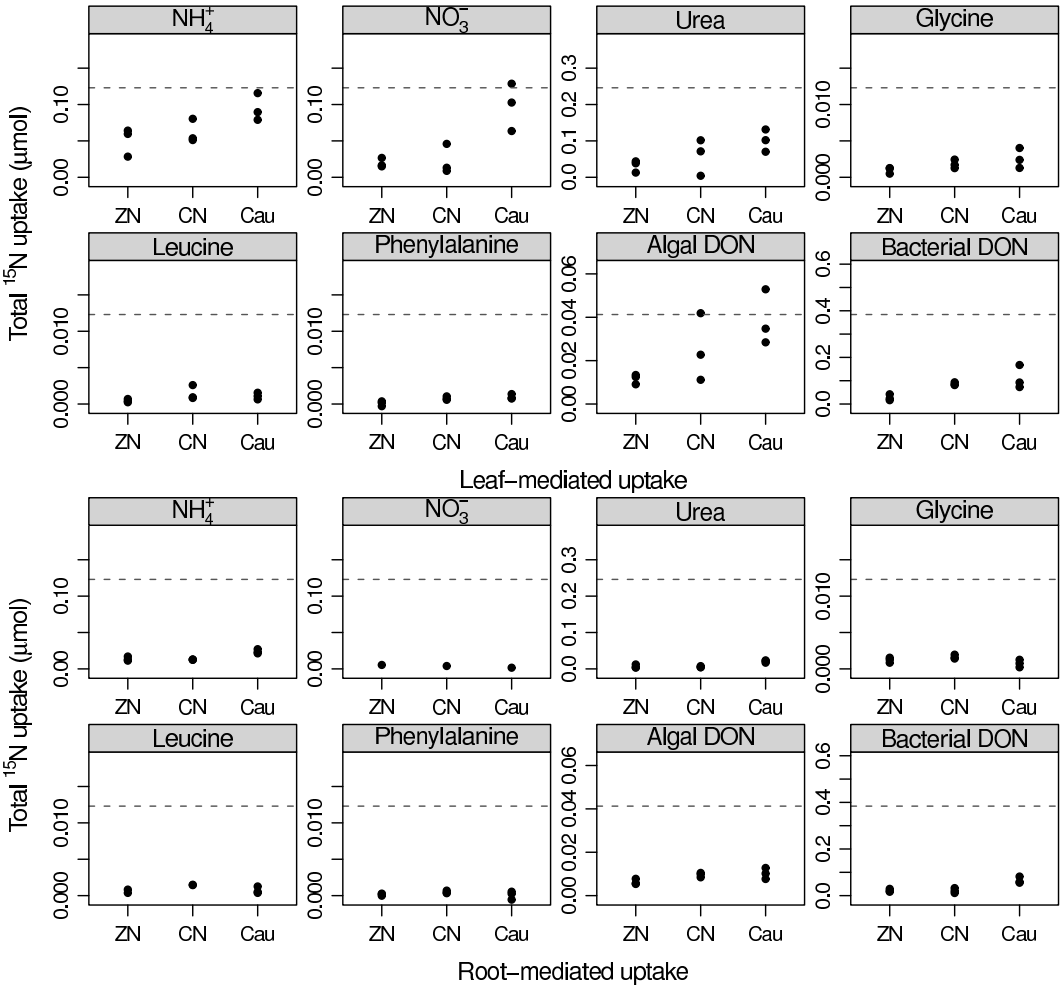

Figure 4.6: Total amount of label incorporated at the end of the incubation (bullets) and the amount added (dashed line) for the leaf (above) and root incubations (below).

dependence of DON reactivity on DON origin, found for other ecosystem compartments (Ziegler and Benner, 1999b; Seitzinger et al., 2002; McCallister et al., 2006).

All individual organic compounds were taken up in significant quantities by the aboveground macrophyte parts. However, the preferences for individual organic compounds were smaller than for the inorganic nitrogen sources and composed DON pools. It therefore seems that a composed pool of substrates is more useful to the macrophytes than larger quantities of one compound. Since one amino acid in large quantities implies a necessity to resynthesize other amino acids this could be expected. It needs to be emphasized that not only the preferences but also the specific uptake rates were higher. This excludes artifacts due to an overcorrection for differential substrate availability, which would occur if only a small fraction of the DON is bioavailable and specific uptake rates were divided by the concentration of the entire DON pool. A preference for a mixture of compounds rather than strong uptake of one specific compound was also hypothesized by Flynn and Butler (1986) in the context of free amino acid uptake.

There were clear differences in the ability of leaves to take up different organic compounds. These differences appeared related to the complexity of the substrates. Urea nitrogen was preferred over amino acid nitrogen, and nitrogen from glycine, a simple achiral amino acid was preferred over more complex amino acids like L-leucine and L-phenylalanine. Since the nitrogen content and the starting concentrations of the amino acids were the same for all treatments, our differential amino acid preferences also reflect the specific uptake rates, meaning that seagrass specific uptake of glycine N was higher than leucine and phenylalnine N. Vonk et al. (2008) also observed higher uptake rates of urea nitrogen than amino acid nitrogen by the leaves of most of the species examined. It is not clear by which mechanisms the amino acid nitrogen enters the macrophytes. Numerous mechanisms exist for phytoplankton, bacteria and macroalgae, including urease activity (Berman and Bronk, 2003, and references therein; Solomon and Glibert, 2008), peptide hydrolysis (Mulholland et al., 2002; Stoecker and Gustafson, 2003), amino acid oxidation (Palenik and Morel, 1990a), and complete uptake of the entire amino acid (Legrand and Carlsson, 1998). Furthermore, the mode of uptake can differ with compound (Tyler et al., 2005) and environmental conditions (Mulholland et al., 2004). More research in this area, particularly for seagrasses, could advance our knowledge significantly. It should also be noted that the complexity gradient also corresponds with a gradient in carbon content. Although we cautiously attribute the differential uptake capacities to the substrate complexity, it is also possible that other factors are at the basis of the pattern. More research, using more substrates of varying complexity, is needed to confirm this complexity dependence and improve our understanding.

With the exception of urea-N and NO_3^- the highest specific uptake rates were found in the seagrasses, contradicting the findings of Vonk et al. (2008), who observed considerably higher specific uptake rates in macroalgae than in seagrass leaves. However, clear distinctions in nitrogen uptake exist between slow-growing and fast-growing macroalgae (Duarte, 1995), and *Caulerpa prolifera* is considered a slow-growing macroalga (Malta et al., 2005). In addition, depletion effects could have occurred in the NH_4^+ and NO_3^- and algal-derived DON treatments of *C. prolifera* implying a potential underestimation of the true specific uptake rates. The amino acid treatments, however, did not exhibit any signs of depletion

supporting the validity of the lower uptake rates in *C. prolifera*.

4.4.2 The nitrogen source spectrum for root systems

The spectrum of available nitrogen sources for uptake by the belowground parts differed from that of the aboveground parts. Nitrate and urea nitrogen uptake through the root systems was statistically significant for all species. However uptake of these compounds was negligible when compared to NH_4^+ uptake. Considering that virtually no NO_3^- is expected to be in the sediment, apart from the shallow oxygenated layer around the roots and at the sediment-water interface, it is not surprising that the root-mediated NO_3^- uptake is low. In addition, root-leaf interactions and interactions between ammonium and nitrate uptake exist in different seagrass species (e.g. Thursby and Harlin, 1982, 1984; Stapel et al., 1996). An explanation for low uptake of urea nitrogen is less obvious. Compared to uptake of NH_4^+, splitting urea molecules induces increased energetic costs and NH_4^+ is usually readily available within sediments from, for instance, microbial urea breakdown (Lomstein et al., 1989).Indeed, the statistical significance of the root-mediated urea uptake by seagrasses could be entirely due to remineralization to NH_4^+. *Caulerpa prolifera* exhibited a somewhat higher affinity for urea than the seagrasses but total uptake remained very low. Urea nitrogen uptake from the sediment has been observed for other faster-growing macroalgae (Tyler et al., 2001).

The spectra of amino acid uptake by the belowground tissue differred between the species. *Zostera noltii* exhibited a pattern similar to the uptake by the aboveground parts, whereas *Cymodocea nodosa* exhibited higher preferences for glycine and not for L-leucine or L-phenylalanine. The patterns for *C. prolifera* were less clear due to the higher variability per treatment, but L-leucine was preferred over L-phenylalanine. The difference in the preferences per plant species imply that consistent distinctions were made by the plants themselves, since the bacterial communities in the cups at the beginning of the experiment are the same. However, endosymbiotic prokaryotes have been found for the genus *Caulerpa* (Chisholm et al., 1996). It is not clear to what extent these bacteria would influence our results, but it is likely that they play a role.

Algae-derived DON was preferred over bacteria-derived DON when root-mediated uptake was considered. This is consistent with the patterns found for leaf-mediated uptake. However, whereas the specific uptake of algae-derived DON uptake was higher through the leaves in *Z. noltii*, the specific uptake rates in *C. nodosa* and *C. prolifera* were highest for the uptake by belowground tissue. *Caulerpa* preferred algae-derived DON even over NH_4^+ (Fig. 4.4). This is contrary to the other data, that suggest a clear preference for NH_4^+. One explanation could be that *C. prolifera* is able to use more of the nitrogen via different pathways. For example, a high uptake of organic compounds combined with some uptake of regenerated NH_4^+. The preference for NH_4^+ in the belowground parts of *Z. noltii* is also lower than that of *C. prolifera*. Thus, it is possible that the regenerated NH_4^+ uptake contributes substantially to the already high organic nitrogen uptake, making this preference for algae-derived DON appear higher than that for NH_4^+.

4.4.3 Carbon versus nitrogen acquisition from DOM

Although some tendencies existed in the ^{13}C excesses per treatment and per plant very few statistically significant results were found, even despite the sometimes high ^{13}C transport rates. We attribute this lack of detection to the higher carbon content and larger variability, compared to nitrogen. A difference in the natural $\delta^{13}C$ value of 1 ‰ would, with an average organic carbon content of 4.4 mmol (average for the *Caulerpa* leaves), account for a difference in uptake of 4.81 μmol of carbon. If we keep in mind that only 0.11 μmol of L-phenylalanine-C was added to 123 ml of medium, it is not surprising that none of the amino acid treatments showed a significant ^{13}C enrichment. The total uptake of ^{13}C did not show any differences between the different treatments. Only after division by the amount added does a pattern corresponding to that in figure 4.5 (low urea C uptake, decreasing uptake for glycine, leucine and phenylalanine carbon respectively and somewhat increased values for the DON treatments) emerge, meaning that this pattern was entirely due to the correction for the substrate addition. This implies that we did not find any indications of ^{13}C uptake at all, neither through direct uptake nor after remineralization. In the latter case, uptake would be obscured by the introduction of $DI^{13}C$ in the large DIC background ($\approx$ 2 mmol l^{-1}; i.e. dilution).

4.4.4 Do macrophytes use DON or only remineralized DIN?

This study has revealed a rapid uptake of nitrogen originating from various organic substances. Despite the removal of epiphytes, phytoplankton and a part of the bacterial community, we can not completely exclude remineralization prior to uptake of the regenerated nitrogen. However, the differential pattern for uptake of nitrogen from organic compounds by leaves relative to that by roots at least supports the idea that the macrophytes distinguish more than just inorganic nitrogen, since the bacterial communities in the medium were the same in all incubations. Whatever the main mode of uptake might be, nitrogen from small well-defined organic compounds is available to macrophytes in a matter of hours, and a complex pool of DON supplies nitrogen in similar or larger amounts than inorganic pools at realistic concentrations found in temperate seagrass-dominated systems.

5. Dissolved organic matter uptake by temperate macrophytes

Van Engeland T., T. J. Bouma, E. P. Morris, F. G. Brun, G. Peralta, M. Lara, I. E. Hendriks, P. van Rijswijk, B. Veuger, K. Soetaert & J. J. Middelburg. (In prep.)

Abstract - *Seagrass-dominated ecosystems are often characterized by very low nutrient concentrations. We assessed the utilization of inorganic and organic nitrogen compounds by primary producers that are co-occuring in a seagrass meadow. Using double-labeled (^{13}C and ^{15}N) substrates of differential complexity the net transfers from the dissolved nitrogen and carbon pools to phytoplankton, planktonic bacteria, epiphytes, seagrasses (Zostera noltii and Cymodocea nodosa), and macroalgae (Caulerpa prolifera) were quantified in field incubations. Phytoplankton was by far the largest nitrogen sink, followed by the epiphytic community. In contrast, the seagrasses and Caulerpa prolifera dominated carbon fixation (≈ 85%). Although compartment-specific variations existed, NH_4^+ was generally preferred over NO_3^- and urea. Specific uptake rates of individual amino acids were inversely proportional to their C/N-ratio and their structural complexity (glycine > L-leucine > L-phenylalanine). In addition, biomarker-specific measurements (polar lipid-derived fatty acids and D-alanine) indicated an increasing bacterial contribution to carbon uptake with increasing amino acids complexity. All primary producers acquired nitrogen from a composite pool of algae-derived dissolved organic matter (DOM), but algae-derived DOC was almost exclusively used by the planktonic compartment. In contrast, a similar complex pool of bacteria-derived DOM was not utilized in significant quantities by any of the primary producers. Our results illustrate that (1) dissolved organic nitrogen plays an important role in nutrient dynamics in seagrass meadows, (2) the role of phytoplankton in seagrass meadows is too often neglected and should be investigated in more detail, and (3) organic nitrogen and carbon dynamics are largely uncoupled and should be investigated as such.*

5.1 Introduction

The high productivity of seagrass-dominated ecosystems in a generally low dissolved inorganic nitrogen (DIN) environment implies a high potential to deal with nitrogen limitation. Biota can cope with this by (1) being the most efficient competitor (e.g. having high affinities for inorganic nitrogen), and/or (2) having exclusive access to a particular nutrient source other than DIN (e.g. urea) and/or utilization or exploiting sediment resources, thus avoiding competition. DON is often the largest constituent of total dissolved nitrogen in oligotrophic marine systems (Bronk, 2002), and thus represents a large potential nutrient source and key component in seagrass meadows. The combination of limited availability of inorganic nitrogen and high biomass points towards efficient recycling of this DON, or towards direct uptake of dissolved organic nitrogen (DON).

Nevertheless, little attention has been paid to DON dynamics in seagrass-dominated systems, apart from research on benthic fluxes (e.g. Eyre and Ferguson, 2002) and temporal variation in bulk DON concentrations (Ziegler and Benner, 1999b). DON is often considered a black box from which inorganic nitrogen is drawn, because it is hard to link the operationally defined fractions within the DON pool with bioavailability (Bronk, 2002). For instance, low-molecular-weight DON (LMW-DON; $<$ 3000 kDalton) is preferred over high-molecular-weight DON (HMW-DON) by estuarine bacteria, but in the end HMW-DON breakdown is more complete and provides nitrogen over longer time-scales (Kerner and Spitzy, 2001). In addition, within the bioavailable DON fraction taxon-specific preferences are expected but not well documented for marine systems (Harrison et al., 2007).

The principal sources of DON in seagrass meadows are autochtonous. First of all, particulate organic matter, trapped by the seagrasses and partially buried breaks down in the sediment and causing significant DON effluxes. Evrard et al. (2005) and Barron et al. (2006) observed quick utilization of dissolved nitrogen originating from labeled detritus injected into the sediment, part of this nitrogen was lost from the seagrass bed to the overlying water, presumably in a reduced form such as NH_4^+ and DON. Other DON sources are phytobenthos (Tyler et al., 2001; Eyre and Ferguson, 2002), active or passive loss of DOM from living and senescent macrophyte leaves and/or roots (Benner et al., 1986; Findlay et al., 1986; Ziegler and Benner, 1999b), and from phytoplankton (Ziegler and Benner, 2000). This DON supply to the water column influences bacterial activity and water column nitrogen cycling (Ziegler and Benner, 1999a,b).

A broad range of taxa utilize dissolved organic nitrogen within a few hours to days. The capabilities to use DON are highly variable within and between taxa (Berman and Chava, 1999; Weigelt et al., 2003). Heterotrophic bacteria (Stepanauskas et al., 1999) and phytoplankton (Bronk et al., 2007) are the most frequently studied, but some macroalgae also take up urea and amino acids (Tyler et al., 2005). Recently, DON utilization by seagrasses was observed in the laboratory and in the field (Vonk et al., 2008).

This is actually not surprising since organic nitrogen utilization is also wide spread in terrestrial macrophytes, their Âtancestors Ât (e.g. Persson et al., 2003). In addition, seagrasses would benefit from direct uptake of amino acids, their main form of N storage (Invers et al., 2002), by avoiding energy-demanding synthesis from NH_4^+ or NO_3^-.

But in spite of these theoretical considerations, the ecology of DON utilization in seagrasses remains virtually unknown. Indeed, except from the study cited above, uptake experiments in seagrass meadows have focussed almost exclusively on DIN uptake (Stapel et al., 1996; Cornelisen and Thomas, 2002; Lepoint et al., 2004; Morris et al., 2008).

Seagrasses and rooting macroalgae take up nutrients from both the water column and the sediment (Stapel et al., 1996), and the leaves can supply up to half of the total N demand in seagrasses (Zimmerman et al., 1987; Lee and Dunton, 1999). They thus potentially compete with phytoplankton, bacteria and (non-)epiphytic phytobenthos for nutrients. Nevertheless, uptake experiments have hitherto only considered seagrasses, avoiding or neglecting uptake by other primary producers (Stapel et al., 1996; Lepoint et al., 2002b; Morris et al., 2008). In addition, studies on interactions between primary producers in seagrass meadows mainly focussed on macrophyte-macrophyte competition for inorganic nutrients or other resources (Fourqurean et al., 1995; Davis and Fourqurean, 2001; Steen, 2004; Stafford and Bell, 2006), or on the influence of epiphyte cover on the uptake of inorganic nutrients by seagrasses (Cornelisen and Thomas, 2002, 2004). However, model simulations suggest that phytoplankton and epiphytic microalgae may be the dominant nutrient consumers in the water column, driving seagrasses to be nutrient limited and largely dependent on sediment nitrogen (Plus et al., 2003).

We investigated the capacity of different co-occuring primary producers (*Zostera noltii*, *Cymodocea nodosa*, *Caulerpa prolifera*, the epiphytes, and the phytoplankton) from the inner bay of Càdiz to acquire dissolved organic and inorganic nitrogen compounds from the water column. Using a spectrum of ^{13}C and ^{15}N double-labeled substrates of differential complexity and composition, we investigated how much of each substrate flows into these ecosystem compartments, whether carbon and nitrogen acquisition was coupled, and how much each source contributed. The bacterial contribution to the plankton uptake was studied using polar lipid-derived fatty acids (PLFA) and hydrolysable amino acids (HAA) as biomarkers.

5.2 Materials & Methods

5.2.1 The study site

The bay of Càdiz encompasses an area of approximately 30,00.0 ha of which 40% is more or less permanently inundated (Carrasco et al., 2003). It is subdivided into a deeper outer bay with a direct input of continental shelf water and riverine runoff with urban waste water, and a shallow inner bay which receives water from the outer bay. It is a system impacted by aquaculture and waste water run-off, as indicated by ^{15}N stable isotope measurements (Morris et al., 2009). There are three dominant seagrass species, *Zostera marina* (not treated in this study), *Zostera noltii*, and *Cymodocea nodosa*, and a small rooting macroalga *Caulerpa prolifera*. This experiment was conducted in the inner bay near Santibañez (36°28'12.79"N, 6°15'7.07"W; Fig. 5.1), where *Zostera noltii*, *C. nodosa* and *C. prolifera* co-occur.

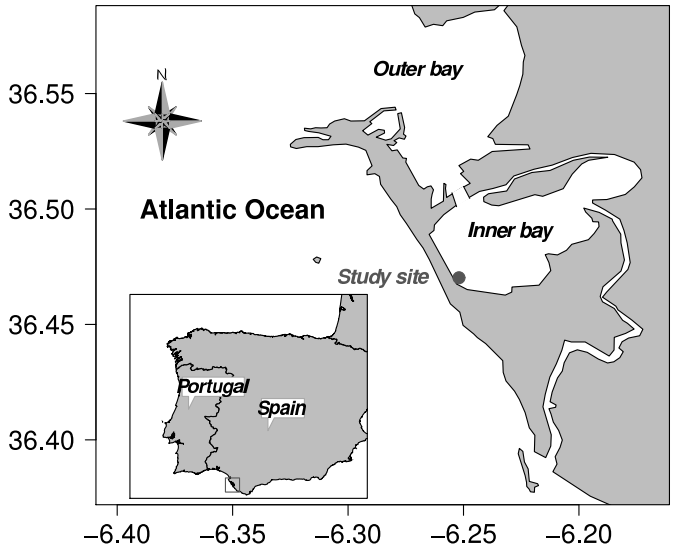

Figure 5.1: Experimental site in the inner bay of Càdiz, Spain.

5.2.2 Experimental Design

The experiment was designed to assess under potential competition the relative contributions of the expected main players (*Zostera noltii*, *Cymodocea nodosa*, *Caulerpa prolifera*, phytoplankton, bacterioplankton, and epiphytes) with regard to nitrogen acquisition from different sources in the water column (Tab. 5.1). Incubations were performed in plastic bags with a screw cap on the lower side. The macrophytes were bundled in a hole in the screw cap with a hydrophobic cotton wool bud wrapped around the basis of their aboveground parts, such that the aboveground parts were in the bag and the belowground parts outside the bag (Fig. 5.2). The cotton wool bud was sufficient to prevent water from leaking through the hole. The macrophyte species were added to the enclosures in similar biomasses. The bag was filled with 5 liters of unfiltered bay water containing the natural plankton community. Each incubation therefore involved not only three macrophytes and the epiphytes, but also suspended algae and bacteria. Eight nitrogen and carbon containing substrates were added in quantities amounting to the final concentrations indicated in table 5.1. The composed DOM substrates (algae- and bacteria-derived DOM) were prepared following Veuger et al. (2004). The algae were grown on $^{15}NH_4^+$ and ^{13}C-bicarbonate, and bacteria on $^{15}NH_4^+$ and ^{13}C-glucose. After a week they were harvested. After removal of the remaining label, the DOM was extruded from the algae/bacteria with hot water (60°C) and the complex organic extract was used as a proxy for algae/bacteria-derived DOM. Since filtration of substrates added to filtered seawater demonstrated that a considerable part of the bacteria-derived DON stuck to the filter (data not shown), the results for bacteria-derived DON should be interpreted with caution, particularly with respect to the incorporation in suspended particulate matter (SPM). $NaH^{13}CO_3$ was added to the NH_4^+ and NO_3^- incubations to assess

the primary production (Tab. 5.1). After the substrates were added, the bags were anchored approximately 0.3 m above the bottom at a depth of 0.5 to 1.5 m (tidal variation). Incubations were started around low water and lasted for approximately 4 hours. After the incubation period the bags were collected one by one in random order to be sampled. This experimental setup was replicated three times on different days to obtain statistical stability (no replicate treatments in one day).

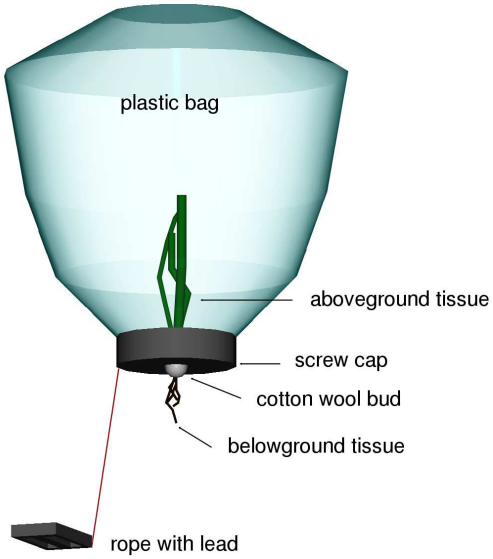

Figure 5.2: Incubation setup: A screw cap with a hole containing three macrophyte species in similar biomasses. A plastic bag contains the incubation medium (water from the bay) with the planktonic microbial community. The enclosure is attached to the bottom with a rope on a weight.

5.2.3 Sampling and sample handling

Post incubation, the dissolved nutrients were collected after filtration over a precombusted GF/F filter (Whatman). The amino acids and DOC were sampled by filtration over a precombusted GF/6 filter (Whatman). Suspended particulate matter (SPM) samples were collected on preweighed precombusted GF/F filters (Whatman) for bulk ^{13}C and ^{15}N analysis, polar lipid-derived fatty acid isotope (PLFA) analysis, and amino acid isotope analysis. All SPM samples were stored on ice in the field and at -20°C in the laboratory until further processing. The macrophytes were dissected and stored in liquid nitrogen in the field and at -20°C in the laboratory. For *Zostera noltii* aboveground and belowground parts were distin-

Table 5.1: The substrates (Cambridge Isotope Laboratories, CIL) used for this experiment and their final concentrations in the incubations. For the protocol of DON preparation we refer to Veuger et al. (2004) and chapter 4.

Treatment	Abbrev.	Labeled substrates	Concentration
NH_4^+/DIC	NH_4^+	NH_4Cl (^{15}N, 99%) + $NaHCO_3$ (^{13}C, 99%)	1 μmol-N l^{-1} / 30 μmol-C l^{-1}
NO_3^-/DIC	NO_3^-	$NaNO_3$ (^{15}N, 98%) + $NaHCO_3$ (^{13}C, 99%)	1 μmol-N l^{-1} / 30 μmol-C l^{-1}
Urea	UR	Urea (^{13}C, 99%; $^{15}N_2$, 98%)	2 μmol-N l^{-1}
Glycine	Gly	Glycine ($U^{13}C_2$, 98%; ^{15}N, 98%)	0.1 μmol-N l^{-1}
Leucine	Leu	L-Leucine ($U^{13}C_6$, 98%; ^{15}N, 98%)	0.1 μmol-N l^{-1}
Phenylalanine	Phe	L-Phenylalanine ($U^{13}C_9$, 98%; ^{15}N, 98%)	0.1 μmol-N l^{-1}
Algae-derived DOM	AD	DOC (8.33% ^{13}C) + DON (65.78% ^{15}N)	25 μmol-C l^{-1} / 2.93 μmol-N l^{-1}
Bacteria-derived DOM	BD	DOC (46.22% ^{13}C) + DON (46.36% ^{15}N)	138 μmol-C l^{-1} / 39 μmol-N l^{-1}

guished, which will be referred to as leaves and roots for simplicity. In *Cymodocea nodosa* aboveground parts (leaves), rhizomes and roots were separated. In *Caulerpa prolifera* rhizoids and the rest of the thallus were distinguished, and will also be referred to as roots and leaves for simplicity. The epiphytes from *C. nodosa* and *Z. noltii* were in the field collected with razor blades, and stored on a precombusted GF/F filter (Whatman) on ice. Reference samples from the environment were taken for all variables mentioned above. In addition GF/F filters for pigment analysis were collected to assess the phytoplankton community composition (also stored on liquid nitrogen in the field and at -20°C in the laboratory). The macrophytes, SPM and epiphytes were later freeze dried. The macrophytes were ground to a fine powder for isotope analysis.

5.2.4 Chemical analyses

DIN components (NH_4^+, NO_2^-, NO_3^-), urea and dissolved inorganic phosphate (DIP) were determined colorimetrically (Middelburg and Nieuwenhuize, 2000). DON was calculated by difference from the total dissolved nitrogen (TDN), determined as NO_3^- after a alkaline persulphate destruction (120°C for 30 min; Grasshoff et al., 1999), and DIN. DOC concentrations were measured with an auto-analyzer (Skalar SK12 organic carbon analyzer). Dissolved free amino acids (DFAA) concentrations were measured by HPLC (Fitznar et al., 1999) on a Waters HPLC system with a 996 photodiode array detector. Total hydrolysable amino acids dissolved in the water column (THAA) were measured using the same procedure after 24 hours of hydrolysis in 6 M HCl at 110°C. Dissolved combined amino acids were determined by subtraction (DCAA = THAA - DFAA). Pigment analysis was performed on a Waters HPLC system with a Waters 474 fluorescence detector (Barranguet et al., 1997). Concentrations and relative abundances of ^{13}C in dissolved inorganic carbon ($DI^{13}C$) were measured with a headspace technique using a Thermo NA2500 elemental analyzer coupled to a Thermo Delta Plus isotope ratio mass spectrometer via a Conflo II interface. Bulk carbon and nitrogen content and relative abundances of ^{13}C and ^{15}N in SPM and plant tissue were measured using a Thermo EA 1112 elemental analyzer coupled to a Thermo Delta V Advantage isotope ratio mass spectrometer with a Conflo II interface (EA-IRMS; Vonk et al., 2008). Concentrations and relative abundances of ^{13}C and ^{15}N for the hydrolysable amino acids in SPM (HAA) were analyzed by gas chromatography-combustion-isotope ratio mass spectrometry (GC-c-IRMS) using a HP 6890 GC with a Thermo type III combustion interface and Thermo Delta Plus IRMS after extracting and derivatizing the amino acids using the protocol of Veuger et al. (2005), modified for extraction from filters. PLFA (polar lipid-derived fatty acid) extractions and derivatization to fatty acid methyl esters (FAME) were performed using a modified Bligh and Dyer protocol (Boschker et al., 1999). FAME concentrations were measured by gas chromatography-flame ionization detection (GC-FID) with separation on a polar column (Scientific Glass Engineering BPX-70; Middelburg et al. 2000). ^{13}C isotope ratios of the individual FAME were measured on a HP 6890 GC gas-chromatograph with a Thermo type III combustion interface and Thermo Delta Plus GC-c-IRMS.

5.2.5 Calculations & statistics

Due to the wide range of labeling intensities we based all our calculations on atomic fractions (F; for ^{15}N or ^{13}C) rather than δ-values (Fry, 2006). The occurrence of uptake was investigated with t-tests to test the difference between the heavy isotope fractions in the treatment samples (F_{sample}) relative to the natural heavy isotope fractions in the reference samples ($F_{nat.ab.}$). Isotope excesses ($E_{sample} = F_{sample}$ - $F_{nat.ab.}$) were used to calculate specific uptake rates of heavy isotope: $V_{sample} = E_{sample} \times$ [X]/time, where [X] is the carbon or nitrogen concentration (μmol gDW^{-1}). Transport rates were calculated as the product: $\rho_{sample} = V_{sample} \times$ dryweight. Corrections for differential substrate concentrations were accomplished (when desirable) by dividing V by the substrate concentration [i]. This rate of uptake per amount available gives an indication of the preference for a particular nutrient source and is eventually expressed in gDW^{-1} h^{-1}.

Three biomarker classes were measured (PLFA, HAA_{SPM}, and pigments) to obtain robust results for the bacterial and phytoplankton biomasses and their contributions to N and C uptake. The chlorophyll a concentration was converted to POC_{phyto} by assuming a carbon content of 45 μg-C per μg of chlorophyll a. No biomarker-based calculations were performed on the algae- and bacteria-derived DON additions because biomarkers were introduced by the additions. Bacterial biomass was determined, following Evrard et al. (2008), from the average PLFA concentration in bacteria as $POC_{bac} = PLFA_{bac}/a$, where a is the average amount of PLFA per amount of bacterial carbon (assumption: a = 0.073 mmol PLFA-C/mmol POC_{bac}, following Brinch-Iversen and King (1990) and Moodley et al. (2000)). The average PLFA concentration in bacteria was calculated based on the concentrations of the bacteria specific markers (aiC15:0, iC15:0, iC14:0, and iC16:0) as $PLFA_{bac} = \sum PLFA_{bact-spec}/b$, with b the amount of bacteria-specific PLFA per amount of total bacterial PLFA (assumption: b = 0.14 mmol $PLFA_{bact-spec}$-C/mmol of $PLFA_{bac}$, following Moodley et al. (2000)). The phytoplankton biomass, POC_{phyto} was estimated from the PLFA data as $POC_{phyto} = PLFA_{phyto}/c$, with $PLFA_{phyto}$ the total PLFA concentration in phytoplankton and conversion factor c (assumption: c = 0.077 $\pm$ 0.034 μg PLFA-C/μg POC_{phyto}, based on averaged results from Dijkman and Kromkamp (2006a) for Chlorophyceae, Trebouxiophyceae, and Bacillariophyceae combined). The amount of phytoplankton PLFA was calculated as the difference to the total amount of PLFA and the total amount of bacterial PLFA: $PLFA_{phyto} = \sum PLFA_{all}$ - $PLFA_{bac}$.

Bacterial contributions in amino acid C and N uptake were measured by means of the hydrolysable amino acids in SPM (HAA). Following Veuger et al. (2005), and using a bacterial D-alanine/L-alanine ratio of the isotope excesses in carbon or nitrogen (D/L) of 0.07, bacterial contributions were estimated as (D/L)/0.07. The D/L ratio was corrected for hydrolysis-induced racemization (Veuger et al., 2007). The bacterial D/L ratio of 0.07 was chosen based on the fact that at lower D/L ratios the phenylalanine addition would result in bacterial contributions to carbon uptake in HAA of more than 100% (see section 5.3.4). This D/L ratio corresponds to an approximate Gram-positive contribution of 42% to the bacterial biomass, which is plausible (Veuger et al., 2007).

Using the area-specific biomasses for *Zostera noltii* (65.6 $\pm$ 4.4 g DW m^{-2}) and *Cy-*

modocea nodosa (123 ± 10 g DW m^{-2}) reported for the inner bay of Càdiz by Brun et al. (2006), the area-specific biomass for *Caulerpa prolifera* (97 ± 52 g DM m^{-2}) from Morris et al. (2009), and the SPM data from this study (21.5 ± 5.2 mg DW m^{-2}), we calculated the nitrogen uptake and turn-over rates per m^2. For the SPM and the nutrient stocks we assumed a water depth of 3.75 meter, based on the average water depth and the difference between average low and high tide reported by Morris et al. (2009).

All calculations were performed in the statistical package R (R Development Core Team, 2009). Significance tests were performed using the gls-function in the nlme package for R (Pinheiro et al., 2008).

5.3 Results

5.3.1 Environmental conditions

DIN concentrations were low (0.29 ± 0.11 μmol-N l^{-1} and 0.72 ± 0.65 μmol-N l^{-1} for NH_4^+ and NO_3^- respectively; data not shown). Nitrite concentrations were negligible. The total DON concentration was 16.41 ± 1.33 μmol-N l^{-1}, and represented 94% of the total dissolved nitrogen. Urea (2.17 ± 0.41 μmol-N l^{-1}) represented 13.2% of the DON. The L-leucine concentration (0.21 ± 0.36 nmol-N l^{-1}) was almost two orders of magnitude smaller than the glycine concentration (18.24 ± 5.91 nmol-N l^{-1}) and exhibited considerably more variation between sampling days. The L-phenylalanine concentration was more stable at 3.47 ± 1.28 nmol-N l^{-1}.

5.3.2 Bacterial versus microalgal contributions to POM

The chlorophyll a (*Chla*) concentration was on average 2.7 ± 2.6 μg-Chla l^{-1}, corresponding to a phytoplankton biomass of 10 ± 10 μmol-C l^{-1} (results not shown). The major part of the variation was between the days. Using the *Chla* derived biomass, phytoplankton contributed on average 25 ± 22 % to the carbon pool of SPM. Fucoxanthin was relatively high (0.62 ± 0.67 μg-Fuco l^{-1}), indicating a high contribution of diatoms. The very low concentration of zeaxanthin on day 3 (0.05 ± 0.01 μg-Zea l^{-1}) indicate negligible contributions of cyanobacteria. The presence of the alloxanthin pigment (0.30 ± 0.43 μg-Allo l^{-1}) gave support to some presence of cryptophytes, particularly on day 3. Chlorophyll b was abundantly present, indicating some contribution of chlorophytes. Part of this concentration is most likely due to *Caulerpa prolifera* derived detritus. Despite the high variation in pigment content between the days and the occurrence of some very low concentrations of accessory pigments on day 3, the pigment ratios relative to *Chla* were rather constant (0.22 ± 0.03 for fucoxanthin), indicating a stable community composition.

Significant concentrations of the bacterial PLFA markers aiC15:0 and iC15:0 indicated the presence of Gram-positive bacteria and Cytophaga/Flavobacter, while C18:1ω7c indicated potentially high abundances of Gram-negative and Proteobacteria However, the latter marker is also present in algal species. We calculated the bacterial and phytoplankton abundances using the PLFA concentrations of all the samples except the complex DOM

additions. The bacterial abundance was 4 ± 1 μmol-C l^{-1}, corresponding to 8 ± 3 % of the POC, whereas phytoplankton comprised 12 ± 5 μmol-C l^{-1} or 25 ± 12 % of the POC, which was in good agreement with the results from the pigments (25 ± 22 %). The high abundance of the diatom related PLFA markers C16:1ω7c and C20:5ω3 also corroborated the high fucoxanthin values, while the presence of the Chlorophyceae-related PLFA marker C16:4ω3 and the comparable abundance of the Trebouxiophyceae related PUFA C16:3ω3 supported the chlorophyll b values. Dinoflagellates were a negligible constituent of the microbial community as indicated by the vanishingly small quantities of C18:5ω3 and peridinin.

5.3.3 Bulk carbon and nitrogen uptake

Suspended particulate matter (SPM) and seagrass epiphytes exhibited significant ^{15}N excesses over background values for all treatments, which differed per substrate (data not shown). *Zostera noltii* and *Cymodocea nodosa* leaves showed significant ^{15}N excesses in all treatments except for phenylalanine (data not shown). $^{15}NO_3^-$ addition did not cause significant ^{15}N excesses in *Caulerpa prolifera* leaves. No excesses were found in the belowground parts of any of the macrophyte species (data not shown), indicating that translocation was not importance during the 4-hour incubation period.

To give an idea of the preference for a particular substrate, specific uptake rates of heavy isotopes (μmol g DW^{-1} h^{-1}) were calculated normalized to the amount of added substrate (μmol) to correct for the differences in substrate concentrations. The highest ^{15}N preferences were found for NH_4^+, except for *C. prolifera* and the epiphytes (Fig. 5.3). For SPM preferences decreased in the order $NH_4^+ > NO_3^- >$ urea. A similar but much weaker pattern was visible in the epiphytes and *C. prolifera*. The seagrasses tended to take up more urea-N than NO_3^- per available amount but the differences were small and not significant. The preferences in seagrasses and their epiphytes were higher for glycine than for leucine, while phenylalanine was not taken up. The preferences for leucine in SPM and *C. prolifera* were similar or slightly higher than for glycine.

The preference of SPM for algae-derived DON was comparable to that for NH_4^+. Other compartments appeared to prefer algae-derived DON over bacteria-derived DON, but preferred DIN over DON. The substrate-corrected ^{15}N specific uptake rates in the bacteria-derived DON additions were quantitatively negligible compared to the other substrates, despite the ^{15}N excesses that were roughly double that of the algae-derived DON treatment. These high excesses were thus only attributable to the high amount that was added (cf. Table 5.1).

Total ^{15}N (or ^{13}C) uptake per enclosure was calculated as a percentage of the added amount (Fig. 5.4). Note that the epiphytes were not mentioned here since no biomass data was available. Contributions of the different ecosystem compartments to total uptake were calculated as percentages of the total uptake (Fig. 5.4). SPM dominated nitrogen uptake for all substrate additions with a minimum of 67% for the urea-N (Fig. 5.4a). However, DIC was predominantly taken up by the macrophytes (≈ 85%; Fig. 5.4b). The seagrasses were responsible for approximately 60% of the DI^{13}C uptake, whereas the SPM accounted for less than 15%. Urea-N uptake was dominated by the SPM, urea-C by the macrophytes.

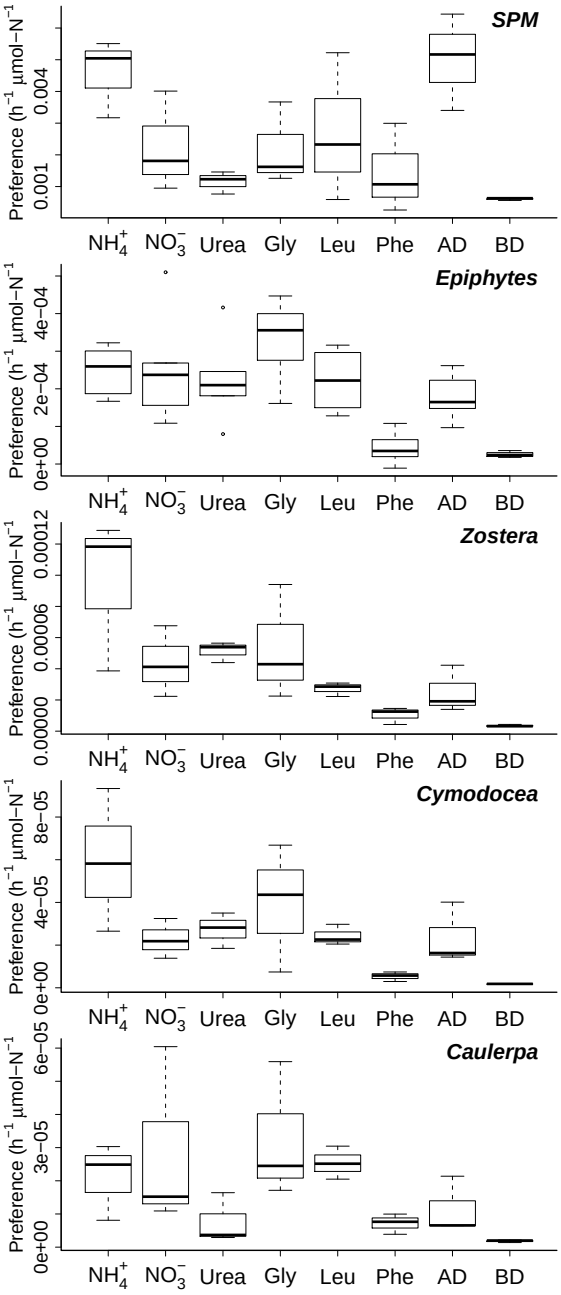

Figure 5.3: Nitrogen specific uptake rate corrected for the initial substrate concentrations for the SPM (suspended particulate matter), the epiphytes an three macrophyte species. See table 5.1 for the abbreviations of the treatments.

The contributions of SPM to ^{15}N uptake increased with increasing complexity (urea < glycine < leucine < phenylalanine; Fig. 5.4a), while total ^{15}N uptake decreased with increasing complexity of the amino acids. The uptake of ^{13}C from glycine and L-leucine was higher than from L-phenylalanine, which was mainly taken up by the *C. prolifera* and SPM (Fig. 5.4b). The complex pools of organic nitrogen, containing a whole spectrum of compounds, were for 95% used by the SPM compartment. Algae-derived DON was taken up to a much larger extent than DIN (Fig. 5.4a). The DOC was only taken up for 44% when derived from algae and for 23% when derived from bacteria (Fig. 5.4b). The uptake of this composed pool was almost exclusively by the SPM compartment but most likely overestimated due to the stickiness of the substrate.

5.3.4 Contribution of bacteria and algae to N and C uptake

Large portions of the ^{13}C that went into biomarkers were found in the HAA. The phytoplankton was mainly responsible for the incorporation of DIC, urea-C and glycine-C (Fig. 5.5). Twenty-six percent of the DI^{13}C, that went into the HAA pool, ended up in the bacterial compartment during this 4 hour incubation period. In the leucine and phenylalanine additions the ^{13}C was predominantly taken up by the bacteria, but they only accounted for 24 and 32 % of the ^{15}N incorporation, respectively (Fig. 5.5). Almost no $^{15}NH_4^+$ went directly into the bacterial compartment, while 6% of the NO_3^- incorporation into HAA was due to bacteria.

The ratios of ^{13}C over ^{15}N in HAA ranged from 0.05 for the NH_4^+ treatment to 0.5 for the glycine addition, indicating that nitrogen was incorporated into amino acids to a much larger extent than carbon. The $^{13}C/^{15}N$ ratio in the urea treatments was of the same order of magnitude as the NH_4^+ and NO_3^- treatments. The $^{13}C/^{15}N$ ratio in the amino acid additions were higher (0.5, 0.24, and 0.46 for the glycine, leucine, and phenylalanine additions respectively), indicating relatively higher carbon incorporation from amino acids than from urea or DIC. For these calculations the added amino acids were excluded to avoid artifacts.

5.3.5 Nitrogen uptake and carbon fixation at ecosystem level

Total carbon fixation per m^2 was mainly accomplished by the seagrasses, in particular *Cymodocea nodosa* (Tab. 5.2). *Caulerpa prolifera* and the SPM had an equal share which was highly variable. Unfortunately, we did not have biomass data on the epiphyte community or the sediment associated microphytobenthos.

In contrast to the DIC consumption, SPM was by far the largest sink for dissolved nitrogen regardless of the source (Tab. 5.2). The area-based DIN turnover rate amounted to 0.39 h^{-1} in our simplified system. The DIN turnover rate if *Zostera noltii* would be the only consumer would be 0.014 h^{-1} and that for *C. nodosa* 0.017 h^{-1}. In the absence of fluxes into the substrate pools, the uptake of NH_4^+ and glycine would drive these pools close to depletion after 1 hour. This was less pronounced for NO_3^- ($\approx$ 4 hours) and urea ($\approx$ 10 hours). The area-based uptake rates of leucine-N and phenylalanine-N were large compared

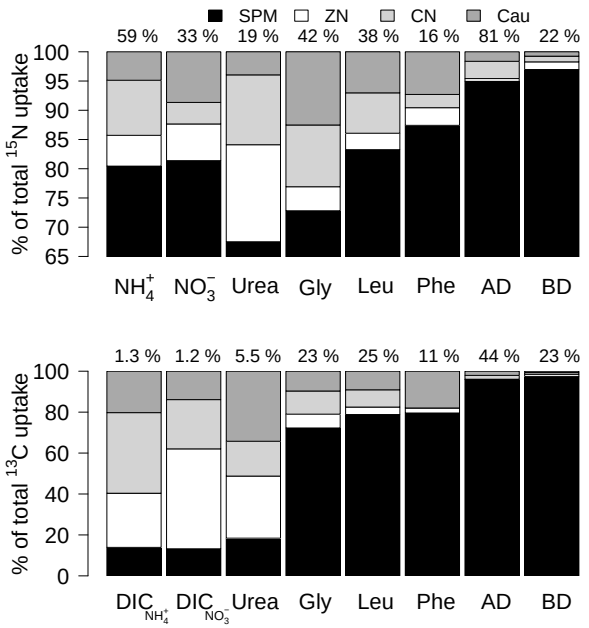

Figure 5.4: Percent contribution to the total amount of ^{15}N (a.) and ^{13}C (b.) taken up per enclosure for each of the treatments. Note that the scale in (a.) starts at 65 % because of the dominant role of nitrogen uptake by SPM. The numbers above the graphs are the percentages of the added ^{15}N (or ^{13}C) that were consumed in the enclosures. The ecosystem compartments indicated with gray scales are SPM (SPM), *Zostera noltii* (ZN), *Cymodocea nodosa* (CN), and *Caulerpa prolifera* (Cau).

to the standing stock, indicating a rapid turnover of these nitrogen compounds as well. The calculations for the algae-derived DON were based on the assumption that the entire DON pool is derived from algae, which is obviously a too crude approximation. These numbers are purely indicative of how 'tasty' algal DON could be.

5.4 Discussion

Seagrass meadows have a tremendous capacity to filter nutrients from the water column (Fernandes et al., 2009). Nutrient limitation and the mechanisms to cope with this are probably among the most studied aspects of seagrasses ecology to date. However, few studies exist on the contribution of different primary producers in these ecosystems to system-level nitrogen uptake and primary production (but see Moncreiff et al., 1992 and Lepoint et al., 2004). In addition, uptake of organic substances by seagrasses only recently started to receive

Table 5.2: Area-based carbon fixation (mmol-C m^{-2} h^{-1}) and nitrogen transport rates (μmol-N m^{-2} h^{-1}) for the various compartments from this study, total uptake rates for all compartments, and the total amount of substrate available to the biota per(mmol-C m^{-2} for DIC, μmol-N m^{-2} for the rest). All calculations were based on the assumption of a water column depth of 3.75 meters, and using biomass values from Brun et al. (2006), Morris et al. (2009) and this study.

Source	SPM	*Zostera noltii*	*Cymodocea nodosa*	*Caulerpa prolifera*	Total uptake	Nutrient stocks
DIC	9.9 ± 9.6	13.9 ± 10.7	27.6 ± 21.7	10.2 ± 15.2	61.6 ± 31.3	6280 ± 739
NH_4^+	746 ± 438	32 ± 21	44 ± 34	26 ± 24	847 ± 440	1100 ± 401
NO_3^-	456 ± 379	19 ± 19	19 ± 9	39 ± 41	533 ± 379	2438 ± 2444
Urea	620 ± 419	53 ± 22	64 ± 36	31 ± 41	767 ± 425	8125 ± 1539
Gly	32 ± 27	1.5 ± 1.3	2.7 ± 2.6	3.8 ± 3.5	40 ± 27	68 ± 23
Leu	35 ± 39	0.7 ± 0.3	1.4 ± 0.7	2.5 ± 1.6	39 ± 39	2.3 ± 2.1
Phe	20 ± 24	0.3 ± 0.2	0.3 ± 0.2	0.7 ± 0.6	21 ± 23	13 ± 5
AD	12548 ± 7943	119 ± 89	254 ± 208	216 ± 236	13138 ± 7967	61525 ± 5016

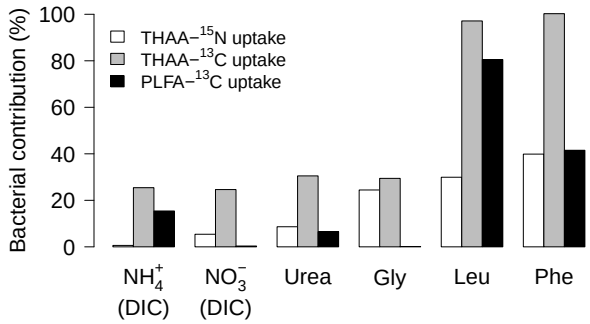

Figure 5.5: Bacterial contribution to the ^{15}N and ^{13}C incorporation in amino acids and PLFAs.

attention (Bird et al., 1998; Vonk et al., 2008; Vonk and Stapel, 2008). To our knowledge this is the first study that addresses the contribution of different primary producers to the concurrent uptake of nitrogen from both inorganic and organic sources in a seagrass meadow.

5.4.1 Nitrogen uptake in a wider context

Our results are in good agreement with uptake values found in literature (Tab. 5.3). The NH_4^+ and NO_3^- transport rates corresponded well with those reported for temperate estuaries (Glibert et al., 1991; Middelburg and Nieuwenhuize, 2000; Andersson et al., 2006). Inorganic nitrogen transport rates by suspended particulate matter (SPM) fell within the range for coasts but this range is large. The NH_4^+ and NO_3^- specific uptake rates by SPM, seagrasses and their epiphytes in a Mediterranean *Posidonia oceanica* meadow were smaller than in this study (Lepoint et al., 2004). However, our specific uptake rates of NH_4^+ in seagrasses were in close agreement with those found by Morris et al. (2008) for *Zostera noltii* and *Cymodocea nodosa* in stagnant water, and those for epiphyte-covered *Thalassia testudinum* (Cornelisen and Thomas, 2004). Our NH_4^+ and NO_3^- uptake rates for the seagrasses and macroalga were lower than those found by Vonk et al. (2008). Our macroalgal specific uptake rates of NH_4^+ and NO_3^- were roughly four times lower than those in the Mediterranean *Posidonia oceanica* (Lepoint et al., 2004), but they fell in the range for macroalgae on rocky shores (Phillips and Hurd, 2004).

Bacteria and phytoplankton can use simple organic compounds such as urea and amino acids for their nitrogen requirements (Bronk, 2002; Bronk et al., 2007). Preference, regulation of the pathways, and whether the carbon is utilized in addition to the nitrogen depends on the species and circumstances (Berg et al., 2003; Fan et al., 2003; Mulholland et al., 2004), complicating literature comparison. The urea uptake by SPM was stronger in our incubations than in the North Sea (Tungaraza et al., 2003) and the Baltic Sea (Tamminen and Irmisch, 1996). *Caulerpa prolifera* took up little urea compared to literature values for macroalgae (Tab. 5.3). The dissolved free amino acid transport rates by SPM were lower than those observed by Andersson et al. (2006), but they used an amino acid mixture

which could be more useful to biota than a large amount of one amino acid (Flynn and Butler, 1986), although the transport rates from Andersson et al. (2006) were two orders of magnitude lower than our DON transport rates (for algae-derived DON). In addition, the biodegradability and mode of uptake is amino acid dependent (Tyler et al., 2005). Amino acid uptake by the seagrasses and *C. prolifera* was similar to that found by Vonk et al. (2008).

Planktonic algal DON transport rates were in the range of those found in Randers Fjord (Denmark; Veuger et al., 2004). SPM took up algae-derived DON at rates comparable to those in temperate estuaries (Kerner and Spitzy, 2001; Badr et al., 2008). This was unexpected since our DON substrate purely consisted of fresh algal material, while their cultures received riverine DON that has been aged, preprocessed, and thus ought to have a lower bioavailability.

5.4.2 Importance of different sinks

SPM was the strongest sink for the nitrogen compounds tested, followed by the epiphytes (Fig. 5.3, Tab. 5.2). The specific uptake rates of the SPM were a lot higher than those of the macrophytes. Even on a areal basis the total transport rates into the planktonic compartment were 10 to 20 times higher than those into the individual macrophyte species (Tab. 5.2). DON uptake was for more than 95% attributable to the SPM. These results support the idea that slow-growing algae, such as Caulerpa (Malta et al., 2005), and seagrasses are inferior competitors for nutrients relative to fast-growers, such as epiphytic phytobenthos and phytoplankton (Duarte, 1995; Plus et al., 2003). Uptake rates of the macrophytes may have been underestimated, because the dependence on water column mixing for some sources (Cornelisen and Thomas, 2004; Morris et al., 2008), and because of root uptake. However, this can not explain the large differences between the SPM and macrophytes. Although we did not measure uptake kinetics, we can expect that on the short term phytoplankton can outcompete the macrophytes for nitrogen sources from the water column, since our nutrient additions occurred at close to ambient concentrations. On the long term, nitrogen limitation in macrophytes is alleviated by root uptake and by utilizing stored nitrogen taken up in late fall and winter and nitrogen withdrawal from senescing leaves (Lepoint et al., 2002a).

Two potentially important sinks have not been quantified because of logistic reasons. The epiphyte biomass is hard to quantify accurately and sediment associated microalgae could not be included in our incubations because of the enclosure design and the decision to exclude sediment associated processes and fluxes. It is estimated that epiphytes contribute up to 17% to NH_4^+ removal from the water column, and 10% to carbon fixation by an assemblage (Heip et al., 1995; Cornelisen and Thomas, 2002). Microphytobenthos is able to modify nutrient fluxes to the water column (Eyre and Ferguson, 2002) and utilize small organic compounds (Linares and Sundback, 2006), implying a serious impact on the available nutrient stocks.

Our biomarker measurements indicate an important contribution of bacteria to the uptake of dissolved organic compounds. Bacteria dominated carbon uptake from L-leucine and L-phenylalanine, and contributed about 20% to glycine, urea and DIC uptake. Bacteria

Table 5.3: Nitrogen uptake rates from this study (V_N and ρ_N, the specific uptake rate and transport rate of nitrogen, respectively) and from literature. All values are taken from graphs, text or were kindly provided by the first author, and converted to as few units as possible.

	NH_4^+	NO_3^+	Urea	Amino Acids	DON	Units	Location
Suspended matter							
V_N	4574 ± 2497	2405 ± 2415	820 ± 519	3105 ± 2602	835 ± 409	nmol-N gDW^{-1} h^{-1}	
ρ_N	185 ± 36	109 ± 62	147 ± 58	7 ± 4.2	3561 ± 594	nmol-N l^{-1} h^{-1}	
Andersson et al. (2006)	48 - 112	7 - 35	30 - 45	29 - 40		nmol-N l^{-1} h^{-1}	estuary
Middelburg and Nieuwenhuize (2000)	3	1	1 - 6	6 - 150		nmol-N l^{-1} h^{-1}	estuary
Glibert et al. (1991)	100 - 350	10 - 100		5 - 90		nmol-N l^{-1} h^{-1}	protected bay
Bode and Dortch (1996)	200 - 1600	500 - 2900				nmol-N l^{-1} h^{-1}	exposed coast
Badr et al. (2008)					3000 ± 2000	nmol-N l^{-1} h^{-1}	estuary
Kerner and Spitzy (2001)					3000 - 6000	nmol-N l^{-1} h^{-1}	estuary
Mulholland et al. (2002)	2830 ± 280			1004 ± 10		nmol-N l^{-1} h^{-1}	coastal bay
Tamminen and Irmisch (1996)			36 - 54			nmol-N l^{-1} h^{-1}	coast
Kokkinakis and Wheeler (1987)	13 - 95	4 - 151	2 - 69			nmol-N l^{-1} h^{-1}	upwelling region
Bronk (2002)			63.5 ± 92.8	134.8 ± 317.3	114 ± 142	nmol-N l^{-1} h^{-1}	[a]
Tungaraza et al. (2003)	10 - 20	0 - 50	0 - 5			nmol-N l^{-1} h^{-1}	offshore
Lepoint et al. (2004)	727 ± 827	270 ± 313				umol-N g-N^{-1} h^{-1}	Mediterranean coastal bay
Epiphytes							
V_N	563 ± 278	876 ± 541	608 ± 599	659 ± 531	39 ± 16	nmol-N gDW^{-1} h^{-1}	
Lepoint et al. (2004)	7.4 ± 7.6	5.3 ± 6.5				umol-N g-N^{-1} h^{-1}	Mediterranean coastal bay
Seagrasses							
V_N	338 ± 151	114 ± 47	110 ± 36	129.1 ± 96	13 ± 5	nmol-N gDW^{-1} h^{-1}	
ρ_N	18 ± 18	7.9 ± 5.9	32 ± 11	0.5 ± 0.6	68 ± 77	nmol-N l^{-1} h^{-1}	
Vonk et al. (2008)	1500 - 2850	330 - 1860	340 - 680	130 - 460		nmol-N gDW^{-1} h^{-1}	offshore
Morris et al. (2008)	1070 - 4790					nmol-N gDW^{-1} h^{-1}	protected bay
Lee and Dunton (1999)	1030 - 1840	770 - 1180				nmol-N gDW^{-1} h^{-1}	protected bay
Cornelisen and Thomas (2004)	257 - 1131	118 - 225				nmol-N gDW^{-1} h^{-1}	protected bay
Thursby and Harlin (1982)	2540					nmol-N gDW^{-1} h^{-1}	protected bay
Lepoint et al. (2004)	3.7 ± 3.2	3.1 ± 4.6				umol-N g-N^{-1} h^{-1}	Mediterranean exposed bay
Macroalgae							
V_N	181 ± 115	217 ± 210	45 ± 53	228.7 ± 147	12 ± 8.9	nmol-N gDW^{-1} h^{-1}	
ρ_N	9.6 ± 6.8	12 ± 6.1	8.4 ± 7.5	0.8 ± 0.6	71 ± 82	nmol-N l^{-1} h^{-1}	
Vonk et al. (2008)	3340 - 5490	3400 - 5010	1670 - 2530	380 - 620		nmol-N gDW^{-1} h^{-1}	offshore area
Probyn and Chapman (1982)	1199		1199			nmol-N gDW^{-1} h^{-1}	
Phillips and Hurd (2004)	220 - 1510	320 - 1240	120 - 1350			nmol-N gDW^{-1} h^{-1}	rocky shore
Tyler et al. (2005)			165	15 - 21		nmol-N gDW^{-1} h^{-1}	protected bay
Lepoint et al. (2004)	19 ± 16	19 ± 20				umol-N g-N^{-1} h^{-1}	Mediterranean coastal bay

[a] Average over different types of locations

also contributed to planktonic nitrogen uptake but always less than 35% (Fig. 5.5), and a gradual increase in contribution was found for more complex compounds. Our results, clearly illustrate the importance of the choice of label: ^{15}N labeling of the molecule may induce a phytoplankton associated bias, whereas the carbon skeleton is taken up by the bacterial community.

5.4.3 Preference for different nitrogen substrates

Ammonium was preferred over NO_3^- by most primary producers, whereas urea was taken up to a smaller extent. Seagrasses did not prefer NO_3^- over urea-N (Fig. 5.3). If the correction for the amount of substrate nitrogen is weakened to a correction for the amount of nitrogen-containing substrate (which is what primary producers see in the first place), urea delivered more nitrogen than NO_3^- per available molecule in the seagrasses and the epiphytes. The epiphytes did not show a pronounced preference for inorganic nitrogen or urea over amino acids (Fig. 5.3). Within the SPM compartment NH_4^+ was exclusively taken up by the phytoplankton (Fig. 5.5). The NO_3^- uptake was only for 6% attributable to bacteria, leaving the remaining 94% to the phytoplankton. As opposed to what is generally believed (see Middelburg and Nieuwenhuize (2000) for an overview), heterotrophic bacteria contributed more to NO_3^- uptake than to NH_4^+ uptake in our incubations.

The preferences for glycine and leucine, as indicated by the specific uptake rates normalized to the amount of added substrate, were comparable to those for NO_3^- and urea, (Fig. 5.3). A clear preference pattern emerged, with glycine uptake dominating over leucine uptake, and a low uptake of phenylalanine (Fig. 5.3). Total uptake of the individual amino acids also reflected the decreasing preference (Fig. 5.4) with increasing complexity. This gradient for seagrasses and epiphytes was less pronounced in the SPM because leucine was preferred over glycine and phenylalanine, probably because of the large contribution of bacteria in SPM (Fig. 5.5). Preferences for simple N-rich amino acids over complex C-rich amino acids were also observed for terrestrial plants (Harrison et al., 2007). The bacterial contribution to ^{15}N incorporation by SPM gradually increased from 0 - 6% for the inorganic nitrogen compounds over urea, glycine, and leucine to 32% for phenylalanine (Fig. 5.5). Note that the C/N ratio and the molecular weight also covary with the complexity in our substrates.

DON was used by all primary producer compartments, particularly by SPM. In fact, the planktonic uptake rate normalized to the amount of nitrogen was for algae-derived DON very similar to that for NH_4^+. The macrophytic contribution to DON incorporation amounted to only 5% of the total DON incorporation (Fig. 5.4). But in view of their overall low nitrogen demand compared to that of SPM this could be expected. The specific $DO^{15}N$ uptake rates per amount of substrate were in the seagrasses comparable to those for leucine, and in the epiphytes comparable to the NO_3^- and urea uptake rates. Algae-derived DON was preferred over bacteria-derived DON (81% of the added amount ended up in the primary producers; Fig. 5.4). Bacteria-derived DON uptake was most likely even overestimated because substrate stuck to the filters.

5.4.4 Carbon uptake relative to nitrogen uptake

Primary production (DIC incorporation) was dominated by the macrophytes, which accounted for ≈85% of the total DIC uptake (Fig. 5.4). SPM only contributed ≈15% to DIC uptake in both inorganic nitrogen additions (Fig. 5.4). These contributions are in perfect agreement with values for the subtropics (Kaldy et al., 2002). Dominance of seagrasses over phytoplankton in primary production is expected considering the larger biomass and C/N ratio of the former relative to the latter (Duarte, 1995; Kaldy et al., 2002), although dominance of epiphyte and phytoplankton production over seagrass production has also been observed (Moncreiff et al., 1992). DIC incorporation into SPM was for 74% accomplished by the phytoplankton, still leaving 26% for the bacterial portion (Fig. 5.5). Since carbon fixing cyanobacteria were not present, DOC uptake by bacteria after exudation or leakage from POC is the most likely pathway (Van den Meersche et al., 2004). DOM loss to the water column occurs in phytoplankton (Carlson, 2002) as well as seagrasses (Findlay et al., 1986).

Urea-C was taken up by all primary producers in similar quantities (Fig. 5.4), probably owing to the high concentrations and a strong urease activity which led to significant labeling of the NH_4^+ and DIC pools. Not only bacteria, but also phytoplankton can utilize urea by splitting it extracellularly or intracellularly (Price and Harrison, 1988). The bacterial contribution to carbon incorporation from urea and glycine was similarly low as from DIC, but carbon uptake from leucine and phenylalanine in the HAA pool was dominated by the bacteria. The latter was also supported by the PLFA analysis (Fig. 5.5).

In contrast to the macrophyte-dominated DIC utilization, DOC uptake occurred almost exclusively by the SPM. Considering the dominance of the macrophytes in DIC utilization, it is likely that the SPM used the DOC either directly or immediately following remineralization since the total uptake of carbon by the macrophytes in the DOM additions was very low compared to the SPM. Both uptake of the total compounds and uptake of parts after breakdown have been documented for phytoplankton (Palenik and Morel, 1991; Legrand and Carlsson, 1998).

5.4.5 From experiment to ecosystem

Comparing the area-specific nutrient stocks with the total uptake of substrate in the same water column, it is obvious that most of the substrates would be depleted even within half a tidal cycle in the absence of fluxes replenishing the substrate pools (Tab. 5.2). Although the calculation of turnover rates is imprecise due to the accumulation of measurement error, those for *Zostera noltii* and *Cymodocea nodosa* fell within the range reported by Lee and Dunton (1999) for *Thalassia testudinum*. Although nutrient limitation is largely species specific (Udy and Dennison, 1997) and should be assessed using proper methods (see for instance Downing et al., 1999), our results underline this possibility for Càdiz Bay. In addition, the nitrogen content of the seagrasses (data not presented) was generally below 1.8%, the approximate limit indicated by Duarte (1990). Irrespective of the presence or absence of nitrogen limitation, our calculations illustrate the vital role of benthic fluxes to

the water column and fast remineralization in the canopy and underlying sediment in Càdiz Bay.

Organic nitrogen uptake exceeds by far that of inorganic nitrogen. Note, however, that the absolute DON uptake values are based on the assumption that all DON present in the water column is of algal origin and of the same composition as the added substrate, both unrealistic assumptions. However, reported DON remineralization rates are very similar to the total uptake rates found here (Tab. 5.2); Kerner and Spitzy (2001) reported a DON removal rate of 43 μg N l^{-1} h^{-1}, corresponding to 11 mmol m^{-2} h^{-1} under the assumptions used in this study (cfr. section 5.2.5). Similarly, Badr et al. (2008) reported a removal of 12% h^{-1} for estuarine DON, corresponding to 7.3 mmol m^{-2} h^{-1} in our system. These rates would be enough to supply all the NH_4^+ and NO_3^- needed to compensate for the uptake of DIN in the bay.

This study has revealed a strong exploitation of the DON pool by both macrophytes and microbes in a temperate seagrass meadow. All primary producers distinguished between individual organic compounds, and preferences were potentially related to the structural complexity. These are strong indications for direct uptake of DON compounds by the primary producers in addition to bacterial remineralization. Our results show that recycling fluxes are not only very high, but also that there are different pathways. More research is needed to gain insight into the ins and outs of DON in general, and in seagrass and other macrophyte-dominated systems in particular. Biomarker-based research and utilization of multiple isotope tracers to characterize different pathways at once is one promising but currently underused strategy.

6. Dissolved organic matter uptake in macrophyte-dominated marine sediments: nitrogen retention and partitioning among algae, bacteria, roots, and shoots

Van Engeland T., T. J. Bouma, E. P. Morris, F. G. Brun, G. Peralta, M. Lara, I. E. Hendriks, P. van Rijswijk, B. Veuger, K. Soetaert & J. J. Middelburg. (In prep.)

Abstract - *Seagrasses enhance their nutrient acquisition by trapping suspended particulate nutrients and stimulation of heterotrophic reworking in the sediment. Although regenerated production is a key aspect of seagrass ecosystems, the mechanisms behind nutrient regeneration are only superficially understood. We used a set of dual-labeled (^{13}C and ^{15}N) dissolved (in)organic nitrogenous compounds to assess nitrogen retention and regeneration in macrophyte-dominated sediments. Two seagrass species (Zostera noltii and Cymodocea nodosa) and one macroalga (Caulerpa prolifera) were studied. Among the simple substrates tested, ammonium and glycine nitrogen were the most retained after 24 hours of incubation in the field. Leucine and phenylalanine nitrogen were retained to a lesser degree. Of a complex substrate consisting of algae-derived dissolved organic matter a fraction similar to that of ammonium and glycine was retained in the sediment-macrophyte system. Macrophyte ^{15}N uptake exhibited a similar pattern, with highest values in the NH_4^+ and glycine additions. Concentrations of ^{15}N were similar in aboveground and belowground tissue, indicating allocation within the macrophytes according to biomass. Biomarker measurements (phospholipid-derived fatty acids, PLFA; D-alanine) indicated that in sediments carbon was exclusively taken up by bacteria and directed predominantly towards PLFAs, whereas nitrogen was taken up by the primary producers (i.e. macrophytes and microphytobenthos) and built into hydrolysable amino acids. ^{13}C enrichment in bacterial PLFAs was highest in the leucine treatments, whereas some algal PLFAs exhibited maximal enrichment according to carbon content of the amino acid added (glycine < leucine < phenylalanine), providing some evidence that regenerated DIC was the main (but quantitatively not significant) carbon source for microphytobenthos. Seagrasses received organic matter-derived carbon through the root system, in proportions dictated by the substrate C/N ratio. Our experiment illustrates compound-specific organic matter retention and destination of regenerated nitrogen.*

6.1 Introduction

Seagrasses and rooting macrophytes can take up substantial amounts of nitrogen from the sediment (Pedersen and Borum, 1993; Lepoint et al., 2002b). In temperate oligotrophic seagrass systems, detritus-derived nitrogen is the most important fixed-nitrogen source since benthic nitrogen fixation is limited (Welsh, 2000). Although N-losses due to benthic efflux and coupled nitrification-denitrification are significant (Hemminga et al., 1991), the nitrogen retention in seagrass systems is stronger than in unvegetated sediments, and detritus-derived nitrogen can be quickly transferred to the seagrasses (Evrard et al., 2005; Barron et al., 2006).

Nitrogen recycling from detritus (PON) usually occurs through dissolved organic nitrogen (DON) as intermediate (Bronk, 2002). The DON can be taken up as such or can be remineralized to dissolved inorganic nitrogen (DIN) before uptake. In seagrass research, it is usually assumed that remineralization of DON to DIN is "the" pathway to organisms (see for instance Boon et al., 1986). However, Vonk et al. (2008) recently reported a quick root-mediated uptake of nitrogen from small organic compounds by tropical seagrasses. However, they did not distinguish between amino acid uptake and ammonium uptake after deamination, as would be possible when using dual-labeled (^{13}C and ^{15}N) compounds (Mulholland et al., 2004; Tyler et al., 2005; Andersson et al., 2006; Harrison et al., 2007). Nevertheless, glutamate uptake was demonstrated for an axenic culture of *Halophila decipiens* (Bird et al., 1998), which makes direct uptake of a wider spectrum of compounds plausible.

Beside seagrasses, many other organisms can utilize DON compounds (Bronk et al., 2007). Given the high productivity in seagrass systems and the low C/N ratio of micro- and macroalgae living within these seagrass ecosystems, competition for nitrogen is conceivable (e.g. Plus et al., 2003). In addition, heterotrophic bacteria are the main drivers behind remineralization, but they may compete with seagrasses for nitrogen when their growth is nitrogen-limited (Lopez et al., 1998). Soil bacteria have also been shown to be competitive with terrestrial plants for amino acids (Bardgett et al., 2003).

The retention and fate of nitrogen in sediments will depend on the consumers and the processes. Retention is compound-specific (Veuger et al., 2006), and will most likely depend on the usefulness of the compounds to organisms. Nitrogen consumers differ in their uptake capabilities and preferences for particular compounds (Admiraal et al., 1987; Lomstein et al., 1998; Berg et al., 2003; Vonk et al., 2008). Some primary producers can utilize organic nitrogen directly, whereas others rely on bacterial remineralization. This can result in either coupled or uncoupled uptake of carbon and nitrogen (Tyler et al., 2005; Veuger and Middelburg, 2007). It is currently unknown (1) how much of the bioavailable nitrogen in sediments is directed towards different sinks (i.e. macrophytes, bacteria, microphytobenthos, sediment), (2) in which form the nitrogen enters the respective compartments, and (3) if (or for which compounds) carbon and nitrogen uptake are (partially) coupled.

We investigated the retention and fate of dissolved inorganic (DIN) and dissolved organic nitrogen (DON) compounds in temperate macrophyte-dominated beds with two seagrass species (*Zostera noltii* and *Cymodocea nodosa*) and a rooting macroalga (*Caulerpa prolifera*). Ammonium additions served as reference. The use of dual-labeled (^{13}C and ^{15}N) amino acids allowed us to track the fate of the carbon and nitrogen separately, and to assess their coupling

in the different components of macrophyte-sediment systems. Three amino acids of varying molecular structure and complexity were followed to assess the compound-specificity of use, retention, and partitioning among micro-organisms and macrophytes. Biomarker analyses (polar lipid-derived fatty acids; PLFA, and D-alanine) enabled us to estimate bacterial contributions to microbial assimilation. In addition, a complex substrate derived from an axenic algal culture was used to mimic the highly complex DON pool found in natural sediments.

6.2 Materials and Methods

6.2.1 Field experiment and sample processing

This in situ incubation experiment was conducted in August 2007 in the inner bay of Cadiz, which is dominated by two seagrass species (*Zostera noltii* and *Cymodocea nodosa*) and one small rooting macroalga (*Caulerpa prolifera*). One of five substrates was added to sediments around subtidal *Zostera noltii*, *Cymodocea nodosa*, or *Caulerpa prolifera* individuals, and left to incubate for 24 hours under calm weather (Tab. 6.1). For each species-treatment combination three replicate incubations were set up.

A total volume of 1 ml, containing the amount of substrate indicated in table 6.1 was injected in situ at four points 1 cm from the base of the plant. The needle was pushed 5 cm into the sediment, and while slowly retracting the syringe the substrate was injected, thus creating a more or less homogeneous vertical distribution over the upper 5 cm of the sediment. After 24 hours of incubation, the sediment including the plant was sampled to a depth of 10 cm by pressing in a tube of 4.2 cm inner diameter. The sediment cores were left in the tubes after removal of the overlying water. They were frozen at -20 °C within the hour until further processing. We decided not to press in the core tubes before the sediment injections to avoid artifacts from cutting plants and altered pore water flow. This, however, implies that the substrate could diffuse away from the direct vicinity of the plant, and that sampling only recovered part of the remaining substrate. In this sense our estimates of nutrient retention in the sediment are minimum but realistic estimates.

During processing the sediment cores were subdivided into two layers: the upper 2 cm and the remainder (2-10 cm), further referred to as the top layer and the bottom layer, respectively. After freeze drying, the plant material was separated from the sediment. Distinction was made between aboveground and belowground macrophyte material. Dry weights were determined, and the tissue was ground to a fine powder. Note that it was not feasible to remove all the plant material (e.g. hair roots) from the sediment due to the brittleness of the plant material after freeze drying. This means that part of the enrichment in the sediment may be due to uptake in the roots of macrophytes, rather than microbial biomass or adsorption.

Table 6.1: The substrates (Cambridge Isotope Laboratories, CIL) used for this experiment. For the protocol of DON preparation we refer to Veuger et al. (2004). For the amino acid composition of the complex DOM substrate we refer to chapter 4.4.4.

Treatment	Abbreviations	Labeled substrates	Added amount
1 NH_4^+	NH_4^+	NH_4Cl (^{15}N, 99%)	2.7 μmol-^{15}N
2 Glycine	Gly	Glycine (U$^{13}C_2$, 98%; ^{15}N, 98%; c/n = 2)	2.7 μmol-^{15}N
3 Leucine	Leu	L-Leucine (U$^{13}C_6$, 98%; ^{15}N, 98%; c/n = 6)	2.7 μmol-^{15}N
4 Phenylalanine	Phe	L-Phenylalanine (U$^{13}C_9$, 98%; ^{15}N, 98%; c/n = 9)	2.7 μmol-^{15}N
5 Algae-derived DOM	DOC_{Alg}	DOC (8.33% ^{13}C)	0.5 μmol-^{13}C
(= DOM_{Alg})	DON_{Alg}	DON (65.78% ^{15}N)	0.5 μmol-^{15}N

6.2.2 Chemical analyses

The macrophytes and sediment samples were analyzed for carbon and nitrogen content and isotopic composition using a Thermo EA 1112 elemental analyzer coupled to a Thermo Delta V Advantage isotope ratio mass spectrometer with a Conflo II interface (EA-IRMS; Vonk et al., 2008). The concentrations and isotope composition of carbon and nitrogen in the sediment hydrolysable amino acids (HAA) were determined by gas chromatography-combustion-isotope ratio mass spectrometry (GC-c-IRMS) using a HP 6890 GC with a Thermo type III combustion interface and Thermo Delta Plus IRMS after extracting and derivatizing the amino acids (Veuger et al., 2005). Following PLFA (polar lipid-derived fatty acid) extractions and derivatization to fatty acid methyl esters (FAME) by a modified Bligh and Dyer protocol (Boschker et al., 1999), FAME concentrations were measured using gas chromatography-flame ionization detection (GC-FID) after separation on a polar column (Scientific Glass Engineering BPX-70; Middelburg et al. 2000). ^{13}C FAME isotope ratios were measured on a HP 6890 GC gas-chromatograph with a Thermo type III combustion interface and Thermo Delta Plus isotope ratio mass spectrometer (GC-c-IRMS). Sediment grainsize distribution parameters were determined using a Malvern 2000 Laser Particle Sizer.

6.2.3 Calculations & statistics

Results on isotopic compositions are all based on atomic fractions (F^{15N} and F^{13C}). The occurrence of uptake was investigated using t-tests to test the difference between the heavy isotope fractions in the treatment samples (F_{sample}) relative to the natural heavy isotope fractions in the natural abundance samples ($F_{reference}$). Isotope excesses were calculated as the difference $E_{sample} = F_{sample}$ - $F_{reference}$. Since the incubations lasted for 1 day, these excesses can be considered either dimensionless or as average specific uptake rates of heavy isotope per day (d^{-1}). Total incorporation of heavy isotope in the macrophytes resulted from the multiplication of the fractional excess by the nitrogen (or carbon) content, and was expressed in μmol-^{15}N (or ^{13}C). Retention in the sediment was calculated as the product of the organic nitrogen (and carbon) concentration and the fractional excess in ^{15}N (and ^{13}C) in the sediment, and was expressed in μmol-^{15}N (or ^{13}C) g DW_{sed}^{-1}. Incorporation in microbial (bacterial or microphytobenthos) biomass, PLFA (phospholipid-derived fatty acids) or HAA (hydrolysable amino acids) was as the product of the relevant concentrations (microbial carbon, PLFA carbon, amino acid carbon or nitrogen) and the fractional excess in the relevant biomarker or biotic compartment. In analogy with the fractional excesses, the total incorporation is either interpreted as an amount taken up, or as a transport rate sensu Dugdale and Wilkerson (1986) expressed on a per-day basis. Macrophyte total uptake rates were divided by the dryweight to obtain dryweight-normalized specific uptake rates of heavy isotope. Contributions to total retention in the macrophyte-sediment system were calculated by dividing individual total incorporations per compartment by the sum over the compartments studied, after the biomarkers and sediment incorporation values were integrated over the relevant sediment layer (multiplication by the dryweight of the sediment layer).

Bacterial biomasses were calculated from PLFA (polar lipid-derived fatty acid) concentration as:

$$Bact = \sum PLFA_{bact-spec}/(a \times b),$$

with $PLFA_{bact-spec}$ = the concentrations of bacteria specific PLFAs (iC15:0, aiC15:0, iC16:0, iC17:0, C18:1ω7c; in μmol g DW_{sed}^{-1}), a = 0.073 mmol bacterial PLFA-C per mmol bacterial C, and b = 0.28 mmol bacteria-specific PLFA-C per mmol bacterial PLFA-C (Brinch-Iversen and King, 1990; Moodley et al., 2000; Evrard et al., 2008). Microphytobenthos biomass was calculated from PLFA concentrations as:

$$MPB = (\sum PLFA_{all} - \sum PLFA_{bact-spec}/b)/c,$$

with $\sum PLFA_{all}$ the total concentration of PLFAs in the sediment and c = 0.062 mmol PFLA-C per mmol microalgal C (Dijkman and Kromkamp, 2006a). ^{13}C incorporation into bacterial and microalgal biomass (bacteria + microphytobenthos)was calculated by multiplying the ^{13}C excesses (atomic fractions) with the PLFA concentrations in the presented formulae.

Bacterial contributions to amino acid ^{13}C and ^{15}N uptake were measured by means of incorporation in D-alanine (a bacterial biomarker) relative to incorporation in L-alanine (present in both prokaryotes and eukaryotes), assuming a bacterial D-alanine-to-L-alanine ratio of 0.065 (Veuger et al., 2005, 2007). Incorporation of nitrogen and carbon into microbial biomass was estimated by means of excesses in HAA (hydrolysable amino acids; E^{HAA}) as follows:

$$I_{^{15}N} = Bactfrac \times \sum E_{HAA}^{^{15}N}/0.53 + (1 - Bactfrac) \times \sum E_{HAA}^{^{15}N}/0.67$$

$$I_{^{13}C} = Bactfrac \times \sum E_{HAA}^{^{13}C}/0.44 + (1 - Bactfrac) \times \sum E_{HAA}^{^{13}C}/0.38$$

with Bactfrac the bacterial fraction in microbial biomass, based on PLFA data (Bact/(MPB + Bact)). The conversion factors were based on data from (Cowie and Hedges, 1992; 0.38 HAA-C/OC and 0.67 HAA-N/ON for microalgae, and 0.43 HAA-C/OC and 0.53 HAA-N/ON for bacteria). These calculations represent essentially the weighted average of the incorporation under the assumption of an incorporation by bacteria only and incorporation by microphytobenthos only, with their share in total microbial biomass, based on PLFA data, as weights.

All calculations were performed in the statistical package R (R Development Core Team, 2009). Significance tests were performed using the gls-function in the nlme package for R (Pinheiro et al., 2008).

6.3 Results

6.3.1 Characterization of the macrophytes and their sediment

The carbon content of *Caulerpa prolifera* tissue was significantly higher than that of seagrasses (t-test, $p < 0.0001$). The higher nitrogen content of *Caulerpa prolifera* relative to

seagrasses was even more pronounced (Tab. 6.2). Overall *Caulerpa prolifera* had a much lower C/N ratio than the seagrasses (Tab. 6.2).

The organic matter content of the *Caulerpa prolifera* sediment was 20 times higher than that of the seagrass sediments, both in terms of carbon and nitrogen (Tab. 6.2). The C/N ratios, based on the organic matter concentrations, were rather close to Redfield values, with a small carbon excess. In contrast to the sandy character of the seagrass sediment, the *Caulerpa prolifera* sediment was black silty mud (Tab. 6.2) with a strong sulphide smell, indicating sulphate reduction.

PLFA concentrations were roughly twice as high in the *Caulerpa prolifera* sediment, compared to the seagrass-inhabited sediments (data not shown). The most abundant PLFA (phospholipid-derived fatty acid) marker was C16:0 (present in most microalgae and bacteria), independent of the macrophyte species. In the seagrass sediments the next most abundant marker was C16:1ω7c, abundantly present in diatoms, followed by C18:1ω7c, a proxy for gram-negative bacteria in sediments. However, in the *Caulerpa prolifera* sediment the bacterial marker C18:1ω7c was more abundant than the diatom marker C16:1ω7c. The bacterial markers aiC15:0 and iC15:0 were in this (presumed highly anoxic) sediment the fourth and fifth in abundance, whereas their relative abundance in the seagrass sediment was lower. Microbial biomass (bacteria + microphytobenthos), estimated from the PLFAs, was largest in the *Caulerpa prolifera* sediment, but contributed the least to sediment total organic carbon (Tab. 6.2).

6.3.2 Nitrogen and carbon retention in the sediment

In the top layer of the sediment (upper 2 cm) ^{15}N excesses over natural abundances were significant in all treatments and for each macrophyte species (Fig. 6.1). The ^{15}N recovery in the NH_4^+ and glycine additions were generally comparable in magnitude (Fig. 6.1). The extent of amino-N recovery decreased in the order glycine > leucine > phenylalanine, according to their molecular weight, complexity and C/N ratio (2, 6, and 9 respectively). After 24 hours of incubation the $DO^{15}N_{Alg}$ concentration was higher in the sediment than phenylalanine ^{15}N but lower than for the other amino acids (Fig. 6.1). This was probably due to the added quantity of DOM being smaller than for all other substrates (Tab. 6.1).

For the additions of dual-labeled substrates bulk ^{13}C excesses in the sediment top layer were generally significant (Fig. 6.1). After 24 hours the highest ^{13}C recovery was observed for leucine carbon. The dryweight-normalized ^{13}C recovery was related to the ^{15}N retention by the substrate C/N ratio (Fig. 6.1; red crosses), but tended to be slightly lower than predicted from the nitrogen (Fig. 6.1; red crosses), indicating some loss of C. This difference was statistically significant in the sediment top layer for the glycine additions to *Zostera noltii* and the glycine, leucine and phenylalanine additions to *Cymodocea nodosa* (Paired t-test; $p <= 0.02$ for all). The differences in the glycine and leucine additions to *Caulerpa prolifera* were not significant (Paired t-test; $p = 0.07$ for both). The bottom layers of the sediment cores exhibited similar patterns (data not shown) but the signals were generally weaker, due to dilution effects (the syringe needle did not penetrate to the lower end of the bottom layer).

Table 6.2: Carbon and nitrogen content, and C/N ratios of the macrophytes (average of aboveground and belowground tissue) and the sediment (top layer only), and microbial biomass (bacteria + microphytobenthos) and contribution to total organic carbon in the sediment, based on PLFA data. All numbers, except the median grainsize of the sediment, are expressed as average ± standard deviations.

		Zostera noltii	*Cymodocea nodosa*	*Caulerpa prolifera*
Macrophytes	C-content (μmol-C g DW^{-1}_{tissue})	12285 ± 2502	13603 ± 3493	16775 ± 3435
	N-content (μmol-N g DW^{-1}_{tissue})	564 ± 278	626 ± 312	1413 ± 397
	C/N ratio	26 ± 9	26 ± 11	12 ± 3
Sediment	C-content (μmol-C g DW^{-1}_{sed})	110 ± 20	103 ± 23	2294 ± 698
	N-content (μmol-N g DW^{-1}_{sed})	14.7 ± 4.0	13.5 ± 4.1	264 ± 52
	C/N-ratio	7.7 ± 1	7.9 ± 1.4	8.6 ± 1.5
	Microbial biomass (μmol-C g DW^{-1}_{tissue})	15.5 ± 3.4	10.3 ± 1.7	30 ± 13
	Microbial contribution to TOC_{sed} (wt%)	16 ± 5	10 ± 2	1.5 ± 0.6
	Median grainsize (μm)	267	252	65

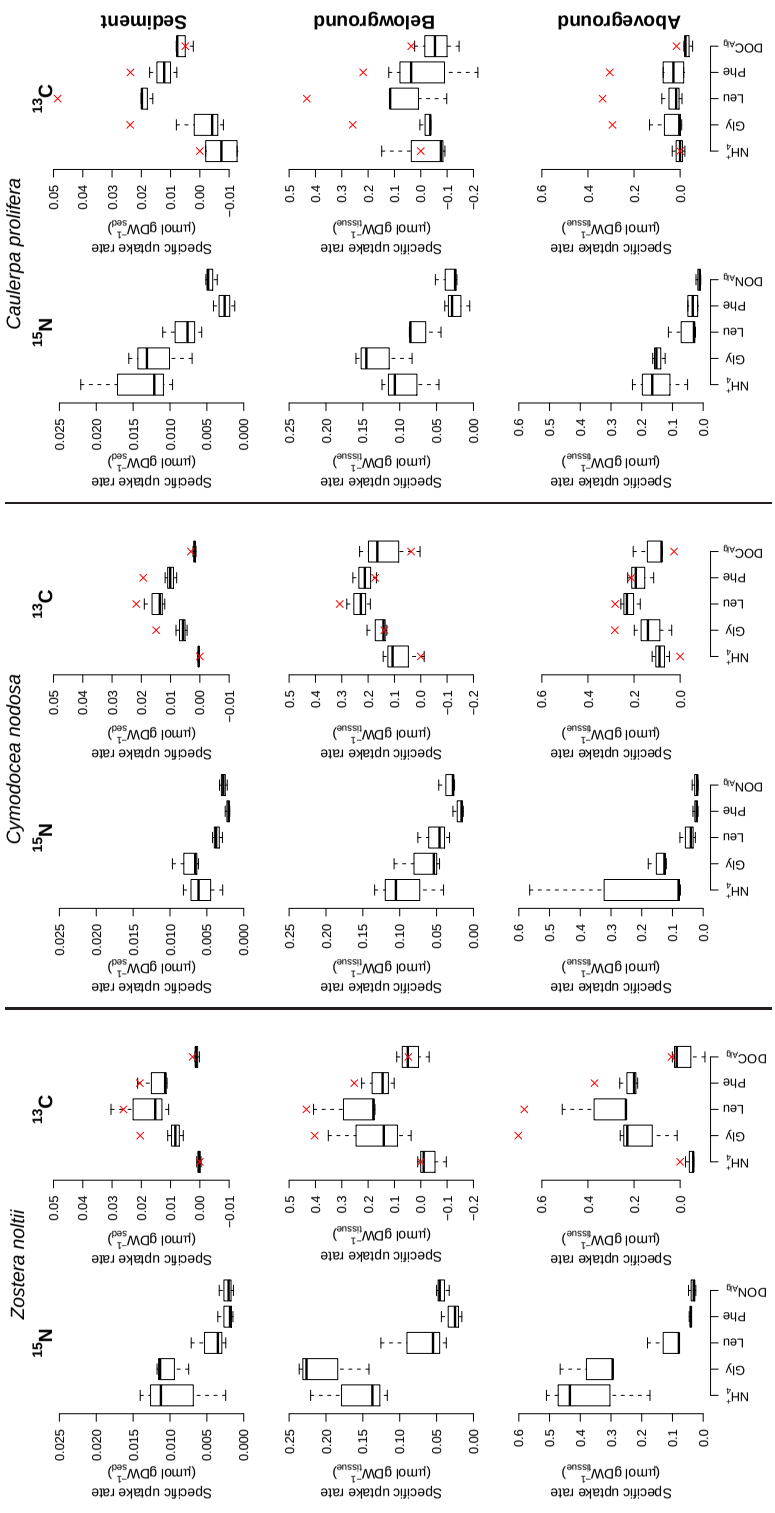

Figure 6.1: ^{15}N and ^{13}C recovery from the top layer of the sediment (upper), belowground tissue (middle), and aboveground tissue (lower) of the three macrophytes after 24 hours of incubation. The red crosses in the ^{13}C panels represent the theoretically expected excess of ^{13}C, based on the C/N ratio of the substrates and the total ^{15}N uptake.

Table 6.3: Specific nitrogen uptake rates in the macrophytes for the various substrates, expressed in nmol-N gDW^{-1} d^{-1} (mean ± sd).

Substrate	*Zostera noltii*	*Cymodocea nodosa*	*Caulerpa prolifera*
NH_4^+	185 ± 62	107 ± 63	121 ± 61
Gly	210 ± 53	79 ± 28	141 ± 19
Leu	76 ± 47	49 ± 23	67 ± 37
Phe	29 ± 13	20 ± 7	33 ± 11
DON_{Alg}	42 ± 9	32 ± 9	18 ± 5

6.3.3 Nitrogen and carbon uptake by the macrophytes

In the belowground parts of the macrophytes significant ^{15}N excesses over the natural background isotope abundance existed for each of the treatments and plants (Fig. 6.1; middle row). The overall pattern in dryweight-normalized total ^{15}N uptake was similar to that of the surrounding sediment. The strongest N uptake occurred in the NH_4^+ and glycine additions, followed by the leucine and phenylalanine additions (Fig. 6.1). The ^{15}N uptake per gram of dryweight in the DON_{Alg} additions were of the same order as those in the leucine and phenylalanine additions (Fig. 6.1). The belowground parts of *Zostera noltii* consistently showed a higher uptake, relative to the other macrophytes. The difference between *Caulerpa prolifera* and *Cymodocea nodosa* were not significant, but tended towards stronger uptake by *Cymodocea nodosa*. The aboveground parts generally exhibited significant excesses in ^{15}N (Fig. 6.1; lower row).

The *Z.noltii* and *Caulerpa prolifera* belowground parts showed no significant ^{13}C excesses, which seemed attributable to a lack of statistical power rather than the absence of uptake in case of *Zostera noltii*, since a similar pattern as for *Cymodocea nodosa* was apparent (Fig. 6.1). For the same reason, the aboveground *Zostera noltii* tissue did show a significant ^{13}C uptake from leucine and phenylalanine. Again nitrogen uptake was a good predictor of the carbon uptake from the presented dual-labeled substrates by the seagrasses, but not in *Caulerpa prolifera* due to very low C uptake (red crosses; Fig. 6.1). Losses (differences between observed and expected uptake, based on the substrate C/N ratio and the nitrogen uptake) were not significant due to large variability in the expected values. The ^{15}N excesses in the macrophytes after addition of DOM_{Alg} substrate were significant but low. This is in part due to to lower amount of added label (0.50 μmol-^{15}N and 0.5 μmol-^{13}C as opposed to the 2.7 μmol-^{15}N in the NH_4^+ and amino acid treatments).

6.3.4 Nitrogen and carbon uptake by the microbial community

Bacterial carbon incorporation based on the phospholipid-derived fatty acid (PLFA) data followed the pattern of bulk ^{13}C retention in the top layer of the sediment (Fig. 6.1 and 6.2), with maximal values in the leucine treatments for all species. Statistically significant excesses were found for the amino acid treatments (Mixed model ANOVA with random macrophyte species-effect, $p < 0.05$ for each amino acid). Microalgal ^{13}C uptake was in

none of the treatments statistically significant (data not shown). Nevertheless, individual microalgal markers showed ^{13}C excesses with particular substrates (Fig. 6.3)

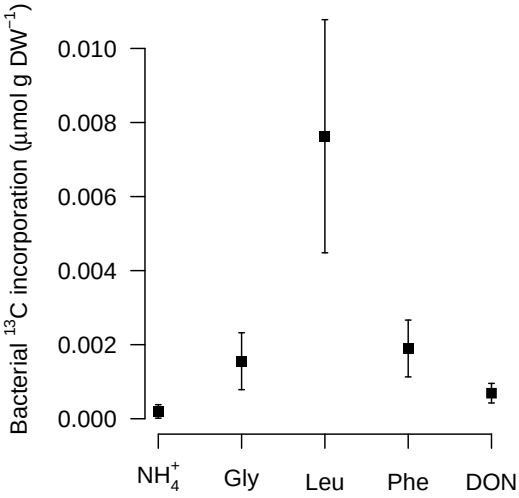

Figure 6.2: Total ^{13}C incorporation in bacterial biomass, based on PLFA data, normalized per gram of sediment dryweight.

Individual PLFA markers exhibited differential uptake patterns. The bacterial markers (e.g. iC15:0, aiC15:0, C18:1ω7c) showed a maximal ^{13}C excess in the leucine additions (shown for aiC15:0 in Fig. 6.3), whereas C18:2ω6c (abundant in the algal taxa Chlorophyceae and Trebouxiophyceae) exhibited a maximal specific ^{13}C uptake rate in the phenylalanine treatment (Fig. 6.3). A principal component analysis (data not shown) revealed an association of this marker alone with phenylalanine carbon excesses, irrespective of the macrophyte species, and the respective sediment types. The mono-unsaturated fatty acid C16:1ω7c and poly-unsaturated fatty acid C20:5ω3, which are abundantly present in diatoms, exhibited maximal specific ^{13}C uptake rates in the glycine and leucine treatments of the seagrasses.

Nitrogen and carbon incorporation in hydrolysable amino acids (HAA) was stronger in the silty *Caulerpa prolifera* sediment than in the sandy seagrass sediment (data not shown). Microbial nitrogen incorporation in biomass differed significantly between the macrophyte species (ANOVA, $F_{2,9} = 4.6$, $p = 0.04$). The C/N ratio of total incorporation of nitrogen and carbon into the HAA pool increased with increasing substrate C/N ratio (in the seagrasses: 0.3 ± 0.1, 0.94 ± 0.1, and 1.7 ± 0.4, and in *Caulerpa prolifera* 3, 4, and 11 for glycine, leucine and phenylalanine respectively). Excess ^{13}C in D-alanine, did not exceed the racemization background, implying that incorporation of carbon in bacterial amino acids is small.

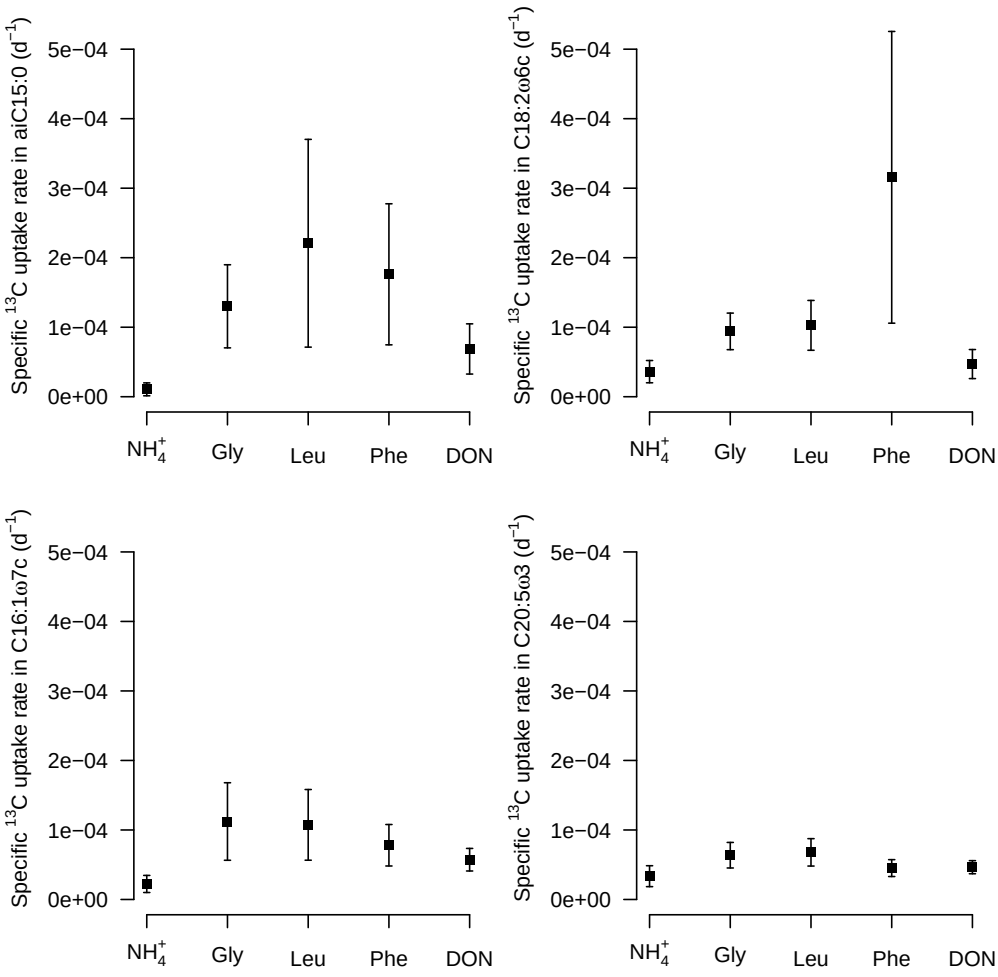

Figure 6.3: Specific ^{13}C uptake rates in individual PLFA markers, averaged over macrophytes species. These markers represent different biotic groups (aiC15:0 : bacterial; C18:2ω6c algal; C16:1ω7c and C20:5ω3: diatom). The NH_4^+ treatment did not receive labeled carbon and can be considered a reference for the natural abundance and variability in the isotope composition of the markers.

6.3.5 Nitrogen and carbon partitioning in the sediment

Less than half of the added nitrogen was recovered in the sediment plots 24 hours after nutrient addition (Fig. 6.4). Algae-derived DOM (both DOC_{Alg} and DON_{Alg}) was efficiently kept within the macrophyte-sediment system. The highest retention of DOM_{Alg} occurred in the *Cymodocea nodosa*-sediment system. The other substrates were most efficiently retained by the *Zostera noltii*-sediment system (Fig. 6.4). In the seagrasses, the ^{15}N was predominantly accumulated in the belowground parts, whereas *Caulerpa prolifera* accumulated the ^{15}N in the aboveground parts (assimilators and stolons; Fig. 6.4). This is not surprising considering the small contribution of their rhizoid system to their overall biomass. For the seagrasses the fraction of DON_{Alg} taken up after 24 hours of incubation was comparable to the fraction of NH_4^+ or glycine nitrogen taken up (Fig. 6.4).

In the *Caulerpa prolifera*-sediment system only the DOC_{Alg} was kept within the sediment, whereas other substrate carbon was almost entirely lost. This seems to disagree with figure 6.1, with minimal enrichment in the DOM_{Alg} addition. This may be attributed to the low addition of DOM compared to the other substrates and the high water content of the silty *Caulerpa prolifera* sediment compared to the sandy seagrass sediments, implying a lower (specific) mass in the core. Bacterial contributions were dominant in carbon incorporation, whereas algal contributions were dominant in nitrogen acquisition. Of the total amount of carbon and nitrogen stored in the sediment only a part was present in microbial biomass. The sum of the bacterial and microalgal ^{13}C and ^{15}N incorporation (thin bars inside black bars in figure 6.4) was in all cases smaller than the total amount recovered from the sediment (black bars in figure 6.4), which is in part attributable to the incomplete recovery of plant tissue (i.e. fine hair roots) from the sediment and the adsorption of substrate to sediment particles.

6.4 Discussion

6.4.1 Nitrogen retention and partitioning

After 24 hours of incubation we recovered significant fractions of the injected inorganic and organic nitrogen from the sediment-macrophyte systems. A substantial part thereof was found in the belowground and aboveground tissue of the macrophytes, indicating a quick transfer of nitrogen from the sediment to the macrophytes and a quick translocation from the belowground to the aboveground parts. These results are in line with earlier findings by Evrard et al. (2005) for tropical seagrasses and Barron et al. (2006) for Mediterranean seagrasses, both based on particulate organic matter additions.

The total recovery, however, differed between substrates, with highest recoveries of NH_4^+ and glycine. This pattern was similar for retention in the sediment and the specific uptake rates in the macrophytes. The similarity in recovery and uptake rates of NH_4^+ and glycine suggests that the substrates were treated in a similar fashion (i.e. a common pathway). Boon et al. (1986) also observed a quick deamination of glycine in sediment inhabited by *Zostera capricorni*, and a subsequent complete uptake of the NH_4^+. A quick glycine deamination

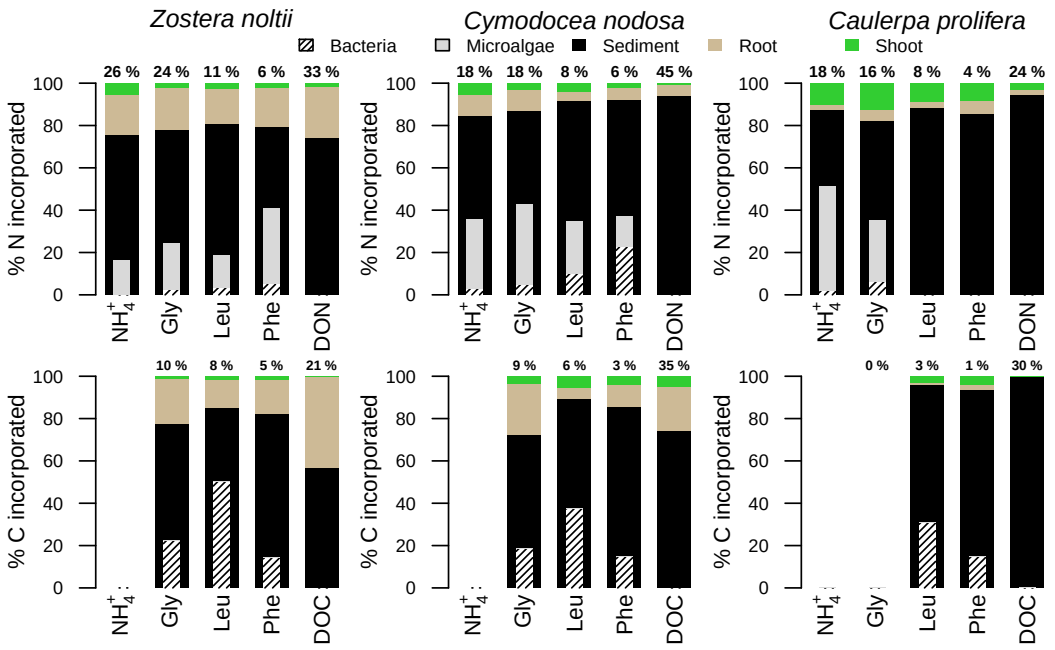

Figure 6.4: Nitrogen and carbon partitioning between different compartments of the macrophyte-sediment systems, expressed as percentages of the total amount taken up. Above the bars the percentage of injected substrate retained are indicated.

combined with an ammonium transport as the dominant limiting factor for the uptake, can indeed explain the similar retention and uptake for NH_4^+ and glycine in our study. This is also in line with the similarity in contributions of macrophytes and microalgae (Fig. 6.4), and their dominance in ^{15}N uptake from these sources. Bacterial incorporation of glycine N and ammonium was negligible, but glycine C was predominantly taken up by bacteria. In addition, the uptake of nitrogen but not carbon by *Caulerpa prolifera* supports this hypothesis.

The fraction of retained amino nitrogen in the macrophytes-sediment system decreased with increasing substrate complexity (Fig. 6.4; glycine > leucine > phenylalanine). However, other factors have to be considered. Their molecule weight, hence diffusion coefficients (Burdige et al., 1999), and C/N ratio also increase with their complexity. In addition, the relative abundance of these hydrolysable amino acids in biota decreases in the order glycine > leucine > phenylalanine (Cowie and Hedges, 1992), and presumably their reactivity and number of pathways starting from the respective amino acid as well. A phenyl-(or benzene-)ring is considered chemically very stable, whereas glycine is achiral and offers the most possibilities to modify. The amino acid concentrations in the sediment, the belowground and the aboveground plant tissue (and hence their apparent specific uptake rates) all decreased in this order (Fig. 6.1). In addition, bacterial contributions to microbial N incorporation

increased for more complex amino acids (glycine < leucine < phenylalanine; Fig. 6.4).

The recovered $DO^{15}N_{Alg}$ concentration (and absolute amount) in the sediment was low due to the almost six times lower amount added, relative to other substrates (Fig. 6.1; Tab. 6.1). Normalization of the nitrogen concentration to the added amount revealed a high fraction of $DO^{15}N_{Alg}$ recovered (Fig. 6.4). Note, however, that diffusive losses of the complex DON substrates are most likely lower due to the larger size of the molecules involved, implying a smaller diffusion rate (Burdige et al., 1999). The fraction of $DO^{15}N_{Alg}$ recovered from the highly organic and muddy *Caulerpa prolifera* sediment was unexpectedly lower than from the sandy seagrass sediments, despite the expected lower diffusion and lower heterotrophic activity in the latter. This was entirely due to the low specific mass of the mud matrix. The $DO^{15}N_{Alg}$ concentration (in μmol gDW^{-1}) was higher than in the seagrass sediment.

The total amount of ^{15}N allocated in roots and aboveground tissue more or less tracked the biomass in these organs. The highest percentage of total nitrogen uptake was found in the seagrass roots and the *Caulerpa prolifera* aboveground tissue (Fig. 6.4). Given that some macrophytes, among which *Cymodocea nodosa*, may store nitrogen in their rhizomes (Invers et al., 2002), this suggests that little storage took place at that time.

Total nitrogen recovery in our study range from 6 to 45 %, which is considerably lower than that reported by Barron et al. (2006). However, their coring tubes were inserted prior to injection, preventing lateral transport through diffusion (but resulting in a homogeneous horizontal distribution). In addition, Barron et al. (2006) added particulate organic matter (POM), which can not diffuse away from the injection location and provides DOM over a prolonged period of time through a steady, slow enzymatic hydrolysis. Furthermore, by only sampling the upper 2 cm in a radius of 2 cm around the plant, we took only a subsample of what was present in the plant and sediment (diffusive transport lateral and deeper into the sediment). Our retention estimates should hence be considered minimal estimates.

Caution is needed in comparing uptake rates without information on background concentrations. Different substrate background concentrations imply different relative abundance of the added heavy isotope, and hence different isotope ratios depending on the substrate. Assuming absence of isotope fractionation during uptake, and given the equal amounts of the different substrates, this would lead to lower uptake rates of heavy isotopes in the substrates with higher background values (Harrison et al., 2007, 2008; von Felten et al., 2008). However, assuming concentrations of 7.5 - 12.5 μmol l^{-1}, 0.6 - 1 μmol l^{-1}, and 1.8 - 3 μmol l^{-1} for glycine, leucine, and phenylalanine respectively, based on results from Hansen et al. (2000) for an Australian seagrass system, dilution effects would actually counteract the observed gradient in specific ^{15}N uptake. In addition, assuming a sediment porosity of 50 - 70 %, typical for the inner bay of Cadiz (Ligero et al., 2005), and using these concentrations, our added amounts of substrate would be 5 - 140 times higher than the amounts present, implying minimal dilution effects. However, the high additions imply that ^{15}N uptake rates in our incubation should be considered potential uptake rates (Tab. 6.4).

Nevertheless, our data (Tab. 6.3) were in good agreement with literature values (Tab. 6.4). Our rates of NH_4^+ and glycine-N utilization in the *Zostera noltii* plots (e.g. 0.29 ± 0.1 μmol cm^{-3} d^{-1} for NH_4^+) fell in the range of those reported by Boon et al. (1986) (0.21 -

Table 6.4: Reference values of specific uptake rates (converted to μmol gDW^{-1} d^{-1}) of seagrass roots. Ranges are calculated from the kinetic parameters for the ammonium concentrations 30 - 100 μmol l^{-1}.

Reference	Specific uptake rate	Species
Boon et al. (1986)	2.5 - 4.4	*Zostera capricorni*
Lee and Dunton (1999)	23 - 133	*Thalassia testudinum*
Lepoint et al. (2002b)	830 *	*Posidonia oceanica*
Stapel et al. (1996)	528	*Thalassia hemprichii*
Thursby and Harlin (1982)	258 - 565	*Zostera marina*
Thursby and Harlin (1984)	878 - 1108	*Ruppia maritima*
Vonk et al. (2008)	7 - 22	*Thalassia hemprichii*, *Halodule uninervis*, *Cymodocea rotundata*

* in μmol-N g $^{-1}_{tissueN}$ d^{-1}

0.39 μmol cm^{-3} d^{-1}), supporting the validity of our measurements. However, the specific uptake rates of the seagrasses were roughly an order of magnitude lower in our experiment (Tab. 6.4), but Boon et al. (1986) reported N uptake, whereas we calculated ^{15}N uptake. Assuming a pore water NH_4^+ concentration of 30 - 50 μmol l^{-1} (Gómez-Parra and Forja, 1993), our specific NH_4^+ uptake rates (2.5 - 3 μmol-N gDW^{-1} d^{-1}) are similar to those of Boon et al. (1986). Overall our NH_4^+ specific uptake rates (1.1 - 3.4 μmol-N gDW^{-1} d^{-1}) were at the lower end of the distribution of literature values (Tab. 6.3 and 6.4).

The root-mediated amino acid specific uptake rates in our incubations were two orders of magnitude lower than those reported by Vonk et al. (2008) (13 - 30 μmol N gDW^{-1} d^{-1}). However, their experiment only lasted for 1 hour and was performed in a water reservoir under laboratory conditions, implying that transport limitation and dilution over time was not an issue. In contrast, a set of incubations using the species and substrates from this study in a laboratory setting with roots put in a water column resulted in specific ^{15}N uptake rates somewhat lower than those for this study (chapter 4.4.4). But the added substrate concentrations were lower than here as well. Our microbial specific uptake rates of amino nitrogen ranged from 0.2 - 2.1 μmol m^{-2} h^{-1} (upper 2 cm of the sediment; data not shown), and corresponded with those reported by Linares and Sundback (2006) (0.3 - 2.2 μmol m^{-2} h^{-1}).

6.4.2 DOM utilization and remineralization

Incorporation of nitrogen and carbon from amino acids can occur along three different pathways (Veuger and Middelburg, 2007): (1) direct amino acid uptake and incorporation into biomass, (2) direct uptake of the amino acids with subsequent intracellular transformation to other amino acids prior to incorporation, and/or (3) uptake of regenerated NH_4^+ after extracellular breakdown. The first two pathways would result in a tight coupling between ^{13}C and ^{15}N uptake from particular amino acids. The third pathway can result in a coupling

or decoupling of ^{13}C and ^{15}N uptake depending on the strength of ^{13}C utilization. This ^{13}C utilization can occur through heterotrophic uptake or as $DI^{13}C$ uptake after remineralization. Given the high DIC background in the marine environment, the latter would imply loss of ^{13}C through dilution (Veuger and Middelburg, 2007).

Carbon was retained in the sediments of all macrophyte species, but significant macrophyte carbon incorporation was only found for the seagrasses (Fig. 6.1 and 6.4). *Caulerpa prolifera* only took up ^{15}N, suggesting that all amino acid nitrogen that went into the macroalga was deaminated (pathway 3). In contrast, both in the seagrasses and the surrounding sediment ^{13}C and ^{15}N concentrations were related through the C/N ratio of the relevant amino acids (Fig. 6.1), indicating a coupling between amino acid carbon and nitrogen uptake in the seagrass-sediment systems (pathway 1 and/or 2). However, the lower carbon enrichment in the seagrass tissue relative to what was expected from the nitrogen uptake and the substrate C/N ratio illustrates that the ^{15}N was taken up to a larger extent than the ^{13}C, particularly in *Zostera noltii*. This suggests at least a partial decoupling of the carbon and nitrogen uptake from amino acids (pathway 3). Decoupling of amino acid carbon and nitrogen during uptake by microorganisms was also reported by Mulholland et al. (2002) and Andersson et al. (2006) for the water column, and by Veuger and Middelburg (2007) for sediments.

Although microbial ^{13}C incorporation, based on PLFA data, was only statistically significant in bacteria (Fig. 6.2), individual microalgal PLFAs were enriched in ^{13}C as well (Fig. 6.3). The ^{13}C was incorporated in C18:2ω6c according to the C-content of the substrates (glycine < leucine < phenylalnine), indicating a carbon uptake according to availability. This pattern can be explained in two ways: (A) All amino acids are remineralized to a large extent, and the resulting $DI^{13}C$ (with relative abundance in the total DIC pool according to the substrate C/N ratio) is taken up (pathway 3). (B) The amino acids are indiscriminately taken up as molecules by the cells and internally reworked (pathway 2). Given the observed discrimination between amino acids in the bulk sediment, and the fact that carbon is predominantly directed towards the bacteria whereas nitrogen is predominantly taken up by the microphytobenthos, explanation (A) is more plausible than (B). The diatom-related PLFA markers from figure 6.3 (C16:1ω7*c* and C20:5ω3) exhibited highest specific uptake rates in the glycine and leucine incubations according to the natural concentrations of the relevant amino acids in seagrass systems (Hansen et al., 2000), and in microbes and macrophytes (Cowie and Hedges, 1992), suggesting uptake of entire molecules and reworking to incorporate carbon in the PLFAs (pathway 2).

Although seagrasses and macroalgae can efficiently utilize organic nitrogenous compounds (Tyler et al., 2005; Vonk et al., 2008, chapter 4.4.4), results from this study suggest that rapid remineralization prior to nitrogen and carbon uptake is the predominant mode of organic matter recycling for the macrophytes, rather than direct uptake. The variation in incorporation into different microbial markers indicate that, depending on the phylogeny, organic matter recycling occurs through remineralization prior to uptake, or direct uptake of the dissolved organic matter.

Regenerated production is a key process in seagrass meadows. However, nitrogen regeneration differs among compounds, and probably among sources that differ in DON compo-

sition. Amino acid nitrogen was retained and utilized by primary producers according to their complexity and natural abundance in biota, suggesting that the amino acids themselves rather than just the nitrogen therein are of importance. However, despite the consistent relationships between carbon and nitrogen uptake by the seagrasses, some carbon was progressively lost during transport in the macrophytes, indicating a partial decoupling between carbon and nitrogen dynamics. The microbial community was an important sink for both nitrogen and carbon, but carbon was mainly transferred to bacterial PLFAs whereas nitrogen was predominantly incorporated in microphytobenthos. Nitrogen partitioning in the microphytobenthos was even similar in magnitude to the fraction taken up by the macrophytes, making microphytobenthos an important sink for pore water nitrogen in this macrophyte-dominated system.

7. General discussion

Continental shelf ecosystems, such as the North Sea, are characterized by strong gradients in nutrients and organic matter, which are maintained by a continuous supply through river runoff (de Vries et al., 1998). These gradients imply an intensive nutrient and organic matter cycling, which contribute a major part of the annual nitrogen demand in, for instance, the North Sea (Hydes et al., 1999). Intensive dissolved organic nitrogen (DON) transformations have been reported during across-shelf transport from rivers to the open ocean (Hedges et al., 1997). DON can thus be regarded as an active player in nitrogen metabolism at the land-ocean interface.

Nevertheless, DON is an often neglected ecosystem variable, particularly in long-term monitoring. This is mainly attributable to the methodological difficulties in measuring total dissolved nitrogen (TDN; Sharp et al., 2002) and the misconception that DON (like dissolved organic carbon; DOC) is not useful to primary producers (Bronk et al., 2007). Apart from the study by Butler et al. (1979) and a few short-term studies, little research has been conducted into the spatio-temporal variation of DON. Therefore, we started this research with an investigation of the spatial distribution and temporal evolution of DON in the Dutch sector of the North Sea. Although this study was largely descriptive, and only considered the net result of a large suite of processes working on the DON pool (i.e. we looked only at concentration changes), several new patterns were revealed that shed some light on, among others, the inconsistency that was found between other studies (Butler et al., 1979; Williams, 1995). These patterns allowed, in the first place to generate a number of hypotheses, that could be tested in this or future research.

Similar to dissolved inorganic nitrogen (DIN), DON concentrations exhibited large gradients with high values in nearshore and lower values in offshore regions (Chapter 3). The fraction of DON in TDN, however, increased with offshore distance, suggesting that DIN was used and DON was not. However, despite the general preference of primary producers for inorganic nitrogen forms (Chapters 4 - 6), organic nitrogen can indeed be a significant source to primary producers, either directly or indirectly after remineralization (Palenik and Morel, 1991; Kerner and Spitzy, 2001; Mulholland et al., 2002; Andersson et al., 2006). Although a part of the DON is not bioavailable time scales of up to a year, a substantial fraction is. In addition, under higher concentrations of substances that are hard to break down, bacterial remineralization is stimulated (Stepanauskas et al., 1999).

One of the more prominent results in this study was the difference in modes of variability between the coastal region, which exhibited a large DON build up until mid-summer and a subsequent decline towards a winter low, and the open sea where the variability was more erratic in nature (occuring at shorter time scales). We hypothesized that this difference in DON variability was caused by shifting balances between influxes into and effluxes out of the DON pool under a varying terrestrial influence (Chapter 3). Rivers deliver large

quantities of inorganic and bioavailable organic nitrogen to the coastal zone (Stepanauskas et al., 1999; Soetaert et al., 2006; Seitzinger and Sanders, 1997; Wiegner et al., 2009), thus fueling both autotrophic and heterotrophic production. As such autotrophic production does not only depend in situ production of inorganic nutrient by remineralization processes, and heterotrophic remineralization is not dependent on in situ production of organic matter (i.e. the autotrophic and heterotrophic states are uncoupled; Dodds, 2006; Dodds and Cole, 2007). In addition, DON exudation by phytoplankton occurs predominantly - but not exclusively - under nutrient sufficient conditions (Bronk, 1999, 2002). This was for the North Sea consistent with the annual chlorophyll maximum that preceded the annual DON maximum (Chapter 3). Furthermore, an increase in grazer biomass towards summer (which can be expected in the presence of larger phytoplankton biomass) could enhance the build up of DON during that period by sloppy feeding and excretion (Bronk, 2002). Moreover, discharge from rivers and consequently (in)organic nitrogen loads exhibit seasonality as well, resulting in seasonal inputs to the coastal zone. Although these direct nitrogen inputs are small on a shelf-wide scale compared to the nitrogen supply from internal reworking (Hydes et al., 1999), a local effect can be expected. Together these processes could lead to a periodic DON input in excess of metabolic or physical DON removal. However, when direct allochtonous nitrogen inputs are too low, autotrophic production depends on nitrogen fixation or heterotrophic nitrogen remineralization. Conversely, bacterial production and remineralization depends on the presence of autochtonous organic carbon and nitrogen. Hence, autotrophic and heterotrophic processes, and thus influxes to and effluxes from the DON pool are more tightly coupled. Such tight couplings between nitrogen remineralization and nitrogen assimilation have been repeatedly reported (Harrison, 1978; La Roche, 1983).

One remarkable finding of this study was a clear change in DON seasonality at the Dogger Bank, where around 1999 the seasonal component of the DON variability shifted from a summer maximum to a spring maximum. From this moment onwards, the ammonium and nitrate pools were depleted more and for longer time spans each year, indicating that either the inorganic nitrogen that was regenerated was quickly used before it could accumulate (i.e. a 1:1 relationship between nitrogen assimilation and nitrogen recycling) or that DON was directly taken up by the primary producers and bacteria.

Since we only had concentration measurements at our disposal, no causal relationships can be inferred, and the presented mechanism remains largely hypothetical. To improve our understanding of DON dynamics, analysis of concentration changes (which is without doubt a first essential step) are not sufficient. Experimental work with stable isotope tracers is one possibility to address specific questions about the processes and fluxes governing the variability in DON. In this thesis I have focussed on nitrogen uptake processes. Using double labeling (^{13}C and ^{15}N) the two most abundant elements in dissolved organic matter and their mutual dependence can be investigated.

7.1 Organic nitrogen uptake

The systematic variability in DON and the changing patterns in time and space imply changing balances between influxes and effluxes and biological processes working on them. From a biological point of view, the fluxes out of the DON pool and into the biota are the most important. Whereas DON utilization has since long been reported for microalgae (Admiraal et al., 1987; Berg et al., 2003; Mulholland et al., 2002, 2004; Andersson et al., 2006), macrophytic DON uptake only received more attention in the past few years (Brun et al., 2003; Tyler et al., 2005; Vonk et al., 2008; Vonk and Stapel, 2008, but see for instance Probyn and Chapman, 1982). In many studies of seagrass ecosystems, which cover a considerable proportion of the coastal systems (Hemminga and Duarte, 2000), nitrogen cycling is still approached via the traditional view of bacterial remineralization and seagrass uptake of inorganics.

We performed several laboratory and field experiments to assess what kind of nitrogen sources are exploited by different biota (phytoplankton, pelagic and benthic bacteria, epiphytes, seagrasses, and a macroalga) in a coastal ecosystem. In a first laboratory experiment, the uptake capabilities and preferences of macrophytes for inorganic nitrogen and organic nitrogen compounds through aboveground and belowground tissue were investigated. This was mainly intended to distinguish between not having the uptake capabilities, and not being able to reach particular sources because of other potentially more competitive consumers. A second experiment, performed in a semi-enclosed coastal bay aimed at assessing the competitive strength of different biotic compartments (phytoplankton, pelagic bacteria, macrophytes, and epiphytes) in the uptake of different (in)organic sources of nitrogen. This allowed to put the physiological uptake capabilities found in the first experiment in an ecological context. A third experiment, conducted in the same bay, focusing on the benthic environment, was performed to determine how much of particular nitrogen sources is directed towards various (a)biotic compartments (microphytobenthos, benthic bacteria, macrophytes, sediment). The first two experiments lasted for a few hours to exclude surge uptake, and to assess what can be taken up immediately. The latter experiment lasted for 24 hours, and allowed to assess the retention of fresh DON and DIN in the sediment.

In the field experiments microalgae were the primary sink for nitrogen. In the water column nitrogen incorporation in suspended matter was at least 67%, and most of the nitrogen entered the phytoplankton compartment, irrespective of the substrate. Epiphytes, including bacteria and microalgae (but most likely also fauna, such as bryozoans), represented a strong nitrogen sink as well, based on their high specific uptake rates (chapter 5), although we did not have biomass measurements for this ecosystem compartment. High contributions to inorganic nitrogen uptake and carbon fixation of this compartment have been reported before (Heip et al., 1995; Cornelisen and Thomas, 2002), supporting our conclusion. The 24-hour sediment incubations also revealed contributions to total nitrogen retention and uptake in microphytobenthos of similar or larger magnitude than for the macrophytes. It is thus safe to conclude that macrophytes are inferior as short-term N sinks, and most likely bad competitors with phytoplankton for N.

Nevertheless, macrophytes were able to acquire nitrogen from all substrates offered, both

organic and inorganic. The seagrasses exhibited a clear preference for inorganic nitrogen, primarily ammonium (chapter 4 and 5). The macroalga *Caulerpa prolifera*, however, appeared to take inorganic nitrogen from the water column as easily as small organic compounds (chapter 5), whereas a clear preference for ammonium was encountered for pore water (sediment) uptake (chapter 6). This contrasts with the results from the laboratory experiment, where clear preferences for inorganic nitrogen were revealed for the uptake by aboveground and belowground tissue. The fact that ammonium uptake was so large compared to the rest in the laboratory incubations of the belowground tissue, suggests that the organic nitrogen in the field was entirely remineralized before it entered the macroalga. This was also supported by the absence of carbon uptake by *Caulerpa prolifera* in this experiment (chapter 6). It appears that nitrogen uptake in *Caulerpa prolifera* is more dependent on the activity of other ecosystem actors (microalgae, seagrasses, and bacteria). Whereas no translocation was found in the laboratory experiment and the water column incubation, a substantial fraction of the nitrogen was transferred to the aboveground tissue in the sediment incubations due to the longer incubation time.

Although inorganic nitrogen was the preferred N source in the laboratory experiment, a complex pool of algae-derive DON was taken up at similar rates normalized to the added concentration (chapter 4). In the in situ water column incubations, however, algae-derived DON was mainly incorporated in the suspended matter, and macrophytic contributions to the DON uptake were not higher than 5% (chapter 5). These findings suggest that macrophytes indeed can take up organic nitrogen, but predominantly rely on N remineralization. Remineralization rates in marine and estuarine systems are very high (Kerner and Spitzy, 2001; Badr et al., 2008), but given the low bacterial biomass in the laboratory experiment and the short incubation times, it is likely that DON was at least in part processed by the seagrasses themselves. Vonk et al. (2008) also reported uptake of small organic compounds in a laboratory setting with a strongly reduced microbial community. Retention in the sediment from the same algae-derived DON pool was higher than that of ammonium, but relatively little of the N entered the macrophytes after 24 hours of incubation in comparison to what was retained in the sediment, supporting the low direct exploitation of DON by macrophytes. However, the high retention in the sediment emphasizes the importance of DON as benthic nitrogen reservoir. DON that is kept in the sediment by incorporation in bacteria or microphytobenthos, or that is bound to sediment particles, may become available to the seagrasses at a later stage.

Both the laboratory and the water-column incubations pointed out that algae-derived DON is preferred over bacteria-derived DON. The higher amino acid content in algae-derived DON (84% and 47% amino acid nitrogen for algal and bacterial DON respectively, mainly as dissolved combined amino acids; DCAA) may explain why this substrate was preferred. Other, possibly refractory, nitrogenous compounds must have been present in larger quantities in the bacteria-derived DON. (Stepanauskas et al., 2000) also reported lower bioavailability of riverine DON with lower fractions of L-amino acids. DOM from Bacteria appear to contribute substantially to refractory DOM in oceanic water as well (McCarthy et al., 1998, 2004). Our findings corroborate the dependence of DON reactivity on DON origin, reported earlier (Ziegler and Benner, 1999b; Seitzinger et al., 2002; McCallister et al., 2006).

The three amino acids used in this research showed a marked and consistent difference in reactivity and retention in the different experiments. Glycine uptake by the primary producers was always higher and phenylalanine uptake most of the time lower than leucine uptake. This increasing uptake coincides with an increasing abundance in biota (Cowie and Hedges, 1992), C/N ratio (3, 6, and 9 for glycine, leucine, and phenylalanine respectively), and concentrations in the seagrass sediment (Hansen et al., 2000). In addition, the molecule complexity of glycine is lower than that of leucine. Glycine is achiral with two hydrogen atoms on the α-carbon, which makes it a versatile building block. Each of the two hydrogen atoms can be replaced by another functional group, resulting in either a D or L enantiomer. Leucine is a chiral amino acid with an isobutyl-group. Phenylalanine has a phenyl residual which is highly chemically stable. All of these properties suggest that the chemical stability of these amino acids should increase in the order glycine < leucine < phenylalanine. Glycine retention in the sediment was similar to ammonium retention, irrespective of the macrophyte species (and sediment type), whereas leucine retention was lower, and phenylalanine retention even lower than that of leucine, which agrees well with their presumed reactivity. However, no clear distinction between amino acids existed in the contribution of macrophytes to total uptake from the sediment, indicating that the different N uptake rates of the macrophytes in the sediment were dictated by what was made available, possibly after remineralization (see below). Bacterial contributions to amino acid uptake showed the gradient in reverse (phenylalanine-N > leucine-N > glycine-N), both in the water column and the sediment. Glycine-N retention and uptake by the macrophytes was similar to that for ammonium, suggesting a common uptake process. Boon et al. (1986) indeed reported a quick deamination of glycine in *Zostera capricorni* sediment, followed by a complete uptake of the ammonium.

Generally, carbon dynamics were uncoupled from nitrogen dynamics. In contrast to their relatively low contribution to N uptake, seagrasses were the dominant DIC consumers. This high carbon fixation combined with relatively low N uptake can be understood in light of their high C/N ratio (Duarte, 1995). In the laboratory incubations no significant carbon uptake was detected from the organic substances despite the significant nitrogen uptake. This indicates either remineralization prior to uptake or exudation of the residual carbon after uptake of complete molecules. Remineralization prior to uptake is well understood for amines in phytoplankton (Palenik and Morel, 1990b,a, 1991; Mulholland et al., 2002). Exudation of residual carbon upon urea uptake has been reported by Price and Harrison (1988). In situ carbon uptake from amino acids and DOC in the water column was low in the macrophytes, compared to the suspended matter. However, carbon uptake from the sediment by the seagrasses was related to nitrogen uptake through the C/N ratio of individual amino acids, albeit with some loss. Since no carbon was taken up in the laboratory incubations, the most plausible explanation for this partial coupling in the sediment is that the remineralized carbon (remineralization by bacteria or primary producers; cf. Price and Harrison, 1988) was not immediately lost due to diffusive transport. This could explain the almost undetectable uptake of labeled DIC by the microphytobenthos, which resides mainly at the sediment surface. The preferential transport of nitrogen relative to carbon in *Zoster noltii* (^{13}C losses were higher in the aboveground than in the belowground tissue) support

this hypothesis of carbon uptake as DIC. *Caulerpa prolifera* only took up ^{15}N, both in the laboratory and in situ sediment incubations, suggesting that all amino acid nitrogen that went into the macroalga was deaminated. Ultimately, carbon and nitrogen uptake by the macrophytes were thus uncoupled, both in the water column and the sediment. Decoupling of the fate of amino acid and urea carbon and nitrogen have been reported repeatedly for the water column (Mulholland et al., 2002; Andersson et al., 2006) and for sediments (Veuger and Middelburg, 2007).

Given the high DOC and DON incorporation in microbial biomass, couplings between N and C uptake may be stronger. Bacteria are considered the dominant users of DOM through (1) remineralization and (2) incorporation. However, remineralization might represent a larger efflux from the DON pool than incorporation, implying that bacteria are not so much a sink, but rather facilitators of larger effluxes from the DON pool. Although we did not measure any net rates of remineralization, the present work supports the inferiority of bacteria as sinks (as defined here) relative to microphytobenthos and phytoplankton. Their contribution to nitrogen uptake, however, increased for more complex amino acids, illustrating that they are indeed better equiped to utilize organic substances than primary producers. One important observation in this work was that, whereas in the water column leucine and phenylalanine carbon was incorporated into bacterial hydrolysable amino acids (HAA) and bacterial PLFAs (phospholipid-derived fatty acids), amino acid carbon in the sediment was mainly inserted in bacterial PLFAs. ^{13}C labeling in D-alanine remained below the racemization background (Kaiser and Benner, 2005; Veuger et al., 2005, 2007). This implies that the ^{13}C enrichment in the sediment HAA was predominantly in the microphytobenthos. The C/N ratio of the incorporation in HAA in the sediment increased with increasing substrate C/N ratio but was always much lower than that of the respective substrates.

7.2 Ecological implications

7.2.1 Net community production

This research has illustrated that the strong erratic variability in DON in the open North Sea is likely due to significant utilization of organic nitrogen compounds by primary producers. Intensive recycling of DON can lift net community production based on DIC concentration changes (i.e. carbon fixation; NCP_{DIC}) above values expected from inorganic nitrogen uptake (net community production based on nitrate; NCP_{NO3}) (Thomas et al., 1999). This discrepancy between NCP_{DIC} and NCP_{NO3} was illustrated for the North Sea by Bozec et al. (2006), but has also been found in a other ecosystems (Copin-Montegut, 2000; Begovic and Copin-Montegut, 2002). This intensive and preferential recycling of DON probably contributes substantially to the high efficiency of the North Sea continental shelf pump, which enhances CO_2 transport from the atmosphere to the deep atlantic ocean (Thomas et al., 2005).

7.2.2 Inorganic nutrient reduction measures and coastal oligotrophication

This work confirms the idea that DON is a highly dynamic pool of nitrogen that is available to primary producers and bacteria on very short time scales, and can contribute substantially to their nitrogen demand. With increasing chlorophyll concentrations under conditions of decreasing total nitrogen over the past few decades (McQuatters-Gollop et al., 2007), internal loading and stronger remineralization are the only possibilities to sustain this high productivity. Nitrogen regeneration supports phytoplankton growth even when concentrations are close to zero (McCarthy and Goldman, 1979). The importance of internal loading in sustaining high chlorophyll concentrations under decreasing nutrient loads was illustrated for the Danish coastal systems (Carstensen et al., 2006). Price et al. (1985) also observed more intense DON utilization in stratified waters, deprived from an upward supply of inorganic nutrients, relative to primary producer communities in frontal systems with high nutrients.

7.3 Future perspectives

The recognition of DOM as nutrient source is relatively recent, compared to inorganic nutrients, and a lot of work still has to be done to increase our understanding of this complex ecosystem component.

7.3.1 Characterization of dissolved organic matter sources and transformations

Since DON is a dynamic ecosystem component, it should be dealt with accordingly. Research on DON release and uptake has to continue to broaden our understanding of the existence and relative importance of pathways in the nitrogen cycle and the connectivity with the carbon and phosphorus cycle. Multiple isotope labeling has proven its worth in elucidating metabolic pathways (Mulholland et al., 2004; Tyler et al., 2005, this research), but needs to be used on a wider scale.

Complete isolation of DOM without altering it, is still a challenge. Some resins have been used in the past to isolate particular fractions, such as humic and fulvic acids (Bronk, 2002; See et al., 2006). However, more recent techniques based on reverse osmosis and electrodialysis (used to turn seawater into drinking water) are promising for isolating more complete fractions (Vetter et al., 2007). Reverse-phase liquid chromatography allows for the isolation of DOM and subdivision into fractions for later use (Koch et al., 2008).

Measurement of carbon, nitrogen, phosphorus in organic matter (DOC, DON, and DOP) has much evolved in the past decades. With respect to DON, some issue still existed in the early years 2000, mainly related to proper referencing and calibration of the measurement equipment (Sharp et al., 2002). But given that proper reference material is used, the accepted methods (UV-destruction, high temperature catalytic combustion, and chemical oxidation,

or a combination thereof) all perform similarly (Sharp et al., 2002). Molecular characterization of DOM or fractions thereof has improved a lot in recent years as well. Ultrahigh mass spectrometry combined with multivariate analysis techniques will probably allow for a more detailed characterization of DOM transformation, for instance by UV-radiation, and the identification of sources and environments (Koch et al., 2008; Kujawinski et al., 2009). A good chemical characterization of DOM is considered a prerequisite for understanding bioavailability (Sulzberger and Durisch-Kaiser, 2009).

7.3.2 Long-term monitoring and data integration

This research has illustrated that DON may play a significant role in nitrogen supply, particularly when DIN concentrations decrease. As such, it could compromise the efforts so reduce eutrophication effects by waste water treatment (Seitzinger and Sanders, 1997). In the light of the Water Framework Directive (WFD), DON thus represents an important nutrient variable that should be taken into account. The DONAR database is, as far as we know, one of the very few that contain time series of DON measurements. With ten years of monthly measurements they only now start to become sufficiently long to properly investigate interannual and long-term DON variability.

A few remarks and words of criticism are, however, in place. In the 1970s the monitoring started with 'good intentions' and an extensive coverage of both marine and inland Dutch waters. However, after cut-backs at the end of the 1980s and beginning of the 1990s the number of stations have been reduced by 35%, due to 'a need to become more cost-effective' (de Jonge et al., 2006). The WFD, nevertheless, dictates that one should endeavor to obtain a good knowledge of ecosystem functioning in order to make well-founded management decisions. Our time series analyses, however, has pointed out that the variability in DON is mainly situated at the finest time scales (2 - 4 months). We could not determine at which time scale the highest variability occurred since the stations were not consistently sampled at higher frequencies. This lack of sufficient frequency resolution was also pointed out for the chlorophyll a concentrations in the Westerschelde estuary (Kromkamp and Van Engeland, 2009). The monitoring of Rijkswaterstaat occurred exactly during the bloom, whereas a monitoring cruise of the NIOO-CEME, 2 weeks later, largely missed it, with a resulting severe underestimation of the primary production. In addition, the spatial coverage was not adequate to properly assess the spatial variability at finer scale than coast versus open sea. These findings support the conclusions of (de Jonge et al., 2006), that also the spatial coverage of the monitoring data is inadequate to sufficiently understand the dynamics of the Dutch marine and estuarine systems. Consequently, we fully support the recommendations made by de Jonge et al. (2006), that the design of the monitoring with more stations should be restored. We further recommend that all stations should be sampled at least at monthly intervals, and that a few stations should be sampled with biweekly frequency throughout the year, particularly in the highly dynamic estuaries.

One of the possibilities to extend and make this monitoring more cost-effective would be to include remote sensing. This has been used since years to assess terrestrial vegetation cover (e.g. Gamon et al., 1995), but appears to be feasible for tidal flats as well (De Wever

et al., in prep). In addition, (Del Castillo and Miller, 2008) used remote sensing technology to investigate DOC transport in a river plume. By including information from teledetection on a regular basis, sampling efforts could be reduced to obtaining ground truthing data in a smaller set of locations. McQuatters-Gollop et al. (2007) used such data integration approach, using data from the continuous plankton recorder and from teledetection, to investigate the evolution of chlorophyll a in the North Sea on a region wide scale. More general, different data sets of a variety of sources could be integrated into a larger data archive, with a flexible monitoring program as back-bone. By enting individual cause-effect studies on this back-bone monitoring program and sharing efforts and data between the governmental and scientific stakeholders, compliance to the WFD and a scientific policy would be unified in a cost-effective manner.

Summary

Eutrophication poses a substantial threat to many coastal ecosystem all over the world. Despite waste water treatment efforts, which have led to dissolved inorganic nitrogen (DIN) reductions in some regions, productivity has not decreased as expected. This is often attributed to internal loading and efficient nutrient recycling of nitrogen, shifting the focus from DIN to DON dynamics. However, DON is still an ecosystem variable that is little understood. This study aims to address some fundamental questions on DON dynamics in coastal systems.

In a first part, the temporal and spatial variability of DON was examined using a large dataset of DON concentration measurement in the Dutch section of the North Sea, in order to increase our understanding of terrestrial influences, temporal behaviour and the relationship with other ecosystem variables. These analyses revealed a strong gradient with high DON concentrations in the coastal zone and low concentrations in the open sea. The contribution of DON to total dissolved nitrogen (TDN), however, increased with offshore distance because of decreases in DIN concentrations. Similar to DOC, DON concentrations exhibited a pronounced seasonal variability in the coastal zone. In the open sea, however, DOC exhibited a seasonality similar to the coastal zone, whereas DON concentrations fluctuated more erratically, without a clear seasonal signal. This apparent random variability suggests that not much is happening in the DON pool, there. However, the opposite is true. While the coastal DON concentration increased throughout spring and a part of summer, and was subsequently broken down or transported, we suggest that DON was quickly recycled in the open sea because DIN concentrations are low and alternative sources have to fuel primary production. This hypothesis is supported by an event that was observed at the Dogger Bank. Based on wavelet analysis, we showed that around 1999-2000, the very weak seasonality at the Dogger Bank changed from a pattern similar to the coast (maxima in summer) to maxima earlier in spring. At the same time the period that DIN was depleted was prolonged, particularly for ammonium, the product of DON remineralization. This suggests that DON that builds up during the phytoplankton bloom, was used more quickly. Despite the absence of a clear relationship with phytoplankton abundance (approximated by chlorophyll a concentrations), concurrent changes in the phytoplankton community composition at that site have been reported by other authors.

To examine this hypothesized quick DON utilization, three experiments were performed in a coastal bay dominated by marine macrophyte species (two seagrasses: *Zostera noltii* and *Cymodocea nodosa*, and one macroalga: *Caulerpa prolifera*). Uptake of nitrogen from various inorganic (NH_4^+ and NO_3^-) and organic (urea, glycine, L-leucine, and L-phenylalanine) compounds by various ecosystem compartments (macrophytes, epiphytes, phytoplankton, microphytobenthos, and planktonic and benthic bacteria) were investigated using stable isotope labeling and biomarker measurements (D-alanine and phospholipid-derived fatty acids: PLFA). Dual-labeling allowed to track the carbon and nitrogen separately, and thus to investigate relationships between DOC and DON uptake. A laboratory experiment, in

which all primary producers except the macrophytes were excluded and bacterial biomass was reduced, was conducted to assess the capacity of the macrophytes to take up organic nitrogen substrates. Two field experiments, one focusing on uptake from the water column and the other focusing on benthic nitrogen processing and uptake, were performed to investigate how much of the different nitrogen compounds was actually taken up by each of the potential consumer groups. The influence of DON origin was assessed by using two additional complex substrates derived from an algal and a bacterial culture. The laboratory experiment showed that all macrophytes had the capability to use DON compounds within hours. However, they appeared to have a preference for inorganic over organic nitrogen. Uptake by aboveground and belowground tissue differed in that the preference for ammonium was more pronounced relative to other nitrogen compounds in the belowground tissue. Carbon uptake by the macrophytes was not detected. A second (field) experiment, focusing on uptake from the water column, revealed a dominant nitrogen uptake by the microbial community (phytoplankton, bacteria, and epiphytes), irrespective of the substrate. Nevertheless, all primary producers, including the macrophytes, took up nitrogen from the inorganic and organic substrates presented to them in a matter of hours, supporting our earlier hypothesis of a quick DON utilization. The three amino acids tested provided decreasing amounts of nitrogen to all primary producers in correspondence with increasing complexity and C/N ratio, and decreasing abundance in biota, illustrating that not all amino nitrogen is similar to them. Bacterial contributions to amino nitrogen uptake, in contrast, showed an increasing tendency with increasing complexity, illustrating their heterotrophic nature and adaptation to using organic matter. A clear preference of algae-derived complex DON over bacteria-derived DON was observed in both experiments, supporting the influence of DON origin and composition on bioavailability. Labeled DIC was predominantly used by the seagrasses, whereas the complex DOC ended up almost exclusively in the microbial community. No relationships between carbon and nitrogen utilization were found in the microbial community or the macrophyte community. A third (field) experiment, focusing on benthic nitrogen uptake, revealed a quick transfer of administered organic nitrogen (NH_4^+, glycine, L-leucine, L-phenylalanine, algae-derived DON; injected into the sediment) from the sediment to the aboveground tissue of the macrophytes. This translocation was not observed in the laboratory and water column incubation due to the much shorter incubation times. Microphytobenthos contributed substantially to nitrogen uptake, based on HAA data, whereas bacterial nitrogen uptake was considerably lower. Carbon was partially retained in the sediment, and also transferred into the seagrasses, but not into the macroalga. The concentrations in the sediment and the seagrasses were related to the nitrogen concentrations by the C/N ratios of the substrates, although a progressive loss from sediment to aboveground tissue was found in *Zostera noltii*. This contrasts to the C/N ratios of incorporation in microphytobenthos HAA, which were much lower than the C/N ratios of the respective administered amino acids. This indicates an uncoupling between carbon and nitrogen uptake. Bacterial carbon incorporation occurred almost exclusively in PLFAs, whereas microalgal carbon incorporation was predominantly found in the HAAs. PLFA markers specific for particular groups of algae or bacteria showed different uptake characteristics per group, indicating that they either preferred different substrates or received DIC

only after remineralization.

This research has illustrated a highly dynamic DON pool, which can be utilized by primary producers in a matter of hours. Carbon dynamics is at all scales largely uncoupled from nitrogen dynamics. Under low DIN availability this results in a different behaviour in carbon and nitrogen dynamics at macroscopic level. The apparent inconsistency in literature that DON seasonality exists in some places but is absent in others is put in perspective, and is probably related to a balance between supply and demand of nitrogen. These findings support the potential role of DON as nutrient, particularly under decreasing DIN concentrations. This has important consequences for limitation of primary productivity and remediation of eutrophication effects.

Samenvatting

Veel kust systemen in de wereld worden bedreigd door eutrofiëring. In een aantal gebieden blijft de primaire productie hoger dan verwacht, ondanks effectieve nutrientreductiemaatregelen. Dit wordt vaak toegeschreven aan interne regeneratie van nutrienten. Hierdoor komt opgeloste organische stikstof (dissolved organic nitrogen; DON) meer centraal te staan binnen de nutrienten problematiek. Ondanks een zekere bewustwording, blijft de kennis over dit complex stikstof reservoir beperkt. Dit onderzoek tracht bij te dragen tot de kennis die fundamenteel nodig is om DON in kust systemen te begrijpen.

In een eerste deel, wordt a.h.v. een omvangrijke databank van DON metingen in het Nederlandse deel van de Noordzee de spatio-temporele variatie in DON onderzocht, ten einde een beter zicht te krijgen op terrestrische invloeden (rivieren), seizoenale en lange-termijn trends en relaties met andere ecosysteem variabelen. Hieruit is gebleken dat er sterke gradienten bestaan loodrecht op de kustlijn. DON concentraties zijn hoog in de kustzone en lager in de open zee. Het aandeel van DON in totale opgeloste stikstof daarentegen neemt toe met toenemende afstand tot de kust, voornamelijk omwille van een afnemende anorganische stikstof concentratie (dissolved inorganic nitrogen; DIN). Seizoenaliteit in DON in de kustzone is gekenmerkt door hogere zomerwaarden en lagere winterwaarden, net als voor de opgeloste organische koolstof (dissolved organic carbon; DOC). In de open zee, daarentegen, vertoont DOC dezelfde karakteristieke seizoenaliteit, maar DON vertoont een zeer zwak seizoenaal signaal met een dominante variabiliteit op een tijdschaal van enkele maanden. Deze schijnbaar willekeurige variabiliteit suggereert dat er niet veel gebeurt met deze stikstofvorm, maar het tegenovergestelde is waar. In de kustzone wordt een hoeveelheid DON opgebouwd doorheen het groeiseizoen, dat in de winter zal worden afgebroken (gerecycleerd tot anorganische voedingstoffen). Anderzijds, in de open Noordzee waar anorganische stikstof minder voorhanden is, moet DON vroeger gerecycleerd worden om voldoende nutrienten te hebben voor het fytoplankton (primaire produktie). Deze hypothese wordt ook gestaafd door een omslag in de (zwakke) DON seizoenaliteit bij de Dogger Bank, een ondiepte in de centrale Noordzee. Rond 1999-2000 veranderde de seizoenaliteit van een patroon gelijkaardig aan dat in de kustzone (hogere waarden in de zomer, lagere waarden in de winter) naar een patroon met maximale waarden in de lente (tijdens de fytoplanktonbloei) en lagere waarden gedurende de zomer en het najaar. Tezelfdertijd verhoogde het aantal maanden dat anorganische stikstof uitgeput was, vooral het eerste produkt van remineralizatie, namelijk ammonium. Dit wil zeggen dat het DON dat geproduceerd werd in de fytoplanktonbloei direct terug werd gebruikt om de primaire produktie te ondersteunen. Hoewel geen duidelijk verband van de veranderende DON dynamiek met de hoeveelheid chlorofyl a (benadering voor fytoplankton biomassa) werd gevonden, zijn er wel meldingen gemaakt in de literatuur over veranderingen in de samenstelling van de fytoplanktongemeenschap.

Om de hypothese van snelle recyclering van DON verder te onderzoeken, werden drie experimenten uitgevoerd in een baai die door macrofyten wordt gedomineerd (twee zeegrassen: *Zostera noltii* en *Cymodocea nodosa*, en een macroalg: *Caulerpa prolifera*). Hi-

erin werd de opname van stikstof afkomstig van anorganische (NH_4^+ and NO_3^-) en organische (ureum, glycine, L-leucine, and L-fenylalanine) substraten door verschillende biotische compartimenten (macrofyten, epifyten, fytoplankton, microfytobenthos en planktonische en benthische bacteriën) nagegaan met behulp van zware isotopen en biomerkers (D-alanine en fosfolipide-afgeleide vetzuren: PLFA). Door de zware koolstof (^{13}C) en stikstof (^{15}N) isotopen in het substraat kon zowel de koolstof als stikstof opname gevolgd worden. De invloed van de DON bron werd nagegaan door incubaties met een complex substraat afgeleid van een algenkultuur en één van een bacteriekultuur. Een eerste laboratoriumexperiment met enkel macrofyten en een sterke reductie van de bacteriële biomassa, moest uitsluitsel brengen over the mogelijkheid tot opname van organische verbindingen. Vervolgens werden twee veldexperimenten, één voor de opname uit de waterkolom en één voor de opname en verdeling in het sediment, opgezet, om na te gaan hoeveel van iedere bron (substraat) door elk van de biotische groepen zou opgenomen worden. In het laboratorium experiment konden alle aangeboden stikstof substraten opgenomen worden door de macrofyten binnen enkele uren. Maar de drie soorten hadden een voorkeur voor anorganisch stikstof boven organische. Opname via het blad verschilde van deze via de wortels vooral doordat de preferentie voor NH_4^+ meer uitgesproken was, en NO_3^- en ureum niet werden opgenomen door de wortels. Koolstof opname werd in dit experiment niet vastgesteld. Het eerste veldexperiment, dat opname vanuit de waterkolom belichtte, toonde een dominantie aan van de microbiële gemeenschap (fytoplankton, bacteriën en epifyten) in de opname van eender welke stikstof bron, hoewel alle primaire producenten binnen enkele uren stikstof opname vertoonden van anorganische en organische substraten. Dit strookt met onze eerdere hypothese van een mogelijk snelle opname van DON. Aminozuurstikstof werd opgenomen in afnemende volgorde van glycine, leucine en fenylalanine, overeenkomstig hun moleculaire complexiteit, C/N-verhouding en concentratie in biota. Dit illustreert dat niet alle aminozuren gelijk zijn en een mogelijk verschillen in reactiviteit of opneembaarheid. Bacteriën droegen meer bij tot de stikstofopname naargelang de moleculen complexer waren, wat hun specifieke adaptatie aan een heterotroof leven onderschrijft. Een complex substraat, afgeleid van microalgen, werd in beide experimenten verkozen boven DON afgeleid van bacteriën. Dit toont aan dat de opname ten dele wordt bepaald door de bron en daarmee-samenhangende samenstelling. Anorganisch koolstof werd vooral opgenomen door de zeegrassen, terwijl organische koolstof (afgeleid van de microalgen) bijna alleen in de microbiële gemeenschap terecht kwam. Er werden geen verbanden gevonden tussen koostof en stikstof opname, noch in the microbiële gemeenschap noch in de macrofyten. Een tweede veldexperiment, waarin stikstof opname en retentie in het sediment werd onderzocht, toonde een snel opname aan van stikstof substraten (NH_4^+, glycine, L-leucine, L-fenylalanine, DON van microalgen) die in het sediment werden geïnjecteerd, en een snel transport tot in de bovengrondse delen. Deze translocatie staat in schril contrast met de afwezigheid van translocatie in de vorige twee experimenten, wat te wijten is aan de veel kortere incubatieduur in deze experimenten. Microfytobenthos droeg in belangrijke mate bij tot de opname van stikstof (gemeten a.h.v. HAA), terwijl bacteriële bijdragen gering waren. Koolstof werd net als stikstof gedeeltelijk vastgehouden in het sediment. Het werd opgenomen in de zeegrassen maar niet in de macroalg. De opname van koolstof en stikstof gebeurde volgens de C/N-verhouding van de substraten, hoewel een licht verlies optrad

in *Zostera noltii*. Een dergelijke koppeling werd echter niet gevonden bij de opname door microfytobenthos in HAA, waar deze verhouding veel lager was dan de C/N-verhouding in de toegevoegde aminozuren. Hieruit leiden we af dat koolstof en stikstof opname ontkoppeld waren voor deze groep. Bovendien, werd koolstof bij bacteriën in hoofdzaak ingebouwd in PLFAs, terwijl dit bij microfytobenthos gebeurde in HAA. Groep-specifieke PLFA merkers vertoonden een verschil in opname van de diverse aangeboden substraten dat teruggevoerd kan worden op een voorkeur voor verschillende substraten of de opname van anorganische koolstof na remineralizatie.

Dit onderzoek heeft aangetoond dat DON een sterk dynamische ecosysteem component is die snel kan gebruikt worden als stikstof bron door primaire producenten. De koostof in de opgeloste organische stof is op alle niveaus ontkoppeld van de stikstof, wat, onder omstandigheden van lage anorganische stikstof beschikbaarheid, kan resulteren in een verschil in seizoenale variatie van koolstof ten opzichte van stikstof. Hiermee worden schijnbare inconsistenties tussen eerder gerapporteerde studies enigszins verduidelijkt, daar de seizoenale variatie kan teruggebracht worden tot een variërende balans tussen productie en consumptie van DON. Deze bevindingen illustreren een potentiëel belangrijke rol voor DON als stikstof bron, vooral tijdens schaarste van anorganische stikstof, wat belangrijke implicaties heeft voor stikstof-limitatie van primaire produktie en remediëring van effecten van eutrofiëring.

Appendix

A Supplementary R-code to chapter 2

Van Engeland T., K. Soetaert

Abstract Functions to generate the figures of the wavelet-based analyses in the statistical package R (R Development Core Team, 2008). These make use of the libraries waveslim (Whitcher, 2007) and wmtsa (Constantine & Percival, 2007).

A.1 Libraries

We need the following libraries.

```
> library(waveslim)
> library(wmtsa)
```

A.2 Construction of the time series objects

The doppler signal:

```
> dopplerSignal <- as.vector(as.matrix(make.signal("doppler")))
```

The dissolved organic nitrogen series:

```
> DONTSCH175 <- ts(c(5.759, 4.593, 3.427, 3.498, 4.212, 4.409, 4.605, 5.747, 2.427, 4.748,
+     4.998, 4.998, 4.998, 7.853, 6.176, 4.498, 7.377, 6.782, 6.64, 4.426, 5.926, 5.283,
+     5.069, 6.069, 4.284, 4.391, 4.498, 5.14, 4.569, 5.497, 3.177, 4.534, 4.658, 4.783,
+     4.498, 4.712, 3.498, 4.212, 5.259, 6.307, 4.248, 3.927, 4.498, 4.426, 5.14, 4.855,
+     4.569, 4.212, 5.497, 4.855, 4.212, 3.784, 3.356, 6.497, 5.247, 1.142, 4.426, 4.23,
+     4.034, 3.837, 3.641, 3.213, 3.498, 2.784, 4.819, 5.997, 2.642, 4.736, 4.51, 4.284,
+     5.712, 4.676, 3.641, 4.117, 4.593, 5.069, 5.545, 6.39, 4.676, 5.212, 4.462, 3.713,
+     4.212, 4.712, 5.783, 4.908, 4.034, 3.927, 4.783, 4.676, 5.283, 4.319, 4.641, 4.819,
+     4.998, 5.712, 5.355, 3.356, 4.462, 4.569, 5.355, 5.783, 5.676, 4.641, 5.569, 5.497,
+     6.425, 6.015, 5.604, 5.194, 4.783, 5.176, 3.927, 4.177, 4.712, 3.891, 5.997, 6.14,
+     7.139, 7.782), start = c(1995, 1), end = c(2004, 12), deltat = 1/12)
```

and nitrate series:

```
> NO3TSCH175 <- ts(c(1.523, 2.689, 3.855, 0.821, 1.606, 0.357, 0.428, 0.357, 0.428, 0.678,
+     0.571, 1.999, 3.427, 10.352, 7.425, 4.498, 0.666, 0.714, 0.464, 0.464, 0.357, 0.357,
+     1.785, 0.928, 1.785, 1.606, 1.428, 0.714, 0.357, 0.357, 0.357, 0.286, 0.428, 0.571,
+     0.214, 3.998, 3.784, 1.713, 1.095, 0.476, 0.214, 0.214, 0.214, 0.214, 0.214, 0.785,
+     1.356, 1.571, 4.926, 3.873, 2.82, 1.517, 0.214, 0.214, 0.214, 0.214, 0.214, 1.464,
+     2.713, 3.962, 5.212, 5.783, 0.857, 2.499, 0.214, 0.214, 0.214, 0.214, 0.25, 0.286,
+     1.071, 3.427, 5.783, 4.391, 2.999, 1.606, 0.214, 0.428, 0.214, 0.25, 0.232, 0.214,
+     0.214, 0.214, 0.357, 1.624, 2.891, 0.214, 0.214, 0.214, 0.214, 0.214, 0.214, 0.393,
+     0.571, 0.857, 6.782, 6.925, 4.069, 0.214, 0.214, 0.214, 0.214, 0.25, 0.214, 0.357,
+     0.214, 1.053, 1.892, 2.731, 3.57, 0.214, 0.214, 0.214, 0.214, 0.214, 0.214, 0.214,
+     0.214, 0.428), start = c(1995, 1), end = c(2004, 12), deltat = 1/12)
```

(both based on data from `http://www.waterbase.nl`)

A.3 The maximal overlap discrete wavelet transforms(MODWT)

Unbiased estimates

Elimination of all boundary coefficients is accomplished by the function "brick.wall", prior to the phase shift correction (function "phase.shift"). This correction is necessary because the filtering with a wavelet filter induces a displacement of features relative to the original time series.

```
> unbiasedModwtDON <- phase.shift(brick.wall(modwt(DONTSCH175, n.levels = 4, wf = "la8",
+     boundary = "periodic"), wf = "la8"), wf = "la8")
> unbiasedModwtNO3 <- phase.shift(brick.wall(modwt(log(NO3TSCH175), n.levels = 4, wf = "la8",
+     boundary = "periodic"), wf = "la8"), wf = "la8")
```

The least asymmetric wavelet of width 8 (Daubechies, 1992) is the template wavelet. Since all boundary coefficients are eliminated by the brick.wall function, we might just as well use the periodic boundary treatment (default).

Biased estimates

Below the brick-wall is NOT applied. All boundary coefficients are kept.

```
> biasedModwtDON <- phase.shift(modwt(DONTSCH175, n.levels = 4, wf = "la8",
+     boundary = "periodic"), wf = "la8")
> biasedModwtNO3 <- phase.shift(modwt(log(NO3TSCH175), n.levels = 4, wf = "la8",
+     boundary = "periodic"), wf = "la8")
```

By eliminating only the coefficients that are severely affected by the circular filtering, the maximal potential bias is reduced. In an attempt to reduce boundary effects the reflection boundary treatment is used because of the dissimilarity between the beginning and end of the signals.

```
> modwtDON <- phase.shift(modwt(DONTSCH175, n.levels = 4, wf = "la8", boundary = "reflection"),
+     wf = "la8")
> modwtNO3 <- phase.shift(modwt(log(NO3TSCH175), n.levels = 4, wf = "la8",
+     boundary = "reflection"), wf = "la8")
```

The output from the modwt function (waveslim) using the reflection boundary option returns the modwt of the extended version after mirroring. Only the first half is needed and corresponds to the original signal. The extended transform vectors (by mirroring the time series) are again reduced to the original size.

```
> n.levels <- 4
> for (i in 1:(n.levels + 1)) {
+     modwtDON[[i]] <- modwtDON[[i]][1:(length(modwtDON[[i]])/2)]
+     modwtNO3[[i]] <- modwtNO3[[i]][1:(length(modwtNO3[[i]])/2)]
+ }
```

e-Folding estimates

Elimination of the e-folding coefficients is accomplished using the following script where a constant zero valued series with a perturbation of value 1 in the middle (=x) is transformed.

```
> x <- rep(0, 10001)
> x[5000] <- 1
> n.levels <- 4
> len <- length(DONTSCH175)
> temp <- phase.shift(modwt(x, n.levels = n.levels, wf = "la8"), wf = "la8")
```

The positions to the left and to the right of the maximal influence of this spike are recorded in a matrix (left, right) together with the position of the maximum itself (top).

```
> waveExtremes <- matrix(nrow = 3, ncol = n.levels + 1)
> colnames(waveExtremes) <- c(paste("d", 1:n.levels, sep = ""), paste("s", n.levels,
+     sep = ""))
> rownames(waveExtremes) <- c("left", "right", "top")
```

The distance to the maximum from both sides of the influence is determined as $1/e^2$ times the maximum within a specific coefficient vector.

```
> for (i in 1:(n.levels + 1)) waveExtremes[, i] <- c(range(which(abs(temp[[i]])
+     >= max(abs(temp[[i]]))/(exp(2)))), which.max(abs(temp[[i]])))
```

The positions (waveExtremes) are used to calculate the distances to the left and to the right of the influence maximum. The distance to the left of the maximum is called "right" because it will serve to calculate the distance at the end of the series.

```
> boundaries <- data.frame(end = len - (waveExtremes[3, ] - waveExtremes[1, ]),
+     start = waveExtremes[2, ] - waveExtremes[3, ])
```

The actual elimination of the coefficients within the margin defined by the e-folding boundaries:

```
> for (j in 1:(n.levels + 1)) {
+     is.na(modwtDON[[i]]) <- c(1:boundaries$start[i], boundaries$end[i]:length(modwtDON[[i]]))
+     is.na(modwtNO3[[i]]) <- c(1:boundaries$start[i], boundaries$end[i]:length(modwtNO3[[i]]))
+ }
```

A.4 MODWT on the Doppler signal

The Doppler signal was decomposed to the 7th scale level, using a reflection boundary treatment. Phase shift corrections were applied, resulting in the reallignment of the coefficients with the features in the original signal.

```
> modwtDoppler <- phase.shift(modwt(dopplerSignal, n.levels = 7, boundary = "reflection",
+     wf = "la16"), wf = "la16")
> for (i in 1:length(modwtDoppler)) {
+     modwtDoppler[[i]] <- modwtDoppler[[i]][1:(length(modwtDoppler[[i]])/2)]
+ }
```

```
> par(mfrow = c(9, 1), mar = c(2, 6, 0, 0), mgp = c(4, 1, 0))
> plot(dopplerSignal, axes = F, type = "l", bty = "n", lwd = 1, ylab = "Doppler", cex.lab = 1.3)
> axis(2, las = 2, cex.axis = 1.3)
> for (i in 1:length(modwtDoppler)) {
+     plot(modwtDoppler[[i]], bty = "n", axes = F, type = "n", ylab = names(modwtDoppler)[i],
+         ylim = range(modwtDoppler), cex.lab = 1.3)
+     polygon(x = c(1, 1:1024, 1024), y = c(0, modwtDoppler[[i]], 0), col = "black")
+     axis(2, las = 2, cex.axis = 1.3)
+ }
> axis(1, cex.axis = 1.3)
```

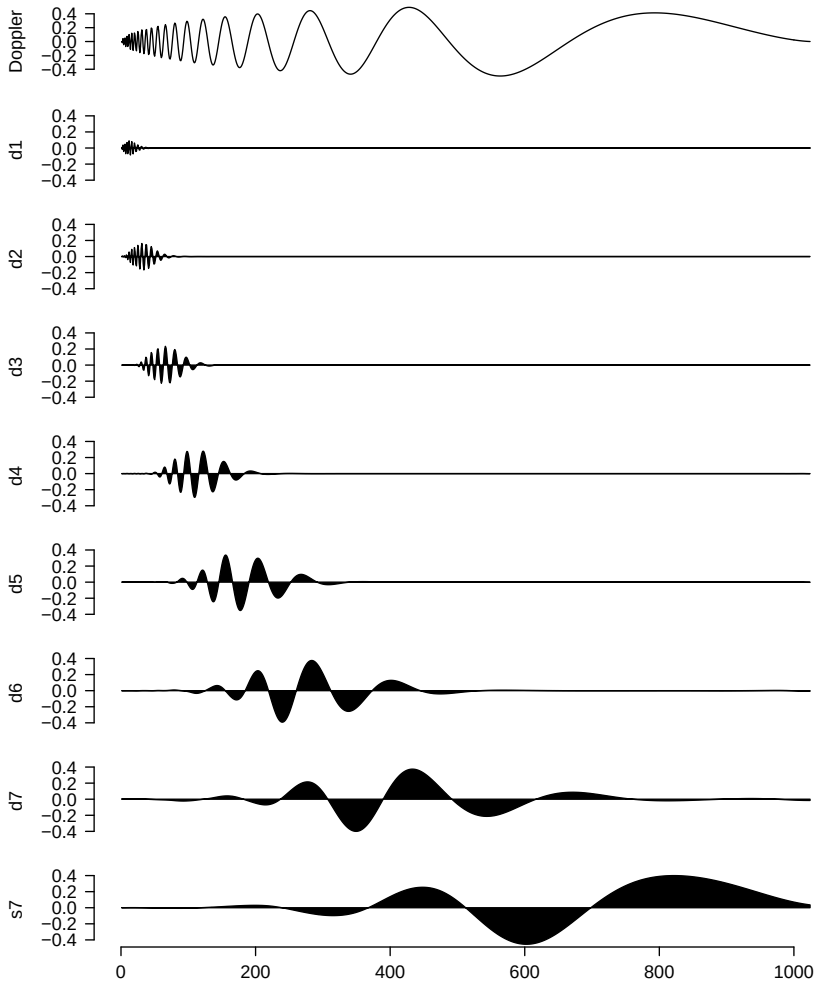

Figure 7.1: Maximal Overlap Discrete Wavelet Transform of the Doppler signal.

A.5 Squared gain of the s8 wavelet

The function `wavGain` calculates the gain function of a given filter (s8 = la8) for a number of scales.

```
> FreqResponsFunctionS8 <- wavGain(wavelet = "s8", n.levels = 4, n.fft = 1024, normalize = TRUE)
> SqrGainHigh <- t(matrix(FreqResponsFunctionS8$sqrgain$high, nrow = 4, byrow = F))
> colnames(SqrGainHigh) <- c("Level1", "Level2", "Level3", "Level4")
> SqrGainLow <- t(matrix(FreqResponsFunctionS8$sqrgain$low, nrow = 4, byrow = F))
> colnames(SqrGainLow) <- c("Level1", "Level2", "Level3", "Level4")
> par(mar = c(3, 4, 1, 0.1))
> plot(1:512, type = "n", axes = F, ylab = "Squared Gain Function", xlab = "", xlim = c(1,
+     512), ylim = c(0, 1), font.lab = 1)
> polygon(x = c(1/16, 1/8, 1/8, 1/16) * 1024, y = c(-0.1, -0.1, 1.1, 1.1), col = "lightgray",
+     border = NA)
> polygon(x = c(1/4, 1/2, 1/2, 1/4) * 1024, y = c(-0.1, -0.1, 1.1, 1.1), col = "lightgray",
+     border = NA)
> polygon(x = c(0, 1/32, 1/32, 0) * 1024, y = c(-0.1, -0.1, 1.1, 1.1), col = "lightgray",
+     border = NA)
> box(bty = "L", lwd = 1)
> matplot(SqrGainHigh[1:512, ], type = "l", lty = "solid", axes = F, ylab = "Squared Gain",
+     xlab = "Scales [month]", add = T)
> lines(1:512, SqrGainLow[1:512, 4], col = "blue")
> abline(v = c(1/24, 1/12, 1/6, 1/3) * 1024, lty = "solid", lwd = 1)
> axis(2, font.axis = 1.3, las = 2)
> mtext(side = 3, line = 0.25, outer = F, text = c(32, 16, 8, 4, 2), at = c(1/32, 1/16,
+     1/8, 1/4, 1/2) * 1024, font = 1, cex = 0.8)
> text(x = c(1/72, 1/24, 1/12, 1/6, 1/3) * 1024, y = rep(0.5, 4), labels = c("s4", "d4",
+     "d3", "d2", "d1"), font = 1, cex = 0.75, pos = 4, offset = 0.1)
> axis(1, font.axis = 1, at = c(1/24, 1/12, 1/6, 1/3) * 1024, labels = c(24, 12, 6, 3),
+     cex.axis = 1)
> mtext(side = 1, line = 1.6, outer = F, at = 256, text = "Periodicity (# obs.)", font = 1)
```

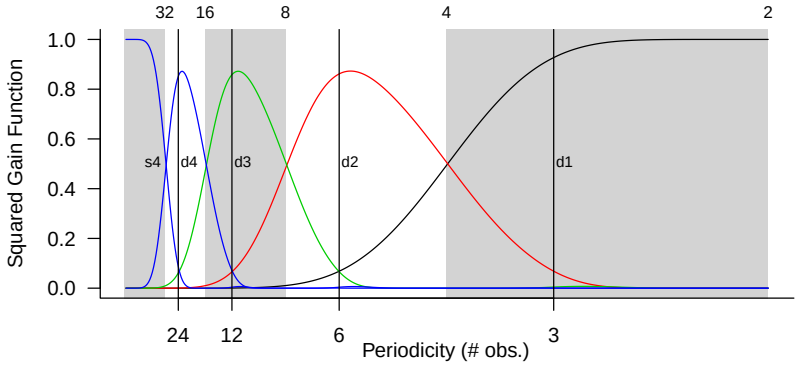

Figure 7.2: The squared gain function of the symlet (s8) or least asymmetric wavelet (la8) of width 8.

The mirrored second half is not shown in our plot. Using 1024 points to calculate the frequency respons function (n.fft=1024), this results in the first 512 values being used. In addition, the frequency respons function of the lowest level scaling filter is included in our graph whereas it is displayed in a separate graph in the `wavGain`-function.

A.6 Fourier and autocorrelation analysis

First the nitrate related graphs, then the DON

```
> par(fig = c(0, 0.48, 0.5, 1), mar = c(3, 5, 0, 0))
> plot((NO3TSCH175), bty = "n", cex.axis = 1.3, ylab = "", xlab = "", axes = F)
> axis(1, cex.axis = 1.3)
> axis(2, cex.axis = 1.3, las = 2)
> box(bty = "L", lwd = 1.1)
> mtext(side = 2, line = 3.5, outer = F, text = expression("[N" * O[3]^"-" * "] (" *
+     mu * "mol/l)"), cex = 1.3)
> par(new = T, fig = c(0, 0.24, 0, 0.5), mar = c(4, 5, 0, 0))
> spec.pgram(log(NO3TSCH175), detrend = T, spans = c(5, 5), bty = "n", main = "", sub = "",
+     xlab = "", ylab = "", demean = T, axes = F)
> axis(1, cex.axis = 1.3)
> axis(2, cex.axis = 1.3, las = 2)
> box(bty = "L", lwd = 1.1)
> mtext(side = 2, line = 3.5, outer = F, at = 0.15, text = "Periodogram", cex = 1.3)
> mtext(side = 1, line = 2, at = 3, outer = F, text = expression("Freq. (year"^"-1" *
+     ")"), cex = 1.3)
> abline(v = 1, col = "red")
> par(new = T, fig = c(0.24, 0.48, 0, 0.5), mar = c(4, 5, 0, 0))
> acf(log(NO3TSCH175), demean = T, ci.type = "white", bty = "n", main = "", sub = "",
+     xlab = "", ylab = "", axes = F)
> axis(1, cex.axis = 1.3)
> axis(2, cex.axis = 1.3, las = 2)
> box(bty = "L", lwd = 1.1)
> mtext(side = 2, line = 3.5, outer = F, at = 0.25, text = "Autocorrelation", cex = 1.3)
> mtext(side = 1, line = 2, at = 0.75, outer = F, text = "Time lag (year)", cex = 1.3)
> Spline <- smooth.spline(seq(1995, 2004 + 11/12, by = 1/12), DONTSCH175, spar = 0.75)$y
> par(new = T, fig = c(0.52, 1, 0.5, 1), mar = c(3, 5, 0, 0))
> plot(DONTSCH175, bty = "n", cex.lab = 1, cex.axis = 1, ylab = "", xlab = "", axes = F)
> axis(1, cex.axis = 1.3)
> axis(2, cex.axis = 1.3, las = 2)
> box(bty = "L", lwd = 1.1)
> mtext(side = 2, line = 3.5, outer = F, text = expression("[DON] (" * mu * "mol/l)"),
+     cex = 1.3)
> lines(seq(1995, 2004 + 11/12, by = 1/12), Spline, col = "red")
> par(new = T, fig = c(0.52, 0.76, 0, 0.5), mar = c(4, 5, 0, 0))
> spec.pgram(DONTSCH175 - Spline, demean = T, spans = c(5, 5), bty = "n", main = "",
+     sub = "", xlab = "", ylab = "", axes = F, ylim = c(0.025, 0.13))
> axis(1, cex.axis = 1.3)
> axis(2, cex.axis = 1.3, las = 2)
> box(bty = "L", lwd = 1.1)
> mtext(side = 2, line = 3.5, outer = F, at = 0.055, text = "Periodogram", cex = 1.3)
> mtext(side = 1, line = 2, at = 3, outer = F, text = expression("Freq. (year"^"-1" *
+     ")"), cex = 1.3)
> abline(v = 1, col = "red")
```

```
> par(new = T, fig = c(0.76, 1, 0, 0.5), mar = c(4, 5, 0, 0))
> acf(DONTSCH175 - Spline, demean = T, ci.type = "white", bty = "n", main = "", sub = "",
+     xlab = "", ylab = "", axes = F)
> axis(1, cex.axis = 1.3)
> axis(2, cex.axis = 1.3, las = 2)
> box(bty = "L", lwd = 1.1)
> mtext(side = 2, line = 3.5, outer = F, at = 0.4, text = "Autocorrelation", cex = 1.3)
> mtext(side = 1, line = 2, at = 0.75, outer = F, text = "Time lag (year)", cex = 1.3)
```

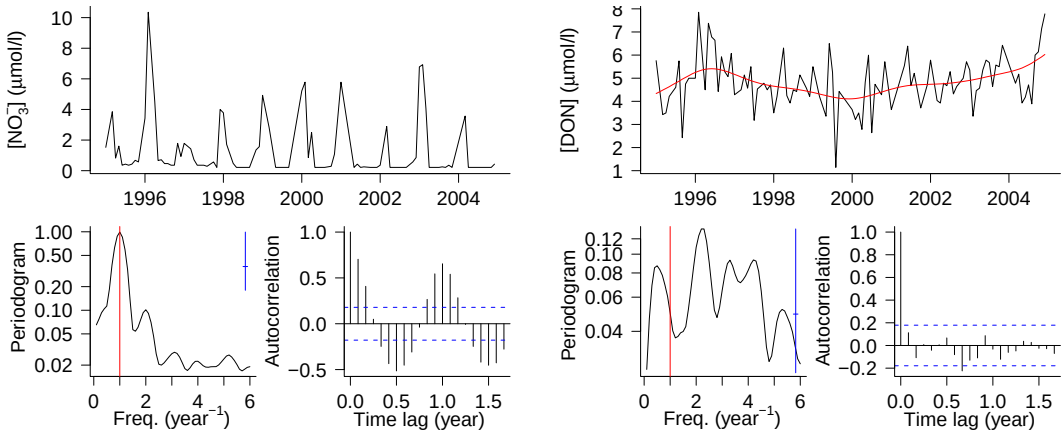

Figure 7.3: Time series plot, smoothed periodogram, and autocorrelation function for nitrate and DON.

A.7 MODWT of the DON signal

The DON concentration series was transformed using a MODWT with the s8 symlet. The limits of the boundary coefficients and e-folding coefficients are indicated with vertical red (solid) and blue (dashed) lines respectively.

```
> par(mfrow = c(n.levels + 1, 1), mar = c(2, 3, 0.5, 0.2))
> for (i in 1:n.levels) {
+     plot(as.vector(time(DONTSCH175)), biasedModwtDON[[i]], xlab = "", ylab = "", type = "h",
+         bty = "n", axes = F, ylim = range(modwtDON[1:n.levels]))
+     axis(2, cex.axis = 1.5, las = 2)
+     abline(v = seq(start(DONTSCH175)[1], end(DONTSCH175)[1], by = 1), col = "gray",
+         lty = "dashed")
+     abline(h = 0)
+     abline(v = time(DONTSCH175)[range(which(!is.na(unbiasedModwtDON[[i]])))], lwd = 2,
+         col = "red")
+     abline(v = time(DONTSCH175)[c(boundaries$start[i], boundaries$end[i])], col = "blue",
+         lwd = 3, lty = "dashed")
+     mtext(side = 4, line = -2, cex = 1.2, outer = F, at = par("usr")[4], text = paste("d",
+         i, sep = ""), las = 2)
+ }
```

```
> plot(as.vector(time(DONTSCH175)), biasedModwtDON$s4, xlab = "", ylab = "", type = "h",
+     bty = "n", axes = F)
> axis(1, cex.axis = 1.5)
> axis(2, cex.axis = 1.5, las = 2)
> mtext(side = 4, line = -2, cex = 1.2, outer = F, at = par("usr")[4], text = paste("s4",
+     sep = ""), las = 2)
> abline(v = time(DONTSCH175)[range(which(!is.na(unbiasedModwtDON[[5]])))], lwd = 2,
+     col = "red")
> abline(v = time(DONTSCH175)[c(boundaries$start[5], boundaries$end[5])], col = "blue",
+     lwd = 3, lty = "dashed")
```

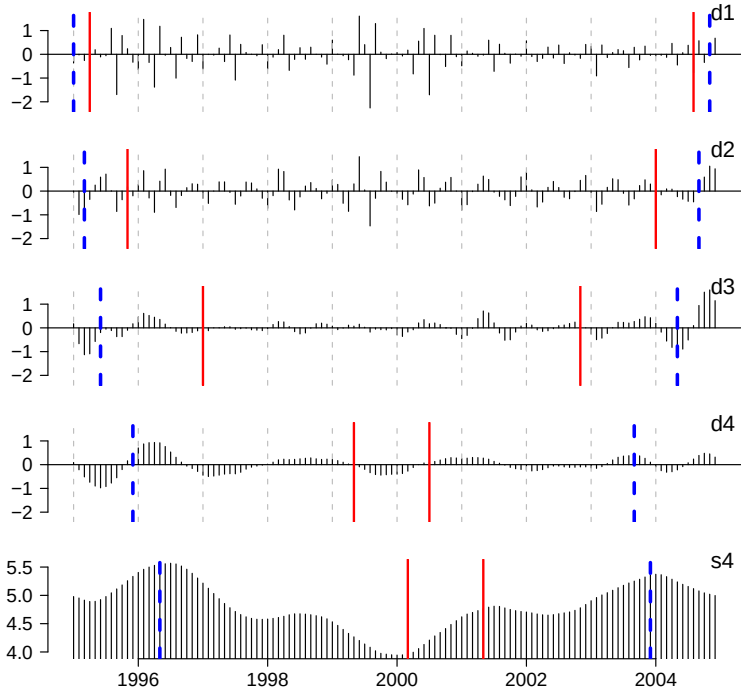

Figure 7.4: MODWT of the DON concentration with indication of the limits of the boundary and e-folding coefficients.

A.8 Analysis of variance

The `wave.variance`-function calculates the scale-dependent wavelet variance with 95%-confidence limits.

```
> wavVarDON <- wave.variance(modwtDON)
> wavVarNO3 <- wave.variance(modwtNO3)

> par(mar = c(5, 5, 0.5, 0.5), mgp = c(4, 1, 0))
> plot(1:4, type = "n", ylim = range(cbind(wavVarDON[1:4, ], wavVarNO3[1:4, ])), xlab = "Scale",
```

```
+     ylab = "Wavelet Variance", log = "y", axes = F, cex.lab = 1.2)
> points((1:4) - 0.05, wavVarDON[1:4, 1], pch = 19, col = "red")
> lines((1:4) - 0.05, wavVarDON[1:4, 1], lty = "dashed", col = "red")
> arrows((1:4) - 0.05, wavVarDON[1:4, 2], (1:4) - 0.05, wavVarDON[1:4, 3], code = 3,
+     angle = 90, length = 0.025, col = "red")
> points(1:4, wavVarNO3[1:4, 1], pch = 18, cex = 1.5, col = "blue")
> lines((1:4), wavVarNO3[1:4, 1], lty = "dashed", col = "blue")
> arrows(1:4, wavVarNO3[1:4, 2], 1:4, wavVarNO3[1:4, 3], code = 3, angle = 90, length = 0.025,
+     col = "blue")
> axis(2, las = 2, cex.axis = 1.2)
> axis(1, at = 1:4, labels = paste("d", 1:4, sep = ""), cex.axis = 1.2)
> box(bty = "l")
> legend("bottomleft", pch = 19:17, lty = "dashed", col = c("red", "blue"),
+     legend = expression("[DON]", "log[NO"[3]^"-" * "]"), bty = "n", cex = 1.5)
```

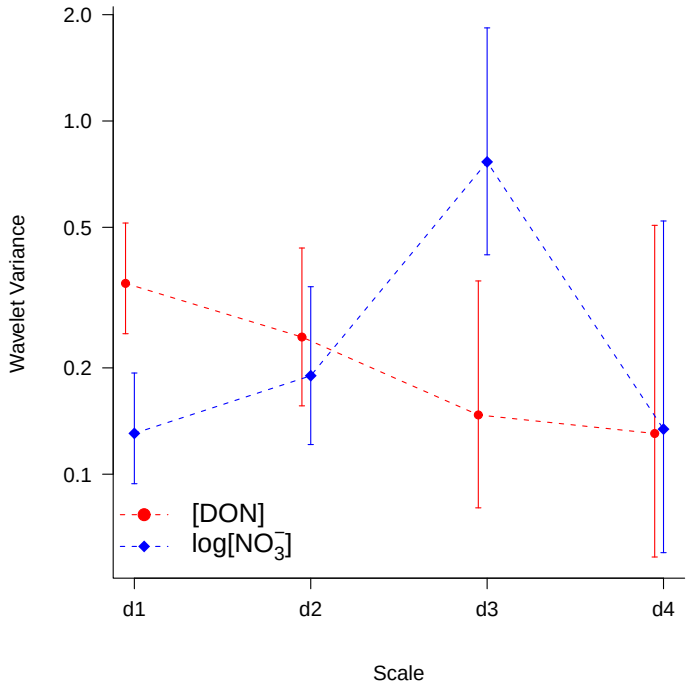

Figure 7.5: The wavelet variance per scale for the nitrate and DON signals.

A.9 Multiresolution analysis

The additive multiresolution decomposition as signal into subsignal that in superposition add up to the orignal signal. This property is used to reconstruct sub-signals at particular set of scales. The result is basically a filtered version of the original signal.

```
> mraDON <- mra(DONTSCH175, boundary = "reflection", J = 3, wf = "la8")

> par(fig = c(0, 1, 0.68, 1), mar = c(0, 4, 0.4, 0.2))
> plot(DONTSCH175, xlab = "", ylab = expression("[DON] (" * mu * "M)"), bty = "n", axes = F)
> axis(2, las = 2)
> mtext(side = 3, outer = F, line = -1, text = expression(bold("Total signal")), at = 2003)
> par(new = T, fig = c(0, 1, 0.35, 0.67), mar = c(0, 4, 0.4, 0.2))
> plot(ts(I(mraDON$D1 + mraDON$D2 + mraDON$D3), start = c(1995, 1), deltat = 1/12), axes = F,
+     xlab = "", ylab = expression("[DON] (" * mu * "M)"), ylim = c(-3, 3))
> axis(2, las = 2)
> mtext(side = 3, outer = F, line = -1, text = expression(bold("Intra-annual")), at = 2003)
> par(new = T, fig = c(0, 1, 0.06, 0.34), mar = c(0.5, 4, 0.4, 0.2))
> plot(ts(I(mraDON$S3), start = c(1995, 1), deltat = 1/12), bty = "L", xlab = "",
+     ylab = expression("[DON] (" * mu * "M)"), ylim = c(3.5, 6.5), axes = F)
> axis(1)
> axis(2, las = 2)
> mtext(side = 3, outer = F, line = -1, text = expression(bold("Inter-annual")), at = 2003)
```

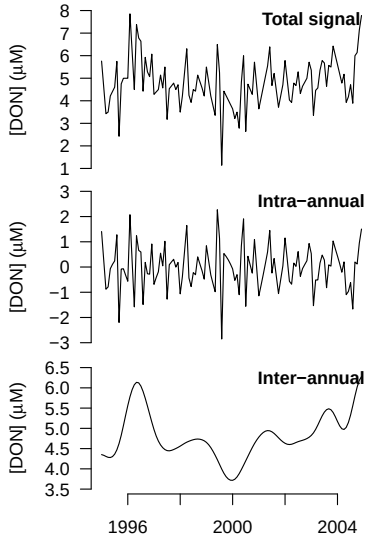

Figure 7.6: The original signal, the reconstructed intra-annual signal, and the interannual trend in the DON concentration.

A.10 Wavelet correlation

Correlation analysis was performed using different strategies: a scale-independent scatterplot, a scale-dependent wavelet correlation, and a scale-dependent cross-correlation. The wavelet correlation gives a scale-wise decomposition of the scale-independent correlation between two signal. The scale-dependent cross-correlation (spin-correlation) decomposes the scale-independent cross-correlation.

To estimate the spin-correlation and the corresponding 95%-confidence intervals, the following function was written:

```
> spincor <- function(modwt1, modwt2, lags) {
+     temp <- list(spincor = vector(), lower = vector(), upper = vector(), lags = -lags:lags)
+     for (i in 1:length(modwt1)) {
+         correlations <- spin.correlation(modwt1[[i]], modwt2[[i]], lag.max = lags)
+         temp$spincor <- cbind(temp$spincor, correlations)
+         temp$lower <- cbind(temp$lower,
+             tanh(atanh(correlations) - qnorm(0.975)/sqrt(rep(trunc(length(modwt2[[1]])/2^i),
+             times = length(-lags:lags)) - 3)))
+         temp$upper <- cbind(temp$upper,
+             tanh(atanh(correlations) + qnorm(0.975)/sqrt(rep(trunc(length(modwt2[[1]])/2^i),
+             times = length(-lags:lags)) - 3)))
+     }
+     colnames(temp$spincor) <- c(paste("d", 1:(length(modwt1) - 1), sep = ""), paste("s",
+         length(modwt1) - 1, sep = ""))
+     colnames(temp$lower) <- c(paste("d", 1:(length(modwt1) - 1), sep = ""), paste("s",
+         length(modwt1) - 1, sep = ""))
+     colnames(temp$upper) <- c(paste("d", 1:(length(modwt1) - 1), sep = ""), paste("s",
+         length(modwt1) - 1, sep = ""))
+     return(temp)
+ }
```

Although this function returns values for all the scale levels, only the d2 scale level is plotted (right):

```
> par(mfrow = c(1, 3), mar = c(4, 5, 0.2, 0.2))
> plot(as.vector(log(NO3TSCH175)), as.vector(DONTSCH175), xlab = expression("log[NO"[3]^"-" *
+     "]"), ylab = expression("[DON]"), bty = "n", pch = 19, cex = 0.5, axes = F, cex.lab = 1.5)
> axis(2, cex.axis = 1.5, las = 2)
> axis(1, cex.axis = 1.5)
> par(mar = c(4, 5, 0.2, 0.2), mgp = c(4, 1, 0))
> wavCor <- as.data.frame(wave.correlation(modwtNO3, modwtDON, N = 120))
> plot((1:4), wavCor$wavecor[1:4], pch = 19, cex = 1, axes = F, xlab = "",
+     ylab = "Wavelet Correlation", ylim = c(-1, 1), xlim = c(0.5, 4.5), col = "black",
+     bty = "n", cex.lab = 1.5)
> abline(h = 0, col = "gray")
> lines((1:4), wavCor$wavecor[1:4], col = "black", lty = "solid")
> arrows(rep(1:4, 2), rep(wavCor$wavecor[1:4], 2), rep(1:4, 2), c(wavCor$lower[1:4],
+     wavCor$upper[1:4]), angle = 90, lwd = 1, length = 0.02, col = "black")
> axis(2, cex.axis = 1.5, las = 2)
> axis(1, cex.axis = 1.5, at = 1:4, labels = c("d1", "d2", "d3", "d4"))
> mtext(1, at = 2.5, line = 2.8, outer = F, text = "Scale", cex = 1)
> spincorrelation <- spincor(modwtNO3, modwtDON, lag = 9)
> par(mar = c(4, 5, 0.2, 0.2), mgp = c(4, 1, 0), xpd = T)
> plot(spincorrelation$lags, spincorrelation$spincor[, 2], xlab = "", ylab = "Correlation",
+     ylim = range(c(spincorrelation$upper, spincorrelation$lower)), type = "l", bty = "n",
+     axes = F, cex.lab = 1.5)
> abline(h = 0, v = 0, col = "gray")
> lines(spincorrelation$lags, spincorrelation$upper[, 2], col = "red", lty = "dashed")
> lines(spincorrelation$lags, spincorrelation$lower[, 2], col = "red", lty = "dashed")
> mtext(3, at = 0, line = -1.5, text = colnames(spincorrelation$spincor)[2], outer = F,
```

```
+     font = 2)
> mtext(1, at = 0, line = 2.8, outer = F, text = "Time Lag (months)", cex = 1)
> axis(1, cex.axis = 1.5)
> axis(2, cex.axis = 1.5, las = 2)
```

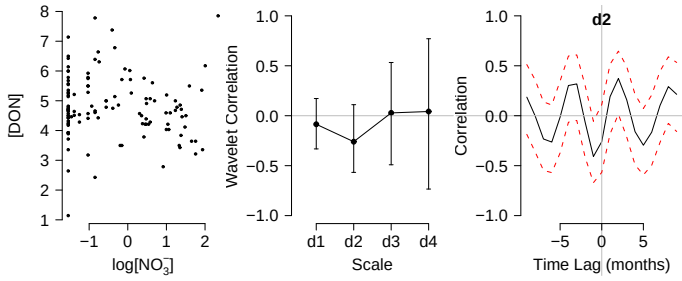

Figure 7.7: Scatterplot, wavelet correlation and d2 spin-correlation between DON and nitrate.

A.11 Coherence/phase analysis

We use the Hilbert wavelet filter template (k313); flength is a smoothing parameter to obtain consistent estimates of the coherence and phase.

```
> wf <- "k313"
> flength <- 12
```

MODHWT transformation of the DON and nitrate series, using the reflection boundary treatment (see above).

```
> modhwtDON <- phase.shift.hilbert(modwt.hilbert(DONTSCH175, wf = "k313",
+     boundary = "reflection"), wf = "k313")
> modhwtNO3 <- phase.shift.hilbert(modwt.hilbert(NO3TSCH175, wf = "k313",
+     boundary = "reflection"), wf = "k313")
> for (i in 1:length(modhwtDON)) {
+     modhwtDON[[i]] <- modhwtDON[[i]][1:(length(modhwtDON[[i]])/2)]
+     modhwtNO3[[i]] <- modhwtNO3[[i]][1:(length(modhwtNO3[[i]])/2)]
+ }
```

Calculation of the coherence and phase difference from the cross-transform of the individual modhwt objects.

```
> coh <- modhwt.coh(modhwtNO3, modhwtDON, f.length = flength)
> phase <- modhwt.phase(modhwtNO3, modhwtDON, f.length = flength)
> tempcoh <- ts(cbind(coh[[1]], coh[[2]], coh[[3]], coh[[4]]), start = c(1995, 1),
+     deltat = 1/12)
> tempphase <- ts(cbind(phase[[1]], phase[[2]], phase[[3]], phase[[4]]), start = c(1995,
+     1), deltat = 1/12)
```

```
> par(mfrow = c(3, 1), mar = c(3, 4.2, 1.2, 4.2))
> for (i in 2:4) {
+     temp <- na.omit(cbind(1:length(tempcoh[, i]), tempcoh[, i]))
+     temp <- rbind(c(temp[1, 1], 0), temp, c(temp[nrow(temp)], 0))
+     plot(0, type = "n", xlim = c(1, length(tempcoh[, i])), ylim = c(0, 1.05), xlab = "",
+         ylab = "", axes = F)
+     polygon(temp, col = "lightgray", lwd = 0.5)
+     axis(2, cex.axis = 1.3, las = 2)
+     axis(1, at = c(0:(length(unique(trunc(time(DONTSCH175)))) - 1)) * 12 + 6,
+         labels = unique(trunc(time(DONTSCH175))), cex.axis = 1.3)
+     par(new = T)
+     plot(1:length(tempphase[, i]), c(tempphase[, i]), type = "n", xlim = c(1,
+         length(tempphase[,i])), ylim = c(-1.5 * pi, 1.5 * pi), axes = F, xlab = "", ylab = "")
+     points(1:length(tempphase[, i]), c(tempphase[, i]), pch = 20, cex = 0.2)
+     axis(4, at = c(-pi, 0, pi), cex.axis = 1.3, labels = c(expression(-pi), 0, expression(pi)),
+         las = 2, hadj = 1, mgp = c(3, 2.7, 0))
+     mtext(side = 4, outer = F, at = 0, text = "Phase", line = 3, cex = 1)
+     mtext(side = 2, outer = F, at = 0, text = "Coherence", line = 3, cex = 1)
+     for (j in -1:1) lines(c(min(c(1:length(tempphase[, i]))[!is.na(tempcoh[, i])],
+         na.rm = T), length(tempphase[, i]) + 10), rep(pi * j, 2), lty = "dotted", col = "red",
+         lwd = 0.6)
+     mtext(side = 3, at = 0, outer = F, line = -0.5, adj = 0, text = paste(2^i, " - ",
+         2^(i + 1), " months (wavelet level ", i, ")", sep = ""), cex = 0.6)
+ }
```

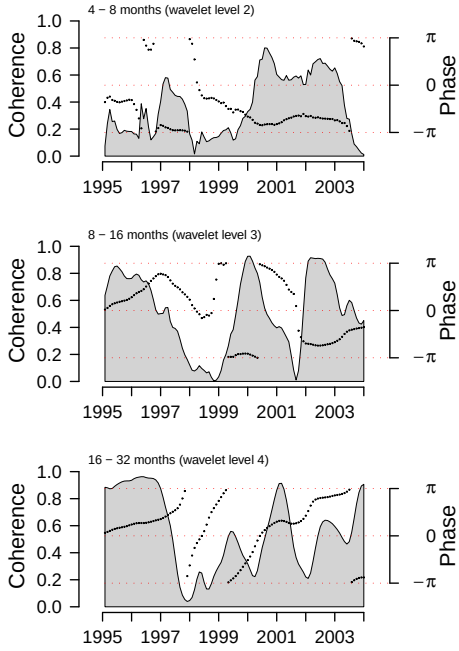

Figure 7.8: Coherence and phase plots of DON versus nitrate for the wavelet levels 2 to 4.

B Acknowledgements by chapter

Chapter 2: The authors would like to thank Prof. Donald Percival and Dr. Maarten Jansen, and Elisa Beninca for the valuable feedback and discussions on wavelet analysis of time series. We also want to express our appreciation to Rijkswaterstaat for supplying the monitoring data. Furthermore, we would like to thank the reviewers and editor for their constructive comments and criticisms. This study was part of the NODCi project.

Chapter 3: The authors wish to thank Johanna Baretta-Bekker for the information on the phytoplankton at the Dogger Bank, and Donald Percival and Maarten Jansen for the fruitful discussions on wavelet analysis of time series. We also want to express our appreciation to Rijkswaterstaat for supplying the monitoring data. Furthermore, we would like to thank the reviewers and editor for their constructive comments and criticisms. This study was part of the NODCi project.

Chapter 4: Edward P. Morris is supported by the regional government of Andalusia project FUNDIV (P07-RNM-2516). Additional support was provided the Spanish Project CTM2008-00012/MAR. Fernando G. Brun holds a European Reintegration Grant (MERG-CT-2007-205675). Transport and travel costs were supported by a travel grant from Schure-Beijerinck-Popping Fund (SBP/JK/2007-32). Thanks to Fidel Echevarrìa Navas (Director of institute) for granting us access to the facilities of the CACYTMAR, and to Bas Koutstaal for helping with sample processing.

Chapter 5 and 6: Edward P. Morris is supported by the regional government of Andalusia project FUNDIV (P07-RNM-2516). Additional support was provided the Spanish Project CTM2008-00012/MAR. Fernando G. Brun holds a European Reintegration Grant (MERG-CT-2007-205675). Transport and travel costs were supported by a travel grant from Schure-Beijerinck-Popping Fund (SBP/JK/2007-32).

I would like to thank the thesis committee for their time and effort. I hope that this work was enjoyable to read.

C Curriculum vitae

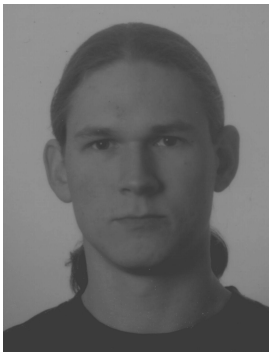

First name: Tom

Last name: Van Engeland

Place of birth: Lommel (Belgium)

Date of birth: January 14, 1979

Nationality: Belgian

Marital status: married

Working address: NIOO-CEME
Korringaweg 7
4401 NT Yerseke
The Netherlands

Webpage: `http://www.nioo.knaw.nl/users/tvanengeland`

Mobile number: +32 (0)474 59 15 37

Education:

2005-2010:	PhD project NIOO-CEME (The Netherlands) Thesis: *Dissolved organic nitrogen dynamics in coastal ecosystems*
2004-2005:	Master of Science in Marine and Lacustrine Sciences Gent University (Belgium) Dissertation: *Using hyperspectral remote sensing data to model microalgal distribution and primary production on an intertidal flat*
2002-2004:	MSc in Biology Leuven University (Belgium) Dissertation: *The relationship between morphology and population genetic aspects in the European Eel (*Anguilla anguilla*): a spatio-temporal analysis*
2000-2002:	BSc in Biology Leuven University (Belgium)
1997-1998:	1^{st} year BSc in Computer Science Leuven University (Belgium)

Courses:

2009/10:	NSG course: Methods for spectral analysis of climatic time series, Amsterdam, The Netherlands
2008/10:	Training course: Data Management, Oostende, Belgium
2006/11:	Writing a Scientific Article, Yerseke, The Netherlands
2006/11:	Longitudinal and Incomplete Data, Leiden, The Netherlands
2006/08:	Aquatic Microbial and Molecular Ecology, Odense, Denmark
2006/03:	Goal Oriented Working and Planning, Utrecht, The Netherlands
2006/05:	Estuarine Ecology, Yerseke, The Netherlands

Additional qualifications:
. IT: operating systems (MS-Windows, Linux), database management software (MySQL, MS-SQL server), statistical packages (R, Statistica, Sigmaplot), GIS (basic; Idrisi, ArcGIS, GRASS)
. CMAS** diver
. Car and motorbike driving license

Language skills:
Dutch: mother tongue
French: basic command
English: fluent

Personal interests:
sports: running, mountain biking, scuba diving), boat renovation, travelling

Scientific meetings:
2008/09: NIOO-days
oral presentation: Dissolved organic nitrogen in the southern North Sea: a wavelet approach

2008/03: 2008 Ocean Sciences Meeting: From the Watershed to the Global Ocean, Orlando, Florida, US.
poster: Van Engeland, T. Knuijt, A., Laane, R. W., Soetaert, K., Middelburg, J. J.: Wavelet analyses show high variability in relationships between dissolved organic nitrogen, primary production and river discharge in the southern North Sea

2007/09: IMBER/LOICZ Continental Margins Open Science Conference, Shanghai, China.
oral presentation: T. Van Engeland, A. Knuijt, R.W.P.M. Laane, K. Soetaert and J.J. Middelburg: Dissolved organic nitrogen: an active ecosystem component at the land-ocean interface

Publications:
Kromkamp, J. C. & T. Van Engeland (2009): Changes in Phytoplankton Biomass in the Western Scheldt Estuary During the Period 1978–2006. Estuaries and Coasts, doi:10.1007/s12237-009-9215-3

Submitted publications:
Van Engeland T., T. J. S. Cox , K. Soetaert, R. W. P. M. Laane, F. J. R. Meysmana , J. J. Middelburg: Wavelet approaches to analyze biogeochemical time series. Submitted to Estuarine, Coastal and Shelf Science

Van Engeland T., K. Soetaert , A. Knuijt , R. W. P. M. Laane, J. J. Middelburg: Dissolved Organic Nitrogen Dynamics in the North Sea: a time series analysis (1995-2005). Submitted to Estuarine, Coastal and Shelf Science.

Bibliography

Admiraal, W., Riauxgobin, C., Laane, R. W. P. M., 1987. Interactions of ammonium, nitrate, and d-amino acids and l-amino acids in the nitrogen assimilation of 2 species of estuarine benthic diatoms. Marine Ecology Progress Series 40, 267–273.

Alexander, R. B., Smith, R. A., 2006. Trends in the nutrient enrichment of us rivers during the late 20th century and their relation to changes in probable stream trophic conditions. Limnology and Oceanography 51, 639–654.

Alvarez-Salgado, X. A., Gago, J., Miguez, B. M., Perez, F. F., 2001. Net ecosystem production of dissolved organic carbon in a coastal upwelling system: the ria de vigo, iberian margin of the north atlantic. Limnology and Oceanography 46 (1), 135–147.

Alves Bolzan, M. J., Vieira, P. C., 2006. Wavelet analysis of the wind velocity and temperature variability in the amazon forest. Brazilian Journal of Physics 36, 1217–1222.

Aminot, A., Kerouel, R., 2004. Dissolved organic carbon, nitrogen and phosphorus in the n-e atlantic and the n-w mediterranean with particular reference to non-refractory fractions and degradation. Deep-Sea Research Part I-Oceanographic Research Papers 51 (12), 1975–1999.

Anderson, D. M., Glibert, P. M., Burkholder, J. M., 2002. Harmful algal blooms and eutrophication: Nutrient sources, composition, and consequences. Estuaries 25 (4B), 704–726.

Andersson, M. G. I., van Rijswijk, P., Middelburg, J. J., 2006. Uptake of dissolved inorganic nitrogen, urea and amino acids in the scheldt estuary: comparison of organic carbon and nitrogen uptake. Aquatic Microbial Ecology 44, 303–315.

Antia, N. J., Berland, B. R., Bonin, D. J., Maestrini, S. Y., 1975. Comparative evaluation of certain organic and inorganic sources of nitrogen for phototrophic growth of marine microalgae. Journal of the Marine Biological Association of the United Kingdom 55, 519–539.

Antia, N. J., Harrison, P. J., Oliveira, L., 1991. The role of dissolved organic nitrogen in phytoplankton nutrition, cell biology and ecology. Phycologia 30 (1), 1–89.

Azam, F., Hodson, R. E., 1977. Size distribution and activity of marine microheterotrophs. Limnology And Oceanography 22 (3), 492–501.

Badr, E. A., Tappin, A. D., Achterberg, E. P., 2008. Distributions and seasonal variability of dissolved organic nitrogen in two estuaries in sw england. Marine Chemistry 110, 153–164.

Baines, S. B., Fisher, N. S., Cole, J. J., 2005. Uptake of dissolved organic matter (dom) and its importance to metabolic requirements of the zebra mussel, dreissena polymorpha. Limnology And Oceanography 50 (1), 36–47.

Banoub, M. W., Williams, P. J. L., 1973. Seasonal changes in organic forms of carbon, nitrogen and phosphorus in sea-water at e1 in english channel during 1968. Journal of the Marine Biological Association of the United Kingdom 53, 695–703.

Bardgett, R. D., Streeter, T. C., Bol, R., 2003. Soil microbes compete effectively with plants for organic-nitrogen inputs to temperate grasslands. Ecology 84, 1277–1287.

Baretta-Bekker, J. G., Baretta, J. W., Latuhihin, M. J., Desmit, X., Prins, T. C., 2009. Description of the long-term (1991-2005) temporal and spatial distribution of phytoplankton carbon biomass in the dutch north sea. Journal of Sea Research 61, 50–59.

Barranguet, C., Herman, P. M. J., Sinke, J. J., 1997. Microphytobenthos biomass and community composition studied by pigment biomarkers: importance and fate in the carbon cycle of a tidal flat. Journal Of Sea Research 38 (1-2), 59–70.

Barron, C., Middelburg, J. J., Duarte, C. M., 2006. Phytoplankton trapped within seagrass (posidonia oceanica) sediments are a nitrogen source: An in situ isotope labeling experiment. Limnology and Oceanography 51 (4), 1648–1653.

Bates, N. R., Hansell, D. A., 1999. A high resolution study of surface layer hydrographic and biogeochemical properties between chesapeake bay and bermuda. Marine Chemistry 67 (1-2), 1–16.

Begovic, M., Copin-Montegut, C., 2002. Processes controlling annual variations in the partial pressure of co2 in surface waters of the central northwestern mediterranean sea (dyfamed site). Deep-Sea Research Part Ii-Topical Studies in Oceanography 49 (11), 2031–2047.

Benner, R., 2002. Chemical composition and reactivity. In: Hansell, D. A., Carlson, C. A. (Eds.), Biogeochemistry of Marine Dissolved Organic Matter. Academic Press, San Diego, pp. 59–90.

Benner, R., Biddanda, B., Black, B., McCarthy, M. D., 1997. Abundance, size distribution, and stable carbon and nitrogen isotopic compositions of marine organic matter isolated by tangential-flow ultrafiltration. Marine Chemistry 57 (3-4), 243–263.

Benner, R., Peele, E. R., Hodson, R. E., 1986. Microbial utilization of dissolved organic-matter from leaves of the red mangrove, rhizophora-mangle, in the fresh creek estuary, bahamas. Estuarine Coastal and Shelf Science 23 (5), 607–619.

Berg, G. M., Balode, M., Purina, I., Bekere, S., Bechemin, C., Maestrini, S. Y., 2003. Plankton community composition in relation to availability and uptake of oxidized and reduced nitrogen. Aquatic Microbial Ecology 30, 263–274.

Berg, G. M., Glibert, P. M., Lomas, M. W., Burford, M. A., 1997. Organic nitrogen uptake and growth by the chrysophyte *Aureococcus anophagefferens* during a brown tide event. Marine Biology 129, 377–387.

Berg, G. M., Repeta, D. J., LaRoche, J., 2002. Dissolved organic nitrogen hydrolysis rates in axenic cultures of aureococcus anophagefferens (pelagophyceae): Comparison with heterotrophic bacteria. Applied and Environmental Microbiology 68 (1), 401–404.

Berman, T., Bronk, D. A., 2003. Dissolved organic nitrogen: a dynamic participant in aquatic ecosystems. Aquatic Microbial Ecology 31 (3), 279–305.

Berman, T., Chava, S., 1999. Algal growth on organic compounds as nitrogen sources. Journal Of Plankton Research 21 (8), 1423–1437.

Biddanda, B., Benner, R., 1997. Major contribution from mesopelagic plankton to heterotrophic metabolism in the upper ocean. Deep-Sea Research Part I-Oceanographic Research Papers 44 (12), 2069–2085.

Billen, G., Garnier, J., Rousseau, V., 2005. Nutrient fluxes and water quality in the drainage network of the scheldt basin over the last 50 years. Hydrobiologia 540, 47–67.

Bird, K. T., Johnson, J. R., Jewett-Smith, J., 1998. In vitro culture of the seagrass halophila decipiens. Aquatic Botany 60 (4), 377–387.

Bjornsen, P. K., 1988. Phytoplankton exudation of organic-matter - why do healthy cells do it. Limnology And Oceanography 33 (1), 151–154.

Bode, A., Dortch, Q., 1996. Uptake and regeneration of inorganic nitrogen in coastal waters influenced by the mississippi river: Spatial and seasonal variations. Journal Of Plankton Research 18 (12), 2251–2268.

Bode, A., Varela, M. M., Teira, E., Fernandez, E., Gonzalez, N., Varela, M. M., 2004. Planktonic carbon and nitrogen cycling off northwest spain: variations in production of particulate and dissolved organic pools. Aquatic Microbial Ecology 37 (1), 95–107.

Boon, P. I., Moriarty, D. J. W., Saffigna, P. G., 1986. Rates of ammonium turnover and the role of amino-acid deamination in seagrass (textitZostera capricorni) beds of moreton bay, australia. Marine Biology 91, 259–268.

Boschker, H. T. S., de Brouwer, J. F. C., Cappenberg, T. E., 1999. The contribution of macrophyte-derived organic matter to microbial biomass in salt-marsh sediments: Stable carbon isotope analysis of microbial biomarkers. Limnology and Oceanography 44 (2), 309–319.

Boschker, H. T. S., Kromkamp, J. C., Middelburg, J. J., 2005. Biomarker and carbon isotopic constraints on bacterial and algal community structure and functioning in a turbid, tidal estuary. Limnology and Oceanography 50 (1), 70–80.

Boschker, H. T. S., Middelburg, J. J., 2002. Stable isotopes and biomarkers in microbial ecology. Fems Microbiology Ecology 40 (2), 85–95.

Boyer, E. W., Goodale, C. L., Jaworski, N. A., Howarth, R. W., 2002. Anthropogenic nitrogen sources and relationships to riverine nitrogen export in the northeastern u.s.a. Biogeochemistry 57-58, 137–169.

Bozec, Y., Thomas, H., Schiettecatte, L. S., Borges, A. V., Elkalay, K., de Baar, H. J. W., 2006. Assessment of the processes controlling seasonal variations of dissolved inorganic carbon in the north sea. Limnology And Oceanography 51 (6), 2746–2762.

Bradshaw, G. A., Spies, T. A., 1992. Characterizing canopy gap structure in forests using wavelet analysis. Journal of Ecology 80, 205–215.

Braswell, B. H., Sacks, W. J., Linder, E., Schimel, D. S., 2005. Estimating diurnal to annual ecosystem parameters by synthesis of a carbon flux model with eddy covariance net ecosystem exchange observations. Global Change Biology 11, 335–355.

Brinch-Iversen, J., King, G. M., 1990. Effects of substrate concentration, growth-state, and oxygen availability on relationships among bacterial carbon, nitrogen and phospholipid phosphorus-content. Fems Microbiology Ecology 74 (4), 345–355.

Brion, N., Baeyens, W., De Galan, S., Elskens, M., Laane, R. W. P. M., 2004. The north sea: source or sink for nitrogen and phosphorus to the atlantic ocean? Biogeochemistry 68, 277–296.

Brockmann, U. H., Kattner, G., 1997. Winter-to-summer changes of nutrients, dissolved and particulate organic material in the north sea. Ocean Dynamics 49, 229–242.

Bronk, D. A., 1999. Rates of nh_4^+ uptake, intracellular transformation and dissolved organic nitrogen release in two clones of marine *Synechococcus spp.* Journal of Plankton Research 21 (7), 1337–1353.

Bronk, D. A., 2002. Dynamics of don. In: Hansell, D. A., Carlson, C. A. (Eds.), Biogeochemistry of Marine Dissolved Organic Matter. Academic Press, San Diego, pp. 153–247.

Bronk, D. A., Glibert, P. M., 1993. Application of a ^{15}n tracer method to the study of dissolved organic nitrogen uptake during spring and summer in chesapeak bay. Marine Biology 115, 501–508.

Bronk, D. A., Glibert, P. M., Ward, B. B., 1994. Nitrogen uptake, dissolved organic nitrogen release, and new production. Science 265, 1843–1846.

Bronk, D. A., See, J. H., Bradley, P., Killberg, L., 2007. Don as a source of bioavailable nitrogen for phytoplankton. Biogeosciences 4, 283–296.

Bronk, D. A., Ward, B. B., 2000. Magnitude of dissolved organic nitrogen release relative to gross nitrogen uptake in marine systems. Limnology And Oceanography 45 (8), 1879–1883.

Bronk, D. A., Ward, B. B., 2005. Inorganic and organic nitrogen cycling in the southern california bight. Deep-Sea Research Part I-Oceanographic Research Papers 52 (12), 2285–2300.

Bruce, A., Gao, H. Y., 1996. Applied Wavelet Analysis with S-Plus. Springer-Verlag New York, Inc., Secaucus, NJ, USA.

Brun, F. G., Vergara, J. J., Navarro, G., Hernández, I., Pérez-Lloréns, J. L., 2003. Effect of shading by *Ulva rigida* canopies on growth and carbon balance of the seagrass *Zostera noltii*. Marine Ecology-Progress Series 265, 85–96.

Brun, F. G., Vergara, J. J., Peralta, G., Garcia-Sanchez, M. P., Hernández, I., Pérez-Lloréns, J. L., 2006. Clonal building, simple growth rules and phylloclimate as key steps to develop functional-structural seagrass models. Marine Ecology-Progress Series 323, 133–148.

Bulthuis, D. A., Axelrad, D. M., Mickelson, M. J., 1992. Growth of the seagrass heterozostera-tasmanica limited by nitrogen in port phillip bay, australia. Marine Ecology-Progress Series 89 (2-3), 269–275.

Burdige, D. J., 2002. Sediment pore waters. In: Hansell, D. A., Carlson, C. A. (Eds.), Biogeochemistry of Marine Dissolved Organic Matter. Academic Press, San Diego, pp. 611–663.

Burdige, D. J., Berelson, W. M., Coale, K. H., McManus, J., Johnson, K. S., 1999. Fluxes of dissolved organic carbon from california continental margin sediments. Geochimica et Cosmochimica Acta 63 (10), 1507–1515.

Burdige, D. J., Zheng, S. L., 1998. The biogeochemical cycling of dissolved organic nitrogen in estuarine sediments. Limnology And Oceanography 43 (8), 1796–1813.

Butler, E. I., Knox, S., Liddicoat, M. I., 1979. Relationship between inorganic and organic nutrients in sea-water. Journal of the Marine Biological Association of the United Kingdom 59, 239–250.

Cadée, G. C., Hegeman, J., 1993. Persisting high levels of primary production at declining phosphate concentrations in the dutch coastal area (marsdiep). Netherlands Journal of Sea Research 31, 147–152.

Cadée, G. C., Hegeman, J., 2002. Phytoplankton in the marsdiep at the end of the 20th century; 30 years monitoring biomass, primary production, and phaeocystis blooms. Journal of Sea Research 48, 97–110.

Carl, G., Kühn, I., 2008. Analyzing spatial ecological data using linear regression and wavelet analysis. Stochastic Environmental Research and Risk Assessment 22, 315–324.

Carlson, C. A., 2002. Production and removal processes. In: Hansell, D. A., Carlson, C. A. (Eds.), Biogeochemistry of Marine Dissolved Organic Matter. Academic Press, San Diego, pp. 91–151.

Carrasco, M., Lopez-Ramirez, J. A., Benavente, J., Lopez-Aguayo, F., Sales, D., 2003. Assessment of urban and industrial contamination levels in the bay of cadiz, sw spain. Marine Pollution Bulletin 46 (3), 335–345.

Carstensen, J., Conley, D. J., Andersen, J. H., Ærtebjerg, G., 2006. Coastal eutrophication and trend reversal: A danish case study. Limnology and Oceanography 51, 398–408.

Cauwet, G., 2002. Dom in the coastal zone. In: Hansell, D. A., Carlson, C. A. (Eds.), Biogeochemistry of Marine Dissolved Organic Matter. Academic Press, San Diego, pp. 579–609.

Cazelles, B., Chavez, M., Berteaux, D., Menard, F., Vik, J. O., Jenouvrier, S., Stenseth, N. C., 2008. Wavelet analysis of ecological time series. Oecologia 156, 287–304.

Chatfield, C., 2004. The analysis of time series: an introduction, 6th Edition. CRC Press, Boca Raton, FL.

Chisholm, J. R. M., Dauga, C., Ageron, E., Grimont, P. A. D., Jaubert, J. M., 1996. 'roots' in mixotrophic algae. Nature 381, 382.

Cloern, J. E., 2001. Our evolving conceptual model of the coastal eutrophication problem. Marine Ecology Progress Series 210, 223–253.

Cloern, J. E., Jassby, A. D., 2008. Complex seasonal patterns of primary producers at the land-sea interface. Ecology Letters 11, 1294–1303.

Collos, Y., Dohler, G., Biermann, I., 1992. Production of dissolved organic nitrogen during uptake of nitrate by synedra-planctonica - implications for estimates of new production in the oceans. Journal Of Plankton Research 14 (8), 1025–1029.

Conley, D. J., Markager, S., Andersen, J., Ellermann, T., Svendsen, L. M., 2002. Coastal eutrophication and the danish national aquatic monitoring and assessment program. Estuaries 25, 848–861.

Conley, D. J., Schelske, C. L., Stoermer, E. F., 1993. Modification of the biogeochemical cycle of silica with eutrophication. Marine Ecology Progress Series 101, 179–192.

Constantine, W., Percival, D. B., 2007. wmtsa: Insightful Wavelet Methods for Time Series Analysis. R package version 1.0-4.

Copin-Montegut, C., 2000. Consumption and production on scales of a few days of inorganic carbon, nitrate and oxygen by the planktonic community: results of continuous measurements at the dyfamed station in the northwestern mediterranean sea (may 1995). Deep-Sea Research Part I-Oceanographic Research Papers 47 (3), 447–477.

Copping, A. E., Lorenzen, C. J., 1980. Carbon budget of a marine phytoplankton-herbivore system with c-14 as a tracer. Limnology And Oceanography 25 (5), 873–882.

Cornelisen, C. D., Thomas, F. I. M., 2002. Ammonium uptake by seagrass epiphytes: Isolation of the effects of water velocity using an isotope label. Limnology and Oceanography 47 (4), 1223–1229.

Cornelisen, C. D., Thomas, F. I. M., 2004. Ammonium and nitrate uptake by leaves of the seagrass *Thalassia testudinum*: impact of hydrodynamic regime and epiphyte cover on uptake rates. Journal Of Marine Systems 49 (1-4), 177–194.

Cowie, G. L., Hedges, J. I., 1992. Sources and reactivities of amino acids in a coastal marine environment. Limnology and Oceanography 37 (5), 703–724.

Craigmile, P. F., Percival, D. B., 2005. Asymptotic decorrelation of between-scale wavelet coefficients. IEEE Transactions on Information Theory 51, 1039–1048.

Dafner, E., De Galan, S., Goeyens, L., 1999. Microwave digestion of organic substances, a useful tool for dissolved organic nitrogen measurements. Water Research 33, 548–554.

Daubechies, I., 1992. Ten lectures on wavelets. Vol. 61 of CBMS-NSF Regional Conference Series in Applied Mathematics. Society for Industrial and Applied Mathematics (SIAM), Philadelphia, PA.

Davis, B. C., Fourqurean, J. W., 2001. Competition between the tropical alga, halimeda incrassata, and the seagrass, thalassia testudinum. Aquatic Botany 71 (3), 217–232.

De Galan, S., Elskens, M., Goeyens, L., Pollentier, A., Brion, N., Baeyens, W., 2004. Spatial and temporal trends in nutrient concentrations in the belgian continental area of the north sea during the period 1993-2000. Estuarine Coastal and Shelf Science 61, 517–528.

de Jonge, V. N., 1997. High remaining productivity in the dutch western wadden sea despite decreasing nutrient inputs from riverine sources. Marine Pollution Bulletin 34, 427–436.

de Jonge, V. N., Elliott, M., Brauer, V. S., 2006. Marine monitoring: Its shortcomings and mismatch with the eu water framework directive's objectives. Marine Pollution Bulletin 53 (1-4), 5–19.

de Jonge, V. N., Elliott, M., Orive, E., 2002. Causes, historical development, effects and future challenges of a common environmental problem: eutrophication. Hydrobiologia 475, 1–19.

de Vries, I., Duin, R. N. M., Peeters, J. C. H., Los, F. J., Bokhorst, M., Laane, R. W. P. M., 1998. Patterns and trends in nutrients and phytoplankton in dutch coastal waters: comparison of time-series analysis, ecological model simulation, and mesocosm experiments. ICES Journal of Marine Science 55, 620–634.

De Wever, A., Forster, R., Engeland, T. V., Adam, S., Sabbe, K., in prep. Exploration of spectral reflectance measures for microphytobenthos mapping on intertidal mudflats in western europe.

Del Castillo, C. E., Miller, R. L., 2008. On the use of ocean color remote sensing to measure the transport of dissolved organic carbon by the mississippi river plume. Remote Sensing of Environment 112, 836–844.

den Meersche, K. V., Soetaert, K., Middelburg, J. J., 2008. A bayesian compositional estimator for microbial taxonomy based on biomarkers. Limnology And Oceanography: Methods 6, 190–199.

Dijkman, N. A., Boschker, H. T. S., Middelburg, J. J., Kromkamp, J. C., 2009. Group-specific primary production based on stable-isotope labeling of phospholipid-derived fatty acids. Limnology And Oceanography-Methods 7, 612–625.

Dijkman, N. A., Kromkamp, J. C., 2006a. Phospholipid-derived fatty acids as chemotaxonomic markers for phytoplankton: application for inferring phytoplankton composition. Marine Ecology-Progress Series 324, 113–125.

Dijkman, N. A., Kromkamp, J. C., 2006b. Photosynthetic characteristics of the phytoplankton in the scheldt estuary: community and single-cell fluorescence measurements. European Journal Of Phycology 41 (4), 425–434.

Dodds, W. K., 2006. Eutrophication and trophic state in rivers and streams. Limnology And Oceanography 51 (1, part 2), 671–680.

Dodds, W. K., Cole, J. J., 2007. Expanding the concept of trophic state in aquatic ecosystems: It's not just the autotrophs. Aquatic Sciences 69, 427–439.

Downing, J. A., 1997. Marine nitrogen: Phosphorus stoichiometry and the global n:p cycle. Biogeochemistry 37, 237–252.

Downing, J. A., Osenberg, C. W., Sarnelle, O., 1999. Meta-analysis of marine nutrient-enrichment experiments: Variation in the magnitude of nutrient limitation. Ecology 80 (4), 1157–1167.

Duarte, C. M., 1990. Seagrass nutrient content. Marine Ecology-Progress Series 67 (2), 201–207.

Duarte, C. M., 1995. Submerged aquatic vegetation in relation to different nutrient regimes. Ophelia 41, 87–112.

Duce, R. A., LaRoche, J., Altieri, K., Arrigo, K. R., Baker, A. R., Capone, D. G., Cornell, S., Dentener, F., Galloway, J., Ganeshram, R. S., Geider, R. J., Jickells, T. D., Kuypers, M. M., Langlois, R., Liss, P. S., Liu, S. M., Middelburg, J. J., Moore, C. M., Nickovic, S., Oschlies, A., Pedersen, T., Prospero, J., Schlitzer, R., Seitzinger, S. P., Sorensen, L. L., Uematsu, M., Ulloa, O., Voss, M., Ward, B., Zamora, L., 2008. Impacts of atmospheric anthropogenic nitrogen on the open ocean. Science 320 (5878), 893–897.

Ducrotoy, J. P., Elliott, M., de Jonge, V. N., 2000. The north sea. Marine Pollution Bulletin 41, 5–23.

Dugdale, R. C., Wilkerson, F. P., 1986. The use of n-15 to measure nitrogen uptake in eutrophic oceans - experimental considerations. Limnology and Oceanography 31 (4), 673–689.

Duursma, E., 1961. Dissolved organic carbon, nitrogen and phosphorus in the sea. Netherlands Journal of Sea Research 1, 1–141.

Elmgren, R., Larsson, U., 2001. Eutropication in the baltic sea area: Integrated coastal management numbers, 15–35.

Engel, A., Goldthwait, S., Passow, U., Alldredge, A., 2002. Temporal decoupling of carbon and nitrogen dynamics in a mesocosm diatom bloom. Limnology and Oceanography 47, 753–761.

Essink, K., 2003. Response of an estuarine ecosystem to reduced organic waste discharge. Aquatic Ecology 37, 65–76.

Evrard, V., Cook, P. L. M., Veuger, B., Huettel, M., Middelburg, J. J., 2008. Tracing carbon and nitrogen incorporation and pathways in the microbial community of a photic subtidal sand. Aquatic Microbial Ecology 53 (3), 257–269.

Evrard, V., Kiswara, W., Bouma, T. J., Middelburg, J. J., 2005. Nutrient dynamics of seagrass ecosystems: N-15 evidence for the importance of particulate organic matter and root systems. Marine Ecology-Progress Series 295, 49–55.

Eyre, B. D., Ferguson, A. J. P., 2002. Comparison of carbon production and decomposition, benthic nutrient fluxes and denitrification in seagrass, phytoplankton, benthic microalgae- and macroalgae-dominated warm-temperate australian lagoons. Marine Ecology-Progress Series 229, 43–59.

Fadili, M. J., Bullmore, E. T., 2002. Wavelet-generalized least squares: A new blu estimator of linear regression models with 1/f errors. Neuroimage 15, 217–232.

Fan, C., Glibert, P. M., Alexander, J., Lomas, M. W., 2003. Characterization of urease activity in three marine phytoplankton species, *Aureococcus anophagefferens*, *Prorocentrum minimum*, and *Thalassiosira weissflogii*. Marine Biology 142 (5), 949–958.

Fan, Y. Q., 2003. On the approximate decorrelation property of the discrete wavelet transform for fractionally differenced processes. IEEE Transactions on Information Theory 49, 516–521.

Farge, M., 1992. Wavelet transforms and their applications to turbulence. Annual Review of Fluid Mechanics 24, 395–457.

Fernandes, M., Bryars, S., Mount, G., Miller, D., 2009. Seagrasses as a sink for wastewater nitrogen: The case of the adelaide metropolitan coast. Marine Pollution Bulletin 58 (2), 303–308.

Findlay, S., Carlough, L., Crocker, M. T., Gill, H. K., Meyer, J. L., Smith, P. J., 1986. Bacterial-growth on macrophyte leachate and fate of bacterial production. Limnology and Oceanography 31 (6), 1335–1341.

Fitznar, H. P., Lobbes, J. M., Kattner, G., 1999. Determination of enantiomeric amino acids with high-performance liquid chromatography and pre-column derivatisation with o-phthaldialdehyde and n-isobutyrylcysteine in seawater and fossil samples (mollusks). Journal Of Chromatography A 832 (1-2), 123–132.

Flynn, K. J., Berry, L. S., 1999. The loss of organic nitrogen during marine primary production may be significantly overestimated when using n-15 substrates. Proceedings Of The Royal Society Of London Series B-Biological Sciences 266 (1419), 641–647.

Flynn, K. J., Butler, I., 1986. Nitrogen-sources for the growth of marine microalgae - role of dissolved free amino-acids. Marine Ecology-Progress Series 34 (3), 281–304.

Fourqurean, J. W., Powell, G. V. N., Kenworthy, W. J., Zieman, J. C., 1995. The effects of long-term manipulation of nutrient supply on competition between the seagrasses thalassia-testudinum and halodule-wrightii in florida bay. Oikos 72 (3), 349–358.

Frazier, A. D., Rowe, J. M., Rentz, C. A., Gobler, C. J., Wilhelm, S. W., 2007. Bacterial lysis of aureococcus anophagefferens ccmp 1784 (pelagophyceae). Journal Of Phycology 43 (3), 461–465.

Fry, B. (Ed.), 2006. Springer, New York.

Gamon, J. A., Field, C. B., Goulden, M. L., Griffin, K. L., Hartley, A. E., Joel, G., nuelas, J. P., Valentini, R., 1995. Relationships between ndvi, canopy structure, and photosynthesis in three californian vegetation types. Ecological Applications 5 (1), 28–41.

Glibert, P. M., Garside, C., Furhman, J. A., Roman, M. R., 1991. Time-dependent coupling of inorganic and organic nitrogen uptake and regeneration in the plume of the chesapeake bay estuary and its regulation by large heterotrophs. Limnology and Oceanography 36 (5), 895–909.

Glibert, P. M., Harrison, J., Heil, C., Seitzinger, S. P., 2006. Escalating worldwide use of urea - a global change contributing to coastal eutrophication. Biogeochemistry 77, 441–463.

Glibert, P. M., Wazniak, C. E., Hall, M. R., Sturgis, B., 2007. Seasonal and interannual trends in nitrogen and brown tide in maryland's coastal bays. Ecological Applications 17, S79–S87.

Gobler, C. J., Hutchins, D. A., Fisher, N. S., Cosper, E. M., Sanudo-Wilhelmy, S. A., 1997. Release and bioavailability of c, n, p, se, and fe following viral lysis of a marine chrysophyte. Limnology And Oceanography 42 (7), 1492–1504.

Gómez-Parra, A., Forja, J. M., 1993. Benthic nutrient fluxes in cadiz bay (sw spain). Hydrobiologia 252, 23–34.

Grasshoff, K., Kremling, K., Ehrhardt, M. (Eds.), 1999. Wiley-VCH, Weinheim.

Grinsted, A., Moore, J. C., Jevrejeva, S., 2004. Application of the cross wavelet transform and wavelet coherence to geophysical time series. Nonlinear Processes in Geophysics 11, 561–566.

Hansell, D. A., Carlson, C. A., 2001. Biogeochemistry of total organic carbon and nitrogen in the sargasso sea: control by convective overturn. Deep-Sea Research Part II-Topical Studies in Oceanography 48, 1649–1667.

Hansen, J. W., Udy, J. W., Perry, C. J., Dennison, W. C., Lomstein, B. A., 2000. Effect of the seagrass *Zostera capricorni* on sediment microbial processes. Marine Ecology-Progress Series 1999, 83–96.

Harrison, K. A., Bol, R., Bardgett, R. D., 2007. Preferences for different nitrogen forms by coexisting plant species and soil microbes. Ecology 88 (4), 989–999.

Harrison, K. A., Bol, R., Bardgett, R. D., 2008. Preferences for different nitrogen forms by coexisting plant species and soil microbes: reply. Ecology 89 (3), 879–880.

Harrison, W. G., 1978. Experimental measurements of nitrogen remineralization in coastal waters. Limnology And Oceanography 23 (4), 684–694.

Hedges, J. I., 2002. Why dissolved organic matter? In: Hansell, D. A., Carlson, C. A. (Eds.), Biogeochemistry of Marine Dissolved Organic Matter. Academic Press, San Diego, pp. 1–33.

Hedges, J. I., Keil, R. G., Benner, R., 1997. What happens to terrestrial organic matter in the ocean? Organic Geochemistry 27 (5-6), 195–212.

Heip, C. H. R., Basford, D., Craeymeersch, J. A., Dewarumez, J. M., Dorjes, J., Dewilde, P., Duineveld, G., Eleftheriou, A., Herman, P. M. J., Niermann, U., Kingston, P., Kunitzer, A., Rachor, E., Rumohr, H., Soetaert, K., Soltwedel, T., 1992. Trends in biomass, density and diversity of north-sea macrofauna. ICES Journal of Marine Science 49, 13–22.

Heip, C. H. R., Goosen, N. K., Herman, P. M. J., Kromkamp, J. C., Middelburg, J. J., Soetaert, K., 1995. Production and consumption of biological particles in temperate tidal estuaries. Oceanography and Marine Biology - An Annual Review, Vol 33 33, 1–149.

Hemminga, M. A., Duarte, C. M., 2000. Seagrass ecology. Cambridge University Press, Cambridge, UK.

Hemminga, M. A., Harrison, P. G., van Lent, F., 1991. The balance of nutrient losses and gains in seagrass meadows. Marine Ecology-Progress Series 71, 85–96.

Hickel, W., Mangelsdorf, P., Berg, J., 1993. The human impact in the german bight - eutrophication during 3 decades (1962-1991). Helgoland Marine Research 47, 243–263.

Hydes, D. J., Kelly-Gerreyn, B. A., Le Gall, A. C., Proctor, R., 1999. The balance of supply of nutrients and demands of biological production and denitrification in a temperate latitude shelf sea - a treatment of the southern north sea as an extended estuary. Marine Chemistry 68, 117–131.

Invers, O., Perez, M., Romero, J., 2002. Seasonal nitrogen speciation in temperate seagrass posidonia oceanica (l.) delile. Journal Of Experimental Marine Biology And Ecology 273 (2), 219–240.

Jansen, M., Oonincx, P., 2005. Second generation wavelets and applications. Springer-Verlag London Limited, London.

Jevrejeva, S., Moore, J. C., Grinsted, A., 2003. Influence of the arctic oscillation and el nino-southern oscillation (enso) on ice conditions in the baltic sea: The wavelet approach. Journal of Geophysical Research-Atmosphere 108, 4677.

Jickells, T. D., 1995. Atmospheric inputs of metals and nutrients to the oceans - their magnitude and effects. Marine Chemistry 48, 199–214.

Kaiser, K., Benner, R., 2005. Hydrolysis-induced racemization of amino acids. Limnology And Oceanography : Methods 3, 318–325.

Kaldy, J. E., Onuf, C. P., Eldridge, P. M., Cifuentes, L. A., 2002. Carbon budget for a subtropical seagrass dominated coastal lagoon: How important are seagrasses to total ecosystem net primary production? Estuaries 25 (4A), 528–539.

Karl, D. M., Bjorkman, K. M., Dore, J. E., Fujieki, L., Hebel, D. V., Houlihan, T., Letelier, R. M., Tupas, L. M., 2001. Ecological nitrogen-to-phosphorus stoichiometry at station aloha. Deep-Sea Research Part II-Topical Studies in Oceanography 48, 1529–1566.

Keil, R. G., Kirchman, D. L., 1994. Abiotic transformation of labile protein to refractory protein in sea-water. Marine Chemistry 45 (3), 187–196.

Keitt, T. H., 2008. Coherent ecological dynamics induced by large-scale disturbance. Nature 454, 331–U39.

Keitt, T. H., Fischer, J., 2006. Detection of scale-specific community dynamics using wavelets. Ecology 87, 2895–2904.

Keitt, T. H., Urban, D. L., 2005. Scale-specific inference using wavelets. Ecology 86, 2497–2504.

Kemp, W. M., Boynton, W. R., Adolf, J. E., Boesch, D. F., Boicourt, W. C., Brush, G., Cornwell, J. C., Fisher, T. R., Glibert, P. M., Hagy, J. D., Harding, L. W., Houde, E. D., Kimmel, D. G., Miller, W. D., Newell, R. I. E., Roman, M. R., Smith, E. M., Stevenson, J. C., 2005. Eutrophication of chesapeake bay: historical trends and ecological interactions. Marine Ecology Progress Series 303, 1–29.

Kerner, M., Spitzy, A., 2001. Nitrate regeneration coupled to degradation of different size fractions of don by the picoplankton in the elbe estuary. Microbial Ecology 41 (1), 69–81.

Kieber, R. J., Whitehead, R. F., Skrabal, S. A., 2006. Photochemical production of dissolved organic carbon from resuspended sediments. Limnology And Oceanography 51 (5), 2187–2195.

Knapp, A. N., Sigman, D. M., Lipschultz, F., 2005. N isotopic composition of dissolved organic nitrogen and nitrate at the bermuda atlantic time-series study site. Global Biogeochemical Cycles 19, GB1018.

Koch, B. P., Ludwichowski, K.-U., Kattner, G., Dittmar, T., Witt, M., 2008. Advanced characterization of marine dissolved organic matter by combining reversed-phase liquid chromatography and ft-icr-ms. Marine Chemistry 111, 233–241.

Kokkinakis, S. A., Wheeler, P. A., 1987. Nitrogen uptake and phytoplankton growth in coastal upwelling regions. Limnology And Oceanography 32 (5), 1112–1123.

Kolaczyk, E. D., 1996. An application of wavelet shrinkage to tomography. In: A., A., M., U. (Eds.), Wavelets in Medicine and biology. CRC Press, Boca Raton, FL, pp. 77–89.

Koroleff, F., 1983. Total and organic nitrogen. In: Methods of seawater analysis. Verlag Chemie, Weinheim, pp. 162–173.

Kroeger, K. D., Cole, M. L., Valiela, I., 2006. Groundwater-transported dissolved organic nitrogen exports from coastal watersheds. Limnology and Oceanography 51, 2248–2261.

Kromkamp, J. C., Van Engeland, T., 2009. Changes in phytoplankton biomass in the western scheldt estuary during the period 1978âĂŞ2006. Estuaries And Coasts.

Kröncke, I., Knust, R., 1995. The dogger bank - a special ecological region in the central north-sea. Helgoland Marine Research 49, 335–353.

Kujawinski, E. B., Longnecker, K., Blough, N. V., Del Vecchio, R., Finlay, L., Kitner, J. B., Giovannoni, S. J., 2009. IdentiiňĄcation of possible source markers in marine dissolved organic matter using ultrahigh resolution mass spectrometry. Geochimica et Cosmochimica Acta 73, 4384–4399.

Kwiatkowski, D., Phillips, P. C. B., Schmidt, P., Shin, Y., 1992. Testing the null hypothesis of stationarity against the alternative of a unit-root - how sure are we that economic time series have a unit-root. Journal of Econometrics 54, 159–178.

La Roche, J., 1983. Ammonium regeneration: its contribution to phytoplankton nitrogen requirements in a eutrophic environment. Marine Biology 75, 231–240.

Lacroix, G., Ruddick, K., Ozer, J., Lancelot, C., 2004. Modelling the impact of the scheldt and rhine/meuse plumes on the salinity distribution in belgian waters (southern north sea). Journal of Sea Research 52, 149–163.

Lacroix, G., Ruddick, K., Park, Y., Gypens, N., Lancelot, C., 2007. Validation of the 3d biogeochemical model miro&co with field nutrient and phytoplankton data and meris-derived surface chlorophyll a images. Journal of Marine Systems 64, 66–88.

Larsson, U., Elmgren, R., Wulff, F., 1985. Eutrophication and the baltic sea - causes and consequences. Ambio 14, 9–14.

Lee, K. S., Dunton, K. H., 1999. Inorganic nitrogen acquisition in the seagrass thalassia testudinum: Development of a whole-plant nitrogen budget. Limnology and Oceanography 44 (5), 1204–1215.

Legrand, C., Carlsson, P., 1998. Uptake of high molecular weight dextran by the dinoflagellate *Alexandrium catenella*. Aquatic Microbial Ecology 16 (1), 81–86.

Lepoint, G., Defawe, O., Gobert, S., Dauby, P., Bouquegneau, J. M., 2002a. Experimental evidence for n recycling in the leaves of the seagrass posidonia oceanica. Journal Of Sea Research 48 (3), 173–179.

Lepoint, G., Gobert, S., Dauby, P., Bouquegneau, J. M., 2004. Contributions of benthic and planktonic primary producers to nitrate and ammonium uptake fluxes in a nutrient-poor shallow coastal area (corsica, nw mediterranean). Journal Of Experimental Marine Biology And Ecology 302 (1), 107–122.

Lepoint, G., Millet, S., Dauby, P., Gobert, S., Bouquegneau, J. M., 2002b. Annual nitrogen budget of the seagrass posidonia oceanica as determined by in situ uptake experiments. Marine Ecology-Progress Series 237, 87–96.

Li, Y., Lark, M., Reeve, D., 2005. Multi-scale variability of beach profiles at duck: A wavelet analysis. Coastal Engineering 52, 1133–1153.

Ligero, R., Barrera, M., Casas-Ruiz, M., 2005. Levels of ^{137}cs in muddy sediments of the seabed of the bay of cadiz, spain. part i. vertical and spatial distribution of activities. Journal of Environmental Radioactivity 80, 75–86.

Linares, F., Sundback, K., 2006. Uptake of dissolved free amino acids (dfaa) by microphytobenthic communities. Aquatic Microbial Ecology 42 (2), 175–186.

Lió, P., 2003. Wavelets in bioinformatics and computational biology: state of art and perspectives. Bioinformatics 19, 2–9.

Liu, Y., Liang, X. S., Weisberg, R. H., 2007. Rectification of the bias in the wavelet power spectrum. Journal of Atmospheric and Oceanic Technology 24, 2093–2102.

Loebl, M., Colijn, F., van Beusekom, J. E. E., Baretta-Bekker, J. G., Lancelot, C., Philippart, C. J. M., Rousseau, V., Wiltshire, K. H., 2009. Recent patterns in potential phytoplankton limitation along the northwest european continental coast. Journal of Sea Research 61, 34–43.

Loh, A. N., Bauer, J. E., Canuel, E. A., 2006. Dissolved and particulate organic matter source-age characterization in the upper and lower chesapeake bay: A combined isotope and biochemical approach. Limnology and Oceanography 51, 1421–1431.

Lomstein, B. A., Blackburn, T. H., Henriksen, K., 1989. Aspects of nitrogen and carbon cycling in the northern bering shelf sediment .1. the significance of urea turnover in the mineralization of nh4+. Marine Ecology-Progress Series 57 (3), 237–247.

Lomstein, B. A., Jensen, A. G. U., Hansen, J. W., Andreasen, J. B., Hansen, L. S., Berntsen, J., Kunzendorf, H., 1998. Budgets of sediment nitrogen and carbon cycling in the shallow water of knebel vig, denmark. Aquatic Microbial Ecology 14, 69–80.

Lopez, N. I., Duarte, C. M., Vallespinos, F., Romero, J., Alcoverro, T., 1998. The effect of nutrient additions on bacterial activity in seagrass (*Posidonia oceanica*) sediments. Journal of Experimental Marine Biology and Ecology 224, 155–166.

Lorite-Herrera, M., Hiscock, K., Jimenez-Espinosa, R., 2009. Distribution of dissolved inorganic and organic nitrogen in river water and groundwater in an agriculturally-dominated catchment, south-east spain. Water Air And Soil Pollution 198 (1-4), 335–346.

Mackey, M. D., Mackey, D. J., Higgins, H. W., Wright, S. W., 1996. Chemtax - a program for estimating class abundances from chemical markers: application of hplc measurements of phytoplankton. Marine Ecology-Progress Series 144, 265–283.

Mak, M., 1995. Orthogonal wavelet analysis - interannual variability in the sea-surface temperature. Bulletin of the American Meteorological Society 76, 2179–2186.

Mallat, S. G., 1999. A Wavelet Tour of Signal Processing, Second Edition (Wavelet Analysis & Its Applications). Academic Press, San Diego, CA.

Malta, E. J., Ferreira, D. G., Vergara, J. J., Pérez-Lloréns, J. L., 2005. Nitrogen load and irradiance affect morphology, photosynthesis and growth of caulerpa prolifera (bryopsidales : Chlorophyta). Marine Ecology-Progress Series 298, 101–114.

Manimaran, P., Panigrahi, P. K., Parikh, J. C., 2008. Difference in nature of correlation between nasdaq and bse indices. Physica A - Statistical Mechanics and its Applications 387, 5810–5817.

Maraun, D., Kurths, J., Holschneider, M., 2007. Nonstationary gaussian processes in wavelet domain: Synthesis, estimation, and significance testing. Physical Review E 75, 016707.

Mayer, L. M., Schick, L. L., Hardy, K. R., Estapa, M. L., 2009. Photodissolution and other photochemical changes upon irradiation of algal detritus. Limnology And Oceanography 54 (5), 1688–1698.

McCallister, S. L., Bauer, J. E., Canuel, E. A., 2006. Bioreactivity of estuarine dissolved organic matter: A combined geochemical and microbiological approach. Limnology And Oceanography 51 (1), 94–100.

McCarthy, J. J., Goldman, J. C., 1979. Nitrogenous nutrition of marine phytoplankton in nutrient-depleted waters. Science 203 (4381), 670–672.

McCarthy, M. D., Benner, R., Lee, C., Hedges, J. I., Fogel, M. L., 2004. Amino acid carbon isotopic fractionation patterns in oceanic dissolved organic matter: an unaltered photoautotrophic source for dissolved organic nitrogen in the ocean? Marine Chemistry 92 (1-4), 123–134.

McCarthy, M. D., Hedges, J. I., Benner, R., 1998. Major bacterial contribution to marine dissolved organic nitrogen. Science 281 (5374), 231–234.

McQuatters-Gollop, A., Raitsos, D. E., Edwards, M., Pradhan, Y., Mee, L. D., Lavender, S. J., Attrill, M. J., 2007. A long-term chlorophyll data set reveals regime shift in north sea phytoplankton biomass unconnected to nutrient trends. Limnology and Oceanography 52, 635–648.

Mejanelle, L., Laureillard, J., Rassoulzadegan, F., 2005. Polar lipid biomarkers of free-living bacteria from oligotrophic marine waters. Biogeochemistry 72 (3), 365–383.

Meyers, S. D., Kelly, B. G., O'Brien, J. J., 1993. An introduction to wavelet analysis in oceanography and meteorology - with application to the dispersion of yanai waves. Monthly Weather Review 121, 2858–2866.

Mi, X., Ren, H., Ouyang, Z., Wei, W., Ma, K., 2005. The use of the mexican hat and the morlet wavelets for detection of ecological patterns. Plant Ecology 179, 1–19.

Middelburg, J. J., Barranguet, C., Boschker, H. T. S., Herman, P. M. J., Moens, T., Heip, C. H. R., 2000. The fate of intertidal microphytobenthos carbon: An in situ c-13-labeling study. Limnology and Oceanography 45 (6), 1224–1234.

Middelburg, J. J., Nieuwenhuize, J., 2000. Nitrogen uptake by heterotrophic bacteria and phytoplankton in the nitrate-rich thames estuary. Marine Ecology-Progress Series 203, 13–21.

Moncreiff, C. A., Sullivan, M. J., Daehnick, A. E., 1992. Primary production dynamics in seagrass beds of mississippi sound - the contributions of seagrass, epiphytic algae, sand microflora, and phytoplankton. Marine Ecology-Progress Series 87 (1-2), 161–171.

Moodley, L., Boschker, H. T. S., Middelburg, J. J., Pel, R., Herman, P. M. J., de Deckere, E., Heip, C. H. R., 2000. Ecological significance of benthic foraminifera: C-13 labelling experiments. Marine Ecology-Progress Series 202, 289–295.

Morris, E. P., Peralta, G., Benavente, J., Freitas, R., Rodrigues, A. M., Quintino, V., Alvarez, O., Valcárcel-Pérez, N., Vergara, J. J., Hernández, I., Pérez-Lloréns, J. L., 2009. Caulerpa prolifera stable isotope ratios reveal anthropogenic nutrients within a tidal lagoon. Marine Ecology-Progress Series 390, 117–128.

Morris, E. P., Peralta, G., Brun, F. G., van Duren, L., Bouma, T. J., Pérez-Lloréns, J. L., 2008. Interaction between hydrodynamics and seagrass canopy structure: Spatially explicit effects on ammonium uptake rates. Limnology and Oceanography 53 (4), 1531–1539.

Motegi, C., Nagata, T., Miki, T., Weinbauer, M. G., Legendre, L., Rassoulzadegan, F., 2009. Viral control of bacterial growth efficiency in marine pelagic environments. Limnology And Oceanography 54 (6), 1901–1910.

Mulholland, M. R., Boneillo, G., Minor, E. C., 2004. A comparison of n and c uptake during brown tide (*Aureococcus anophagefferens*) blooms from two coastal bays on the east coast of the usa. Harmful Algae 3, 361–376.

Mulholland, M. R., Gobler, C. J., Lee, C., 2002. Peptide hydrolysis, amino acid oxidation, and nitrogen uptake in communities seasonally dominated by *Aureococcus anophagefferens*. Limnology and Oceanography 47, 1094–1108.

Nason, G. P., Silverman, B. W., 1995. The stationary wavelet transform and some statistical applications. In: Lecture Notes in Statistics 103. Springer-Verlag, New York, pp. 281–300.

Neff, J. C., Holland, E. A., Dentener, F. J., McDowell, W. H., Russell, K. M., 2002. The origin, composition and rates of organic nitrogen deposition: A missing piece of the nitrogen cycle? Biogeochemistry 57-58, 99–136.

Nezlin, N. P., Li, B. L., 2003. Time-series analysis of remote-sensed chlorophyll and environmental factors in the santa monica-san pedro basin off southern california. Journal of Marine Systems 39, 185–202.

Nienhuis, P. H., 1992. Eutrophication, water management, and the functioning of dutch estuaries and coastal lagoons. Estuaries 15, 538–548.

Nixon, S. W., 1995. Coastal marine eutrophication - a definition, social causes, and future concerns. Ophelia 41, 199–219.

Osterroht, C., Thomas, H., 2000. New production enhanced by nutrient supply from non-redfield remineralisation of freshly produced organic material. Journal Of Marine Systems 25 (1), 33–46.

Otake, T., Nogami, K., Maruyama, K., 1993. Dissolved and particulate organic-matter as possible food sources for eel leptocephali. Marine Ecology-Progress Series 92 (1-2), 27–34.

Palenik, B., Morel, F. M. M., 1990a. Amino-acid utilization by marine-phytoplankton - a novel mechanism. Limnology and Oceanography 35, 260–269.

Palenik, B., Morel, F. M. M., 1990b. Comparison of cell-surface l-amino acid oxidases from several marine-phytoplankton. Marine Ecology-Progress Series 59, 195–201.

Palenik, B., Morel, F. M. M., 1991. Amino oxidases of marine-phytoplankton. Applied and Environmental Microbiology 57, 2440–2443.

Pedersen, M. F., Borum, J., 1993. An annual nitrogen budget for a seagrass *Zostera marina* population. Marine Ecology-Progress Series 101, 169–177.

Peeters, J. C. H., Peperzak, L., 1990. Nutrient limitation in the north-sea - a bioassay approach. Netherlands Journal of Sea Research 26, 61–73.

Percival, D. B., 1995. On estimation of wavelet variance. Biometrika 82, 619–631.

Percival, D. B., Mofjeld, H. O., 1997. Analysis of subtidal coastal sea level fluctuations using wavelets. Journal of the American Statistical Association 92, 868–880.

Percival, D. B., Rothrock, D. A., Thorndike, A. S., Gneiting, T., 2008. The variance of mean sea-ice thickness: Effect of long-range dependence. Journal of Geophysical Research-Oceans 113, C01004.

Percival, D. B., Sardy, S., Davison, A. C., 2000. Wavestrapping time series: Adaptive wavelet-based bootstrapping. In: Fitzgerald, W. J., Smith, R. L., Walden, A. T., Young, P. C. (Eds.), Nonlinear and Nonstationary Signal Processing. Cambridge University Press, Cambridge, pp. 442–471.

Percival, D. B., Walden, A. T., 2000. Wavelet Methods for Time Series Analysis (Cambridge Series in Statistical and Probabilistic Mathematics). Cambridge University Press, New York.

Percival, D. B., Wang, M., Overland, J. E., 2004. An introduction to wavelet analysis with applications to vegetation time series. Community Ecology 5, 19–30.

Persson, J., Hogberg, P., Ekblad, A., Hogberg, M. N., Nordgren, A., Nasholm, T., 2003. Nitrogen acquisition from inorganic and organic sources by boreal forest plants in the field. Oecologia 137 (2), 252–257.

Philippart, C. J. M., Beukema, J. J., Cadée, G. C., Dekker, R., Goedhart, P. W., van Iperen, J. M., Leopold, M. F., Herman, P. M. J., 2007. Impacts of nutrient reduction on coastal communities. Ecosystems 10, 95–118.

Phillips, J. C., Hurd, C. L., 2003. Nitrogen ecophysiology of intertidal seaweeds from new zealand: N uptake, storage and utilisation in relation to shore position and season. Marine Ecology-Progress Series 264, 31–48.

Phillips, J. C., Hurd, C. L., 2004. Kinetics of nitrate, ammonium, and urea uptake by four intertidal seaweeds from new zealand. Journal Of Phycology 40 (3), 534–545.

Pinheiro, J., Bates, D., DebRoy, S., Sarkar, D., the R Core team, 2008. nlme: Linear and Nonlinear Mixed Effects Models. R package version 3.1-90.

Plus, M., Chapelle, A., Menesguen, A., Deslous-Paoli, J. M., Auby, I., 2003. Modelling seasonal dynamics of biomasses and nitrogen contents in a seagrass meadow (zostera noltii hornem.): application to the thau lagoon (french mediterranean coast). Ecological Modelling 161 (3), 213–238.

Price, N. M., Cochlan, W. P., Harrison, P. J., 1985. Time course of uptake of inorganic and organic nitrogen by phytoplankton in the strait of georgia: Comparison of frontal and stratified communities. Marine Ecology-Progress Series 27, 39–53.

Price, N. M., Harrison, P. J., 1988. Uptake of urea-c and urea-n by the coastal marine diatom thalassiosira-pseudonana. Limnology and Oceanography 33 (4), 528–537.

Probyn, T. A., Chapman, A. R. O., 1982. Nitrogen uptake characteristics of *Chordaria flagelliformis* (phaeophyta) in batch mode and continuous mode experiments. Marine Biology 71, 129–133.

Prokoph, A., Patterson, R. T., 2004. Application of wavelet and regression analysis in assessing temporal and geographic climate variability: Eastern ontario, canada as a case study. Atmosphere-Ocean 42, 201–212.

R Development Core Team, 2009. R: A Language and Environment for Statistical Computing. R Foundation for Statistical Computing, Vienna, Austria, 3-900051-07-0.
URL `http://www.R-project.org`

Ramsey, J. B., 2002. Wavelets in economics and finance: Past and future. Studies in Nonlinear Dynamics and Econometrics 6, 1.

Renaud, S. M., Thinh, L. V., Lambrinidis, G., Parry, D. L., 2002. Effect of temperature on growth, chemical composition and fatty acid composition of tropical australian microalgae grown in batch cultures. Aquaculture 211 (1-4), 195–214.

Retamal, L., Vincent, W. F., Martineau, C., Osburn, C. L., 2007. Comparison of the optical properties of dissolved organic matter in two river-influenced coastal regions of the canadian arctic. Estuarine Coastal And Shelf Science 72, 261–272.

Rijkswaterstaat, 2009. Waterbase: Online interface to the donar database (data opslag natte rijkswaterstaat). `http://www.waterbase.nl`.

Romero, J., Lee, K. S., Pérez, M., Mateo, M. A., Alcoverro, T., 2006. Nutrient dynamics in seagrass ecosystems. In: Larkum, A. W. D., Orth, R. J., Duarte, C. M. (Eds.), Seagrasses: Biology, Ecology and Conservation. Springer, Dordrecht, pp. 227–254.

Santos, I. R., Burnett, W. C., Chanton, J., Mwashote, B., Suryaputra, I. G. N. A., Dittmar, T., 2008. Nutrient biogeochemistry in a gulf of mexico subterranean estuary and groundwater-derived fluxes to the coastal ocean. Limnology And Oceanography 53 (2), 705–718.

Schaefli, B., Maraun, D., Holschneider, M., 2007. What drives high flow events in the swiss alps? recent developments in wavelet spectral analysis and their application to hydrology. Advances in Water Resources 30, 2511–2525.

See, J. H., Bronk, D. A., Lewitus, A. J., 2006. Uptake of spartina-derived humic nitrogen by estuarine phytoplankton in nonaxenic and axenic culture. Limnology and Oceanography 51, 2290–2299.

Seitzinger, S. P., Sanders, R. W., 1997. Contribution of dissolved organic nitrogen from rivers to estuarine eutrophication. Marine Ecology Progress Series 159, 1–12.

Seitzinger, S. P., Sanders, R. W., 1999. Atmospheric inputs of dissolved organic nitrogen stimulate estuarine bacteria and phytoplankton. Limnology and Oceanography 44, 721–730.

Seitzinger, S. P., Sanders, R. W., Styles, R., 2002. Bioavailability of don from natural and anthropogenic sources to estuarine plankton. Limnology And Oceanography 47 (2), 353–366.

Selesnick, I. W., 2001. Hilbert transform pairs of wavelet bases. IEEE Signal Processing Letters 8, 170–173.

Selesnick, I. W., 2002. The design of approximate hilbert transform pairs of wavelet bases. IEEE Transactions on Signal Processing 50, 1144–1152.

Selesnick, I. W., Baraniuk, R. G., Kingsbury, N. G., 2005. The dual-tree complex wavelet transform. IEEE Signal Processing Magazine 22, 123–151.

Serroukh, A., Walden, A. T., 2000a. Wavelet scale analysis of bivariate time series i: Motivation and estimation. Journal of Nonparametric Statistics 13, 1–36.

Serroukh, A., Walden, A. T., 2000b. Wavelet scale analysis of bivariate time series ii: Statistical properties for linear processes. Journal of Nonparametric Statistics 13, 37–56.

Serroukh, A., Walden, A. T., Percival, D. B., 2000. Statistical properties and uses of the wavelet variance estimator for the scale analysis of time series. Journal of the American Statistical Association 95, 184–196.

Sharp, J. H., Rinker, K. R., Savidge, K. B., Abell, J., Benaim, J. Y., Bronk, D. A., Burdige, D. J., Cauwet, G., Chen, W. H., Doval, M. D., Hansell, D. A., Hopkinson, C., Kattner, G., Kaumeyer, N., McGlathery, K. J., Merriam, J., Morley, N., Nagel, K., Ogawa, H., Pollard, C., Pujo-Pay, M., Raimbault, P., Sambrotto, R., Seitzinger, S. P., Spyres, G., Tirendi, F., Walsh, T. W., Wong, C. S., 2002. A preliminary methods comparison for measurement of dissolved organic nitrogen in seawater. Marine Chemistry 78 (4), 171–184.

Shumway, R. H., Stoffer, D. S., 2006. Time Series Analysis and Its Applications: With R Examples (Springer Texts in Statistics), 2nd Edition. Springer, New York.

Siddaiah, P., V. V. K. D. V. Prasad, Rao, B. P., 2008. Denoising of biological signals using different wavelet based methods and their comparison. Asian Journal of Information Technology 7, 146–149.

Smith, V. H., 2003. Eutrophication of freshwater and coastal marine ecosystems - a global problem. Environmental Science and Pollution Research 10, 126–139.

Soetaert, K., Middelburg, J. J., Heip, C. H. R., Meire, P., Van Damme, S., Maris, T., 2006. Long-term change in dissolved inorganic nutrients in the heterotrophic scheldt estuary (belgium, the netherlands). Limnology and Oceanography 51, 409–423.

Solomon, C. M., Glibert, P. M., 2008. Urease activity in five phytoplankton species. Aquatic Microbial Ecology 52 (2), 149–157.

Sondergaard, M., Williams, P. J. L., Cauwet, G., Riemann, B., Robinson, C., Terzic, S., Woodward, E. M. S., Worm, J., 2000. Net accumulation and flux of dissolved organic carbon and dissolved organic nitrogen in marine plankton communities. Limnology And Oceanography 45 (5), 1097–1111.

Stafford, N. B., Bell, S. S., 2006. Space competition between seagrass and caulerpa prolifera (forsskaal) lamouroux following simulated disturbances in lassing park, fl. Journal Of Experimental Marine Biology And Ecology 333 (1), 49–57.

Stålnacke, P., Vandsemb, S. M., Vassiljev, A., Grimvall, A., Jolankal, G., 2004. Changes in nutrient levels in some eastern european rivers in response to large-scale changes in agriculture. Water Science and Technology 49, 29–36.

Stapel, J., Aarts, T. L., van Duynhoven, B. H. M., de Groot, J. D., van den Hoogen, P. H. W., Hemminga, M. A., 1996. Nutrient uptake by leaves and roots of the seagrass thalassia hemprichii in the spermonde archipelago, indonesia. Marine Ecology-Progress Series 134 (1-3), 195–206.

Stapel, J., Hemminga, M. A., Bogert, C. G., Maas, Y. E. M., 2001. Nitrogen (n-15) retention in small thalassia hemprichii seagrass plots in an offshore meadow in south sulawesi, indonesia. Limnology And Oceanography 46 (1), 24–37.

Stedmon, C. A., Markager, S., 2005. Tracing the production and degradation of autochthonous fractions of dissolved organic matter by fluorescence analysis. Limnology and Oceanography 50 (5), 1415–1426.

Steen, H., 2004. Interspecific competition between enteromorpha (ulvales : Chlorophyceae) and fucus (fucales : Phaeophyceae) germlings: effects of nutrient concentration, temperature, and settlement density. Marine Ecology-Progress Series 278, 89–101.

Stepanauskas, R., Edling, H., Tranvik, L. J., 1999. Differential dissolved organic nitrogen availability and bacterial aminopeptidase activity in limnic and marine waters. Microbial Ecology 38 (3), 264–272.

Stepanauskas, R., Laudon, H., Jorgensen, N. O. G., 2000. High don bioavailability in boreal streams during a spring flood. Limnology and Oceanography 45 (6), 1298–1307.

Stoecker, D. K., Gustafson, D. E., 2003. Cell-surface proteolytic activity of photosynthetic dinoflagellates. Aquatic Microbial Ecology 30 (2), 175–183.

Sulzberger, B., Durisch-Kaiser, E., 2009. Chemical characterization of dissolved organic matter (dom): A prerequisite for understanding uv-induced changes of dom absorption properties and bioavailability. Aquatic Science 71, 104 – 126.

Suratman, S., Jickells, T. D., Weston, K., Fernand, L., 2008. Seasonal variability of inorganic and organic nitrogen in the north sea. Hydrobiologia 610, 83–98.

Suttle, C. A., 2005. Viruses in the sea. Nature 437 (7057), 356–361.

Tamminen, T., Irmisch, A., 1996. Urea uptake kinetics of a midsummer planktonic community on the sw coast of finland. Marine Ecology-Progress Series 130 (1-3), 201–211.

Tarutani, K., Niimura, Y., Uchida, T., 2004. Short-term uptake of dissolved organic nitrogen by an axenic strain of ulva pertusa (chlorophyceae) using n-15 isotope measurements. Botanica Marina 47 (3), 248–250.

Thomas, H., Bozec, Y., de Baar, H. J. W., Elkalay, K., Frankignoulle, M., Schiettecatte, L. S., Kattner, G., Borges, A. V., 2005. The carbon budget of the north sea. Biogeosciences 2 (1), 87–96.

Thomas, H., Ittekkot, V., Osterroht, C., Schneider, B., 1999. Preferential recycling of nutrients - the ocean's way to increase new production and to pass nutrient limitation? Limnology And Oceanography 44 (8), 1999–2004.

Thursby, G. B., Harlin, M. M., 1982. Leaf-root interaction in the uptake of ammonia by *Zostera marina*. Marine Biology 72, 109–112.

Thursby, G. B., Harlin, M. M., 1984. Interaction of leaves and roots of *Ruppia maritima* in the uptake of phosphate, ammonia, and nitrate. Marine Biology 83, 61–67.

Torrence, C., Compo, G. P., 1998. A practical guide to wavelet analysis. Bulletin of the American Meteorological Society 79, 61–78.

Tungaraza, C., Rousseau, V., Brion, N., Lancelot, C., Gichuki, J., Baeyens, W., Goeyens, L., 2003. Contrasting nitrogen uptake by diatom and phaeocystis-dominated phytoplankton assemblages in the north sea. Journal Of Experimental Marine Biology And Ecology 292 (1), 19–41.

Tupas, L., Koike, I., 1990. Amino-acid and ammonium utilization by heterotrophic marine-bacteria grown in enriched seawater. Limnology and Oceanography 35 (5), 1145–1155.

Tyler, A. C., McGlathery, K. J., Anderson, I. C., 2001. Macroalgae mediation of dissolved organic nitrogen fluxes in a temperate coastal lagoon. Estuarine Coastal and Shelf Science 53 (2), 155–168.

Tyler, A. C., McGlathery, K. J., Macko, S. A., 2005. Uptake of urea and amino acids by the macroalgae ulva lactuca (chlorophyta) and gracilaria vermiculophylla (rhodophyta). Marine Ecology-Progress Series 294, 161–172.

Udy, J. W., Dennison, W. C., 1997. Growth and physiological responses of three seagrass species to elevated sediment nutrients in moreton bay, australia. Journal Of Experimental Marine Biology And Ecology 217 (2), 253–277.

Urban-Rich, J., 1999. Release of dissolved organic carbon from copepod fecal pellets in the greenland sea. Journal Of Experimental Marine Biology And Ecology 232 (1), 107–124.

van Beusekom, J. E. E., Brockmann, U. H., Hesse, K.-J., Hickel, W., Poremba, K., Tillmann, U., 1999. Ocean Dynamics 51, 245–266.

van Beusekom, J. E. E., de Jonge, V. N., 2002. Long-term changes in wadden sea nutrient cycles: importance of organic matter import from the north sea. Hydrobiologia 475, 185–194.

Van den Meersche, K., Middelburg, J. J., Soetaert, K., van Rijswijk, P., Boschker, H. T. S., Heip, C. H. R., 2004. Carbon-nitrogen coupling and algal-bacterial interactions during an experimental bloom: Modeling a ^{13}c tracer experiment. Limnology and Oceanography 49 (3), 862–878.

van der Veer, H. W., van Raaphorst, W., Bergman, M. J. N., 1989. Eutrophication of the dutch wadden sea: External nutrient loadings of the marsdiep and vliestroom basin. Helgoland Marine Research 43, 501–515.

van der Weijden, C. H., Middelburg, J. J., 1989. Hydrogeochemistry of the river rhine: Long-term and seasonal variability, elemental budgets, base level and pollution. Water Research 23, 1247–1266.

van der Zee, C., Chou, L., 2005. Seasonal cycling of phosphorus in the southern bight of the north sea. Biogeosciences 2, 27–42.

Van Engeland, T., Knuijt, A., Soetaert, K., Laane, R. W. P. M., Middelburg, J. J., submitted. Dissolved organic nitrogen dynamics in the north sea: a time series analysis. Estuarine, Coastal and Shelf Science.

van Es, F. B., Laane, R. W. P. M., 1982. The utility of organic matter in the ems-dollard estuary. Netherlands Journal of Sea Research 16, 300–314.

Vetter, T. A., Perdue, E. M., Ingall, E., Koprivnjak, J. F., Pfromm, P. H., 2007. Combining reverse osmosis and electrodialysis for more complete recovery of dissolved organic matter from seawater. Separation and Purification Technology 56, 383–387.

Veuger, B., Middelburg, J. J., 2007. Incorporation of nitrogen from amino acids and urea by benthic microbes: role of bacteria versus algae and coupled incorporation of carbon. Aquatic Microbial Ecology 48 (1), 35–46.

Veuger, B., Middelburg, J. J., Boschker, H. T. S., Houtekamer, M., 2005. Analysis of n-15 incorporation into d-alanine: A new method for tracing nitrogen uptake by bacteria. Limnology And Oceanography-Methods 3, 230–240.

Veuger, B., Middelburg, J. J., Boschker, H. T. S., Houtekamer, M., 2007. Update of "analysis of ^{15}n incorporation into d-alanine: A new method for tracing nitrogen uptake by bacteria"(veuger et al. 2005, limnol. oceanogr. methods 3: 230-240). Limnology And Oceanography-Methods 5, 192–194.

Veuger, B., Middelburg, J. J., Boschker, H. T. S., Nieuwenhuize, J., van Rijswijk, P., Rochelle-Newall, E. J., Navarro, N., 2004. Microbial uptake of dissolved organic and inorganic nitrogen in randers fjord. Estuarine Coastal and Shelf Science 61, 507–515.

Veuger, B., van Oevelen, D., Boschker, H. T. S., Middelburg, J. J., 2006. Fate of peptidoglycan in an intertidal sediment: An in situ c-13-labeling study. Limnology And Oceanography 51 (4), 1572–1580.

Vidakovic, B., 1999. Statistical Modeling by Wavelets. Wiley Series in Probability and Mathematical Statistics. Wiley-Interscience, New York.

Viso, A. C., Marty, J. C., 1993. Fatty-acids from 28 marine microalgae. Phytochemistry 34 (6), 1521–1533.

von Felten, S., Buchmann, N., Scherer-Lorenzen, M., 2008. Preferences for different nitrogen sources by coexisting plant species and soil microbes: comment. Ecology 89 (3), 878–879.

Vonk, J. A., Middelburg, J. J., Stapel, J., Bouma, T. J., 2008. Dissolved organic nitrogen uptake by seagrasses. Limnology And Oceanography 53 (2), 542–548.

Vonk, J. A., Stapel, J., 2008. Regeneration of nitrogen (n-15) from seagrass litter in tropical indo-pacific meadows. Marine Ecology-Progress Series 368, 165–175.

Weigelt, A., King, R., Bol, R., Bardgett, R. D., 2003. Inter-specific variability in organic nitrogen uptake of three temperate grassland species. Journal Of Plant Nutrition and Soil Science-Zeitschrift Fur Pflanzenernahrung und Bodenkunde 166 (5), 606–611.

Weijerman, M., Lindeboom, H., Zuur, A. F., 2005. Regime shifts in marine ecosystems of the north sea and wadden sea. Marine Ecology Progress Series 298, 21–39.

Weilguni, H., Humpesch, U. H., 1999. Long-term trends of physical, chemical and biological variables in the river danube 1957-1995: A statistical approach. Aquatic Sciences 61, 234–259.

Welsh, B. L., Eller, F. C., 1991. Mechanisms controlling summertime oxygen depletion in western long-island sound. Estuaries 14, 265–278.

Welsh, D. T., 2000. Nitrogen fixation in seagrass meadows: Regulation, plant-bacteria interactions and significance to primary productivity. Ecology Letters 3, 58–71.

Weston, K., Jickells, T. D., Fernand, L., Parker, E. R., 2004. Nitrogen cycling in the southern north sea: consequences for total nitrogen transport. Estuarine Coastal and Shelf Science 59, 559–573.

Whitcher, B., 2007. waveslim: Basic wavelet routines for one-, two- and three-dimensional signal processing. R package version 1.6.1.
URL `http://www.image.ucar.edu/~whitcher/`

Whitcher, B., Byers, S. D., Guttorp, P., Percival, D. B., 2002. Testing for homogeneity of variance in time series: Long memory, wavelets, and the nile river. Water Resources Research 38, 1054.

Whitcher, B., Craigmile, P. F., Brown, P., 2005. Time-varying spectral analysis in neurophysiological time series using hilbert wavelet pairs. Signal Processing 85, 2065–2081.

Whitcher, B., Guttorp, P., Percival, D. B., 2000. Wavelet analysis of covariance with application to atmospheric time series. Journal of Geophysical Research-Atmosphere 105, 14941–14962.

Wiegner, T. N., Tubal, R. L., MacKenzie, R. A., 2009. Bioavailability and export of dissolved organic matter from a tropical river during base- and stormflow conditions. Limnology And Oceanography 54 (4), 1233–1242.

Williams, P. J. L., 1995. Evidence for the seasonal accumulation of carbon-rich dissolved organic material, its scale in comparison with changes in particulate material and the consequential effects on net c/n assimilation ratios. Marine Chemistry 51, 17–29.

Yndestad, H., 2004. The cause of barents sea biomass dynamics. Journal of Marine Systems 44, 107–124.

Ziegler, S., Benner, R., 1999a. Dissolved organic carbon cycling in a subtropical seagrass-dominated lagoon. Marine Ecology-Progress Series 180, 149–160.

Ziegler, S., Benner, R., 1999b. Nutrient cycling in the water column of a subtropical seagrass meadow. Marine Ecology-Progress Series 188, 51–62.

Ziegler, S., Benner, R., 2000. Effects of solar radiation on dissolved organic matter cycling in a subtropical seagrass meadow. Limnology And Oceanography 45 (2), 257–266.

Ziegler, S., Kaiser, E., Benner, R., 2004. Dynamics of dissolved organic carbon, nitrogen and phosphorus in a seagrass meadow of laguna madre, texas. Bulletin Of Marine Science 75 (3), 391–407.

Zimmerman, R. C., Smith, R. D., Alberte, R. S., 1987. Is growth of eelgrass nitrogen limited - a numerical-simulation of the effects of light and nitrogen on the growth dynamics of zostera-marina. Marine Ecology-Progress Series 41 (2), 167–176.

Dankwoord / Acknowledgements

We zijn er bijna: jullie nog even lezen, ik nog even schrijven...☺ Maar dit is het aangenaamste deel, waarbij ik rustig over mijn vier jaren als doctoraatstudent kan reflecteren. Daarbij komen direct een hoop namen en gezichten op de voorgrond. In eerste instantie wil ik mijn beide promotoren, Jack en Karline, bedanken voor de degelijke begeleiding. De snelheid en gerichtheid waarmee raad terugkwam wanneer ik een probleem aangaf werkte echt inspirerend. Jullie hebben zeker de handen vol gehad met het verbeteren van hoofdstukken en vooral met me in te tomen, zodat we de bomen door het bos bleven zien. Zonder jullie waardevolle raad zou dit proefschrift er heel anders uit zien (en meer dan waarschijnlijk niet onder de noemer "proefschrift" vallen). Tjeerd, hierbij kan ik jou ook zeker vermelden. Je hebt me met raad en daad bijgestaan tijdens de veldcampagne in Cádiz en lang daarna bij het uitschrijven van de bevindingen. Bedankt voor de aangename tijd. Ik wil ook Carlo Heip, onze centrumdirecteur, bedanken voor de fijne werkplek die ik 4 jaren heb gehad.

Als ik naar die grote kartonnen doos en overvolle plastic bak met stalen kijk, besef ik dat ik deze hoeveelheid sediment, plantenmateriaal en water monsters nooit zelf had kunnen verwerken. Gelukkig kon ik hiervoor rekenen op een klein leger laboranten. Pieter, bedankt voor de hulp bij het uitwerken en opzetten van experimenten, het extraheren van PLFA en aminozuur monsters, al de logistiek van bestellingen en het uren lang filteren van Oosterschelde water (alle metingen zijn binnen, dus ik kan terug vol enthousiasme werken aan een nieuw artikel, dat helaas niet meer in de thesis is geraakt). Marco, ik vrees dat ik er met één appeltaart niet ga geraken na al die keren dat ik in jou deur opening stond met vragen en stalen (of monsters). Peter, Yvonne, Cobie, Jan, Jurian, Anton, Lennart, jullie hebben mij waarschijnlijk evenveel in jullie deuropening zien verschijnen als Marco, en om dezelfde redenen. Bedankt voor de waardevolle raad en hulp wanneer er dingen onduidelijk waren of extra metingen moesten gebeuren. Ik weet niet wat ieder van jullie lekker vindt, maar ga er zeker voor zorgen dat Marco genoeg taart heeft om uit te delen. Hoewel de gegevens niet in de thesis zijn opgenomen, heb ik tijdens mijn promotie traject aan boord van de Luctor experimenten uitgevoerd. Peter, Ko, Anton, Marcel, Jan (Sinke) en Jan (Peene), bedankt voor de fijne sfeer, de hulp bij de bemonstering en uiteraard voor de stevige omeletten tijdens de lunch. Hoewel het grotere deel van deze thesis gebaseerd is op experimenteel werk, is er een aanzienlijke hoeveelheid tijd in de data analyse van monitoring data gestoken. Deze werd vakkundig verzameld en gestroomlijnd op de CEMEDATA server gestockeerd door Adri. Adri, bedankt voor de hulp bij het maken en gebruiken van die lokale databank, en het bieden van eerste hulp bij computer problemen.

Since my Italian, German, Japanese, and Rwanda language skills are slightly worse than my English, I will stick to the latter. Beside progress in your research, the most important determining factor for your job satisfaction is the atmosphere among colleagues. And I

certainly had good colleagues, of which some became real friends. Many have come during my PhD career, and about just as many have gone (assuming that the institute is more or less in a steady-state over the relevant time scale ☺), and some have even returned. It is thus likely that I will forget to mention some names. Karel, Andreas, Johan, I've enjoyed you all as roommates. The quick conversations during working hours were pleasant distractions. R, Latex and Linux became so much easier to master with your background knowledge. I am now at the last stage of the 'stoelendans' with a nice view on the Oosterschelde. Johan, I will stay a bit longer. Unfortunately, you will have to wait longer for the best view in the office. Bart, Dick, Filip, Tom, thanks for the feedback on my work or work in general, and the enjoyable conversations. Hopefully, we can continue to work together for some time and even increase collaboration. I also want to thank the people with whom I've spent quite some time in the guesthouse. James en Laura doen voortreffelijk werk om het iedereen in 'de Kêête' naar zijn zin te maken, waarvoor mijn dank. *It's been exciting with the parties, evenings at Yerseke Beach, movie evenings, swimming (Ina, Ellen, Pieter), ..., and at many times educational, with, for instance, the international cooking (like preparation of fermented rabbit ☺). I've also enjoyed (and continue to enjoy) the carpooling with our small but steadily growing Belgian delegation (Eugène, Tom, Tom, Johan, Kristiaan). The most memorable moments, however, were those with my friends, Andreas, Silke, Tetsuro, Sayuri, and Karel. Thank you for the wonderful time of diving, skiing, boating, biking, barbecues, 'fünf-stunden-fleisch' in copper kettles, conversations, inspiration, trips, weekends, in short: for your friendship. Now, we start to explore different horizons, but the world is not as big as it used to be ...*

Ik kan nu als ervaringsdeskundige zeggen dat het een hele onderneming is om een doctoraat met succes af te ronden, en dat daarbij je naaste familie een cruciale rol speelt. Na een niet te onderschatten taak om me tot volwassenheid te brengen, hebben mijn ouders ook nog het geduld moeten hebben om me te laten studeren. Ma en pa, wie had er tien jaar geleden gedacht dat ik een universitaire studie met succes ging afronden, laat staan een doctoraat zou behalen. De beste keuze die ik gemaakt heb in mijn studenten-carriére was de opleiding als 'Licentiaat (MSc) in de Informatica'overboord gooien, maar het was allesbehalve evident dat ik hierna nog eens vier jaar kon studeren. Op de koop toe maakte ik er nog vijf jaar van door een extra opleiding in mariene wetenschappen in Gent te volgen, waar ik uiteindelijk mijn promotoren ontmoette. Heel erg bedankt voor jullie geduld en al de steun die nodig was om zover te geraken. Moeke, Lieve, Darah, Sofie bedankt om er te zijn en voor de nodige afleiding te zorgen. Paul, Nelly, Nico, Eline en Bopa, bedankt voor de aanmoedigingen en de goede raad.

Saving the best for last...! Els, mijn vrouwke, jij bent vanaf het eerste jaar dat we mekaar kenden de belangrijkste schakel geweest in het behalen van mijn doctoraat. Je hebt me getoond hoeveel discipline nodig was, en hoewel ik er nog steeds minder heb dan jij, bleek het voldoende. Je hebt me altijd gesteund, raad gegeven, en als het nodig was 'achter mijn vodden gezeten'. De laatste maanden waren hectisch met het schrijven van de thesis en de aankoop van het huis, waarbij dat tweede voor een groot deel op jouw schouders terecht kwam. Bedankt voor je steun en om er steeds te zijn. Na de korte pijn is de thesis nu afgerond en kunnen we weer vol frisse moed aan iets nieuws beginnen.